Texas Tech University
Multidisciplinary Research in Transportation

Develop Design Details for CRCP Whitetopping and Unbonded Overlays

Niwesh Koirala, Christopher Jabonero, Tito Nyamuhokya,
Darlene Goehl, and Moon Won

Performed in cooperation with the Texas Department of Transportation and the Federal Highway Administration

Research Project 0-7148
Research Report 0-7148-R1
http://www.techmrt.ttu.edu/reports.php

1. Report No. FHWA/TX-26/0-7148-1	2. Government Accession No.:		3. Recipient's Catalog No.:
4. Title and Subtitle: Develop Design Details for CRCP Whitetopping and Unbonded Overlays			5. Report Date: July 2025 6. Performing Organization Code
7. Author(s): Niwesh Koirala, Christopher Jabonero, Tito Nyamuhokya, Darlene Goehl, and Moon Won			8. Performing Organization Report No. 0-7148 – R1
9. Performing Organization Name and Address: Texas Tech University College of Engineering Lubbock, Texas 79409-1023 Texas A&M Transportation Institute 1111 RELLIS Parkway College Station, TX 77843			10. Work Unit No.(TRAIS): 11. Contract or Grant No.: Project 0-7148
12. Sponsoring Agency Name and Address: Texas Department of Transportation Research and Technology Implementation Office P.O. Box 5080 Austin, TX 78763-5080			13. Type of Report and Period Research Report 14. Sponsoring Agency Code:
15. Supplementary Notes: Project performed in cooperation with Texas Department of Transportation and the Federal Highway Administration			
16. Abstract: Existing design methodologies for concrete overlays often rely on outdated empirical approaches or complex mechanistic models that lack adequate field validation. This has resulted in a significant gap in practice, particularly the design of Continuously Reinforced Concrete Pavement (CRCP) overlays, for which no standardized procedure exists in many jurisdictions. To address this deficiency, this research presents an innovative and rational design method for CRCP overlays grounded in the foundational principle that pavement deflection is a primary and reliable indicator of structural capacity and future performance. The methodology is developed through a holistic approach that combines extensive field testing, a nationwide agency survey, and mechanistic modeling. A field program on new CRCP construction projects quantified the direct correlation between the deflection of the base layer prior to paving and the final deflection of the completed CRCP system. To expand upon the limited scope of the field data, a calibrated Finite Element Method (FEM) model using dynamic analysis was developed to accurately simulate Falling Weight Deflectometer (FWD) loading. The calibrated model generated a comprehensive set of correlation curves relating base deflection to CRCP deflection for slab thicknesses from 4-in. to 15-in. over a wide range of subgrade conditions. These findings were then synthesized into two practical engineering tools: a graphical Design Nomograph and a Python-based software program. Both tools seamlessly integrate design traffic (ESALs), existing pavement deflection, and new correlation data to determine the required CRCP overlay thickness. This deflection-based approach offers a validated, data-driven, and accessible framework for designing durable and cost-effective CRCP overlays, thereby filling a critical void in current pavement rehabilitation practice.			
17. Key Words: Whitetopping, Unbonded Overlays, Deflection design	18. Distribution Statement No Restrictions. This document is available to the public through the National Technical Information Service, Springfield, VA 22161, www.ntis.gov		
19. Security Classif. (of this report) Unclassified	20. Security Classif. (of this page) Unclassified	21. No. Of Pages	22. Price

DEVELOP DESIGN DETAILS FOR CRCP WHITETOPPING AND UNBONDED OVERLAYS

by

Niwesh Koirala,
Graduate Student
Texas Tech University

Christopher Jabonero, Ph.D.
Post-Doctoral Researcher
Texas Tech University

Tito Nyamuhokya, Ph.D.
Associate Research Scientist
Texas A&M Transportation Institute

Darlene Goehl, P.E.
Research Engineer
Texas A&M Transportation Institute

Moon Won, P.E., Ph.D.
Professor
Texas Tech University

Project Report 0-7148-1
Project Number 0-7148-1

Performed in Cooperation with the
Texas Department of Transportation
and the
Federal Highway Administration

Center for Multidisciplinary Research in Transportation
Department of Civil. and Environmental and Construction Engineering
Texas Tech University
Box 41023
Lubbock, TX 79409-1023

Texas A&M Transportation Institute
1111 RELLIS Parkway
College Station, TX 77843

AUTHOR'S DISCLAIMER

The contents of this report reflect the views of the authors who are responsible for the facts and the accuracy of the data presented herein. The contents do not necessarily reflect the official view of policies of the Texas Department of Transportation or the Federal Highway Administration. This report does not constitute a standard, specification, or regulation.

PATENT DISCLAIMER

There was no invention or discovery conceived or first actually reduced to practice in the course of or under this contract, including any art, method, process, machine, manufacture, design or composition of matter, or any new useful improvement thereof, or any variety of plant which is or may be patentable under the patent laws of the United States of America or any foreign country.

ENGINEERING DISCLAIMER

Not intended for construction, bidding, or permit purposes.

TRADE NAMES AND MANUFACTURERS' NAMES

The United States Government and the State of Texas do not endorse products or manufacturers.

Trade or manufacturers' names appear herein solely because they are considered essential to the object of this report.

ACKNOWLEDGMENTS

This research study was sponsored by the Texas Department of Transportation in cooperation with the Federal Highway Administration. The support provided by the project team—Enad Mahmoud, Andy Naranjo, Ruben Carrasco, Rachel Cano, Soojun Ha, Pangil Choi, and Lori Jaramillo is greatly appreciated. Special thanks are extended to Project Manager Danny Sourapath from the Research and Technology Implementation (RTI) Division at TxDOT for his invaluable guidance, insightful feedback, and continuous support throughout the duration of this project, which were essential in bringing the research to its final outcome.

TABLE OF CONTENTS

LIST OF FIGURES

LIST OF TABLES

CHAPTER 1
INTRODUCTION

1.1 Background

America's roads face a persistent challenge. Despite billions allocated through federal funding, the percentage of roads rated in poor condition increased from 14% to 20% between 2009 and 2017 (Bellis et al., 2019). This trend signals that the problem may not be merely a lack of funding, but perhaps a misalignment of priorities. States have often continued to invest heavily in expanding the road network rather than concentrating on the upkeep of existing infrastructure. This focus has led to a significant and growing maintenance backlog, with estimates suggesting an annual need of $231.4 billion to restore and preserve the current network (Bellis et al., 2019).

A glance at state-level figures confirms this emphasis on upkeep. For instance, the Texas Department of Transportation's (TxDOT) legislative appropriations request for the 2026-2027 fiscal years shows a major commitment to maintenance and rehabilitation. In practical terms, nearly 45 cents of every dollar TxDOT plans to spend is directed toward addressing the condition of existing roads (Figure 1-1).

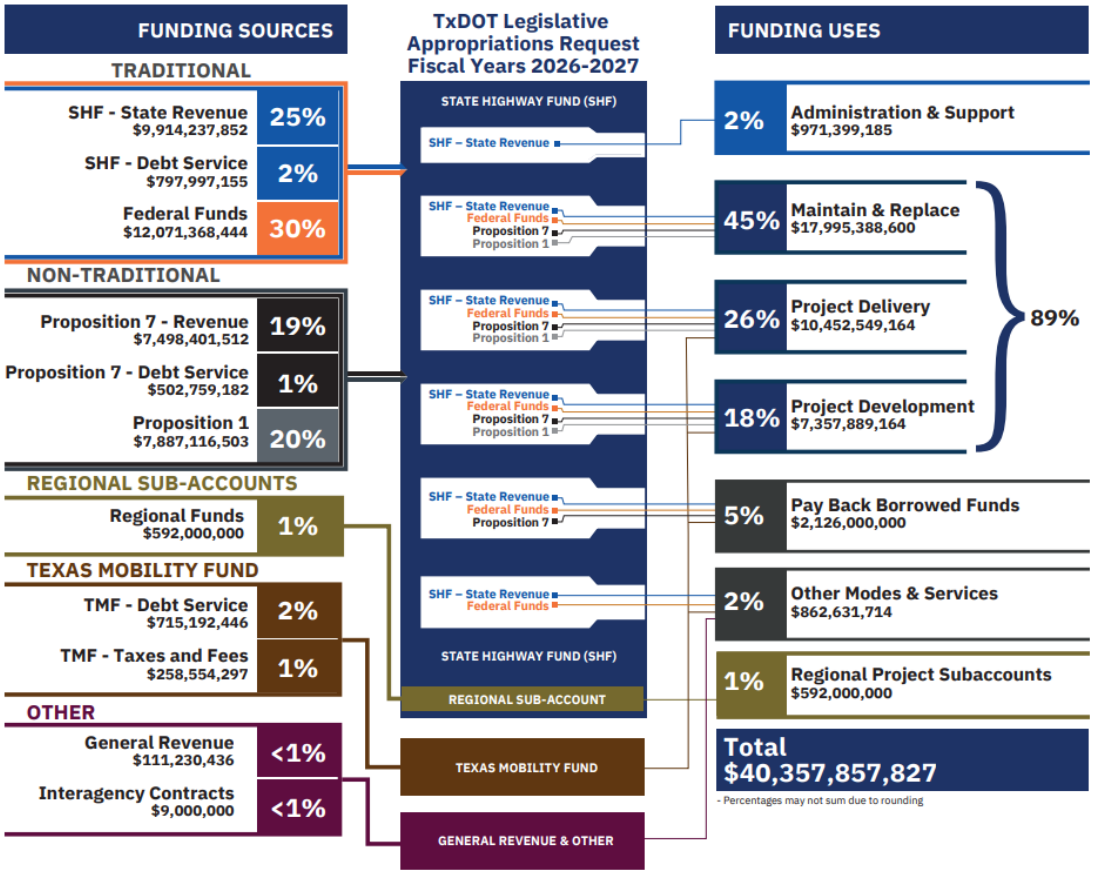

Figure 1-1 TxDOT legislative appropriations request for fiscal years 2026-2027

So, we spend a considerable amount getting things fixed. However, is it truly effective in the long run? Does it make a lasting difference? If every repair was perfect and permanent, future maintenance costs might diminish. Realistically, however, this is not the case. Every maintenance action and every repair come with an implicit lifespan. Roads degrade, and interventions eventually require further attention. Now, consider the compounding effect: we are already investing heavily in current repairs, new lane-miles are added to the system annually, and roads that have already been maintained will inevitably need maintenance again. The crucial debate, therefore, shifts from simply fixing roads to ensuring those fixes are durable and sustainable. This means implementing strong, reliable design and construction strategies from the outset strategies focused on long-term performance. This research centers on the very idea of ensuring the roads we fix stay fixed for longer.

To tackle this, we first need to understand how pavement performance is typically viewed. A key concept is the Present Serviceability Index (PSI), a scale (often 0-5, zero being awful and five being the best) measures the road's ability to serve traffic. As shown in Figure 1-2, a newly constructed road might start with a high PSI, say Pi=4.5, representing excellent condition. Over time, as traffic loads (measured in Equivalent Single Axle Loads, or ESALs) accumulate, the serviceability naturally declines.

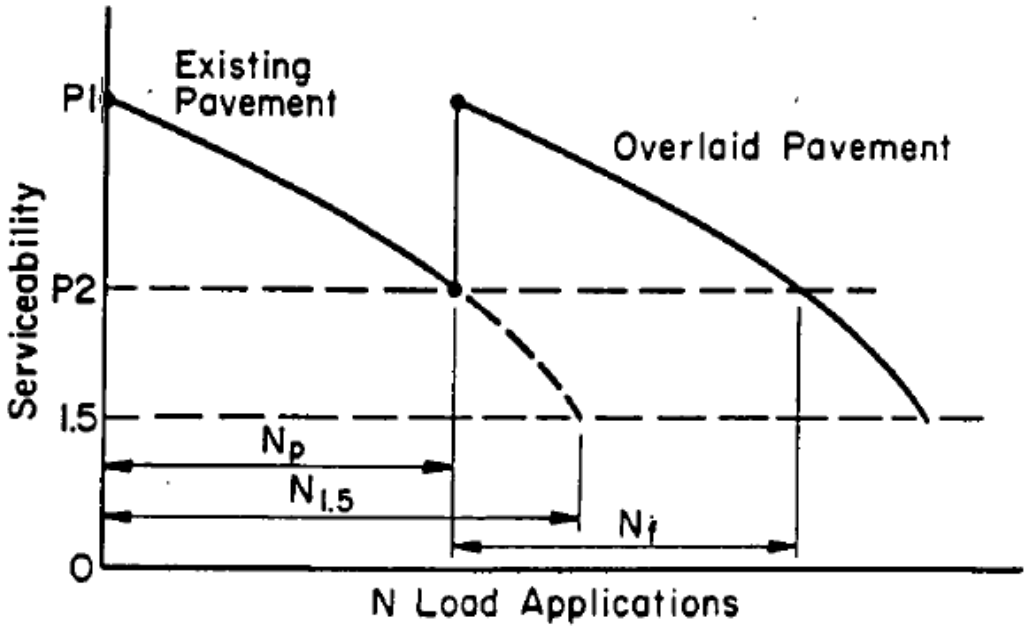

Figure 1-2 Serviceability loss over time with traffic (McGhee, 1994)

Eventually, the PSI drops towards a minimum acceptable level, the terminal serviceability (Pt), perhaps around 1.5 or 2.0. Allowing the road to deteriorate beyond this point is highly undesirable, as it approaches a state of functional failure and necessitates far more extensive and costly intervention. The goal of rehabilitation is typically to intervene before the pavement reaches its end of life and restore its serviceability. A common and often efficient method for doing this, assuming the underlying structure is sound, is applying an overlay.

Let us understand this in a more realistic setting. Consider you are an Area Engineer in 2015 working in TxDOT's Houston District, Harris County. A resident on Almeda Road complains about the condition of the road in front of their apartment, as shown in Figure 1-3.

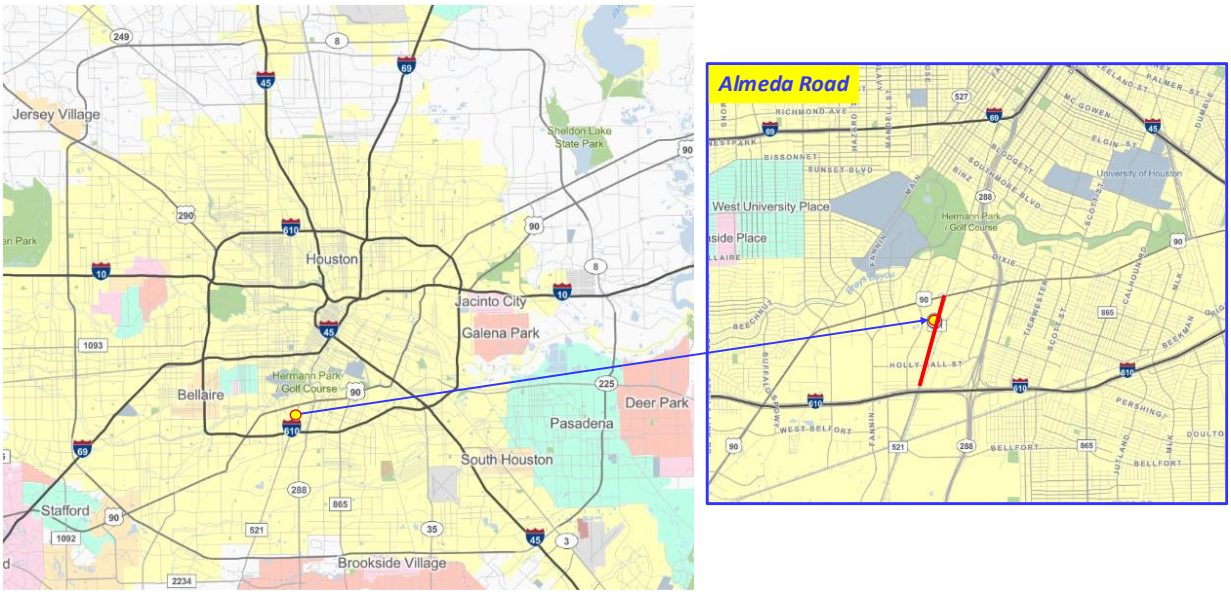

Figure 1-3 Almeda Road in Harris County, Houston

You investigate it, and you find it is noisy and provides a rough ride. Driving the road confirms the poor ride quality. Traffic data indicates a substantial Average Annual Daily Traffic (AADT) of 24,893, including a significant truck volume of 2,800 trucks per day. Checking the original plans, specifications and estimates (PS&E), as shown in Figure 1-4, you find a robust structure: 8-inch Continuously Reinforced Concrete Pavement (CRCP) over a 1-inch bond breaker, 6-inch Cement Stabilized Base (CSB), and 6-inch lime-treated subgrade.

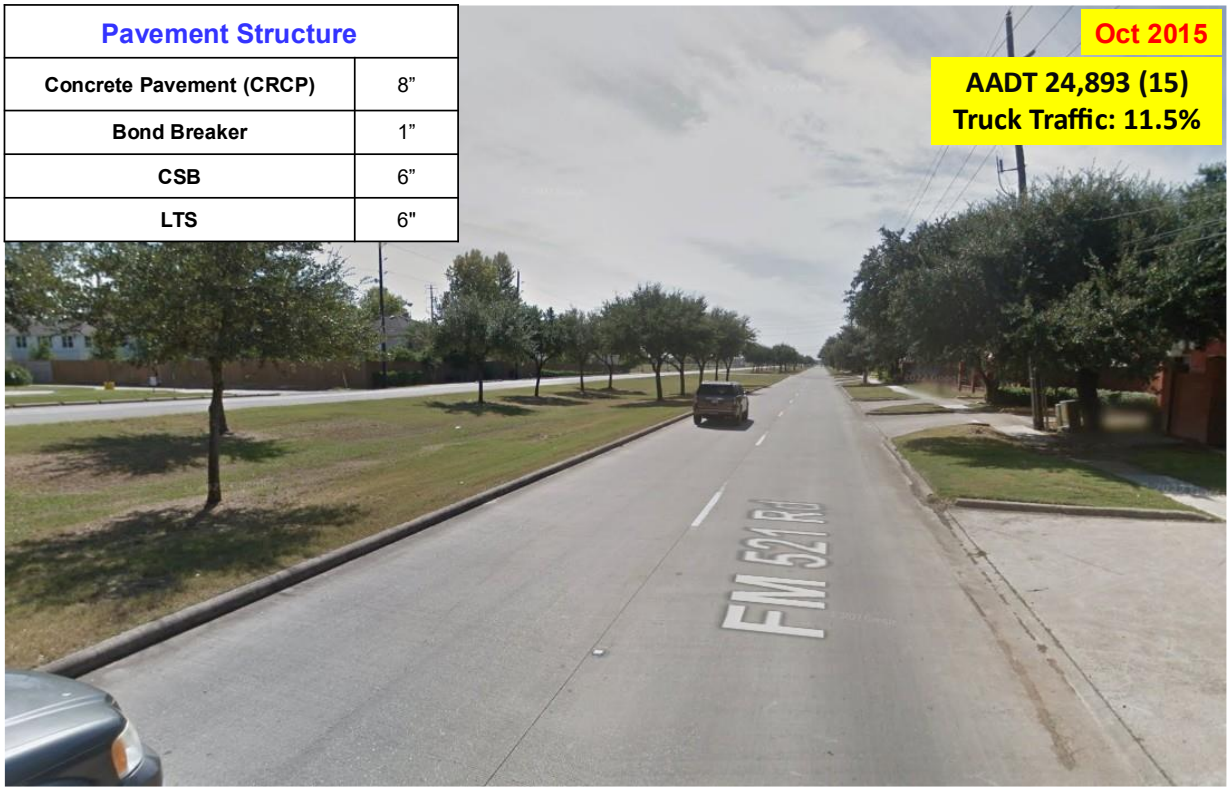

Figure 1-4 Investigated Almeda Road in 2015

To get objective data, you consult TxDOT’s Pavement Management Information System (PMIS). Figure 1-5 confirms the residents’ concerns: conditions and ride scores have indeed declined over time. In 2014, the ride score was 2.7 (indicating roughness, although drivable), and the condition score was approximately 70 (borderline, possibly showing minor cracking or weathering). It is clear that some action is needed.

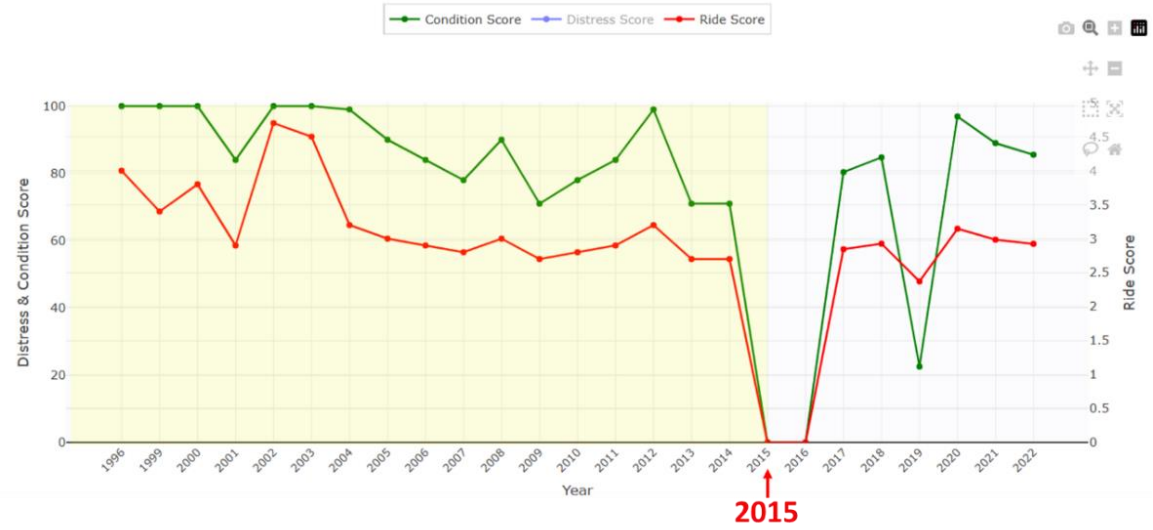

Figure 1-5 Condition Score and Ride Score of Almeda Road

Faced with this situation, the engineer evaluates potential actions:

a) Do Nothing: Unacceptable, as it fails to address the documented deficiencies and user complaints.
b) Reconstruct: A viable long-term solution, but it typically involves substantial capital expenditure, lengthy project timelines, and significant traffic disruptions, making it less suitable for immediate needs.
c) Rehabilitation: Offers a pathway to restore serviceability more rapidly and often at a lower initial cost than reconstruction.

Comparing all three options, it seems the most practical path forward is rehabilitation. But what kind? An overlay seems appropriate. The immediate choice is often between asphalt and concrete. The decision is fairly straightforward in this case as asphalt overlay is often the quicker, initially less disruptive option. Moreover, TxDOT frequently uses 2–4-inch asphalt overlays to address ride quality, friction, and noise issues. Figure 1-6 shows a 2-inch asphalt overlay placed on top of the existing 8-inch CRCP. Though this is a quick fix, there are some repercussions. Especially under heavy traffic, such as on Almeda Road, overlays typically do not significantly increase the structural capacity or fundamentally enhance the pavement's load-bearing ability. They address symptoms but might not be a long-term structural fix.

Figure 1-6 Asphalt overlay on existing pavement in Almeda Road

If we look at 2023 traffic data, the truck traffic has increased by 10% compared to 2015. This information suggests that the road will likely need attention again, potentially requiring a more substantial solution next time, adding to future backlogs. This highlights the core issue, which is fixing for now versus fixing for the long haul. This leads us to explore another viable option,

which is Concrete Overlays. However, before leveraging these options, let us consider another realistic scenario.

In this scenario, consider you are an Area Engineer working in TxDOT's Corpus Christi District, specifically in Live Oak County. As shown in Figure 1-7, this time, you receive a call from a local business owner in Three River City complaining about poor ride quality at two intersections.

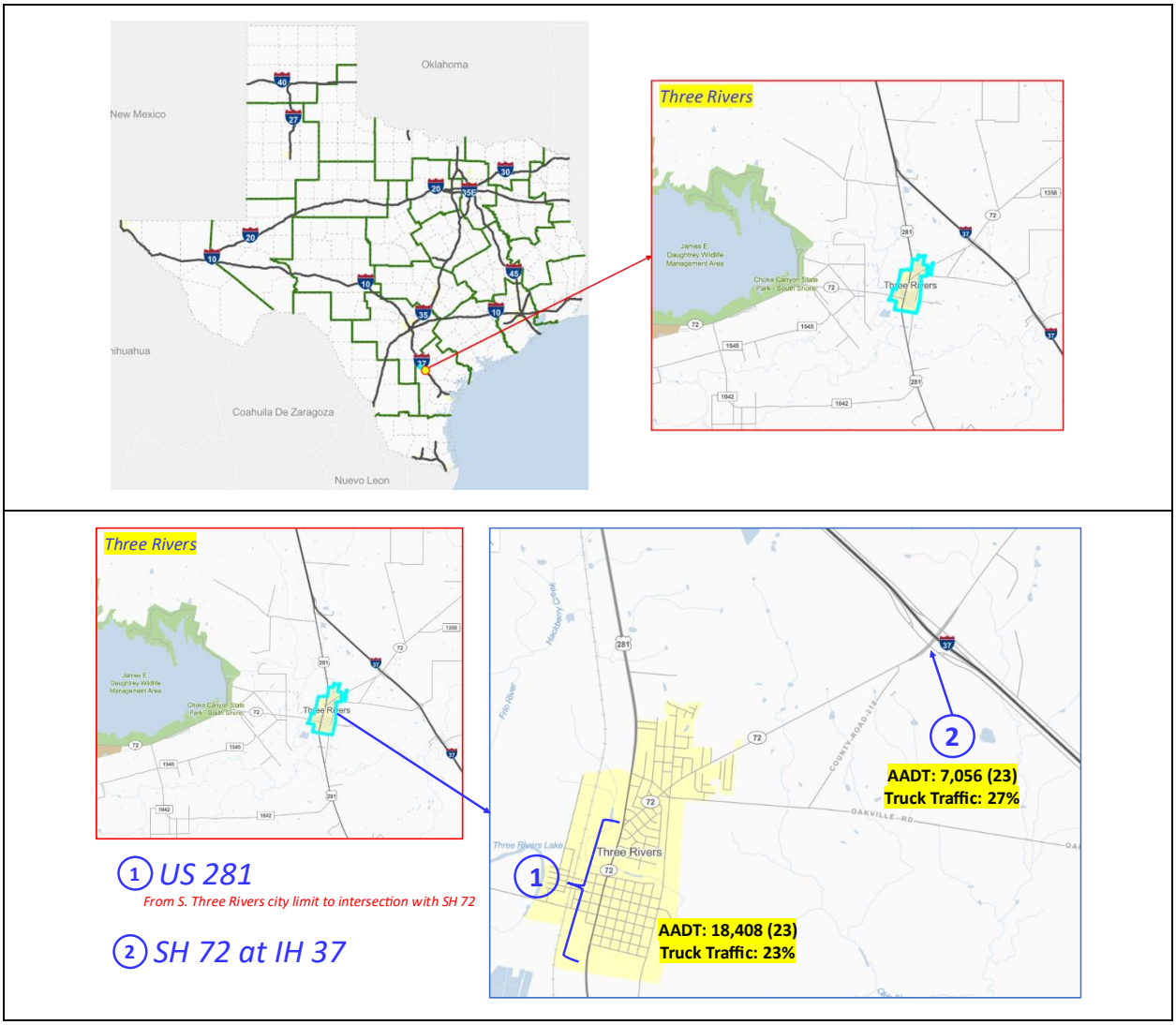

Figure 1-7 Two intersection in Three Rivers, Texas

Driving down the two intersections, you see quite a dire situation. Firstly, the US 281 Intersection has severe rutting in the outside lanes in both directions, as shown in Figure 1-8. Rut depths were measured up to 2-3 inches in some areas. The rutting appeared as uniform depressions, primarily in the wheel paths, without significant associated cracking (e.g., fatigue or longitudinal cracking). This pattern often suggests potential instability or plastic deformation

within the asphalt mixture itself, possibly related to the mix design properties or compaction, which can lead to deformation under channelized traffic loads.

Figure 1-8 Rutting observed in US 281 Intersection

Secondly, the SH 72 intersection at IH 37 also showed considerable pavement problems. Figure 1-9 shows that the distress, including bleeding, distortion (leading to roughness), and rutting, was concentrated near the IH 37 underpass. These issues were observed in both travel lanes in both directions, extending from the eastern limit of the last project (immediately east of IH 37) to where the divided roadway ends west of IH 37. The combination of bleeding and rutting, especially in relatively new pavement sections, often indicates issues with the asphalt mixture's volumetric properties. This could involve insufficient air voids (Va) or Voids in Mineral Aggregate (VMA) in the compacted mix or an excessive asphalt binder content. Such conditions can reduce the mix's resistance to shear stress under heavy traffic loads, leading to instability, deformation (rutting), and migration of free asphalt binder to the surface (bleeding).

Figure 1-9 Distress like bleeding, rutting and distortion observed in US71 in IH37

Selecting an effective rehabilitation strategy is required to address the issues identified at both intersections. Although an asphalt overlay represents an immediate option, its previously noted limitations in providing a durable, structurally significant solution make it less ideal for long-term performance goals. Therefore, achieving substantial structural enhancement and extended service life necessitates focusing on concrete overlays. Figure 1-10 shows the flowchart of the different categories of concrete overlays. It can be broadly divided into two classifications:

A. Whitetopping: Placement of a Portland Cement Concrete (PCC) layer over an existing AC pavement. This can be further classified based on the concrete type (e.g., Contraction Design Concrete Pavement - CPCD or CRCP). While design methods exist for CPCD whitetopping, dedicated methodologies, particularly for CRCP whitetopping are not

developed. A detailed discussion of the present design methodologies and their limitations will be presented in Chapter II. Relating this to our example of the intersection in Three Rivers, if we were to overlay the intersection with concrete, we would perform a Whitetopping.

***B. Concrete Overlay on Existing Concrete Pavement*:** This involves placing a new PCC layer over an existing PCC pavement. These are classified based on the interface condition:

- *Bonded Concrete Overlay (BCO):* Assumes a direct bond between the new overlay and the existing PCC, requiring careful surface preparation. Although CPCD Whitetopping exists, there are very few examples, such as US75 in Sherman and Loop 286 in Paris, of CRCP Whitetopping used as a bonded concrete overlay.
- *Unbonded Concrete Overlay (UBOL):* Incorporates an interlayer (commonly a thin AC layer, 1-4 inches) between the existing PCC and the new PCC overlay. This interlayer prevents bonding and allows the layers to act somewhat independently, mitigating the reflection of distress from the old pavement into the new overlay. A primary drawback is the increased pavement thickness, which can potentially cause issues with vertical clearances under structures such as bridges. However, UBOL is often an excellent structural solution.

Within the UBOL category, while design procedures for CPCD unbonded overlays are available, a significant gap exists: There is a lack of established, validated design methodologies specifically for CRCP unbonded overlays. This deficiency limits the ability of engineers to confidently specify and design a highly effective and durable rehabilitation solution for existing CRCP structures that experience significant traffic loading. A detailed discussion on this will be presented in chapter 2. Additionally, relating this to our example of Almeda Road, if we were to overlay a composite pavement of 2-inch asphalt and 8-inch CRCP with concrete, we would perform an Unbonded Concrete Overlay.

It is important to note that the above two scenarios presented in this section set the stage for this research.

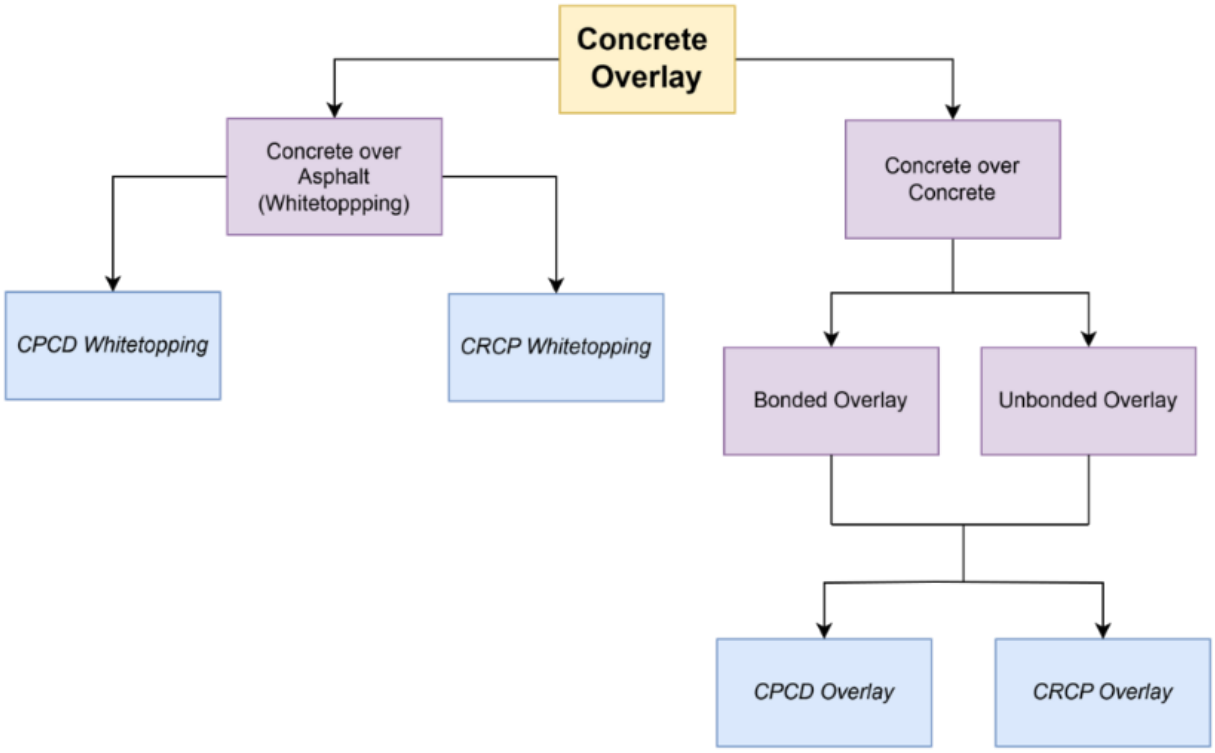

Figure 1-10 Flowchart with categories of Concrete Overlay

1.2 Problem Statement

Building on contextual scenarios, let us dive deeper into the technical limitation embedded in the existing pavement overlay design methodologies used by TxDOT. By revisiting the asphalt overlaid road rigid pavement in Almeda Road and intersections in Three Rivers, this section underscores the need for more adaptable and performance-driven design solutions.

To begin with, consider the case of the US 281 intersection in Three Rivers. A designer intending to implement a concrete overlay over the existing asphalt pavement would typically consult section 8.2 of the TxDOT Pavement Manual. For thin whitetopping (TWT) designs, the manual references guidance derived from the American Concrete Pavement Association (ACPA) design tables, exemplified in Table 1-1.

Table 1-1 Whitetopping thickness design used by TxDOT

Trucks per Day per Lane	Design Life (yr.)					
	5	6	7	8	9	10
≤ 200	4	4	4	4	4	4
250	4	4	4	4	5	5
300	4	4	4	5	5	5
350	4	4	5	5	5	5
400	4	5	5	5	5	5
450	5	5	5	5	5	6
500	5	5	5	5	6	6
600	5	5	5	6	6	6
700	5	5	6	6	7	7
800	6	6	6	7	7	7
900	6	6	6	7	7	n/a
1000	6	6	7	7	n/a	n/a

Applying these values to current conditions reveals an inherent disconnect. The 2023 AADT at US 281 exceeds 18,400 vehicles per day, of which approximately 23% are trucks (Figure 1-7). This translates to over 1,050 trucks per lane per day, well beyond the upper limit of the design table. Moreover, the methodology supports a maximum design life of 10 years, which is increasingly insufficient given contemporary infrastructure planning goals that often target 20- to 30-year service lives. This presents two major limitations. First, the method is strictly tailored to CPCD whitetopping applications and lacks applicability to CRCP overlays. Second, the truck traffic ceiling and capped design life indicate that the approach is not scalable to meet the demands of modern urban freight corridors. For critical intersections experiencing substantial commercial vehicle volumes and requiring long-term durability, the existing design approach is fundamentally constrained and outdated. This reinforces the need for more robust and adaptable methodologies.

Directing to the scenario at Almeda Road, where an existing CRCP was previously overlaid with asphalt, the next logical rehabilitation step might involve a concrete overlay over this composite section. According to Section 7.3 of TxDOT Pavement Manual, designers are advised to utilize the AASHTO 1993 method in such instances. However, the application of this methodology introduces a separate class of complications that merits critical examination. As illustrated in Figure 1-11, the AASHTO 1993 approach requires the designer to calculate the required slab thickness of the overlay, denoted as D_{ol} . This is done by first estimating the effective thickness of the existing pavement D_{eff}, and then determining the slab thickness D_f needed to carry future traffic assuming a new pavement structure.

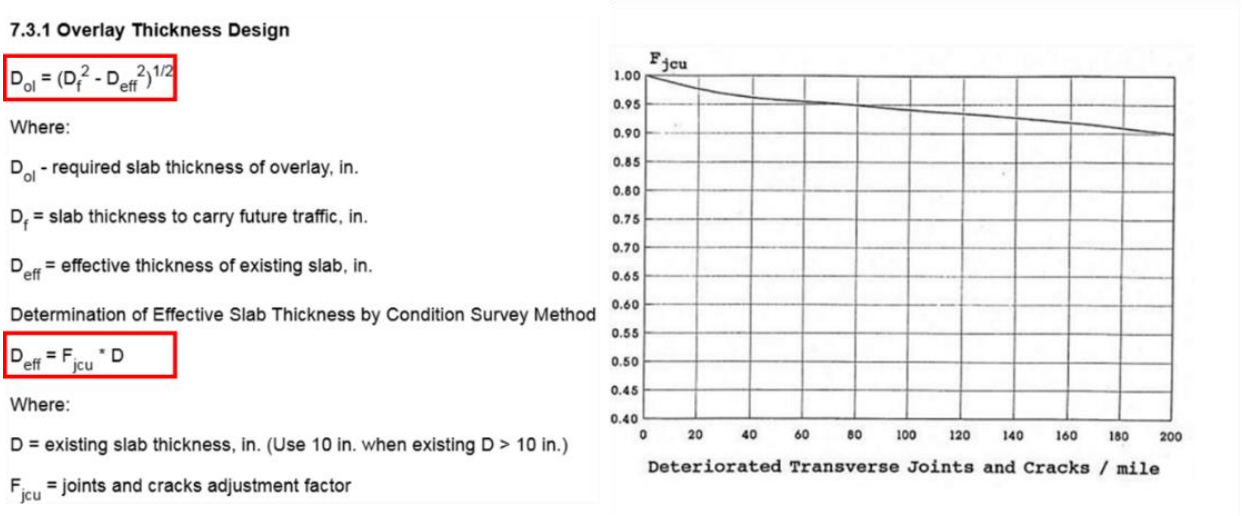

Figure 1-11 AASHTO 1993 method for Unbonded Overlay Thickness Design

The challenge arises in computing D_{eff}. This involves applying joint and crack adjustment factor F_{jcu} to the actual slab thickness D. The factor F_{jcu} is derived from a graph that relates the number of deteriorated transverse joints and cracks per mile to an adjustment coefficient. However, the origin and empirical foundation of this graph remain poorly documented. Literature offers scant explanation regarding its derivation or validation, leaving practitioners to apply it with limited contextual understanding. In practice, the designer is instructed to conduct a field survey and count the number of deteriorated transverse joints and cracks per mile. While this approach may seem reasonable for CPCD systems, it introduces multiple ambiguities when applied to CRCP. In CRCP, transverse cracks are intentionally engineered and are inherent to the system's performance. Hence, quantifying them as "deteriorated" without appropriate context leads to mischaracterization. Furthermore, the methodology does not account for other prevalent forms of distress that may be more representative of structural degradation. Even if the framework were hypothetically acceptable, it lacks guidance for scenarios where the count exceeds 200 cracks per mile, which is not uncommon in CRCP sections.

This absence of clarity raises both theoretical and practical concerns. The lack of traceable provenance for the adjustment factor graph challenges its scientific credibility, while its limited applicability undermines its relevance for Texas, a state that maintains the largest inventory of CRCP pavements. As these assets age and require rehabilitation, reliance on a method that fails to accommodate the characteristics of CRCP becomes increasingly untenable. Moreover, another fundamental shortcoming of the AASHTO 1993 method lies in the calculation of the slab thickness D_f needed to support future traffic. It is important to recognize that the AASHTO 1993 guide is an evolution of the original AASHO Road Test, a landmark empirical study conducted in the 1950s. While its historical significance is undeniable, the method's empirical underpinnings and narrow inference space limit its applicability to modern pavement structures and loading conditions. These constraints are further explored in subsequent chapters.

Consequently, while the AASHTO 1993 method remains institutionalized within the TxDOT Pavement Manual, its usefulness for modern CRCP overlay design is highly constrained. This highlights the urgent need for methodological advancements that integrate mechanistic principles, accommodate realistic distress characterization, and leverage modern field data collection tools objectives that form the foundation of this research. However, the question may arise, "*How should we even begin the quest for solving this design issue?*" This is exactly what the next section will discuss.

1.3 Research Approach

A research framework was developed to solve the present design problem, employing two primary approaches to identify the solution. The first was an evidence-based approach. Here, we traced back the detailed field evaluations conducted in the TxDOT Rigid Pavement Database (RPDB) project to identify the mechanisms of structural failures, specifically punchouts, in CRCP. These findings indicated that deterioration in the slab support was the primary cause for the punchouts. For example, Figure 1-12 illustrates a recent punchout distress observed in IH 45 in the Dallas District. This 8-inch CRCP was completed in 1975, making the pavement 46 years old when the picture was taken. The depression in the asphalt shoulder is a clear indicator of repeated slab deflections at the slab edge. Figure 1-13 provides another example of CRCP structural failure, this one on an 8-inch CRCP on US 287 in the Wichita Falls District, built in the early 1970s, where larger slab deflections resulted in fatigue failure of the concrete.

The second approach focused on understanding the fundamental principles of rigid pavement performance. This evidence-based approach aligns quite well with the insights from the AASHO Road Test, which complement our second approach. The failure mechanism identified in both the IH 45, and US 287 projects is consistent with the findings at the AASHO Road Test, where it was observed that "All failures in rigid pavements were preceded by pumping of material from beneath the concrete slabs." The reference further states, "At the end of the test traffic, data indicated that pumping increased as load increased (the greater the load, the more the pumping, given equal slab thickness) and decreased as slab thickness increased (the thicker the slab, the lesser the pumping, given equal load)."

Even though CRCP was not included in the AASHO Road Test, this finding has an important implication: improvements in rigid pavement performance will be achieved by limiting slab deflections. Thus, this very principle forms the basis of what we call the 'deflection method.' This is the concept we will examine, explore, dissect, connect, and use in this research report to develop a deflection-based design method.

Figure 1-12 Pumping and edge punchout in IH 45

Figure 1-13 Pumping and Punchout in US 287

Figure 1-14 presents the proposed research framework for developing a deflection-based CRCP overlay design method. This framework is organized into five interrelated phases, each building upon the insights and data from the previous stage.

Phase 1: Comprehensive Data Collection

The initial phase focuses on gathering essential data through field surveys and testing. Deflection data was collected from both ongoing new CRCP construction projects to facilitate Phase 2 and evaluations of existing composite pavements to facilitate Phase 4. This information includes deflections measured on existing bases such as asphalt-stabilized base (ASB) and those observed on newly placed CRCP slabs of varying thicknesses. The objective was to generate a robust dataset that forms the foundation for all subsequent analyses.

Phase 2: Data Analysis and Correlation Development

Using the data collected in Phase 1, this phase aimed to establish statistically sound correlations between subbase deflections and those on CRCP overlays. Advanced statistical methods were applied to ensure the reliability and accuracy of these relationships. Additionally, mechanistic modeling using ANSYS was conducted to validate field results, providing theoretical support for the observed behavior, refining correlations and filling the gaps in-between.

Phase 3: Systematic Evaluation Framework for Existing Pavement

Concurrent with Phase 4, this phase focuses on using field data from Phase 1 to create a structured process for evaluating existing pavements as potential base support. It defines criteria for reusability and integrates NDT (Non-Destructive Testing) data to facilitate pavement sectioning, distress identification, and selection of appropriate rehabilitation strategies.

Phase 3: Development of the Deflection-Based Design Procedure

Building on the correlations developed in Phase 2, this phase formulates a new design methodology for determining required CRCP slab thicknesses based on deflection data. The design procedure incorporated very crucial factors such as Equivalent Single Axle Loads (ESALs) and a statewide deflection curve. Ultimately, step-by-step overlay design process is presented tailored for use in Texas conditions in this research report.

Phase 5: Deliverables and Implementation

Phases 3 and 4 converge on producing final deliverables. These include a comprehensive research report, a user-friendly design tool, and detailed implementation guidelines. Recommendations will be provided to TxDOT to support the seamless adoption of this new deflection-based design method into their statewide pavement rehabilitation practices.

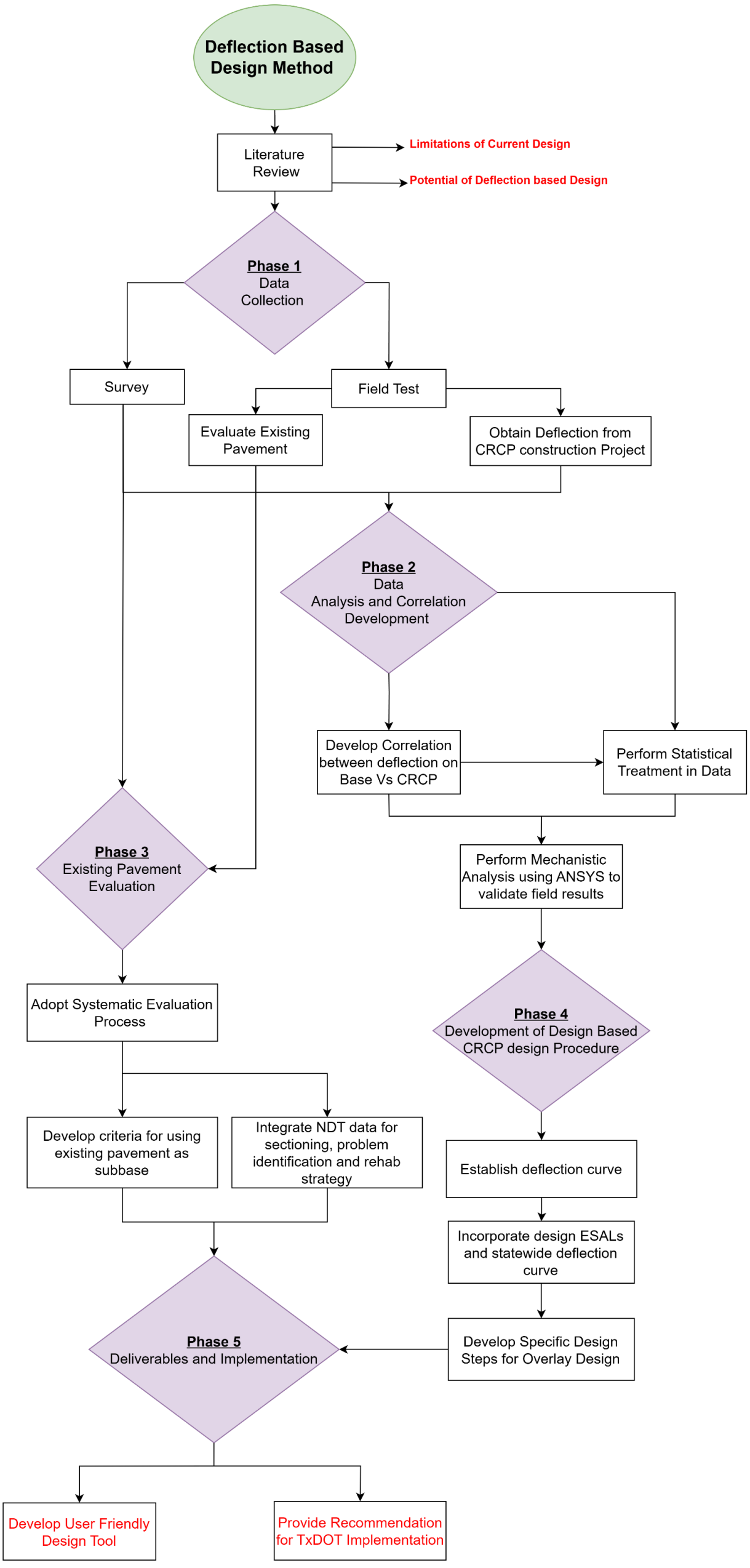

Figure 1-14 Deflection based Design method research Framework

1.4 Objectives of the Study

The objective of this study stems from the void that's evident in current design methods for Whitetopping and Unbonded Overlay. The primary goal of this research is to propose developing and validating a practical, deflection-based design methodology for CRCP Whitetopping and Unbonded Concrete Overlays.

1.5 Scope and Limitations

The scope of this research is centered on improving the design methodologies for concrete overlays, with a specific emphasis on CRCP systems used in roadway rehabilitation. The study encompasses the following key areas:

- Examining the historical evolution of rigid pavement and its rehabilitation practices.
- Critically evaluating existing design methods and international approaches for concrete overlays (Whitetopping and UBOL), identifying their theoretical bases, key assumptions, and limitations, especially concerning CRCP applications.
- Characterizing current nationwide practices, common challenges, and desired improvements in the evaluation, design, and performance of CRCP overlays via a targeted survey of state transportation agencies and industry professionals.
- Establishing systematic procedures and criteria for evaluating existing pavement conditions using non-destructive testing (FWD, GPR) and targeted destructive testing (coring, DCP).
- Developing a framework (e.g., decision matrix or flowchart) for utilizing pavement evaluation data to determine project suitability and derive essential inputs for a deflection-based overlay design methodology.
- Developing a mechanistic-empirical design procedure for determining CRCP Overlay thickness, leveraging field deflection data and validated Finite Element (FE) modeling.
- Generating a practical design aid based on the developed methodology.
- Analyzing factors influencing CRCP reinforcement requirements at intersections and limitations of existing models.
- Proposing refined reinforcement design strategies, potentially including optimized steel configurations and saw-cutting recommendations, tailored for intersection-specific demands.
- Evaluating and demonstrating the applicability and accuracy of the proposed deflection-based slab thickness design through case studies.
- Finally, formulate recommendations for integrating the developed CRCP overlay design methodologies into practice, potentially including proposed modifications to existing standards (e.g., TxDOT) and outlining elements for a practical design toolkit and knowledge transfer.

Limitations: The study acknowledges limitations inherent in pavement engineering research, including the historical lack of CRCP in the AASHO Road Test, the empirical nature and known

deficiencies of some existing design methods (especially for Texas conditions), variability in field conditions and construction practices affecting data, the complexity of accurately modeling phenomena like PCC-asphalt bond, and the reliance on ongoing field data collection for final calibration. FEM analysis also involves necessary assumptions and approximations. All these limitations would be discussed in detail in their respective chapters and sections.

1.6 Report Organization

This research report is a collaborative effort undertaken as part of Project 0-7148, funded through a Cooperative Research and Implementation Agreement (CRIA) by the Texas Department of Transportation (TxDOT) and the Federal Highway Administration (FHWA). The research was primarily performed by Texas Tech University (TTU) as the lead agency, in collaboration with the Texas A&M Transportation Institute (TTI).

We express our sincere gratitude to the Project Monitoring Committee (PMC) members: Enad Mahmoud, Andy Naranjo, Ruben Carrasco, Rachel Cano, Soojun Ha, Pangil Choi, and Lori Jaramillo and particularly to Project Manager Danny Sourapath from the Research and Technology Implementation (RTI) Division at TxDOT for their invaluable guidance, insightful feedback, and continuous support throughout the duration of the project. The research team comprised Moon Won (Principal Investigator, TTU), Darlene Goehl (Research Engineer, TTI), Tito Nyamuhokya (Assistant Research Scientist, TTI), Christopher Jabonero (Postdoctoral Research Associate, TTU), and Niwesh Koirala (Graduate Research Assistant, TTU).

It comprises seven chapters, each addressing distinct yet interrelated aspects of CRCP overlays.

- **Chapter 1**: introduces the reader to the underlying issues confronting pavement rehabilitation through the lens of real-world scenarios, including case studies from Houston and Corpus Christi Districts in Texas. This chapter establishes the rationale for exploring more durable and sustainable concrete overlay solutions, particularly CRCP and outlines the overall objectives, scope, and limitations of the study.
- **Chapter 2**: Literature Review provides a thorough historical overview and critical examination of pavement rehabilitation practices. It explores existing concrete overlay techniques including Whitetopping and Unbonded Overlays and surveys established design methodologies from AASHTO, MEPDG, ACPA, BCOA-ME, various state Departments of Transportation (DOTs), and international standards.
- **Chapter 3**: Survey presents findings from a comprehensive nationwide survey directed toward state transportation agencies. This chapter characterizes current practices, identifies prevalent challenges, and highlights specific needs related to the evaluation and design of CRCP overlays within the United States.
- **Chapter 4**: Pavement Evaluation Procedures elaborates on the development and practical application of comprehensive protocols to assess existing pavement conditions. It combines both non-destructive methods such as Falling Weight Deflectometer (FWD) and Ground Penetrating Radar (GPR), along with destructive techniques including coring

and Dynamic Cone Penetrometer (DCP) tests. This chapter primarily focuses on detailed case study analyses of selected pavement sites in Texas.

- **Chapter 5:** Deflection-Based Thickness Design describes systematic collection and analysis of deflection data, particularly employing FWD measurements on base layers, newly constructed CRCP, and existing asphalt-overlaid rigid pavements. Further, mechanistic analyses through Finite Element Modeling (FEM) using ANSYS software support empirical findings, culminating in the development of an innovative deflection-based thickness design protocol.
- **Chapter 6:** Reinforcement Details investigates advanced reinforcement strategies specifically tailored for CRCP overlays, addressing the unique requirements at intersections characterized by shorter slab lengths and potential steel congestion. Alternative reinforcement designs, including cost-benefit analyses of saw cutting methods, are explored in detail.
- **Chapter 7:** Conclusion succinctly synthesizes the key contributions, acknowledges the study's limitations and inherent assumptions, and proposes future research directions. This chapter concludes the report with reflective and forward-looking insights.

Through this structured approach, the report aims to provide comprehensive guidance for practitioners, policymakers, and researchers, thus contributing significantly to the field of pavement engineering and infrastructure development.

CHAPTER 2
LITERATURE REVIEW

In chapter 1, we examined the critical issues in the existing design methods for Whitetopping and unbonded concrete overlays in Texas. Now let's transition into a more structured assessment of rigid pavement design in general. Having established the central problem, we will first trace the chronological development of rigid pavement technologies and design philosophies. Next, we will conduct a comprehensive review of existing national and international design practices, positioning us to critically assess their theoretical assumptions, field applications, and limitations. This will be followed by a reflection of Whitetopping in Texas, highlighting emerging concerns, particularly with current Concrete Pavement Contraction Design (CPCD) Whitetopping applications, and how these may pose significant challenges in the future. The chapter concludes with a synthesis of findings that sets the stage for Chapter 3, which presents results from a nationwide survey aimed at characterizing current practices and identifying practitioner needs in CRCP overlay design.

2.1 Historical Perspective on Rigid Pavement

The origin of concrete pavement in the United States dates back to 1891 and is credited to George W. Bartholomew. As shown in figure 2-1, this pioneering work took place in Bellefontaine, Ohio, between 1891 and 1893. Bartholomew successfully persuaded city officials to test an 8-foot-wide strip of concrete on Main Street. By 1893, an entire street block of Court Avenue with a 6-inch-thick concrete pavement was paved with the intention of withstanding horse traffic. Interestingly, the cost of placing concrete at the time was $2.25 per square yard which is roughly equivalent to $75.85 in today's cost accounting for the inflation over 133-year period. Remarkably, this pavement is still in use today and is celebrated as the "Oldest Concrete Street in America." Since then, concrete pavement evolved significantly throughout the 20th century as horse traffic was replaced by automobiles, and the advent of industrialization demanded more durable roadways. The advancement of concrete pavement design over the period can be categorized into four distinct timeframes.

Figure 2-1 First concrete street in America built in 1891 at Bellefontaine, Ohio

Early 1900s-1940s: Initial Developments

In the early 1900s, concrete pavements were designed without reinforcement, relying solely on slab thickness to resist cracking and deterioration. This approach was primarily based on field engineers' and contractor's experience rather than systematic research. As concrete pavements became more common, it became clear that they suffered from cracking due to shrinkage and temperature changes. This led to the introduction of CPCD, which incorporated dowel bars to allow for controlled movement, reducing cracking due to temperature fluctuations.

Late 1940s-1950s: Introduction of Reinforced Concrete

As the understanding of concrete behavior advanced, engineers began experimenting with reinforcement, primarily using steel bars, to control crack widths and enhance the pavement's load-carrying capacity. This led to the development of Jointed Reinforced Concrete Pavement (JRCP). While JRCP improved crack control, the joints remained points of weakness, often leading to deterioration. Recognizing these limitations, engineers introduced Continuously Reinforced Concrete Pavement (CRCP) in the late 1940s and early 1950s. CRCP utilized continuous steel reinforcement, eliminating joints and allowing fine, closely spaced cracks to form naturally without compromising the pavement's structural integrity.

Late 1950s-1960s: AASHO Road Test and Design Evolution

The introduction of CRCP presented a new challenge: determining the appropriate slab thickness to withstand traffic loads. Until then, concrete pavement design had largely been based on experience, lacking a logical engineering framework for CRCP. The AASHO Road Test, conducted in the late 1950s and early 1960s, provided crucial data that influenced CRCP thickness design methods, even though the test did not include any CRCP sections. This marked a pivotal moment in the evolution of CRCP design, as engineers adapted inputs from CPCD design to develop CRCP thickness guidelines. However, this approach introduced several conservative assumptions that have persisted over time.

1970s-Present: Modern Design Approaches

The 1972 AASHTO Interim Guide for Design of Pavement Structures, which forms the fourth timeframe, incorporated these conservative assumptions in CRCP slab thickness design:

- ***Load Transfer Coefficient:*** CRCP lacks joints like CPCD, making the use of load transfer coefficients from CPCD design overly conservative.
- ***Distress Mechanisms:*** In CRCP, transverse cracking is normal and does not degrade serviceability as it does in CPCD.
- ***Performance Exceeding Design Life:*** The inherent conservatism in design has often resulted in CRCP exceeding its intended design life.

Despite advancements in materials science, pavement analysis techniques, and computational tools like the Finite Element Method (FEM), modern CRCP design still relies on these conservative principles.

2.2 Review of Existing Thickness Design Procedure

There are numerous design methods and tools currently available for rigid pavement thickness design procedures. As a result, understanding these various procedures remains a significant challenge and, at times, confusing. Nevertheless, if one were to structure them within a single overarching framework, Figure 2-2 attempts to provide a quick and coherent overview for the reader.

Conceivably, the early road tests form the backbone of today's pavement thickness design practices. This becomes apparent when we trace the lineage of pavement design back to 1909, when the first controlled pavement test was conducted in Detroit using a rudimentary horse-and-wagon simulator. This experimental effort culminated in the construction of the first mile of rural concrete pavement on Woodward Avenue in Wayne County, Michigan.

Building upon this, between 1912 and 1923, the Bates Test Road was conducted by the State of Illinois. Using WWI-era trucks with a range of wheel loads, this ambitious testing program evaluated various pavement materials and thicknesses. The outcomes of this test were pivotal: they revealed optimal slab thicknesses and underscored the critical importance of longitudinal center joints to mitigate cracking. Concurrently, in 1921–1922, a separate test road was constructed in Pittsburgh, California, to compare the performance of reinforced versus plain concrete pavements. Although the results of that study were inconclusive, it added another valuable layer of insight.

Synthesizing the outcomes of these tests, early stress-based design equations emerged most notably by Goldbeck, Older, and Sheets. These formulations marked the birth of mechanistic-empirical thickness design procedures, a blend of engineering mechanics and empirical calibration from field data that continues to define modern pavement design.

Around this same transformative period, rigid pavement engineering experienced a major theoretical breakthrough from the work of Professor H.M. Westergaard. Thus, it would be uncanny not to pay homage to him, the pioneer whose pioneering equations on stress and deflection triggered a profound ripple effect in the field. Developed in the 1920s, Westergaard's analytical models were the first widely accepted methods for evaluating concrete pavement behavior under wheel loads and thermal gradients. He introduced now, fundamental concepts such as the radius of relative stiffness, capturing the interplay between slab rigidity and subgrade support, and pinpointed the critical stress locations (interior, edge, and corner), which remain central to pavement evaluations.

Westergaard's work laid the theoretical foundation for understanding how concrete slabs respond to structural loading and environmental variations. This foundational understanding was not only essential for interpreting field performance but was also instrumental in shaping the design philosophies that followed. His models were subsequently refined by engineers like Pickett and Spangler, whose work brought Westergaard's theory into closer alignment with empirical data from studies such as the Bureau of Public Roads' test in Arlington, Virginia.

Figure 2-2, therefore, is not just a schematic summary, it is a conceptual bridge, tracing the evolution of knowledge from rudimentary experiments to refined theoretical formulations.

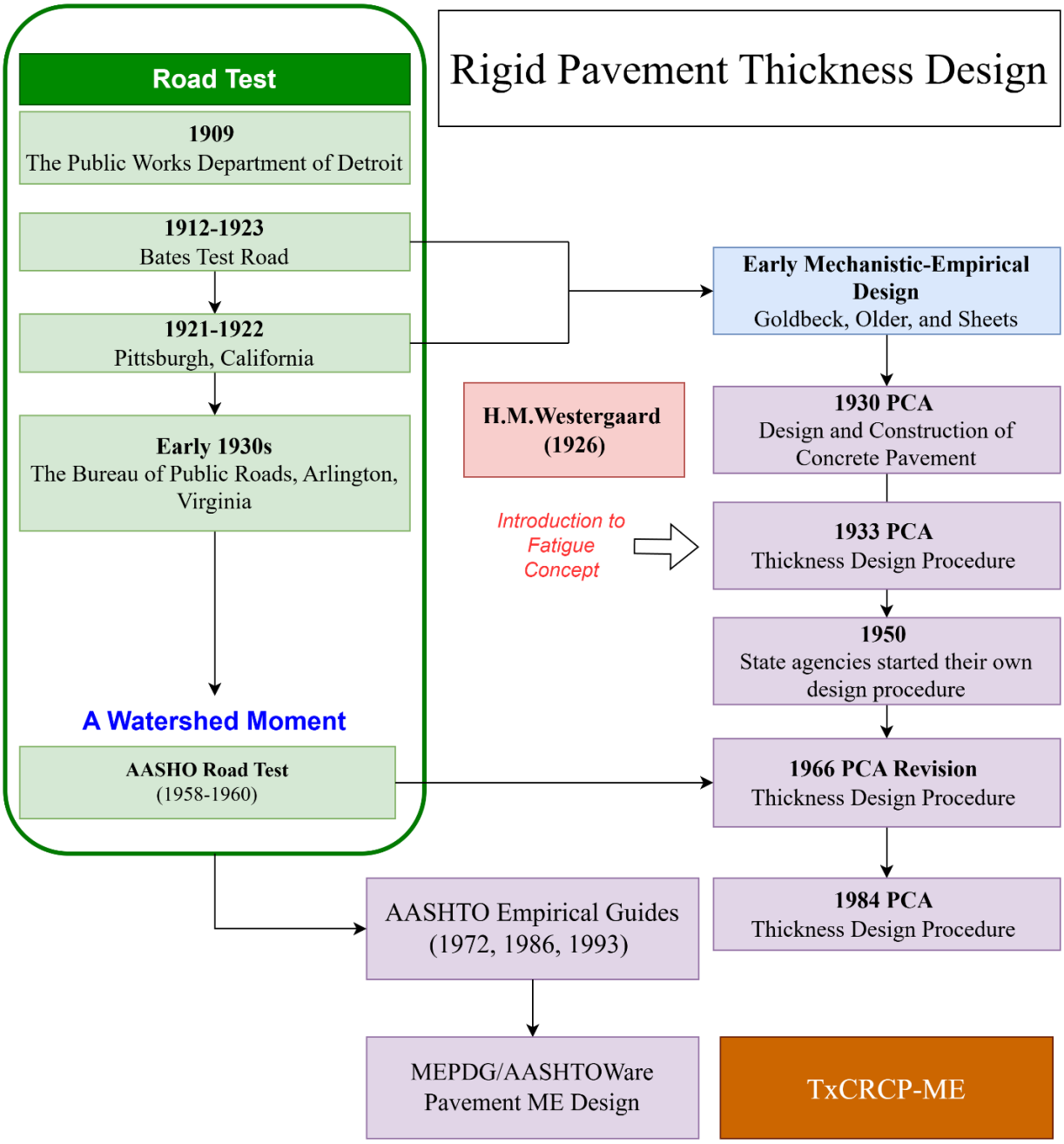

Figure 2-2 Rigid pavement thickness design overview

The translation of theory into practice began taking a more structured form when, in 1930 and later in 1933, the Portland Cement Association (PCA) introduced its design procedure using Older's equation. This was a landmark moment: pavement thickness could now be directly related to induced stress, and the concept of fatigue in concrete was formally recognized. The designs incorporated uniform thickness as well as thickened edge sections to manage increased

edge stresses, an approach that remained prevalent until the 1950s. By the mid-20th century, state agencies had begun to develop their own design methods, bringing greater regional nuance and adaptation to pavement design. This wave of innovation culminated in the AASHO Road Test (1958–1960) in Illinois, a landmark $26 million study that would profoundly shape pavement engineering. The study introduced the serviceability index, a measure of pavement performance from a user's perspective, and the concept of Equivalent Single Axle Loads (ESALs), which simplified mixed traffic load analysis.

The findings of the AASHO Road Test led to a significant revision of the PCA design method in 1966 and again in 1984, the latter of which incorporated finite element analysis to evaluate not only stresses but also pavement distress mechanisms such as erosion, pumping, and joint faulting. This comprehensive modeling approach represented a major leap toward mechanistic-empirical design rooted in realistic field behavior.

Having established this rich historical and theoretical context, we now aim to examine three cornerstone design frameworks that continue to influence current practice: the AASHO Road Test methodology, the AASHTO design guide, and the Mechanistic-Empirical Pavement Design Guide (MEPDG). Exploring each in detail will help us understand how today's complex pavement design practices are built on the layered legacy of both experimental evidence and analytical rigor.

2.2.1 AASHO Road Test & Early Version of Design Equations

Building upon the theoretical foundations established by Westergaard, the need for comprehensive empirical validation and data became paramount. The AASHO (American Association of State Highway Officials) Road Test emerged as a landmark endeavor in direct response to this need. Perhaps it would not be an understatement to recognize AASHO Road Test as a watershed moment in the history of concrete pavement. It was a two-year period of research work which was carried out near Ottawa, Illinois along the alignment of Interstate Route 80. Figure 2-3 shows the layout of the road test. It consisted of 6 loops numbered 1 to 6. The tangent length of loop 1 and 2 was 2,000-ft and 4,400 ft, respectively. The tangent length of 3 to 6 was 6,800-ft. As shown in Figure 2-4 the centerlines divided the pavements into inner and outer lanes, called Lane 1 and Lane 2, respectively. Different axle loadings were applied, with heavier loading at Lane 2.

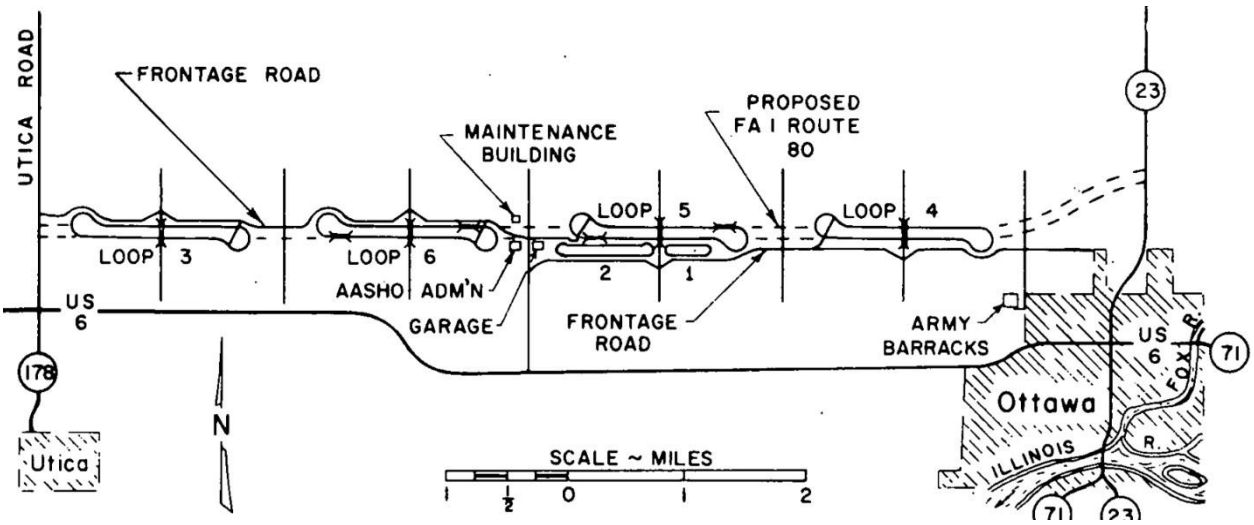

Figure 2-3 Layout of AASHO Road Test (AASHO, 1962)

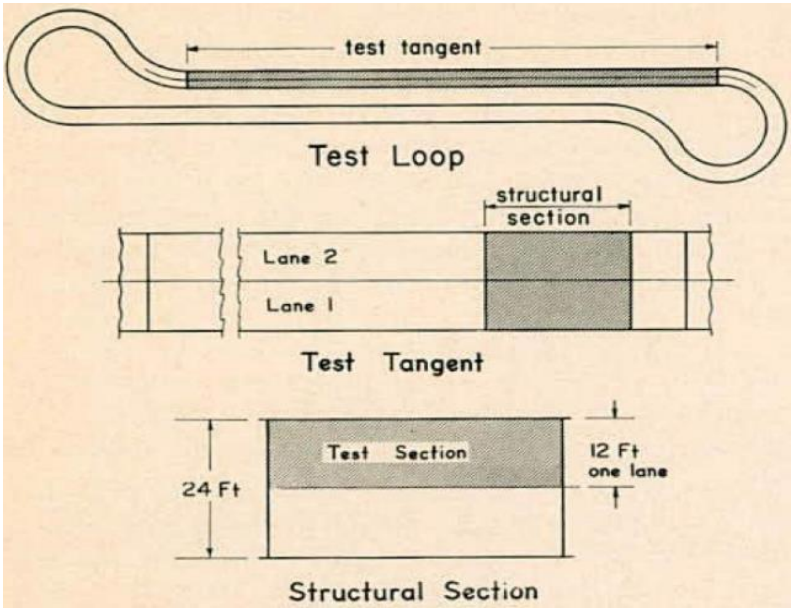

Figure 2-4 Overview of individual test loop (AASHO, 1962)

The construction of these loops started in August 1956. The first test traffic was applied in October 1958. The Road Test included experiments on:

- Flexible pavement with asphalt concrete surfacing
- Rigid pavement with concrete surfacing
- Short-span bridges with steel beams
- Short-span bridges with concrete beams

These lanes were tested under different ranges of loading. After 2 years of loading, the total loading amounted to 1,114,000 axle load applications. The Road Test was completed on November 30, 1960.

The primary objective of this Road Test was to gather answers to relevant questions that are related to pavement design, which included the traffic volume that affects pavement performance, the number of heavy axles load that would affect life expectancy and economic viability of roads. This science-based investigation established the relationship among various factors needed for the design of highway pavements, which are important for highway administrators. Other factors investigated were pavement structure, traffic load magnitude and load frequency. The application of traffic loads in the test loops accelerated the failure of the pavement, thereby providing valuable information on the performance of the pavements.

There were few general assumptions that were accounted in the test loops. One of them is that the method of pavement performance is based on empirical techniques. In addition, the test could not fully incorporate all the factors affecting pavement behavior and performance since this was a controlled experiment, i.e., with one environmental condition, a given soil condition, so forth.

Despite the said limitations, the findings came out to be remarkable.

- First, it was noted that the pavement responses and performance do change with the specific change in axle loads and number of load repetitions.
- Second, it was identified that the pavement performance, which was measured in terms of serviceability to traveling public with time or load, decreased over time. So, when a pre-determined level of terminal serviceability was reached, then the road needed major maintenance or reconstruction.
- Third, all the failures in the rigid pavement were preceded by pumping of material from beneath the concrete slabs. This finding is quite significant because the failures observed at the Road Test were not due to typical fatigue failure of concrete with the assumption of uniform slab support. This finding, even though it was made more than 60 years ago, is still valid in today's rigid pavement in Texas. Also, all these pumping occurred along the pavement edge. This shows that larger deflections in pavement edge contributed to pumping, which has a significant implication on pavement design. In short, limiting slab deflections by selecting an appropriate slab thickness should be an essential consideration in slab thickness design.
- Fourth, if the quality of subgrade is improved, it would increase the life of pavements appreciably. This finding also supports what's been observed in rigid pavement in Texas. In Texas, poor performance of rigid pavements in 1950s and 1960s was primarily due to poor slab support, along with pumping, with resulting increased slab deflections.
- Fifth, faulting occurred at cracks only, but never at the doweled transverse joints. This finding is also ascertained in Texas. Even when the slab support is quite poor and distresses such as slab cracking developed, faulting was not observed, since dowels were used. On the other hand, severe faulting was observed where dowels were not used, and slab support was poor.

- Sixth, future performance of rigid pavement was accurately predicted by slab deflections or concrete strains. This finding validates the efforts made by TxDOT and researchers for measuring slab deflections with Falling Weight Deflectometer (FWD) for rigid pavement condition evaluations.

Based on the analysis of the data collected, a slab thickness design equation was developed as shown in Equation 2-1. Later this very same equation was modified in AASHTO which will be fully discussed in subsequent sections.

$$Log(ESAL) = 7.35 * Log(D+1) - 0.06 + \left[\frac{Log\left[\frac{4.5 - p_t}{4.5 - 1.5}\right]}{1 + \frac{1.624 * 10^7}{(D+1)^{8.46}}}\right] \quad (Equation\ 2-1)$$

It is to be noted that the concept and computation of ESAL (Equivalent Single Axle Load) and pavement performance were from this equation. As discussed earlier, all the terms used in this equation were derived from millions of load repetitions, performance surveys, and regression analysis. Though they are empirical, they incorporate insights from mechanics and performance modelling. Also noted is that the types of rigid pavement included in the Road Test were plain and reinforced jointed concrete pavement, and CRCP was not placed in the Road Test.

2.2.1 AASHTO 1993

Since the AASHO Road Test was conducted in only one location, subjected to one environmental condition and a given soil condition, the "inference space" of the original design equation developed based on the data obtained from the Road Test is quite limited. To expand the applicability of the original design equation, research effort was made, which concentrated on incorporating mechanistic behavior of concrete slabs as affected by concrete material properties, slab support conditions and slab continuity condition, into the design equation. Original equation did not include any of those variables. Based on the research effort, the initial version was published in 1986. Further research effort was made to include overlay design, and the findings were published in 1993. The design equation from the 1993 publication, The AASHTO Guide for Design of Pavement Structure, is referred to as 1993 Design Equation, which is shown below (Equation 2-2).

$$Log(ESAL) = Z_R * s_o + 7.35 * Log(D+1) - 0.06 + \left[\frac{Log\left[\frac{\Delta PSI}{4.5-1.5}\right]}{1+\frac{1.624*10^7}{(D+1)^{8.46}}}\right] + (4.22 - 0.32 * \rho_t) * Log\left[\frac{S_c' * C_d * (D^{0.75} - 1.132)}{215.63 * J * \left[D^{0.75} - \frac{18.42}{\left(\frac{E_c}{k}\right)^{0.25}}\right]}\right] \quad (Equation\ 2-2)$$

There are a total of 11 inputs for the above equation which are:

- Slab Thickness = D
- Traffic = $ESAL$
- Change in serviceability = ΔPSI
- Modulus of Elasticity = E_c

- Modulus of Subgrade Reaction = k
- Modulus of Rupture = S_c'
- Standard Normal Deviate = Z_R
- Overall standard Deviation = s_o
- Terminal Serviceability = ρ_t
- Drainage Coefficient = C_d
- Load Transfer Coefficient = J

The first and last term is the portion added to the original equation based on the regression analysis and fatigue component respectively. What they really were trying to achieve with the last term is the idea that concrete fails in fatigue. Well to be technically correct, they were trying to overcome the fatigue induced distresses in the first place. The key variables that were included are modulus of subgrade reaction(k), concrete modulus(E), modulus of rupture (S_c'), drainage coefficient (C_d), and load transfer coefficient(J). However, there are inherent issues with this addition.

The first issue is in regards of reliability which is introduced as a statistical safety factor to accommodate variability in traffic, material performance, and environmental conditions. The AASHTO Guide suggests values ranging from 50% to 99.9%, with higher reliability applied to critical roadways. Somehow, this factor hugely impacts the final slab thickness output, however, the practical basis for assigning these values is vague. TxDOT typically adopts 95% for pavements expected to carry more than 5 million ESALs and 90% for lighter traffic levels. However, increasing reliability from 90% to 99% can add as much as 4 inches to slab thickness. This is a concern because it appears like it simply inflates the design based on uncertain assumptions.

The second issue is of modulus of subgrade reaction(k). If you notice k is raised to the power of 0.25 (a very small exponent), inside a logarithmic term, further reducing its impact. This means that even if we were to double k, it does not result in a large reduction in thickness(D). Also reducing k by half doesn't massively increase D either. The influence of k has diminishing effects which contradicts AASHO Road test findings. This contradicts the very important premise of AASHO Road test regarding the better slab support leading to better pavement performance.

The third issue is of modulus of rupture (S_c'). It is directly tied to how well concrete resists tensile fatigue. As we know concrete, though strong in compression, experiences progressive microcracking under repeated flexural stresses, especially at slab corners or midspans. This can lead to fatigue cracking over time even if individual loads are within elastic limits. However, calculating the modulus of rupture itself is a challenge. As it isn't truly a material constant, it's a test-dependent property. Unlike compressive strength, flexural strength is rarely measured in the field, so values are often estimated from empirical correlations which can be wildly inaccurate depending on mix design and materials.

The fourth issue is in the very conceptualization of Load Transfer coefficient (J). This is valid for CPCD as it is functionally linked with concrete volume change. However, when it comes to CRCP, CRCP lacks joints. Therefore, using this coefficient from CPCD design makes it impractical. In the formula, J is treated as an adjustable input, higher J values (representing poor load transfer) can lead to offsetting the equation by simply increasing slab thickness. This gives an idea that it is okay to use no dowels as long as the slab is made thick enough. In practice, however, this has not held up. If we reflect back to AASHO Road Test it stated that rigid pavements failed almost exclusively at cracks due to pumping, not at joints, as long as load transfer was effective. This raises the question of why J was retained as a key variable in the design equation if it does not directly capture the true failure mechanisms observed in the test.

The fifth issue is the use of drainage coefficient (C_d). There is no doubt that proper drainage is an essential part of long-lasting pavement structure. This is voiced in AASHO road test findings as well, which says that pumping water and fines leads to failures. In practicality this makes absolute sense, however AASHTO 1993 tries to incorporate it as a multiple factor. This leads to a notion that they were trying to compensate for poor drainage solely by increasing slab thickness. Further, it attempts to capture how quickly water leaves the pavement system, but this is inherently difficult to quantify during design, before any construction has occurred. It is important to note that the solution to this issue is not in altering design thickness rather it is more to do with construction job performed in the field. Until and unless the grading issue is resolved, whatsoever thick pavement is used it is simply not going to work.

With the above underlying issues, it's fair to point out AASHTO93 is outdated. Therefore, to compensate for the above impracticalities, MEPDG, aka AASHTOWare Pavement ME design, was developed in 2004 under NCHRP project 1-37A which is discussed next.

2.2.3 MEPDG

MEPDG, is implemented in a professional software package called AASHTOWare Pavement ME design. It is not a free tool and incurs yearly subscription. This is the most sophisticated overlay design procedure currently available in the US. While MEPDG boasts improvements over AASHTO 93, it shares similar limitations. One of the main differences with AASHTO 93 is the inference space. AASHTO 93 has limited structure sections, whereas in MEPDG, there is a wide range of structural and rehabilitation designs. Some remarkable differences can be seen in Table 2-1.

Table 2-1 Comparison between AASHTO 93 and MEPDG

Parameters	AASHTO 93	MEPDG
Traffic	1.1 million load repetitions	50+ million load repetitions
Design	Limited structural sections	Wide range of structural and rehabilitations designs
Climate	1 climate/ 2 years	All climates over 20-50 years
Materials	1 set of Materials	New and diverse materials

When it comes to the thickness design of CRCP, MEPDG represents a more advanced approach but is fraught with significant challenges due to its complexity and reliance on questionable assumptions, which often fail to align with real-world observations. As iterated earlier, TxDOT has chosen not to adopt MEPDG for CRCP designs in totality due to deficiencies in its punchout mechanism. The assumption that the crack spacing and crack width are strong predictors of long-term CRCP performance is flawed. The MEPDG adopted this view and used crack width, along with the associated load transfer efficiency (LTE) at transverse cracks, as a primary input in predicting punchout development.

To begin, the estimation of zero-stress temperature using a simplified equation based on mean monthly temperatures during construction has proven inaccurate in Texas, where field measurements show significant variability in ZST within a single day and across seasons. This leads to inaccuracies in predicting crack width, load transfer efficiency, and punchout development. As illustrated in Figure 2-5 and Figure 2-6, MEPDG assumes crack widths increase over time, reducing LTE and increasing punchout risk, whereas field data in Texas as shown in Figure 2-7 indicate that crack widths often decrease, which is attributed to the long-term development of transverse cracks, the progressive stress redistribution within the concrete, and resulting stress relaxation. Also, as shown in Figure 2-8, LTE values remain high even for older pavements over the period of 17 years, questioning the validity of the MEPDG's assumptions.

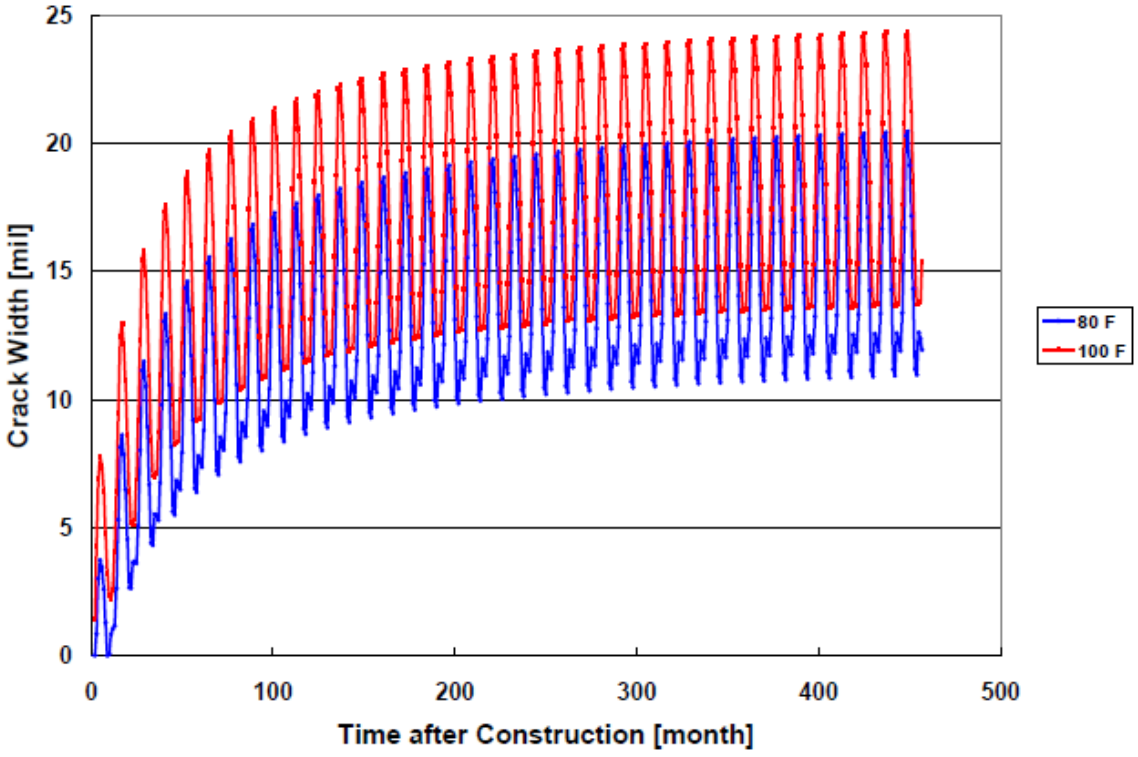

Figure 2-5 Effect of ZST on crack width

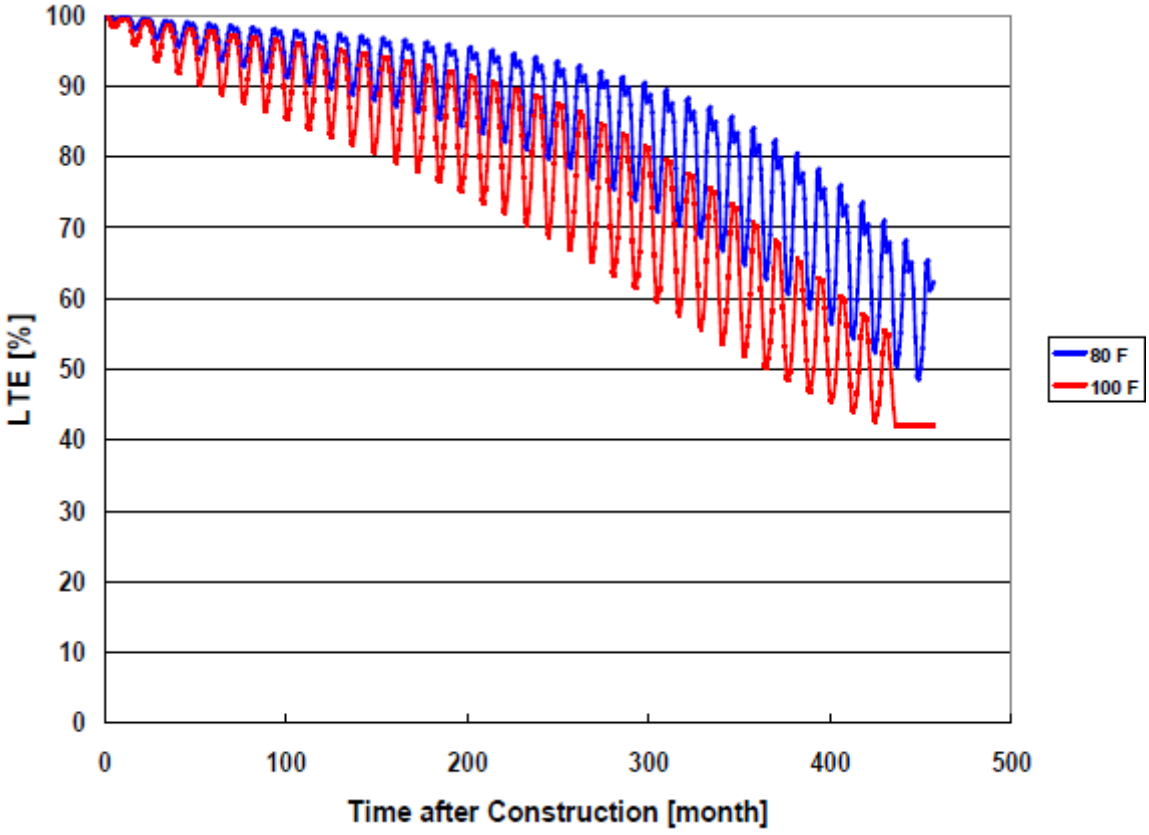

Figure 2-6 Effect of ZST on LTE

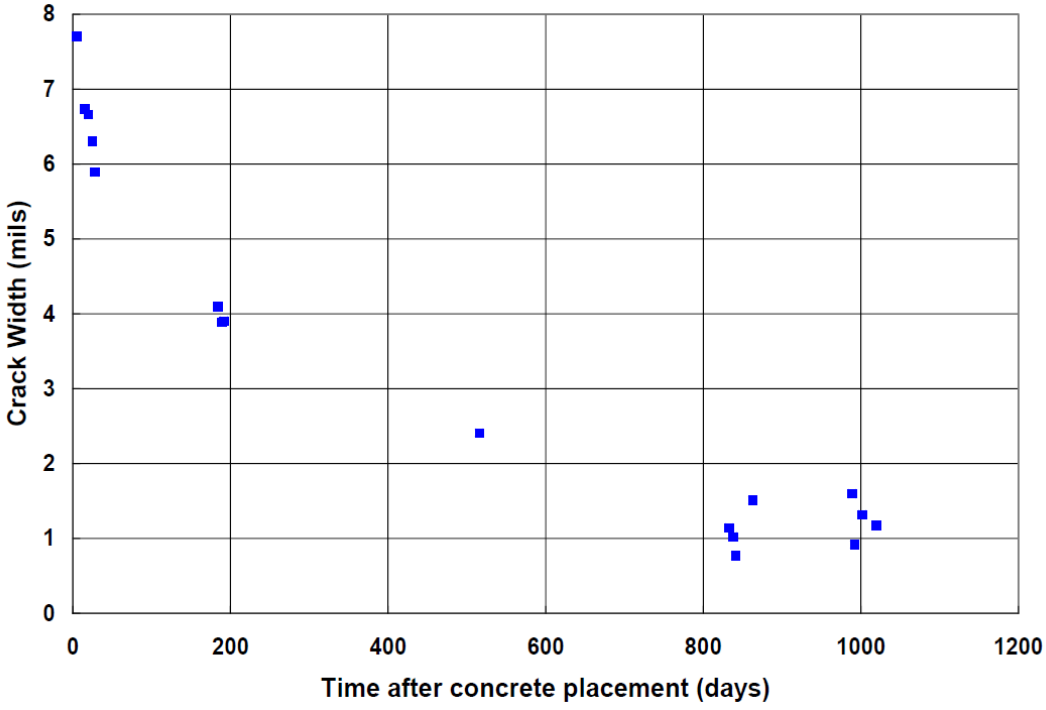

Figure 2-7 Measured crack widths over time (Nam 2005)

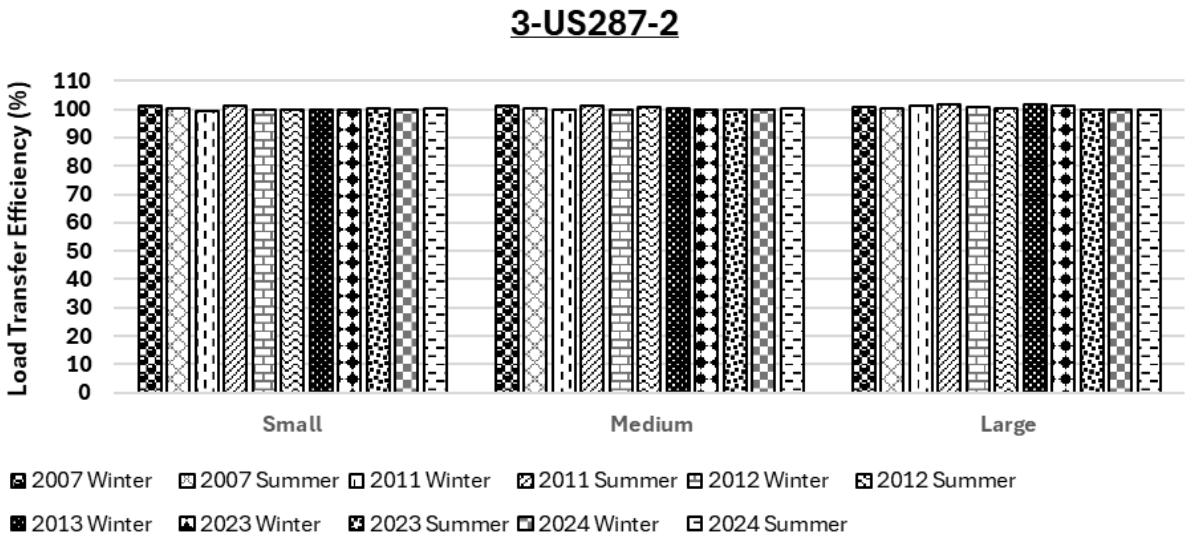

Figure 2-8 Field data in US287-2 Texas indicating LTE over a period of 17 years

Another limitation of MEPDG is its subbase erosion modeling, which assumes erosion is independent of slab thickness or traffic and is solely influenced by material properties and rainfall. This does not align with real-world observations in Texas, where subbase erosion is significantly affected by slab thickness, traffic loading, and drainage conditions. Additionally, MEPDG's assumptions regarding shoulder type further reduce its applicability in Texas. The model assumes asphalt shoulders, where critical transverse stress occurs at the slab's top, while Texas uses tied-concrete shoulders, which shift critical transverse stress to the bottom of the slab and cause bottom-up longitudinal cracking.

Probably, one of the critical issues with existing MEPDG is that though it starts with mechanical calculations, the final distress predictions still depend on empirical transfer functions. These models relate stresses and strains to cracking, faulting, and roughness based on field performance data. If the calibration was done using data that does not represent local conditions, the predictions can be inaccurate. An instance of this was in the MEPDG, where the test section used for the calibration was only 500 ft long, leading to gross overestimation of punchouts predicted when the transfer function is used. For example, 5 punchouts recorded within 500 ft would translate to about 50 punchouts in one mile, which is unrealistic. Therefore, going forward, it is very crucial to understand transfer functions in the first place. It is quite a sad state within academia that the gravity of this is often neglected, and researchers attempt to overuse this by performing tasks in domains beyond their resolution capabilities. If reader is interested to comprehend the problem with transfer function, it is recommended to read a research article titled, "Reflections on the Use of Transfer Functions in Pavement Engineering" by Anastasios M. Ioannides and Jeb S. Tingle from US Army Corps. It does a great job on pointing out that today's transfer function is just a blunt, policy-driven guardrail rather than a statistical formula.

Therefore, in an academic sense, MEPDG does fall in the bracket for its robust and rather comprehensive approach. It attempts to incorporate a wide range of factors like climate, materials, traffic, and existing pavement conditions. Also, the iterative design process allows for greater control over design parameters and provides options for both bonded and unbonded overlays. The caveat or the crucial pitfalls underlying MEPDG is its overly dependence on complex algorithms which seem out of touch with what happens in reality. Thus, it could be considered as a mere academic pursuit of excellency.

2.2.4 TxCRCP-ME

Amid all the misunderstandings and misguided approaches in CRCP slab thickness design across the United States, the Texas Department of Transportation (TxDOT) has distinguished itself by developing a more accurate slab thickness design method for CRCP. This distinction took a head start after the NCHRP 1-37 report and the Mechanistic-Empirical Pavement Design Guide (MEPDG) software were released in March 2004. By 2005, TxDOT initiated research to evaluate the MEPDG for potential implementation but concluded against it. Consequently, in 2007, TxDOT began research project 0-5832 to develop its own mechanistic-empirical CRCP design procedures, resulting in the TxCRCP-ME program. With its easy-to-use tools and simple user interface all the new CRCP project constructed within Texas uses this program for their slab thickness design.

However, even TxCRCP-ME is not without its limitations and cannot be considered a fully robust or foolproof system. Its reliance of the final distress predictions on empirical transfer function is one of its weak links. Nevertheless, it does a great job addressing most of the issues that MEPDG fails to recognize. The crucial being its descriptive approach to defining true punchout and accepting the limitations poised by data collected from its pavement management information systems (PMIS) which are: (1) reasonably accurate traffic information, (2) availability of design and construction data and (3) accurate distress information.

Another pitfall in all the existing thickness design procedure is Concrete fatigue. It is accepted fact, at least among field practitioners, that concrete fatigue behavior is quite complicated. The relationship between stress/strength ratio and fatigue life of concrete is not unique, as shown in Figure 2-9. A large variance is observed among fatigue curves depending on the testing condition as well as how to define “failure.” This is why developing purely mechanistic-based rigid pavement design is a real challenge. However, the accuracy of rigid pavement designs based on ME principles does not depend on the reasonableness of the fatigue equation, because a transfer function partially nullifies the “bias” of the fatigue equation. In other words, if an accurate transfer function is obtained, a selection of fatigue curve among many does not influence the accuracy of the pavement design. On the other hand, developing an accurate transfer function requires both correct information on concrete stresses and a large number of data points. Since most of the rigid pavements in Texas are concrete slabs on base, developing an accurate transfer function for new rigid pavement design is less of a challenge. Unbonded

overlay or whitetopping is a different story, since there are only a limited number of existing UBCO or whitetopping projects.

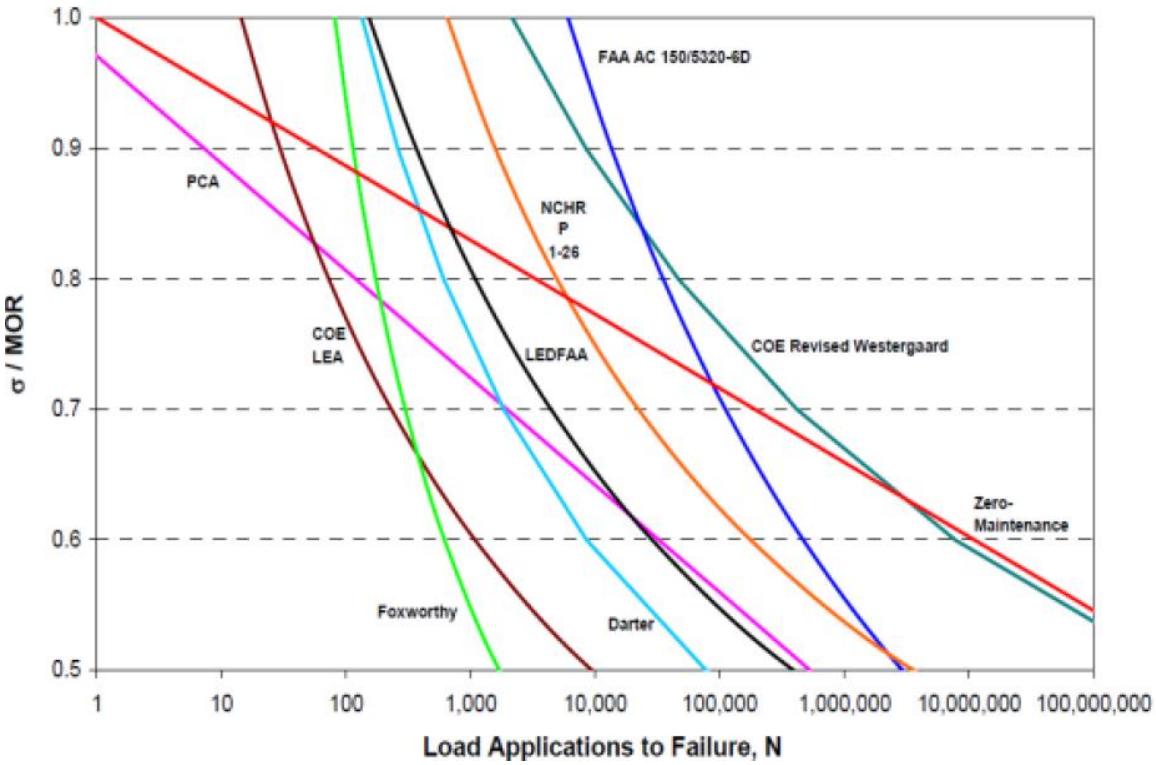

Figure 2-9 Various concrete fatigue curves

2.3 Review of Existing Overlay thickness design procedure

When it comes particularly to the thickness design procedure for concrete overlays, there are currently three different approaches:

- Effective thickness approach
- Mechanistic empirical approach
- Deflection approach

It is to be noted that this research is in lieu of proposing another approach known as a deflection approach which is part of subsequent chapter in this research report.

2.3.1 Effective thickness approach

This approach is based on the principle that the overlay thickness is the difference, not necessarily linear, between thickness required for new pavement and effective thickness of the existing pavement. The effective thickness is a function of existing pavement conditions and thickness of each layer. Therefore, it is also called component analysis procedure.

U.S. Amry Corps of Engineers Method

The method advocated by U.S. Army Corps of Engineer was probably the first overlay design. The design proposed by them was for the PCC overlays over PCC airport pavements. The design procedure introduced empirical coefficients into equation based on the results of full-scale traffic tests.

$$h_{ol}^{n} = h_{f}^{n} - C(h_{e})^{n} \qquad (Equation\ 2-3)$$

Where

h_{ol} = required overlay thickness

h_f = new concrete thickness

h_e = existing thickness

C = condition correction coefficient

C =1 for existing pavements in good overall structural condition with little or no cracking

C = 0.75 for existing pavements with initial transverse and corner cracking due to loading but without progressive structural distress or recent cracking

C = 0.35 for existing pavements that are badly cracked or structurally shattered

n = 1 for bonded (C =1); Structurally sound concrete – No fatigue damage

n = 1.4 for partially bonded

n = 2 for unbonded

Figure 2-10 illustrates the data points from the experimentation of full-scale traffic tests. This graph can be used to find the overlay thickness based on the existing thickness and the type of bond. It is important to note that for the same effective thickness, unbonded overlay thickness is greater than bonded overlay thickness. This is because of the shape of the curve since bonded is linear curve whereas partially bonded and unbonded curve are nonlinear curve.

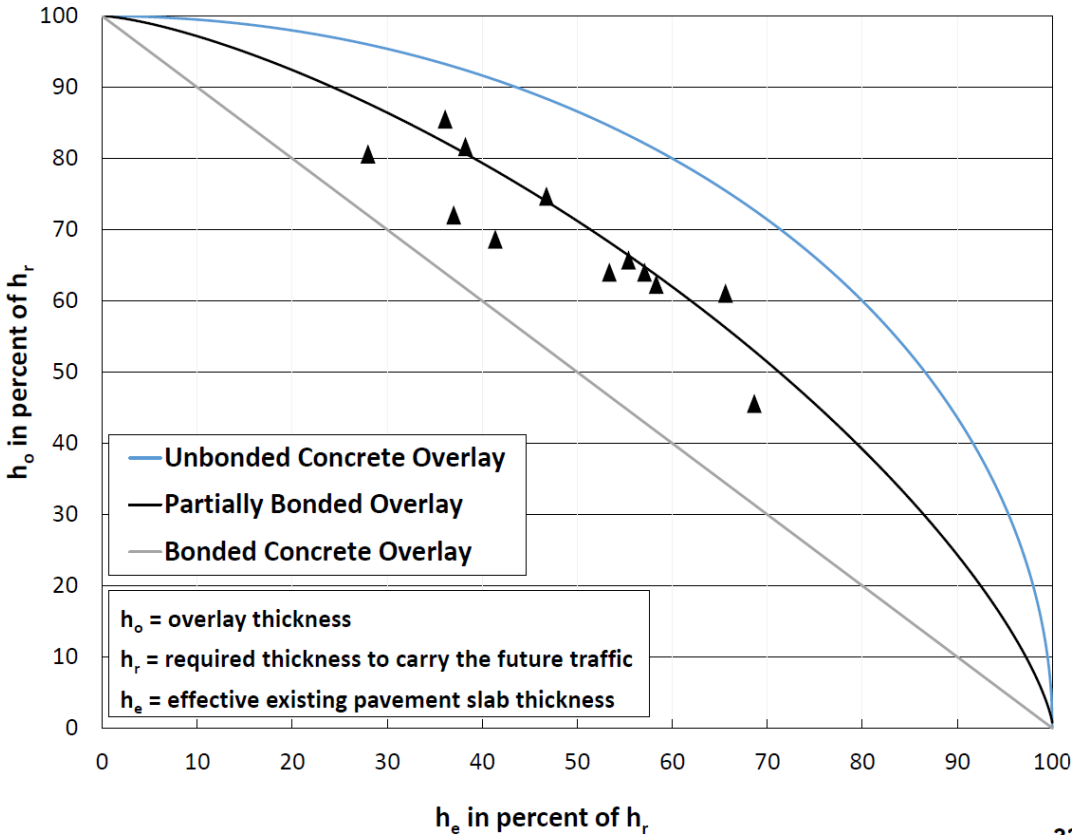

Figure 2-10 U.S. Army Corps of Engineer Method for calculating overlay thickness

AASHTO 1993

In the AASHTO 1993, two methods are suggested: one is visual survey method and the other remaining life method. The main formula to calculate required overlay thickness remained the same as U.S. Army Corps. The only difference was the approach on which the existing effective slab thickness was calculated. Here we will go over those two methods.

Visual Survey Method

The existing pavement is evaluated visually, and the structural capacity of the existing pavement is converted to "equivalent" brand new concrete slab thickness, which is called "effective slab thickness". The formula is given as:

$$D_{eff} = F_{jc}\ X\ F_{dur}\ X\ F_{fat}\ X\ D \qquad (Equation\ 2-4)$$

where,

D_{eff} = Effective slab thickness (in)

F_{jc} = Joints and cracks adjustment factor

F_{dur}= Durability adjustment factor

F_{fat}= Fatigue damage adjustment factor

D = Thickness of the existing concrete slab (in)

The assumption made in the above equation is that pavement condition manifested by visual observation can represent "remaining structural capacity" of the existing pavement accurately. Unfortunately, this assumption has never been proven, even though there should be a correlation, albeit loosely, between visual condition and structural capacity of the pavement.

Figure 2-11 shows the joints and cracks adjustment factor (F_{jc}) graph. The x-axis shows the number of deteriorated transverse joints and cracks per mile and y-axis shows the value that would be used as F_{jc}. The factor is drawn based on deteriorated transverse joints and cracks when we trace the factor with the curve that defines a function. However, there is no description of what constitutes deteriorated transverse joints and cracks provided in this design method.

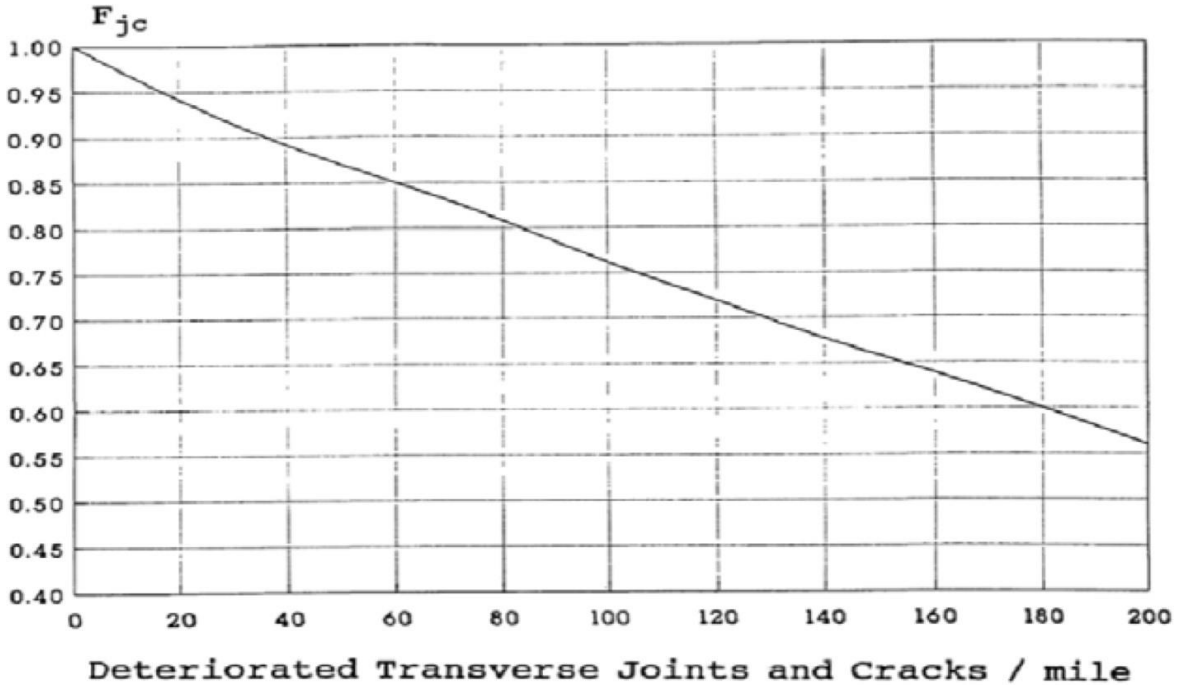

Figure 2-11 Graph showing the joint and crack adjustment factor (AASHTO, 1993)

Table 2-2 illustrates the durability adjustment factor F_{dur} based on the existing pavement condition.

Table 2-2 Summary of the durability adjustment factor (AASHTO, 1993)

F_{dur}	**Description**
1.00	No sign of PCC durability problems
0.96-0.99	Durability cracking exists, but no spalling
0.88-0.95	Substantial cracking and some spalling exist
0.80-0.88	Extensive cracking and severe spalling exist

The durability problems selected for the overlay design are D cracking or reactive aggregate distress, and spalling. Unfortunately, the condition of the pavement is classified qualitatively, not quantitatively, which makes the implementation of this method subjective and difficult.

Table 2-3 illustrates how one can determine the fatigue adjustment factor (F_{fat}) for various rigid pavement types. The values range from 0.88 to 1.00.

Table 2-3 Summary of the fatigue adjustment factor (AASHTO, 1993)

F_{fat}	Description
0.97-1.00	Few transverse cracks/punchouts exist (none caused by" D" cracking or reactive aggregate distress) - JPCP: < 5% slabs are cracked - JRCP: < 25 working cracks per mile - CRCP: < 4 punchouts per mile
0.94-0.96	A significant number of transverse cracks/punchouts exist (none caused by "D" cracking or reactive aggregate distress) - JPCP: < 5 - 15% slabs are cracked - JRCP: < 75 working cracks per mile - CRCP: < 4 - 12 punchouts per mile
0.88-0.95	Many transverse cracks/punchout exist (none caused by "D" cracking or reactive aggregate distress) - JPCP: <>15% slabs are cracked - JRCP: > 75 working cracks per mile - CRCP: > 4 - 12 punchouts per mile

Remaining Life Method

The other method to estimate the effective slab thickness of the existing pavement is to use the remaining life of the existing pavement. The condition factor of the existing pavement is used to calculate the effective thickness per the following equation:

$$D_{eff} = CF\ X\ D \qquad (Equation\ 2-5)$$

where,
CF = condition factor of existing pavement
D = thickness of existing concrete slab (in)

The condition factor (CF) is based on the remaining life of the existing pavement, which is computed by equation below:

$$RL = 100\left[1 - \frac{N_p}{N_{1.5}}\right] \qquad (Equation\ 2-6)$$

where, RL = remaining life (percent)

N_p = Total traffic to date, 18-kip ESAL

$N_{1.5}$ = Total traffic to pavement failure ($P_t = 1.5$), $18 - kip$ ESAL

Once the remaining life is calculated, the condition factor is determined from the curve in Figure 2-12.

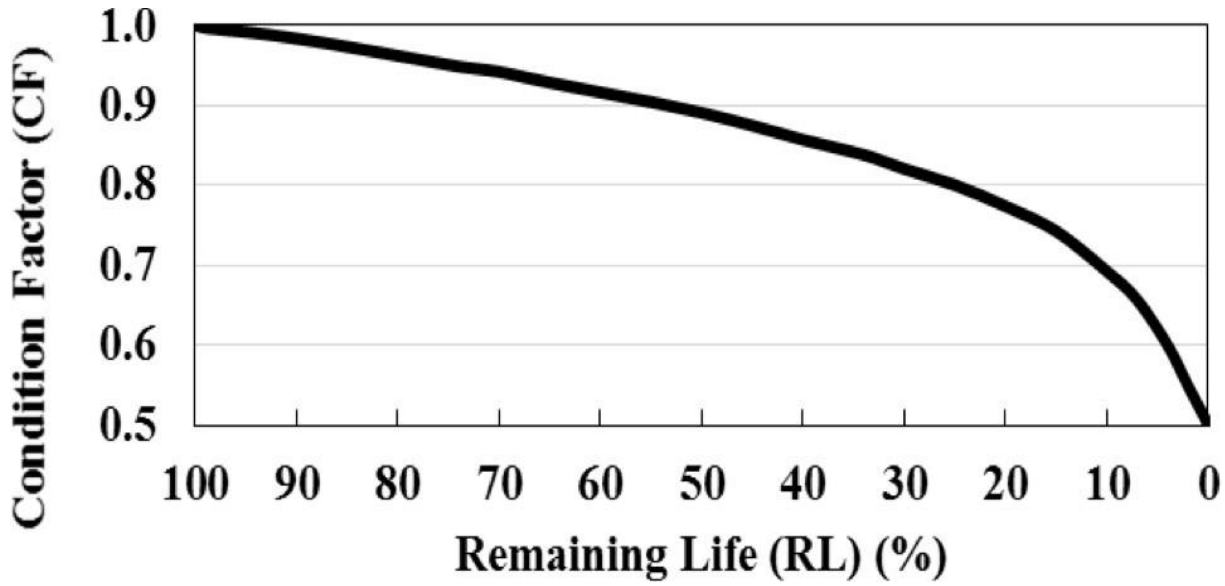

Figure 2-12 Graph showing remaining life and respective condition factors (AASHTO, 1993)

For Unbonded Concrete overlay thickness design, the effective thickness of existing pavement is determined using following equation

$$D_{eff} = F_{jcu}\ X\ D \qquad (Equation\ 2-7)$$

where,

F_{jcu} = Joints and cracks adjustment factor for UBCOs

D = existing PCC slab thickness, inches

The joints and cracks adjustment factor for UBCOs is determined using Figure 2-11. Since there is little evidence for reflection cracking and other problems caused by the existing slab, the F_{dur} and F_{fat} are not needed for UBCO design.

Limitation

The theoretical limitation of using effective thickness approach stems from the fact that it uses principle of the structural moment equivalence (Equation 2-8) proposed by Tabatabaie as shown in Figure 2-13.

$$M_e = M_1 + M_2 \qquad (Equation\ 2-8)$$

Where

$$M = \frac{\sigma\ X\ I}{y} \qquad (Equation\ 2-9)$$

$$I = \frac{bh^3}{12} \qquad (Equation\ 2-10)$$

Substituting M and I we get,

$$\sigma_e h_e^2 = \sigma_1 h_1^2 + \sigma_2 h_2^2 \qquad (Equation\ 2-11)$$

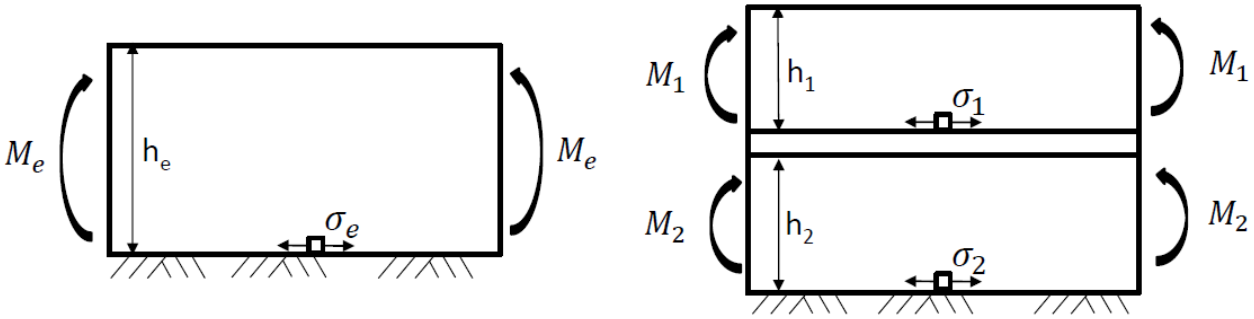

Figure 2-13 Structural moment equivalence concept

If $\sigma_e = \sigma_1 = \sigma_2$, then the equation becomes same as the unbonded overlay formula as proposed. However, this is not found to be true. Figure 2-14 shows the stress ratio of σ1/σ2 for various slab thicknesses with a k-value of 100 pci. It shows that the ratio is larger than 1.0 for all the cases, which violates the basic assumption made in the AASHTO UBCO design method Therefore, the Crops of Engineer and the AASHTO methods for unbonded concrete overlay appear to be not correct, at least from a theoretical standpoint.

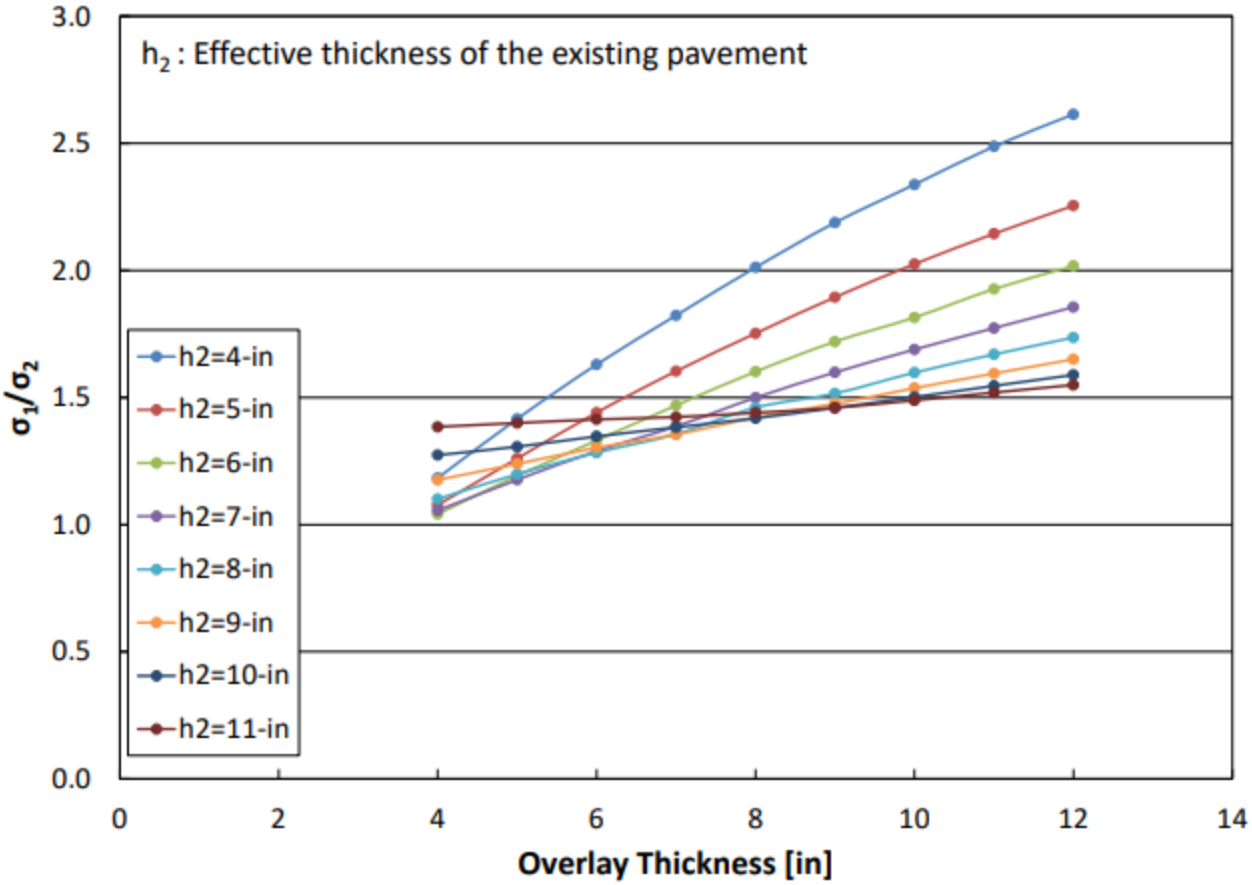

Figure 2-14 The stress ratio of UBCO for the case of K-value=100pci

2.3.2 Mechanistic empirical approach

This approach is based on the principle that the overlay thickness should be sufficient to keep pavement damage within acceptable limits. It involves determining critical responses such as stress, strain, or deflection using mechanistic models, and then estimating the resulting damage through empirical failure criteria. A key component of this method is the use of a transfer function. However, as mentioned earlier, the limited number of overlay projects makes it difficult to develop a reliable and comprehensive dataset for establishing such a transfer function. In this section we will go through two ME approach currently in use for overlay design.

ACPA

American Concrete Pavement Association (ACPA) Thickness Design Procedure has evolved over time. It was only after 2016 that the concrete pavement industry, which included ACPA, NRMCA (National Ready-Mixed Concrete Association) and the PCA (Portland Cement Association) consolidated various concrete pavement design tools and created a more definitive design approach for concrete pavement. They created a free tool, which is based on the mechanistic-empirical design principles and has a more robust design method compared to AASHTO 1993. The name of the design tool is PavementDesigner.org. It was formerly known

as StreetPave or PCA method. This design procedure is primarily used by small entities, such as cities and counties, but not by state DOTs.

Figure 2-15 shows the flowchart of the design procedure. For overlay design, there are 2 classes. The first one is unbonded on HMA or PCC, or bonded on PCC, while the second one is bonded (partially bonded) on HMA. The design for the first category uses a previously known PCA method, while the design method for bonded on HMA utilizes BCOA-ME method. PCA method will be discussed in this section for the thickness design procedure for unbonded overlay, while the BCOA-ME for bonded overlay will be presented in the next section. It should be recognized that there is no good definition of bonded or unbonded overlay on HMA. Since the surface of HMA pavement has substantial amounts of air voids, when concrete is placed, cement paste will penetrate to the voids in HMA surface, resulting in substantial bond. In Texas, when concrete coring is made, 1-in HMA layer is almost always attached to the concrete, indicating a solid bond between asphalt and concrete. Accordingly, it may be academic to classify concrete overlay on HMA as either bonded or unbonded.

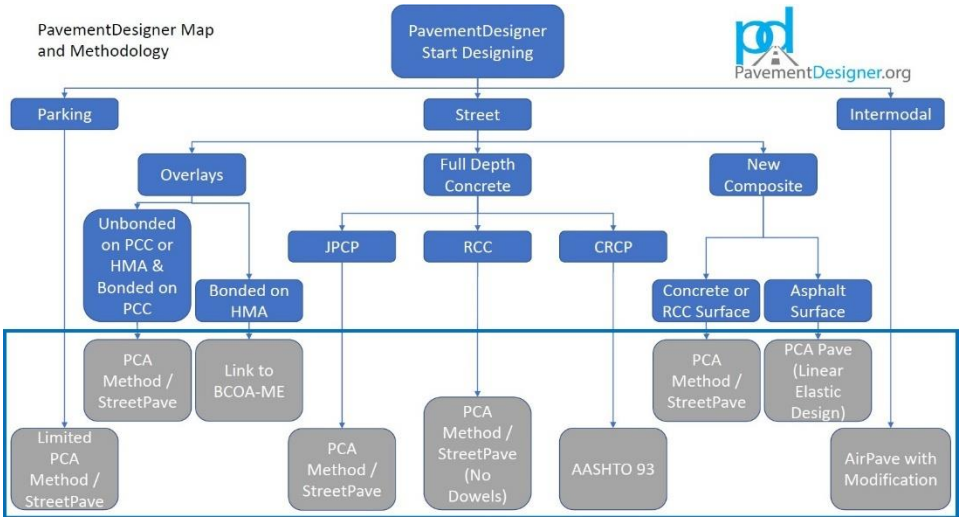

Figure 2-15 Overview of Pavement Designer tool for design procedure

The ACPA design procedure can be summarized and described in 5 steps. The method requires 4 input variables: (1) k-value of the subgrade, (2) flexural strength of the concrete, (3) design period and (4) traffic. The design period is defined as the expected service life of the pavement before any major structural rehabilitation is required. The traffic is defined as the amount of truck-traffic that is expected during the design period.

STEP 1 – Estimating the k -value of the subgrade

Based on the characteristics of the base layer (its thickness and modulus), layer thickness of the existing asphalt, and the k value of the subgrade, the k-value at the top of the existing asphalt layer is estimated. The chart to estimate the k-value on top of the existing asphalt pavement is based on Figure 2-16a and Figure 2-16b. Figure 2-16a is for the estimation of the k-value with

granular base, whereas Figure 2-16b shows the chart to estimate the k-value with cement treated base.

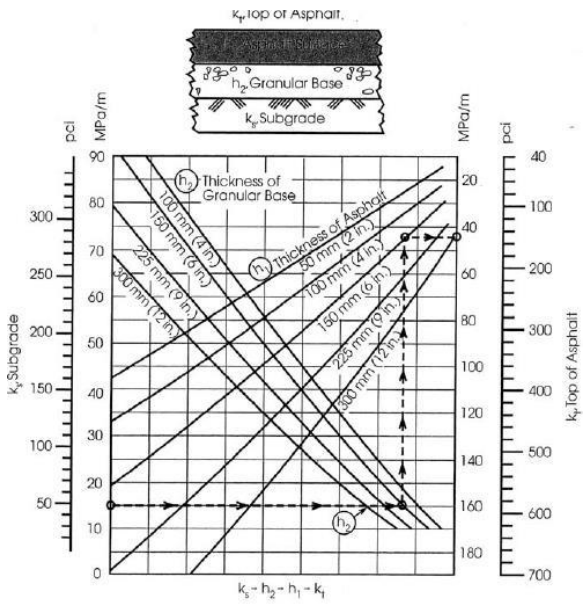

(a) K-value on top of asphalt pavement with granular base

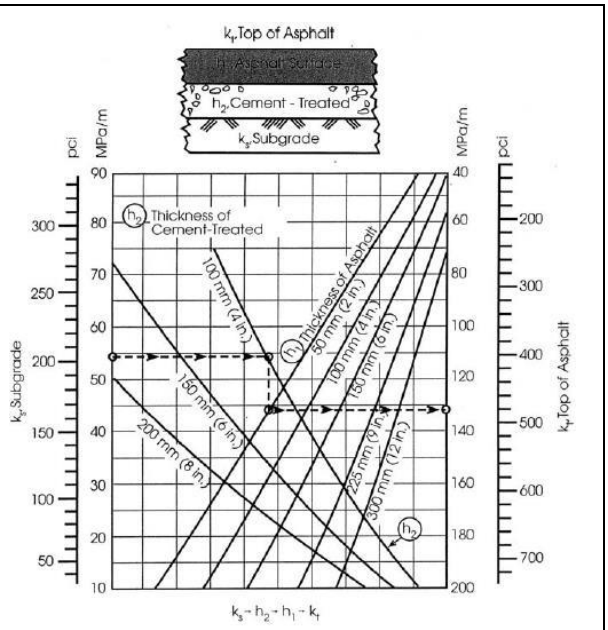

(b) K-value on top of asphalt pavement with cement-treated base

Figure 2-16 k -value on top of asphalt pavement with granular base and cement-treated base

Table 2-4 shows the approximate k-values for different soil types. The k-value of the subgrade was determined using plate load test or FWD test.

Table 2-4 Subgrade soil types and approximate k-value

Type of Soil	Support	k (MPa/m) (pci)	CBR	R
Fine-grained soils in which silt and clay-size particles predominate	Low	20-30 (75-120)	2.5-3.5	10-22
Sand and sand-gravel mixtures with moderate amounts of silt and clay	Medium	35-45 (130-170)	4.5-7.5	29-41
Sand and sand-gravel mixtures relatively free of plastic fines	High	50-60 (180-220)	8.5-12	45-52
CBR=California Bearing Ratio, ASTM D1183 R=Resistance R-Value, ASTM D2844				

STEP 2 – Flexural strength design value for concrete

Table 2-5 shows the relationship between compressive strength and flexural strength in the design procedure, which was derived the following Eq. 7.

$$f_r = C(f_{cr}^{'})^{0.5}$$

Where, f_r = flexural strength (modulus of rupture) in psi, C is a conversion factor, which is 9, and $f_{cr}^{'}$ is compressive strength in psi.

Table 2-5 Relationship between compressive strength and flexural strength

Metric		**U.S.**	
Compressive, MPa	**Flexural, MPa**	**Compressive, psi**	**Flexural, psi**
24	3.7	3500	530
28	4	4000	570
32	4.2	4500	600
36	4.5	5000	640
Note: For individual concrete, the constant, C may vary +/- 10 percent; concretes made with crushed aggregates usually have higher flexural strengths than those made with gravel or rounded aggregate.			

STEP 3 – Estimation of Truck traffic

The design considers the weight and daily load repetitions of the trucks. In this design procedure, only truck traffic is considered

STEP 4 – Design Period of an Overlay

The general design period of an overlay is considered as 20 years.

STEP 5 – Determination of Pavement Thickness

This ACPA design procedure was represented with Table for two traffic categories. The slab thickness is determined based on the amount of truck traffic, flexural strength of concrete and support strength (k-value) on the top of the existing asphalt pavement. Table 2-6 is for light to medium truck traffic.

Table 2-6 Slab thickness, Light to Medium Truck Traffic

Trucks per day per lane	**Design flexural strength, psi (average)**	**k-value, pci**				
		k = 700	**k = 500**	**k = 300**	**k = 200**	**k = 100**
2	650	4.5 (4.0)	5.0 (4.0)	5.0 (4.0)	5.5 (4.5)	6.0 (5.0)
	600	5.0 (4.0)	5.0 (4.0)	5.5 (4.5)	5.5 (4.5)	6.5 (5.0)

	550	5.5 (4.5)	5.5 (4.5)	5.5 (5.0)	6.0 (5.0)	6.5 (5.5)
10	650	4.5 (4.0)	5.0 (4.0)	5.5 (4.0)	5.5 (4.5)	6.0 (5.0)
	600	5.0 (4.0)	5.0 (4.5)	5.5 (4.5)	6.0 (5.0)	6.5 (5.5)
	550	5.5 (4.5)	5.5 (4.5)	6.0 (5.0)	6.5 (5.5)	7.0 (6.0)
40	650	5.0 (4.0)	5.5 (4.5)	6.0 (5.0)	6.0 (5.0)	6.5 (5.5)
	600	5.0 (4.5)	5.5 (4.5)	6.0 (5.0)	6.5 (5.5)	7.0 (6.0)
	550	5.5 (4.5)	6.0 (5.0)	6.5 (5.5)	6.5 (5.5)	7.0 (6.0)

Dowels are not required
Parenthesis = pavement with edge support (concrete shoulder. Widened lane, curb and gutter, or adjacent concrete lanes on both sides)
Minimum thickness = 4in.

Whereas Table 2-7 is for heavy truck traffic. It is to be noted that the determination of an accurate support reaction of the existing asphalt pavement is crucial. If the flexural strength of concrete and traffic are constant, then the slab thickness depends on the support reaction on top of existing asphalt pavement.

Table 2-7 Slab thickness, Heavy Truck Traffic

Trucks per day per lane	**Design flexural strength, psi (average)**	**k-value, pci**				
		k = 700	**k = 500**	**k = 300**	**k = 200**	**k = 100**
80	650	7.0 (6.0)	7.0 (6.0)	7.5 (6.5)	8.0 (7.0)	9.0 (7.5)
	600	7.0 (6.5)	7.5 (6.5)	8.0 (7.0)	8.5 (7.5)	9.5 (8.0)
	550	7.5 (6.5)	8.0 (7.0)	8.5 (7.5)	9.0 (8.0)	10.0 (8.5)
400	650	7.5 (7.0)	8.0 (7.0)	8.5 (7.5)	9.0 (7.5)	9.5 (8.0)
	600	7.5 (7.0)	8.0 (7.0)	8.5 (7.5)	9.0 (8.0)	10.0 (8.5)
	550	8.0 (7.0)	8.5 (7.5)	9.0 (8.0)	9.5 (8.5)	10.5 (9.0)
1200	650	7.5 (7.5)	8.0 (7.5)	8.5 (8.0)	9.0 (8.0)	9.5 (8.5)
	600	8.0 (7.5)	8.5 (8.0)	9.0 (8.5)	9.5 (8.0)	10.5 (9.0)
	550	8.5 (7.5)	9.0 (8.0)	9.5 (8.0)	10.0 (8.5)	11.0 (9.5)

Red colored = doweled joints, uncolored = undoweled joints
Parenthesis = pavement with edge support (concrete shoulder. Widened lane, curb and gutter, or adjacent concrete lanes on both sides)

If you notice this very design method is what TxDOT has derived and currently uses as its Thin Whitetopping design table as presented earlier in Table 1-1.

BCOA-ME

BCOA-ME is fairly the newest addition and is based on the mechanistic-empirical design principles and is specifically for concrete overlay of asphalt. This was developed at the

University of Pittsburgh under FHWA Pooled Fund TPF-5(165). Compared to other methods, BCOA-ME used field performance data from a number of actual overlay projects. This indicates that the design procedure was calibrated in terms of structural response and fatigue. The BCOA-ME is applicable for the design of concrete overlay from 3 inches to 6 inches with slab length ranging from 2 ft to 12 ft.

In this design procedure, the interface between concrete and asphalt is partially bonded. The overall design concept and procedure is similar to those of MEPDG. One important factor incorporated in this design procedure is the joint spacing as an input. One can control what the joint spacing will be, which in turn changes the thickness of overlay. For example, if a user chooses a shorter joint spacing, stresses in concrete slab due to environmental loading (temperature and moisture variations) and wheel loading decreases, resulting in thinner slab.

Figure 2-17 shows how the change in joint spacing results in changes in the performance of the pavements. If we have a very smaller slab joint spacing less than 4.5 ft (e.g., 4 ft x 4 ft panel), the failure mode is assumed to be corner cracks. Corner cracking is selected as the critical distress mechanism. For the slab joint spacing ranging from 5 ft to 7 ft (e.g., 6 ft x 6 ft panel), the failure mode is observed to be longitudinal crack. Longitudinal cracking is assumed to start at the transverse joints. When the slab joint spacing is above 7 ft (e.g., 12 ft x 12 ft), the failure mode is observed to be a transverse crack. Transverse cracking is supposed to start at the longitudinal edge. A closed form equation is used for three distress modes to estimate tensile stresses under traffic loading. For tensile stresses at corner and longitudinal edges, the equation developed by ACPA and Colorado DOT is used. As noted earlier, ACPA procedure focused on UTW, which exhibits corner cracking, and Colorado DOT procedure focused on transverse cracking. For longitudinal cracking, a new equation was developed. This equation was developed based on a database of analysis results from a finite element model where full bonding was assumed. Later, an analytical model was formulated, and its parameters were determined in a best-fit regression analysis process. It should be noted that BCOA-ME provides no experimental data for the estimation of transverse tensile strains at the bottom of the slab. For corner cracking, concrete stresses due to temperature curling were estimated using ACPA procedure, whereas for longitudinal cracking, concrete stresses were estimated using Colorado DOT approach. These are the driving failure criteria for the BCOA-ME.

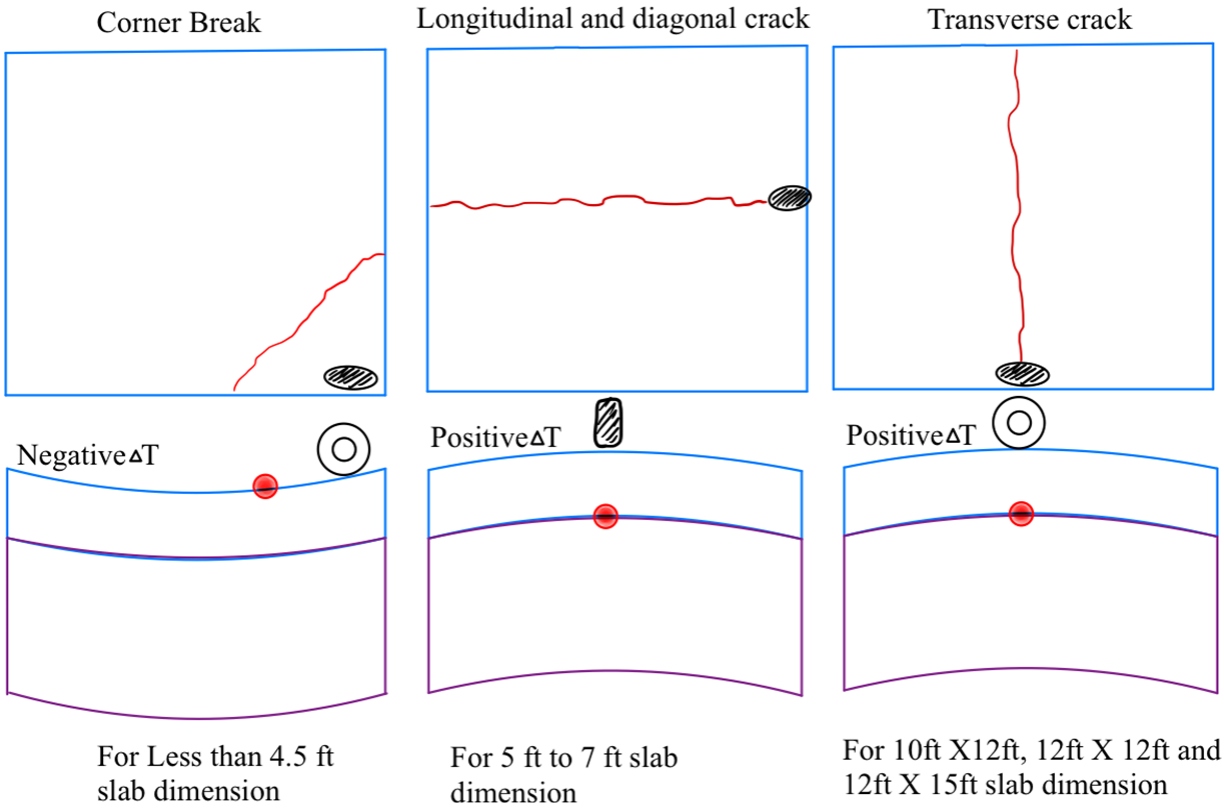

Figure 2-17 Different performance of the pavement in terms of respective slab sizes

The thickness design of the overlay using BCOA-ME can be processed in 5 steps as shown:

STEP 1 – Traffic consideration

It uses traffic based on the concept of 18kip ESAL. It is to be noted that no information is provided in BCOA-ME regarding the extrapolation of load equivalency factors for overlay thickness below 6 inches. Wandering of traffic is only considered for predicting longitudinal cracking.

STEP 2 – Temperature gradient

A mechanistic approach is used to estimate the temperature gradient throughout PCC slabs. The approach uses Enhanced Integrated Climate Model (EICM) and then uses mechanistic-empirical principles to determine the effective equivalent linear temperature gradient (EELTG). Figure 2-18 shows the flowchart to generate the effective linear temperature gradient. This produces the same damage throughout the design life of the overlay. Analytical equations were fitted to the results for each distresses mechanism.

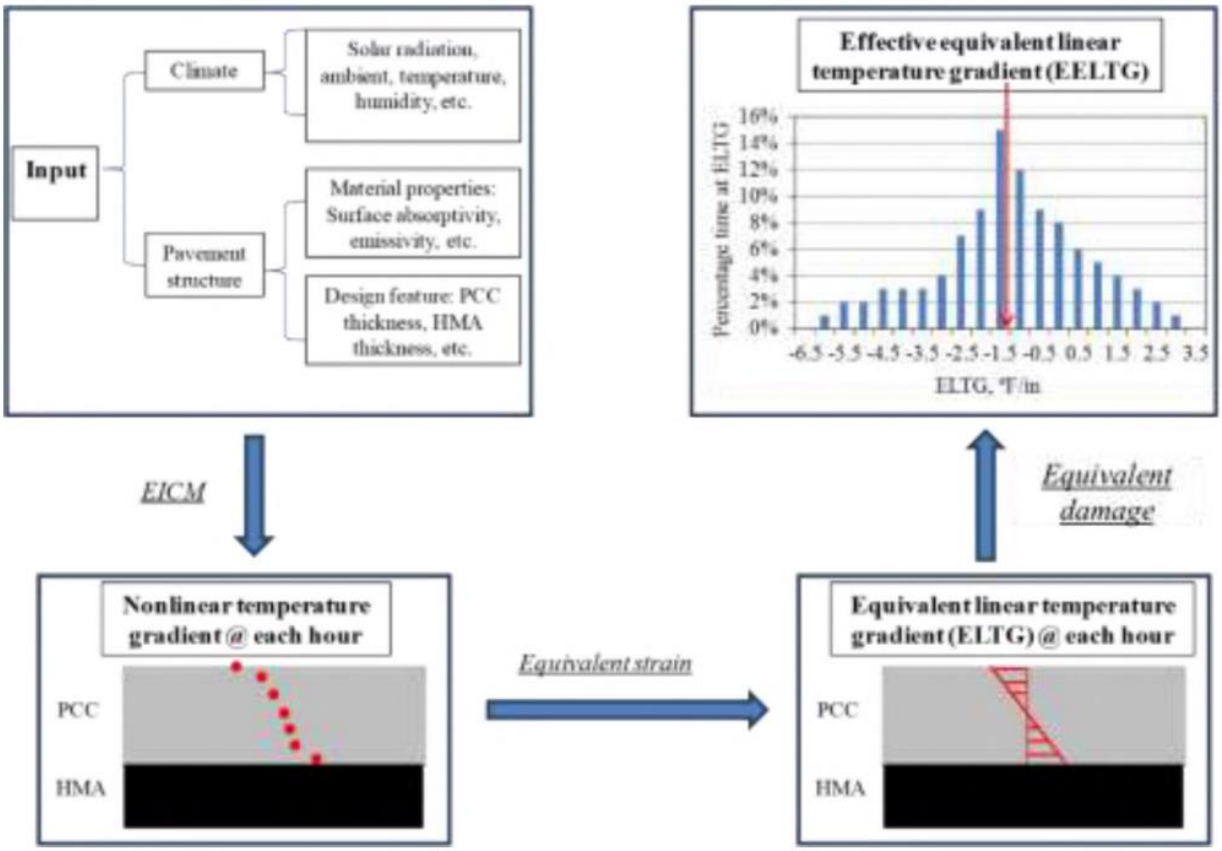

Figure 2-18 Flowchart to generate the effective equivalent linear temperature gradient

STEP 3 – Characterization of the HMA Modulus

This method considers the hourly variation of the stiffness of the asphalt mixture layer, which it estimates monthly. This is calculated using EICM. The stiffness changes depend on the climate zone and the characteristics of the BCOA section.

STEP 4 – Fatigue Model

It uses the fatigue model developed for the ACPA procedure and reliability can be introduced into the design process. It estimates concrete residual strength ratio as a function of fiber dosage using "FRC calculator". Further, it checks the risk of reflective cracking through the PCC overlay.

STEP 5 – Faulting Model

It uses the fatigue model developed for the ACPA procedure and reliability can be introduced into the design process. It estimates concrete residual strength ratio as a function of fiber dosage using "FRC calculator". Further, it checks the risk of reflective cracking through the PCC overlay.

In summary, while robust in theory (Figure 2-19), the BCOA-ME faces several practical limitations. The major being the limited availability of long-term performance data, which

hampers the development of reliable empirical transfer functions, for accurate damage prediction. The approach also relies on idealized assumptions in mechanistic models, such as perfect bonding and simplified temperature gradients, which may not fully reflect field conditions. Additionally, environmental and material variations are often represented by generalized values, potentially overlooking localized effects like freeze-thaw cycles or excessive moisture. The method is also data-intensive, requiring detailed traffic, material, and climatic inputs that may not always be readily available or precise. Lastly, it is sensitive to panel size and geometry, yet the existing models may not fully account for performance variations across different joint configurations or slab dimensions. These factors collectively introduce uncertainty in predicting real-world pavement behavior.

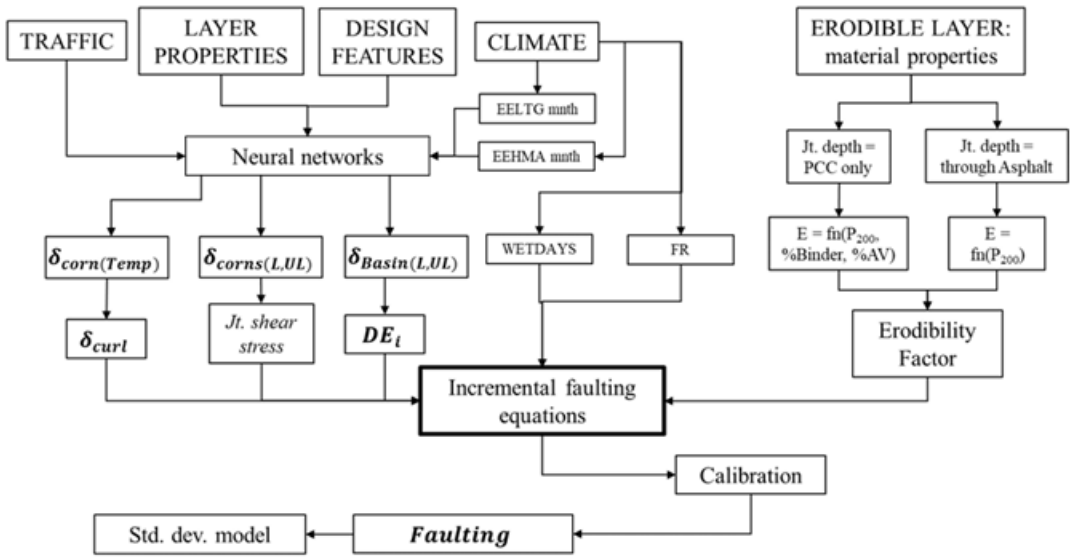

Figure 2-19 Flowchart for incremental prediction of faulting

2.4 State DOT Practices

This section summarizes the experiences and methodologies of several U.S. State Departments of Transportation (DOTs) regarding concrete overlays, particularly whitetopping.

2.4.1 MnDOT

MnDOT has utilized its full-scale pavement test facility, MnROAD, since 1997 to evaluate various pavement designs, including six whitetopping cells. Initial cells with thinner Portland Cement Concrete (PCC) layers (3-4 inches) and small slab dimensions (e.g., 4 ft x 4 ft) experienced significant drops in serviceability and were replaced after approximately seven years due to distresses like corner cracking, particularly when sawcut joints fell under the wheel path. Thicker sections (6-7 inches) with larger slab dimensions generally performed better with minimal distress. A key lesson from MnDOT's experience is the critical importance of joint spacing and its interaction with wheel loading paths.

2.4.2 CDOT

CDOT has been a proponent of Bonded Concrete Overlay over Asphalt (BCOA), with research dating back to 1998 and 2004. Their "Thickness Design of Bonded Whitetopping Pavement" was developed based on experimental data from four thin BCOA sections (4-7 inch PCC thickness). CDOT's approach involved instrumenting sections to measure strains, traffic, and temperature variations, leading to findings that underscored the necessity of good bonding between concrete and asphalt and recommending a joint spacing of 6 feet in both directions. Their design process is mechanistic-empirical, involving determination of critical load locations, analysis of load-induced stresses (accounting for partial bond and temperature effects), and culminating in revised design equations for concrete stress and asphalt strain.

2.4.3 NJDOT

NJDOT developed a mechanistic-empirical design procedure for ultra-thin whitetopping (UTW) based on field experience from an instrumented I-295 ramp project (initiated in 1994) and Finite Element Analysis (FEM). Their objective was to identify critical factors for UTW performance through field testing (HWD, FWD, DCP, etc.) and FEM simulations. The resulting interim design procedure is a multi-step process that includes traffic data analysis (ESALs), characterization of the existing asphalt, calculation of allowable tensile stresses in asphalt and UTW (considering axle loads and temperature differentials), and iterative thickness determination based on fatigue considerations and comparison of bonded and unbonded design scenarios.

2.4.4 Caltrans

Caltrans is in the process of refining its approach to thin BCOA. While their current guide offers limited information on bonded overlays, Caltrans initiated research (Project 4.67) to develop a mechanistic-empirical design method suitable for its network by evaluating existing methods like MEPDG and BCOA-ME. Caltrans' evaluation identified several limitations in these existing methods, including inadequate modeling of faulting, the influence of asphalt base fatigue resistance, slab size effects, concrete properties (CTE, shrinkage), asphalt base type, shoulder type, and the need for California-specific climatic calibration. They also noted concerns regarding reliability approaches and the lack of support for rapid-strength concrete. The recommendation is through local calibration if existing methods are to be adopted.

2.5 International Methods

2.5.1 British

Table 2-8 presents the summary of the UK concrete overlay. As shown in the table, CRCP overlays may be used as rehabilitation method for existing flexible pavements. It also mentions that the existing flexible pavement which undergoes overlay will be acceptable and no surface treatment will be necessary other than remedial works. This method is discussed on RILEM (The International Union of Laboratories and Experts in Construction Materials, Systems and

Structures) state-of-the-art report (Bissonnette et al., 2011). The overlay is based on the flow chart shown in Figure 2-20.

Table 2-8 Summary of UK concrete overlay on concrete pavement

Overlay	Existing Pavement		
	Flexible or flexible composite	URC or JRC	CRCP
URC	2	3	1
JRC	2	3	1
CRCP	1	4	1

Notes:
1. Acceptable and no surface treatment other than remedial works is normally necessary.
2. Separation membrane required.
3. No treatment other than remedial works is normally necessary, but joints should occur above one another.
4. This combination not normally appropriate.
5. URC = Unreinforced concrete
   JRC = Jointed reinforced concrete CRCP = Continuously reinforced concrete pavement

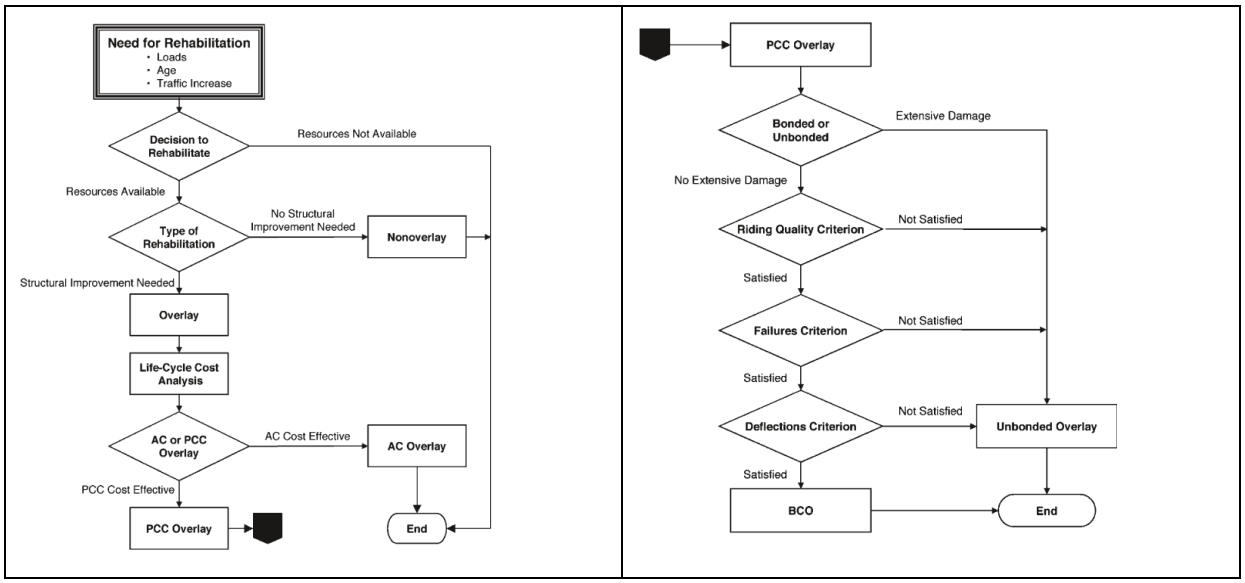

Figure 2-20 Flowchart of overlay design for British Method (BritPave, 2018)

The thickness design used in UK or British Method is a function of structural capacity of existing pavement and structural capacity of BCO to fulfill future traffic requirements. The overlay design is carried based on charts which gives thickness for CRCP overlay which is shown in Figure 2-21 (O' Flaherty, 2007). It utilizes the equivalent surface foundation modulus (ESFM) as a measure of the strength of the existing road structure. It is modulus of a uniform elastic

foundation which gives the same deflection under the same wheel load as that of the existing structure.

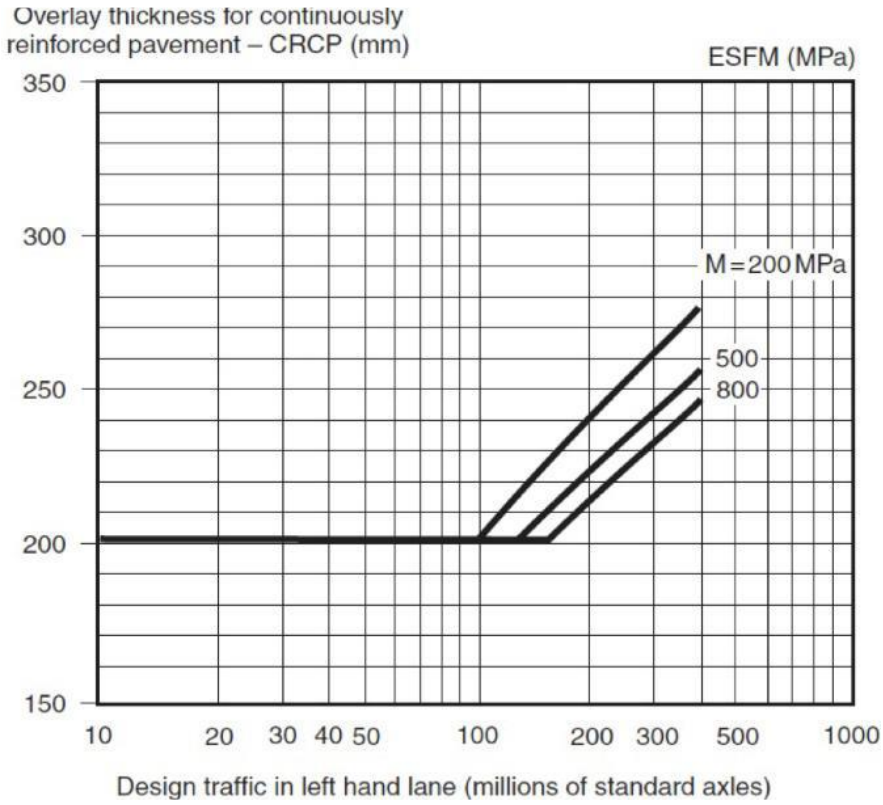

Figure 2-21 Deign thickness for CRCP overlay (O' Flaherty, 2007)

2.5.2 Austria

The Austrian mechanistic-empirical (ME) design method for bonded whitetopping overlays combines detailed structural analysis with empirical data to optimize the rehabilitation of asphalt pavements. This method was formalized through a doctoral research effort at the Vienna University of Technology. Figure 2-22 illustrates the design methodology. Key to this approach is a thorough assessment of the existing HMA pavement's residual bearing capacity, determined either visually or through FWD testing. The method also specifies design considerations for the overlay structure itself, including nearly square slab geometries with undoweled joints, and emphasizes keeping longitudinal joints out of wheel paths to prevent high edge stresses. Input parameters meticulously account for temperature-dependent material behavior (especially for the HMA and the interface bond), standardized traffic loads using equivalence factors for regional applicability, and seasonal climatic variations affecting subgrade support and thermal gradients.

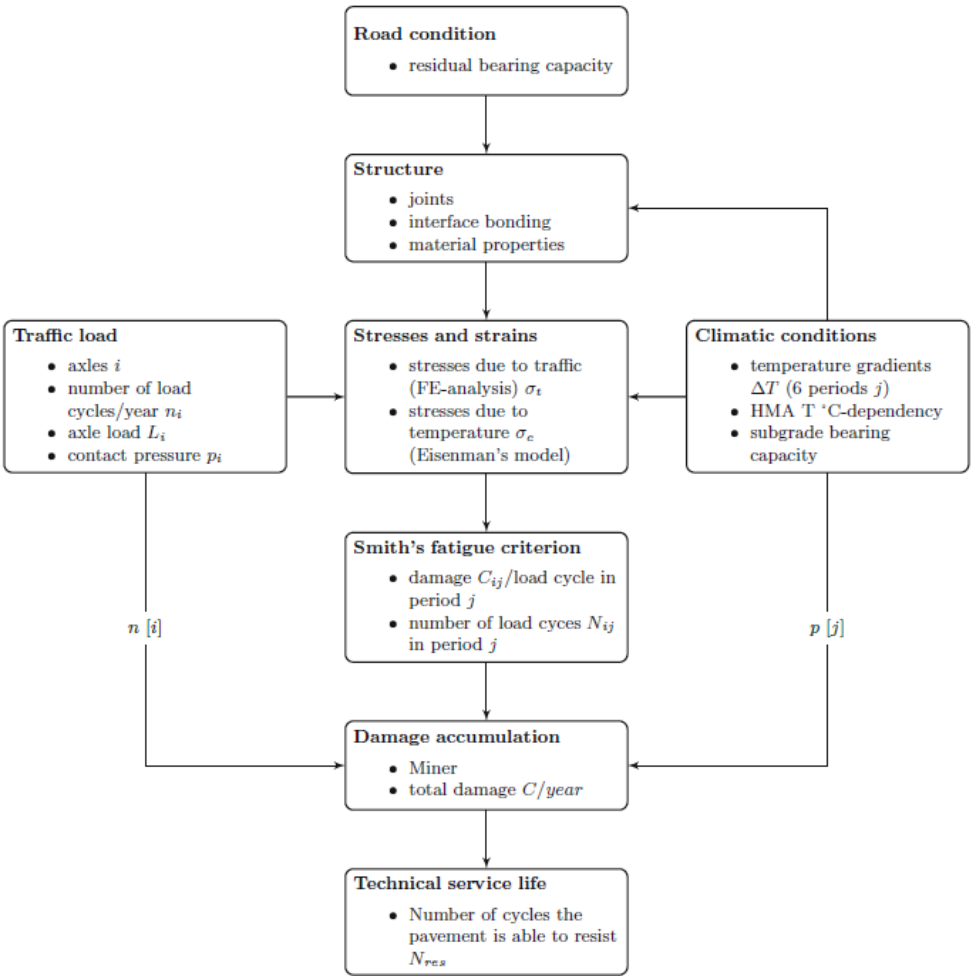

Figure 2-22 Austra Design Methodology

A significant aspect of the Austrian method is its sophisticated consideration of the interface bonding conditions between the concrete overlay and the existing asphalt, moving beyond simple assumptions of full bonding. It utilizes a Cohesive Zone Model (CZM), implemented in Abaqus FE software, with parameters derived from experimental tests (pull-off, wedge splitting, shear resistance) conducted at various temperatures to reflect seasonal changes in bond behavior. Stresses are determined by combining curling stresses (from Eisenmann's model using locally derived temperature gradients) and traffic load stresses (from detailed 3D FE models incorporating the CZM and other inputs). The design life is then assessed by comparing the number of load cycles the pavement can resist (N_{res}), calculated using Smith's fatigue criterion and Miner's rule for cumulative damage, against the expected number of imposed load cycles (N_{imp}) over the design period.

The application of this ME design method, considering various slab sizes, thicknesses, and existing HMA conditions, has led to the development of a practical design catalogue for bonded concrete overlays in Austria (Figure 2-23). This catalogue provides required overlay thicknesses for typical regional road load classes and carriageway widths, based on a 70% residual bearing

capacity of the HMA and a minimum 5 cm (2-inches) HMA thickness. It also includes adjustment factors for deviations in residual bearing capacity, existing HMA thickness, and selected joint spacing, allowing for a more tailored and potentially economical overlay design. This performance-based approach aims for more realistic and durable whitetopping solutions by integrating detailed, site-relevant parameters.

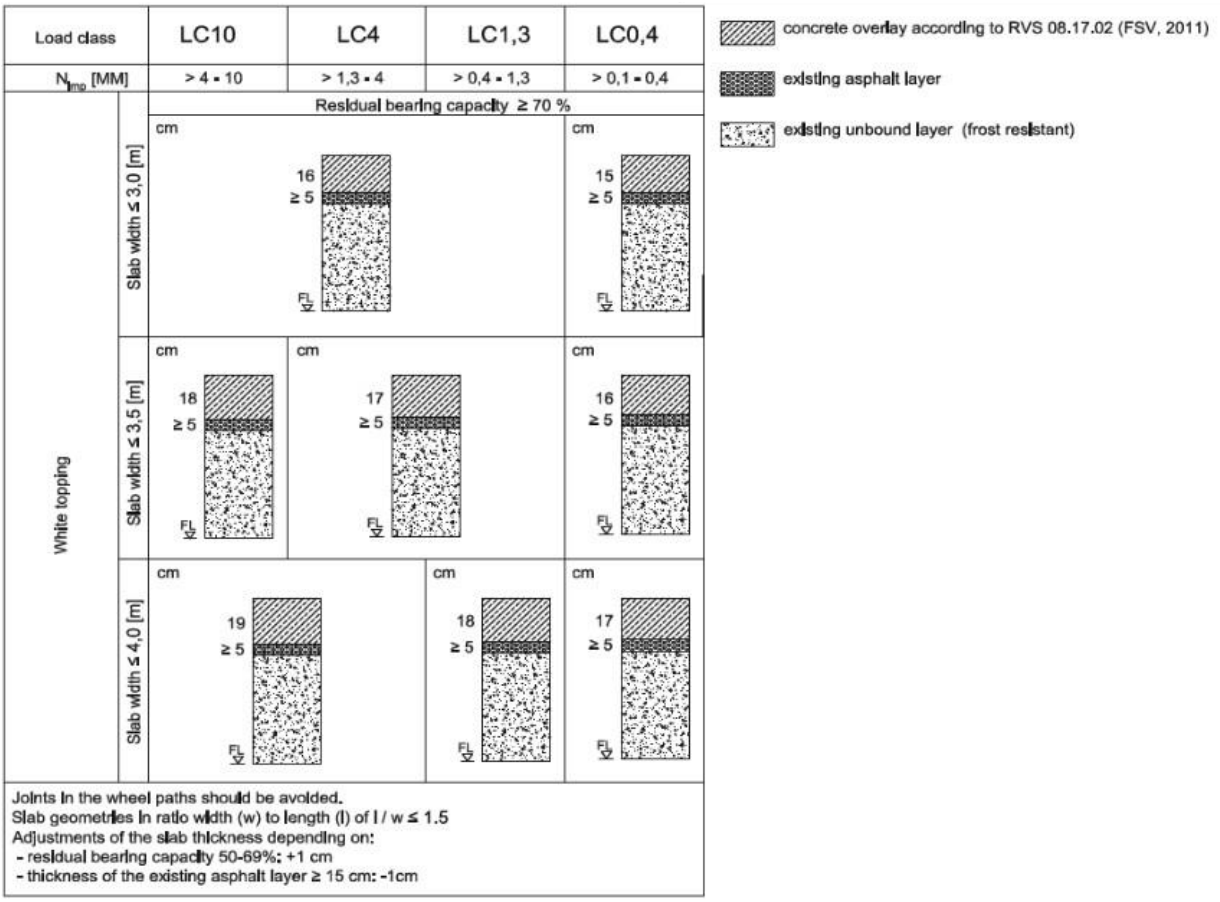

Figure 2-23 Design Catalogue

2.6 Overview of existing CPCD Whitetopping in Texas

The concept of whitetopping, placing a concrete overlay over existing asphalt, dates back over a century. The first known whitetopping project in the U.S. was constructed around 1918 on South 7th Street in Terre Haute, Indiana. This early project used Jointed Reinforced Concrete Pavement (JRCP) at a thickness of approximately 3 to 4 inches (McGhee, 1994). Nearly five decades later, the first documented application of CRCP over asphalt was undertaken at Midway Airport in Chicago, Illinois in 1967. This airfield project featured an 8-inch concrete slab. Unfortunately, no long-term performance records are available for that installation.

It wasn't until after the mid-1970s that whitetopping began gaining widespread popularity as a pavement rehabilitation strategy. Historically, most early whitetopping projects utilized CPCD, while very little research or design guidance was developed specifically for CRCP placed over

asphalt. Challenges with CPCD over asphalt, such as poor load transfer and premature joint distress, have prompted interest in CRCP as a more durable alternative. This section focuses on the performance and considerations of CPCD whitetopping, with an emphasis on its application in Texas.

Whitetopping has proven to be a viable option for rehabilitating deteriorated Hot Mix Asphalt Concrete (HMAC) pavements. However, its success heavily depends on the structural integrity of the underlying asphalt. Unfortunately, many whitetopping projects lack a thorough evaluation of the existing HMAC pavement, leading to designs that may not be well-suited for actual field conditions. Furthermore, many whitetopping designs rely on rigid pavement design principles similar to those outlined in the AASHTO(2008) Guide. These principles often assume that the high stiffness of the concrete slab minimizes the impact of sub-base support on long-term performance. Additionally, they propose that thicker concrete layers can sufficiently distribute wheel loads, thereby reducing stress on the sub-base. However, applying these assumptions to whitetopping, particularly when using thin overlays between 2 to 4 inches, can lead to two major problems.

First, the assumption that sub-base stress is negligible becomes invalid for thinner whitetopping sections, which do not have enough stiffness to shield the sub-base effectively. Second, the jointing systems used in conventional whitetopping do not typically account for the flexural (bending) behavior of the slab unless very tight joint spacing is adopted. In reality, wheel load-induced stresses are influenced not only by slab thickness and load magnitude but also by slab size and support conditions. This is evident in Figures 2-24a and 2-24b, which compare the deflection behavior of 12-ft × 12-ft and 6-ft × 6-ft slabs, respectively. The smaller slab behaves more like a rigid block being pushed downward, whereas the larger slab shows more bending-induced deflection.

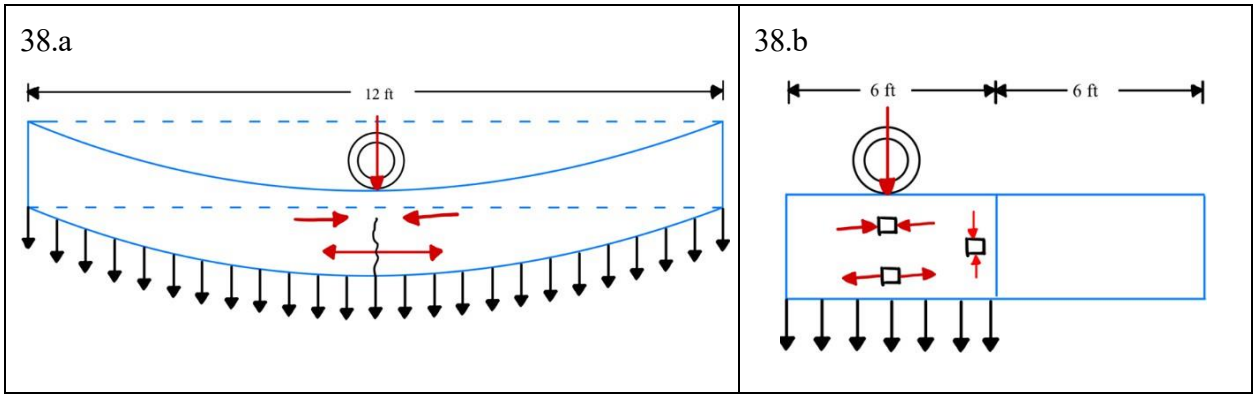

Figure 2-24a. Wheel Load bending at the intersection on 12ft slab size and 24b. Wheel load bending at the intersection of 6ft slab size

Thus, the use of smaller joint spacing aligns with the beneficial utilization of one of the concrete properties, which is that concrete is stronger in compression than in bending or tension. However, when the Minnesota DOT implemented this concept in their test projects, distresses

known as diamond cracks developed at the intersections of joints as shown in Figure 2-25 (Burnham, 2005).

Figure 2-25 Diamond cracking as seen in Minnesota (Burnham, 2005)

The primary reason for these distresses was due to the wheel load path. It was observed that engineers overlooked the fact that heavy truck traffic wanders as any vehicles would. This made the intersecting joints' weak points in the pavement, i.e., the loading condition became "corner loading", rather than "interior loading", which increased concrete stresses and deflections and resulted in diamond cracking. From the Westergaard's closed form equations for stress and deflection for three conditions: interior, edge, and corner, subjecting the slab with that sawcut configuration leads to corner loading. The stress and deflections are larger at the corner compared to the interior loading condition. This points out the limitations of some of the whitetopping design philosophies discussed above.

2.6.1 Field Performance Evaluation of Whitetopping Sections in Texas

Texas so far has been able to work around this philosophy while implementing the design methods for whitetopping. However, as iterated earlier its current slab thickness design requires further improvement. It is believed that a better whitetopping design considering the structural condition of existing asphalt pavement needs to be developed, and this research study attempts to address this needed improvement. It is also important to note that currently Texas has been mainly using its whitetopping design at intersections and as well as in some main lanes. The reason for using whitetopping at the intersection is due to the fact that the traffic at intersections is mostly a stop-and-go operation and that asphalt pavement undergoes rutting and shoving

distresses, with a potential for hydroplaning (Zhou et al., 2013). Figure 2-26a and Figure 2-26b shows the image of rutting and shoving at the intersection.

40a.

40b.

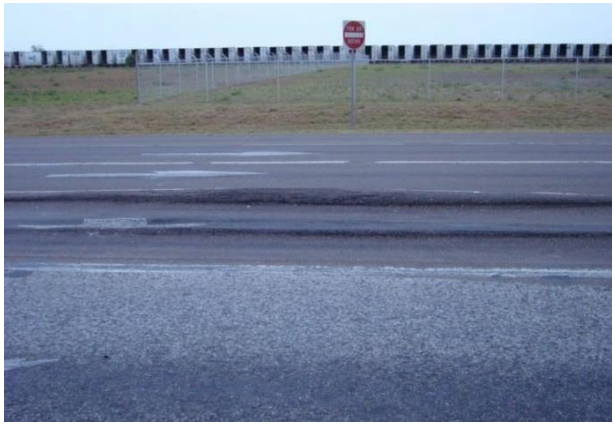

Figure 2-26a. Image of rutting at Intersection 26b. Image of shoving at Intersection

During rainfall events, water will accumulate, and hydroplaning may occur. Whitetopping could address this issue quite effectively and be a cost-effective rehabilitation solution. There are several whitetopping projects at the intersections in Texas, such as SH36 in Abilene, US69 in Emory, West Loop 250 North in Midland, 42nd Street in Odessa, and SH-206 in Cross Plains. In addition, these projects have been in service beyond its design life and are, generally, in good condition.

To better understand the performance of the existing whitetopping section in Texas, we surveyed a few whitetopping sections. This includes the Emory whitetopping (Paris District), the Baytown whitetopping (Beaumont District), and the Midland whitetopping (Odessa District). The primary objective of these surveys was to document the in-service performance characteristics and identify prevalent distress mechanisms, particularly focusing on factors influencing ride quality. The observations suggest potential limitations in the long-term performance of CPCD whitetopping designs under specific traffic and environmental conditions.

Site Descriptions and Traffic Characteristics

Detailed information for each surveyed location is as follows (Figure 2-27):

- **Emory Whitetopping (Paris District):** Constructed in 2012, this section had accumulated approximately 13 years of service life at the time of the survey. It experiences substantial traffic loading, with a reported Average Annual Daily Traffic (AADT) of approximately 24,422 vehicles, of which 13.7% constitutes truck traffic.
- **Baytown Whitetopping (Beaumont District):** This section was constructed in 2016, corresponding to an approximate service life of 9 years. The traffic volume is lower than Emory, with an AADT of roughly 7,634 vehicles, but with a higher proportion of heavy vehicles, indicated by 16.4% truck traffic.

- **Midland Whitetopping (Odessa District):** Representing the oldest section, this whitetopping was constructed in 2001, yielding an approximate service life of 24 years. The performance evaluation focused on three distinct intersections within this section, exhibiting varied traffic demands:
    - Midland Drive Intersection: AADT ≈ 18,225 vehicles; Truck Traffic = 20.3%
    - N Midkiff Intersection: AADT ≈ 16,616 vehicles; Truck Traffic = 14.5%
    - N Garfield Intersection: AADT ≈ 9,662 vehicles; Truck Traffic = 15.6%

27a.

27b.

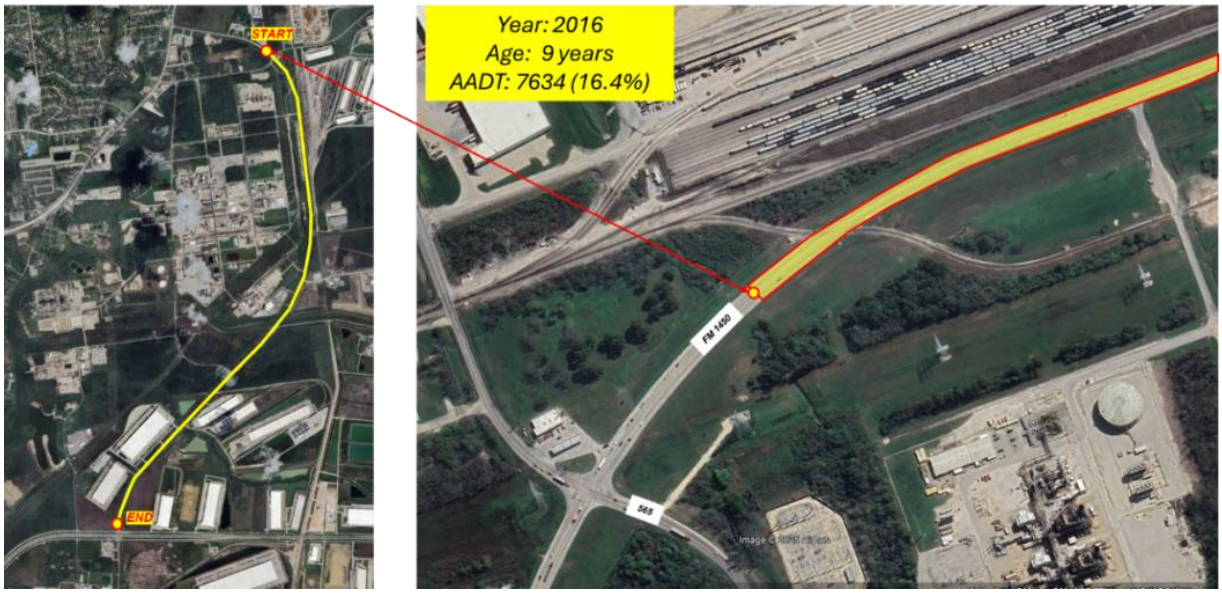

27c.

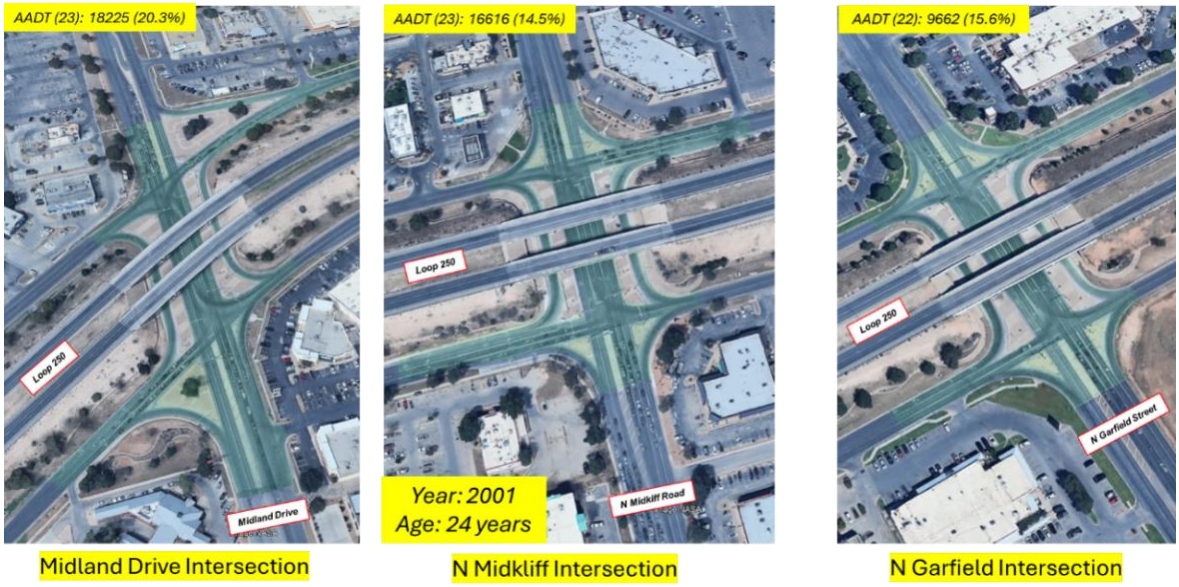

Figure 2-27a. Emory Whitetopping, 41b. Baytown Whitetopping and 41c. Midland Whitetopping

Observed Pavement Distresses

Consistent distress patterns were observed across all three surveyed locations, challenging some of the fundamental design assumptions for whitetopping.

Slab Separation

A prominent observation was the separation occurring between adjacent PCC slabs, both longitudinally and transversely (as depicted in Figure 2-28 from Emory and Figure 2-29 from Midland). This separation, reaching magnitudes as large as 2 inches in some instances, indicates a loss of continuity within the pavement structure. This phenomenon is largely attributed to the absence of dowel bars at the transverse joints. Dowel bars are critical for load transfer between adjacent slabs and for maintaining horizontal alignment. Their absence permits independent slab movement under thermal stress and traffic loading. Furthermore, the observed separation suggests that the assumption of a persistent, perfect bond between the PCC overlay and the underlying HMA layer may be invalid under field conditions. Debonding allows for greater independent movement of the PCC slabs, exacerbating separation. The primary functional consequence of slab separation is a degradation of pavement smoothness and ride quality.

Figure 2-28 Slab Separation of 2-inches observed in Emory, Texas

Figure 2-29 Slab Separation of 1-inches observed in Midland, Texas

Slab Sliding

Closely associated with, and likely a precursor to, slab separation is the phenomenon of slab sliding (Figures 2-30 & Figure 2-31). This refers to the horizontal displacement of slabs relative to the underlying HMA layer and adjacent slabs. This distress mechanism is again linked to the failure or absence of an effective bond between the PCC and HMA layers, negating the assumed composite behavior. The lack of lateral confinement, potentially due to inadequate shoulder support or absence of integrated curbs, can further facilitate this sliding movement.

19a.

19b.

Figure 2-30 Slab Sliding observed in Emory, Texas

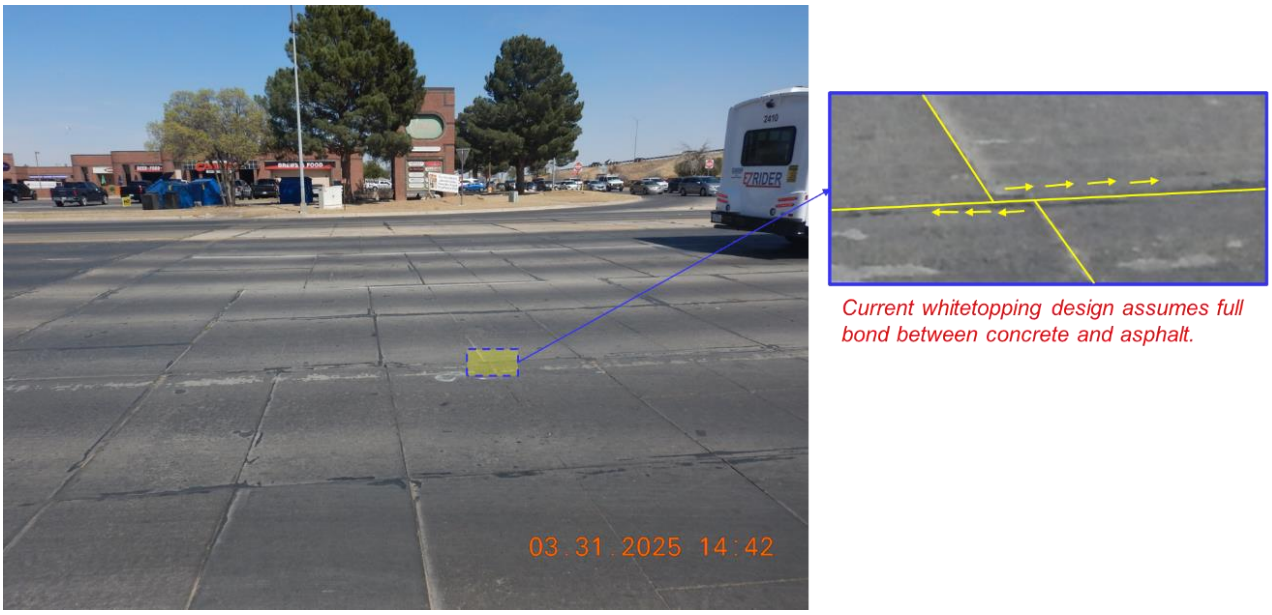

Figure 2-31 Slab Sliding observed in Midland, Texas

Faulting

Consequent to the lack of load transfer mechanisms (i.e., no dowels) and the potential for independent slab movement (sliding and separation), faulting was observed (Figure 2-32). Faulting is the differential vertical displacement between adjacent slabs at joints or cracks. As traffic loads traverse a joint, the unloaded slab edge may experience upward movement or rotation ("twisting"), while the loaded slab deflects downwards. This creates an elevation difference, resulting in impact loading and a characteristic "bumpy" or rough ride experienced by vehicle occupants.

Figure 2-32 Faulting observed in Emory, Texas

Ride Quality Assessment

To quantitatively assess the impact of these distresses on ride quality, a preliminary investigation was conducted using a vehicle-mounted GoPro camera equipped with an accelerometer. Comparative measurements were taken over an initial 300-foot section of CRCP immediately followed by the adjacent whitetopping section. Analysis of the accelerometer data (Figure 2-33) revealed significantly higher amplitude fluctuations and variability when the vehicle traversed the whitetopping section compared to the smoother profile observed on the CRCP. This provides objective evidence correlating the observed distresses (separation, sliding, faulting) in the un-doweled whitetopping with diminished ride quality.

Figure 2-33 Ride Quality Assessment between CRCP and CPCD Whitetopping section

Repair Strategy and Implications

Field observations indicated that localized distresses and areas exhibiting poor ride quality on the surveyed whitetopping sections were being repaired using CRCP patching techniques (Figure 2-34). The selection of CRCP as a repair material is significant. It implies that restoring ride quality and structural integrity in these distressed areas necessitates a pavement type with inherent mechanisms for maintaining smoothness and structural continuity, namely continuous reinforcement. This suggests that the performance limitations observed in the surveyed (presumably JPCP) whitetopping sections may be inherent to the design's lack of reinforcement and load transfer devices. Consequently, mitigating these ride quality issues may require transitioning towards designs incorporating positive load transfer (e.g., doweled JPCP whitetopping) or continuous reinforcement (CRCP whitetopping) for similar applications and traffic levels.

Figure 2-34 Localized distress in CPCD Whitetopping repaired using CRCP

The field surveys of the Emory, Baytown, and Midland whitetopping sections highlight significant performance challenges associated with undoweled designs, particularly concerning slab separation, sliding, and faulting. These distresses appear linked to the absence of dowel bars for load transfer and the apparent failure of the assumed PCC-HMA bond under long-term traffic and environmental loading. The resulting degradation in ride quality, confirmed by accelerometer measurements, necessitates intervention. The observed use of CRCP for repairs suggests its perceived superiority in addressing these specific failure modes, potentially guiding future design considerations for whitetopping applications in Texas.

2.7 Summary and Research Gaps

The major findings from the Literature Review are as follows:

1. Lack of Field Validation for Existing Design Algorithms

Many existing design procedures for concrete overlays use complex computational models, but:

- They are not adequately validated using real-world field performance data.
- This raises concern over the accuracy and reliability of these models.

Core Issue: There's a disconnect between theoretical models and actual field performance, making designs potentially untrustworthy.

2. Limited Research on CRCP Overlays over Asphalt

There is very little published information on how CRCP overlays perform when placed on asphalt bases, and:

- The AASHTOWare MEPDG uses the same failure criteria (punchout and IRI) for CRCP overlays as it does for new CRCP, which may be inappropriate.
- Its punchout model relies heavily on load transfer efficiency (LTE) and crack spacing, yet these factors may not influence punchouts as much in overlays.

Core Issue: Failure mechanisms specific to CRCP-over-asphalt overlays are misunderstood or misrepresented, potentially leading to incorrect designs.

3. Unclear Understanding of PCC-Asphalt Bonding Mechanism

The bonding behavior between concrete and asphalt is poorly understood:

- Field observations (e.g., in Texas whitetopping) suggest bond strength diminishes over time.
- It is unclear whether debonding occurs at the concrete-asphalt interface or within the asphalt layer itself.
- Existing design procedures do not account for or monitor bonding degradation over time.

Core Issue: Lack of understanding of bonding mechanisms between overlay and base layers introduces uncertainty in performance predictions and durability.

4. Absence of Deflection-Based Design in Current Methods

Current design methods:

- Do not incorporate pavement deflection response as part of the design process.
- Rely instead on sophisticated modeling tools to simulate behavior and performance (e.g., fatigue, thermal cracking, IRI).
- But deflection is a direct indicator of structural adequacy and base support, especially critical for overlays.

Core Issue: Deflection behavior, a critical field-measurable parameter, is missing from design protocols, despite its strong relevance to structural health.

CHAPTER 3
NATIONWIDE PRACTICE SURVEY

This chapter details the findings from a nationwide survey conducted to understand the current state of practice, experiences, and design methodologies related to Continuously Reinforced Concrete Pavement (CRCP) overlays and other concrete overlay systems.

3.1 Survey Design and Distribution

The survey was developed and distributed by the research team. The primary objective was to gather fact-based information on the prevailing practices across various transportation agencies.

The survey was distributed to two main groups:

- The TxDOT Project Team.
- The AASHTO Committee on Materials and Pavements.

The survey instrument was designed to cover a comprehensive range of topics pertinent to CRCP and White-Topping (WT) overlays. It was basically divided into four parts.

- ***Part 1: Definitions and General Practices***

The survey question in this part was to determine whether other transportation agencies align with TxDOT's definition for bonded and unbonded overlays, and whitetopping.

- ***Part 2: Continuously Reinforced Concrete Pavement (CRCP) Overlays***

This part was to assess the extent of use, design preferences, and experience levels of agencies with CRCP overlays.

- ***Part 3: Thin Whitetopping (TWT) Overlays***

This part was to explore national practices, specifications, and project considerations around WT.

- ***Part 4: Pavement Evaluation and Overlay Candidate Selection***

This part was to understand how agencies evaluate existing pavement to decide on overlay suitability and type.

3.2 Respondent Profile

Responses were received from a range of transportation agencies across North America.

Geographical Distribution

A total of 36 percent of U.S. States and the Canadian Province of Ontario responded to the survey. The U.S. states that participated include Alabama, Delaware, Illinois, Indiana, Kentucky, Minnesota, Missouri, Nebraska, Nevada, Ohio, South Carolina, South Dakota, Texas, Utah, Virginia, Washington, and West Virginia as shown in Figure 3-1. The respondents primarily represented the State Departments of Transportation (DOTs). The survey requested information on "Agency or University," with the vast majority of detailed responses attributable to state agencies.

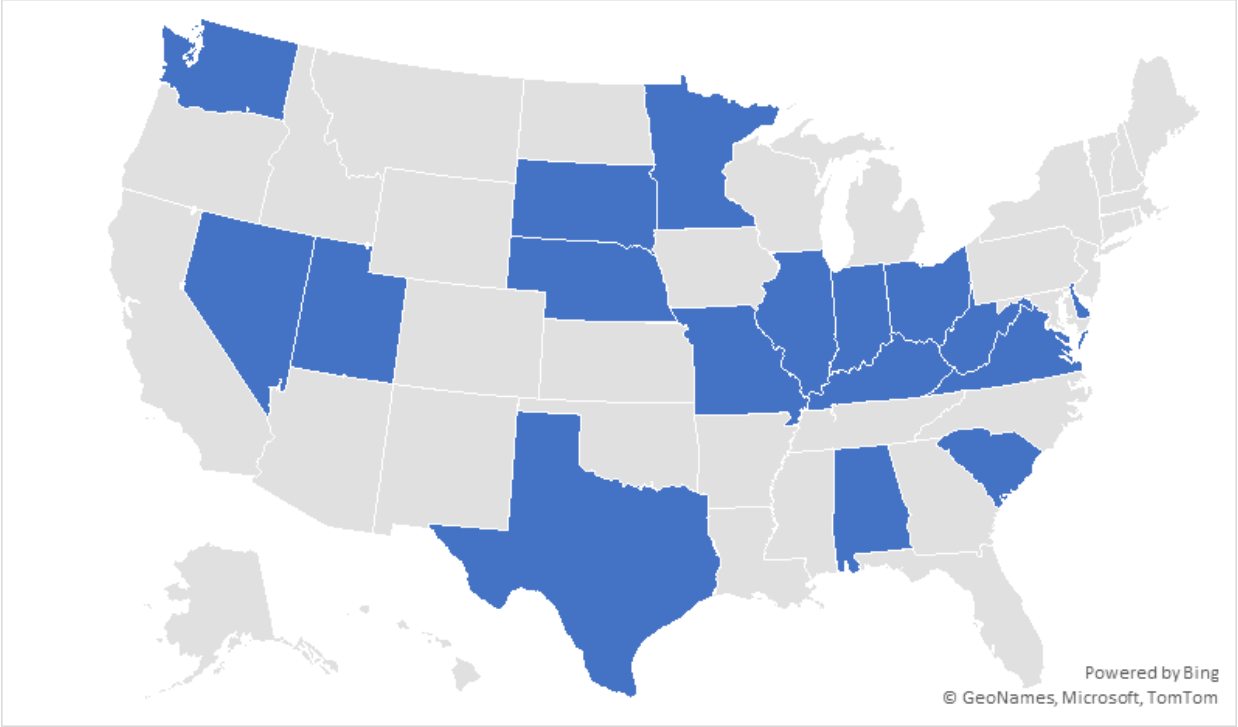

Figure 3-1 States that participated in the survey

3.3 Survey Response

3.3.1 Part 1 - Definitions and General Practices

Three questions were asked in this part. The idea was to understand whether other transportation agencies align with TxDOT's definitions for bonded and unbonded overlays, and thin whitetopping (TWT).

The definition as defined by TxDOT for each overlay practice is as follows:

Bonded Concrete overlay(BCO)

"Bonded concrete overlay (BCO) consists of a 2-in. to 8-in. thick concrete layer placed on top of the existing concrete pavement with operations conducted to ensure full bond between new and old concrete layers."

Unbonded Concrete overlay(BCO)

"Unbonded concrete overlay consists of a concrete layer (5 in. or greater) on top of an existing concrete with HMA interlayer to separate new overlay and existing concrete."

Thin Whitetopping(TWT)

"Thin white-topping (TWT) is a 4- to 7-in. thick concrete overlay bonded to an existing asphalt concrete pavement (ACP) to create a composite section."

Figure 3-2 shows the responses from the agencies. There is a significant lack of uniform, standardized definitions for common concrete overlay types (Bonded Concrete Overlay, Unbonded Concrete Overlay, and Thin White-Topping) across responding transportation agencies when compared to TxDOT's definitions.

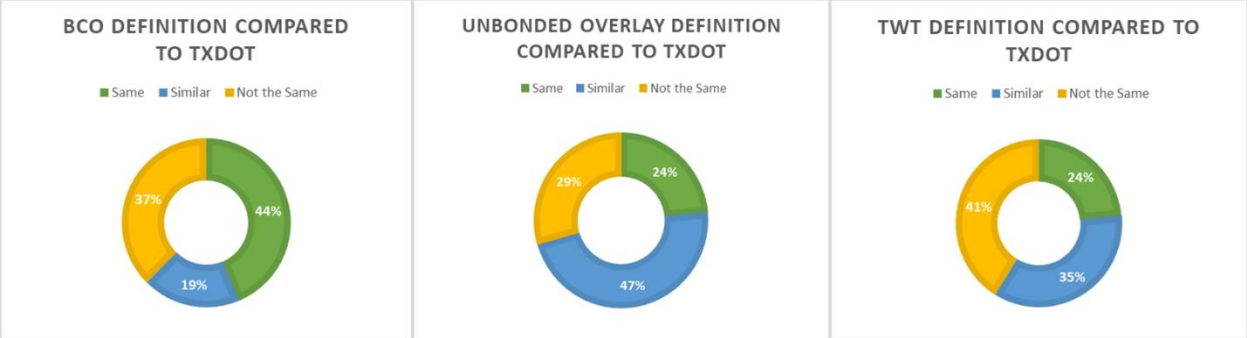

Figure 3-2 Responses from agencies on each definition

As noted by respondents in the survey that the divergence is not merely semantic but often stems from absence of formal definitions, particularly if the practice is not common within their jurisdiction. The most notable variation is in the specified thickness range for each overlay type. Other technical details, like the type of interlayer for unbonded overlays, also differ. Some agencies also noted that they do not use certain overlay types and therefore have not developed or adopted specific definitions.

3.3.2 Part 2 - Continuously Reinforced Concrete Pavement (CRCP) Overlays

Six questions were asked in this part of the survey. The main objective was to:

- Understand who is using CRCP and at what stages (design, construction, maintenance, evaluation).
- Gather detailed data on minimum thickness, construction practices, and joint/repair design standards.
- Discover how agencies adapt CRCP for intersections and what data they rely on for performance evaluations.

The primary insight emerging from questions on CRCP overlays is that CRCP is a specialized and not widely adopted practice among the responding transportation agencies. As shown in Figure 3-3, a large majority of agencies surveyed do not utilize CRCP.

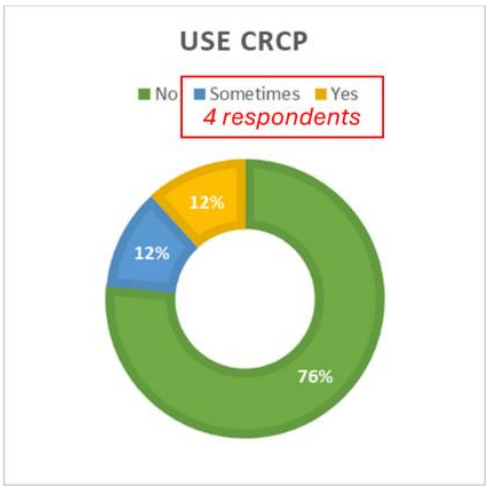

Figure 3-3 Percentage of agencies using CRCP

As shown in Figure 3-4, Among the agencies that do use CRCP, direct experience is not evenly distributed. There's a notable gap between a small pool of highly experienced veterans (over 10 years of experience) and a larger group with minimal to no personal experience in various facets of CRCP projects. This suggests that a deep knowledge of CRCP expertise is concentrated and polarized at the same time.

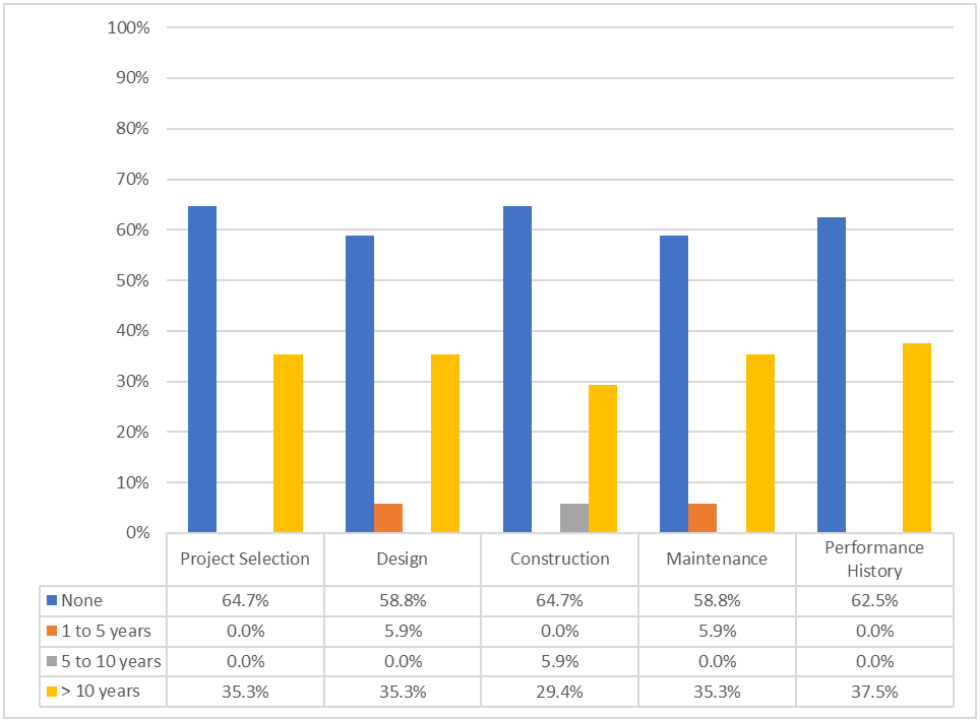

	Project Selection	Design	Construction	Maintenance	Performance History
None	64.7%	58.8%	64.7%	58.8%	62.5%
1 to 5 years	0.0%	5.9%	0.0%	5.9%	0.0%
5 to 10 years	0.0%	0.0%	5.9%	0.0%	0.0%
> 10 years	35.3%	35.3%	29.4%	35.3%	37.5%

Figure 3-4 CRCP experience level for project selection, design, construction, maintenance, and performance evaluation

It was also noted that CRCP when implemented, it is generally designed with substantial minimum thickness (7-9 inches). Figure 3-5 illustrates that standardized details for many

structural components are common. However, its application and specialized design considerations are predominantly geared towards mainline pavements. As shown in Figure 3-6 most agencies, with the exception of TxDOT, do not report making specific design adjustments for CRCP in more complex scenarios like urban intersections, often because its use is limited in such areas. Two agencies' respondents did mention using high early strength concrete and changing curing time or curing compound requirements.

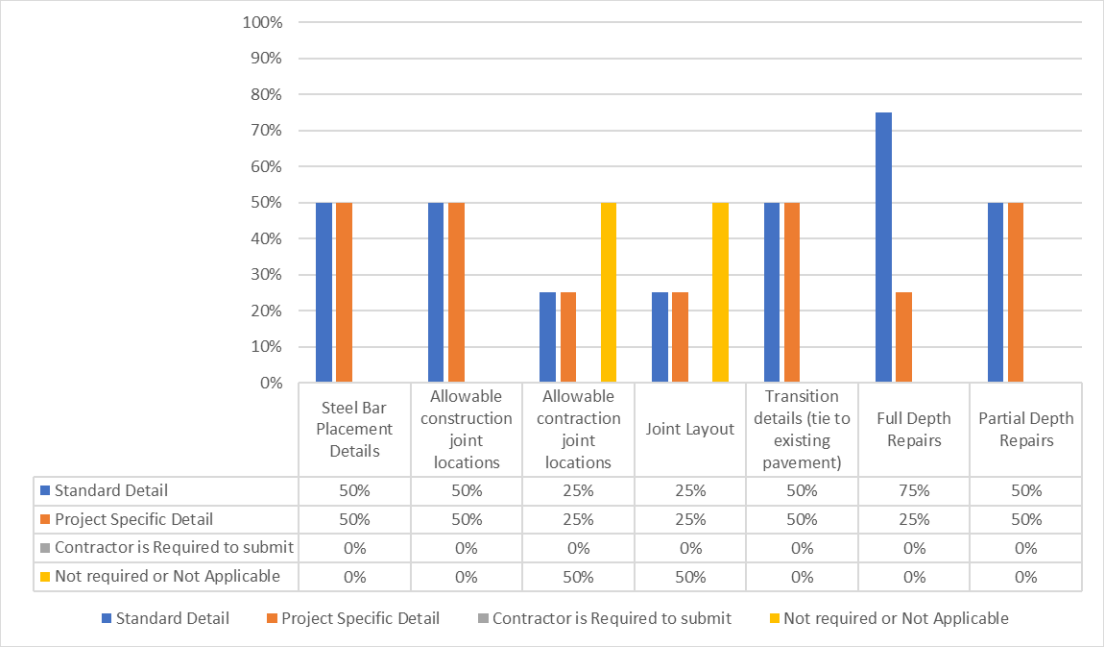

Figure 3-5 CRCP Design Details

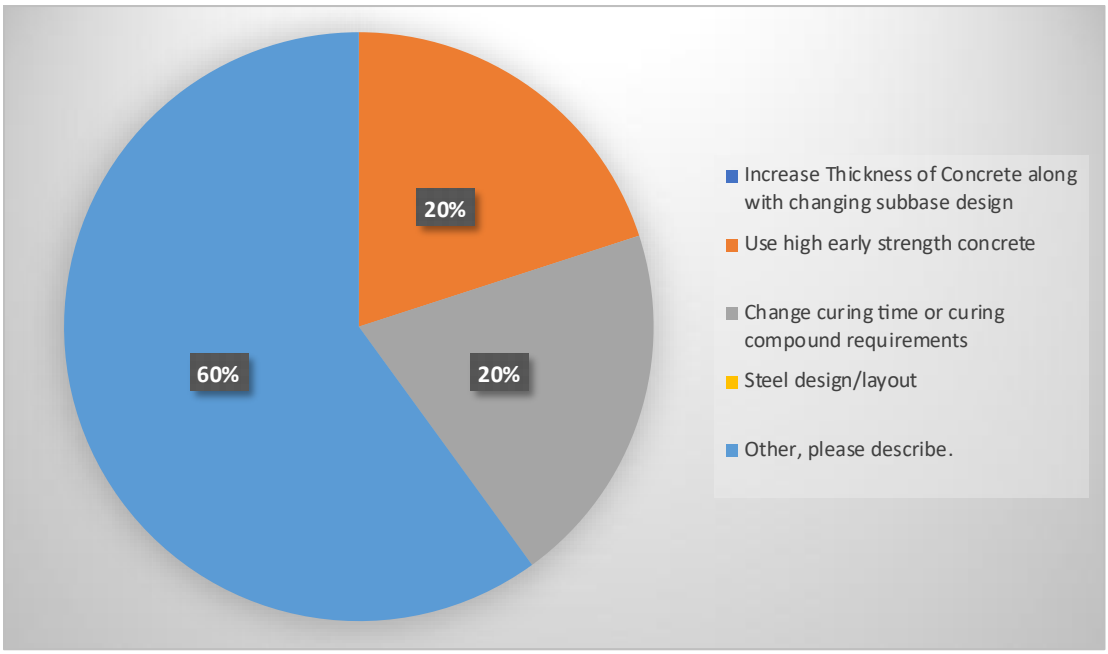

Figure 3-6 CRCP design conditions at intersections

Also, Agencies that use CRCP employ a fairly comprehensive and standard set of metrics to evaluate their long-term performance, focusing on common distress types, ride quality, and overall condition (Figure 3-7).

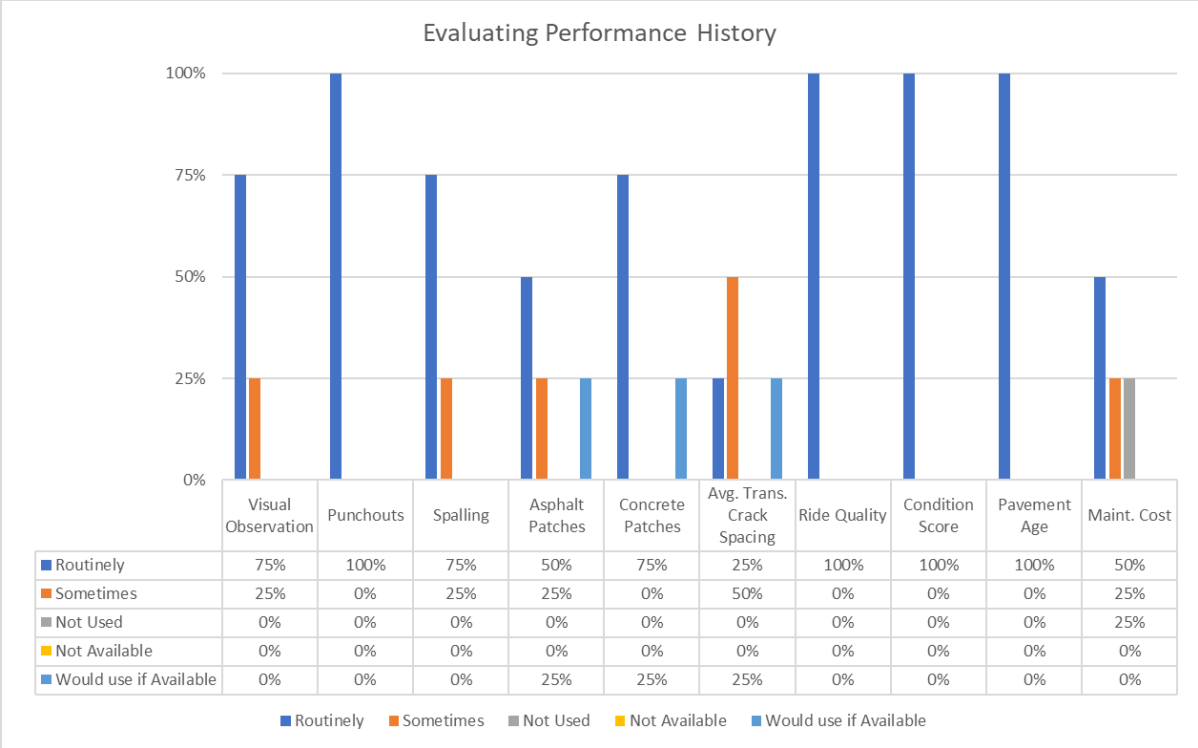

	Visual Observation	Punchouts	Spalling	Asphalt Patches	Concrete Patches	Avg. Trans. Crack Spacing	Ride Quality	Condition Score	Pavement Age	Maint. Cost
Routinely	75%	100%	75%	50%	75%	25%	100%	100%	100%	50%
Sometimes	25%	0%	25%	25%	0%	50%	0%	0%	0%	25%
Not Used	0%	0%	0%	0%	0%	0%	0%	0%	0%	25%
Not Available	0%	0%	0%	0%	0%	0%	0%	0%	0%	0%
Would use if Available	0%	0%	0%	25%	25%	25%	0%	0%	0%	0%

Figure 3-7 Evaluation of Performance history

In essence, while there are established practices for designing and evaluating CRCP among its users, the limited adoption, the nature of existing expertise, and the predominant focus on mainline applications suggest that any efforts to broaden its use or refine its design for specific contexts (like intersections) would need to address potential knowledge gaps and draw from specialized experience of entities like TxDOT.

3.3.3 Part 3 – Thin White-Topping (TWT) Overlays

Ten questions were asked in this part of the survey. The main objective was to:

- Identify which agencies use TWT and their level of involvement at each project stage.
- Understand TWT thickness ranges, design specs, and reinforcement strategies used across agencies.
- Learn how agencies select candidate sites, what construction concerns they prioritize, and how they track long-term performance.
- Overall, this part helps shape a comprehensive picture of current TWT practice and uncover areas for improvement or standardization.

TWT was found to be quite rarely used as an overlay option among the majority of responding agencies. As shown in Figure 3-8, only 6% use it regularly, accounting for almost 71% not using it at all and 23% sometimes.

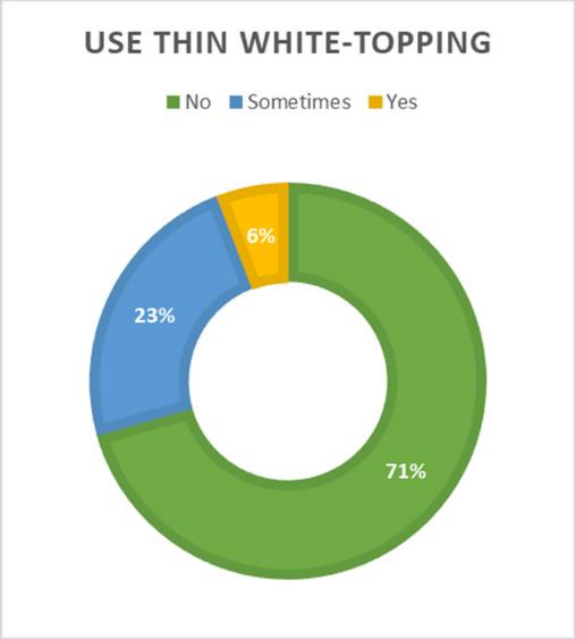

Figure 3-8 Agency using TWT

Figure 3-9 shows that the selection of TWT projects is heavily reliant on the structural integrity and distress condition of the existing pavement, along with anticipated truck volume and traffic loads. However, widely standardized quantitative thresholds for these selection criteria appear uncommon. Table 3-1 summarizes the threshold values set by agencies utilizing thin whitetopping (TWT). The maximum design traffic for which TWT has been applied is 7.5 million ESALs, with a truck volume of up to 500 trucks per day. Several agencies also emphasized the importance of HMA core sampling to assess the structural condition of the existing pavement prior to overlay placement. Notably, one agency specified that at least 85% of the pavement area must retain a minimum of 4 inches of HMA thickness after milling for a project to qualify. Additionally, a maximum of 5% of the surface may consist of exposed PCC or brick beyond which the site is considered unsuitable for TWT application.

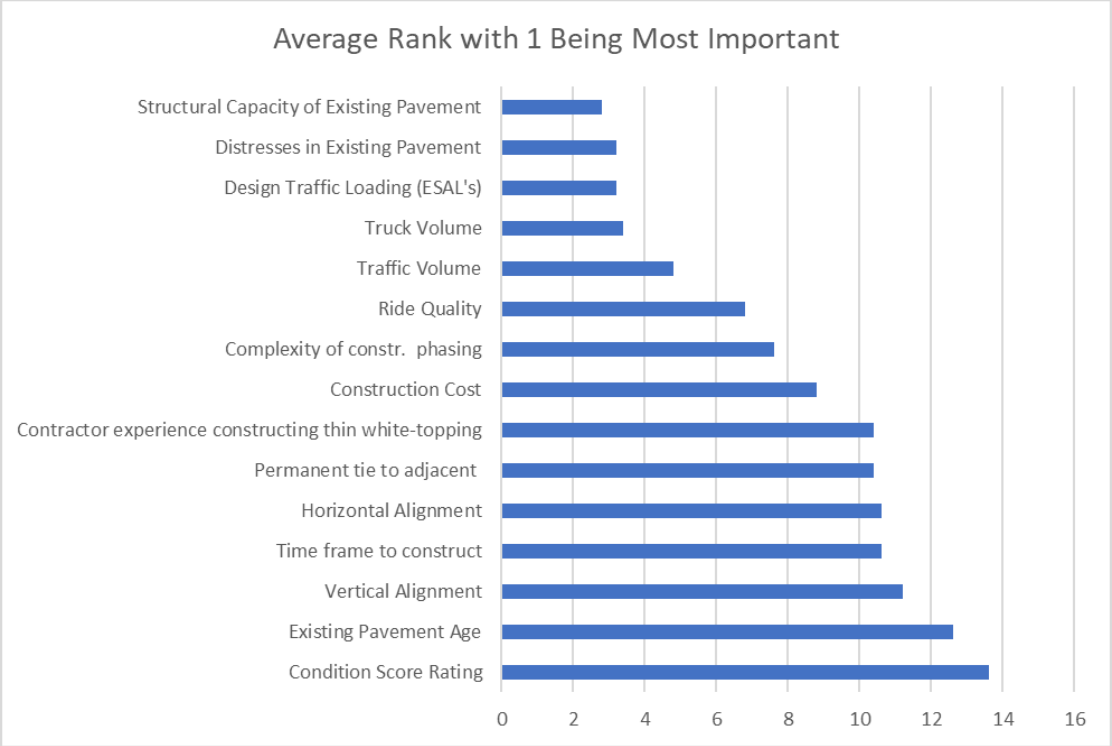

Figure 3-9 Ranking of Selection criteria for TWT Whitetopping

Table 3-1 TWT Candidate Project Evaluation Criteria

Criteria	Minimum	Maximum
Traffic Volume	-	-
Truck Volume	-	500
Design Traffic Loading (ESAL's)	-	7,500,000
Structural Capacity of Existing Pavement	At least three inches of intact HMA remain after milling.	-
Ride Quality/Smoothness	-	-
Distresses in Existing Pavement	No raveling/stripping	-
Contractor experiences constructing thin white-topping	-	-
Time frame to construct Existing Pavement Age	-	-
Condition Score/Rating	-	-

Horizontal Alignment	-	-
Vertical Alignment	-	-
Other, please describe.	• 85% equal or greater than 4" after HMA milling • HMA Cores	5% limit of bare PCC or brick

Figure 3-10 shows the construction of TWT is perceived as technically sensitive, with paramount importance placed on meticulous surface preparation, precise timing of saw cuts, and appropriate curing to ensure performance.

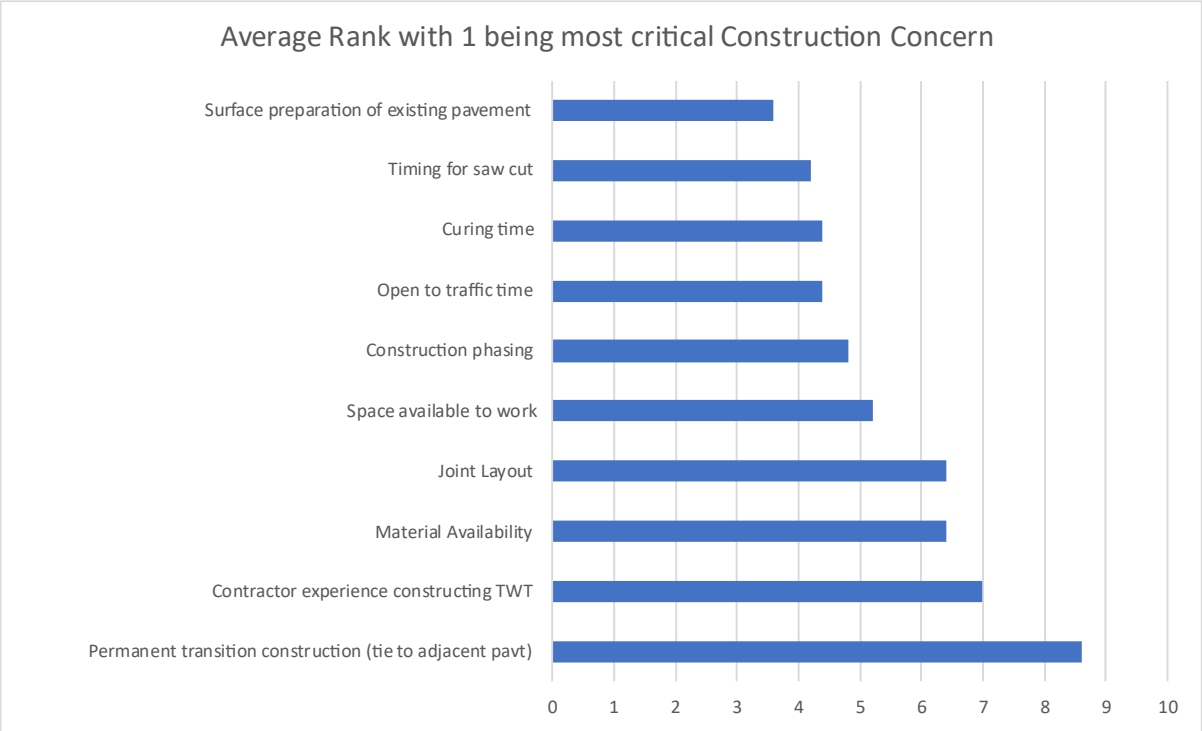

Figure 3-10 Ranking of Construction Concerns

A significant number of agencies using TWT operate without their own formal, documented design procedures, suggesting a potential reliance on broader industry guidelines or manufacturer recommendations. While some states have developed their own specifications, this is not universal. Similar to CRCP, extensive TWT experience tends to be concentrated as illustrated in Figure 3-11. However, the data suggests a slightly broader base of professionals with more recent (1-5 years) experience compared to CRCP, possibly indicating more recent adoption or training initiatives in TWT by some agencies. Figure 3-12 shows the performance is typically monitored using a comprehensive range of distress indicators and condition metrics, and agencies express a willingness to utilize even more detailed data if it were accessible.

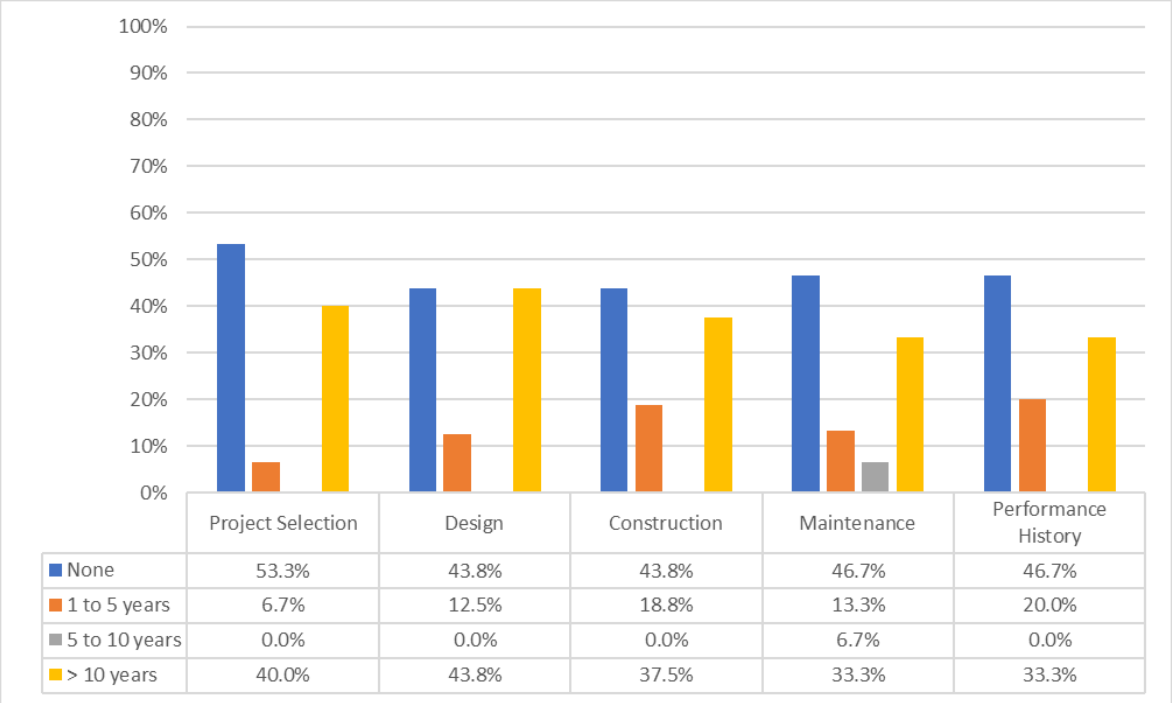

	Project Selection	Design	Construction	Maintenance	Performance History
None	53.3%	43.8%	43.8%	46.7%	46.7%
1 to 5 years	6.7%	12.5%	18.8%	13.3%	20.0%
5 to 10 years	0.0%	0.0%	0.0%	6.7%	0.0%
> 10 years	40.0%	43.8%	37.5%	33.3%	33.3%

Figure 3-11 TWT Experiences

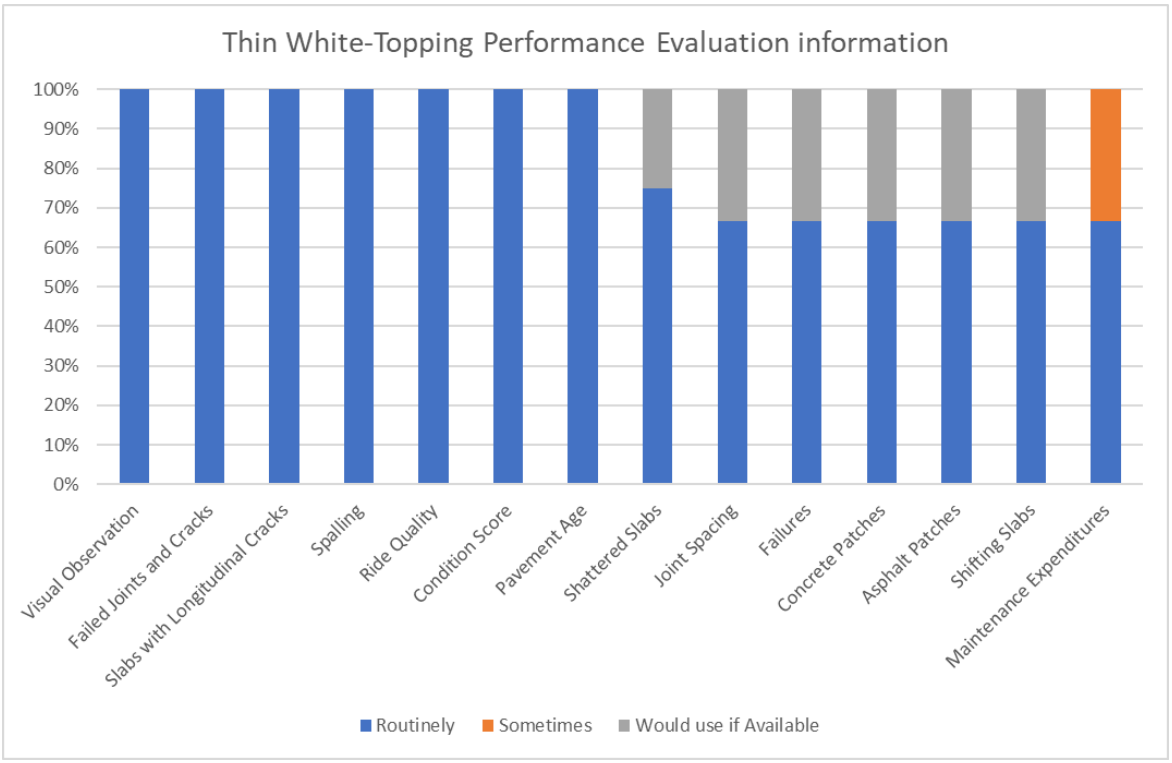

Figure 3-12 TWT Performance Evaluation

In summary, TWT is viewed as a viable but technically demanding overlay option, with success hinging on careful project selection and precise construction control. The current state of practice

indicates opportunities for developing more standardized design guidance and sharing best practices to support its effective implementation.

3.3.4 Part 4 – Pavement Evaluation and Overlay Candidate Selection

There was a total of five questions asked in this part. The main objective was to:

- Learn about agencies' screening processes and decision-making frameworks.
- Identify which data types and evaluation tools are most commonly used (visual inspection, FWD, GPR, cores, etc.).
- Understand how agencies prioritize criteria when comparing overlay options (like cost, performance, traffic).

The collective responses regarding general pavement evaluation and overlay candidate selection highlight that agencies make overlay decisions through varied, pragmatic processes. Figure 3-13 shows the candidate evaluation are heavily influenced by economic considerations (overall cost) and the structural integrity of the existing pavement, while predominantly relying on established, traditional methods for detailed site assessment.

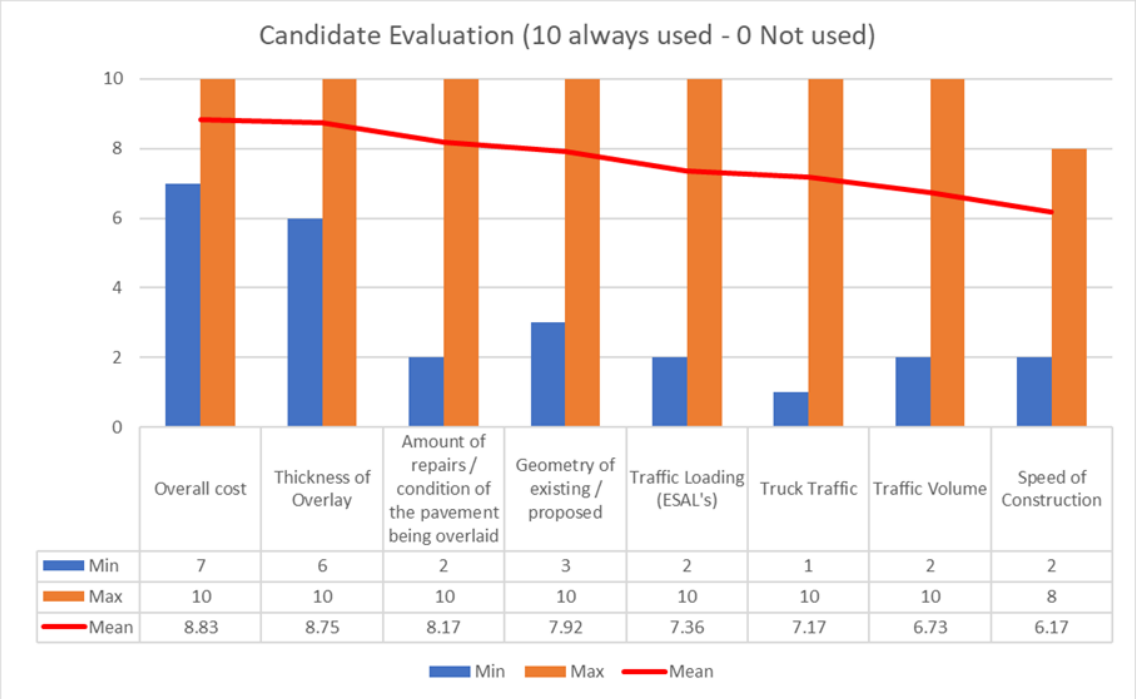

	Overall cost	Thickness of Overlay	Amount of repairs / condition of the pavement being overlaid	Geometry of existing / proposed	Traffic Loading (ESAL's)	Truck Traffic	Traffic Volume	Speed of Construction
Min	7	6	2	3	2	1	2	2
Max	10	10	10	10	10	10	10	8
Mean	8.83	8.75	8.17	7.92	7.36	7.17	6.73	6.17

Figure 3-13 Most critical determining factors for candidate evaluation

There's a strong continued reliance on visual observation as the primary method for initial pavement condition assessment. While some agencies have access to advanced NDT tools like various GPR systems, LiDAR, or Electrical Resistivity Tomography, their integration into typical, routine pavement evaluation for overlay design appears limited. These tools might be reserved for specialized research or forensic investigations rather than widespread field application for project-level decisions. For more detailed structural input, Falling Weight

Deflectometer (FWD) for stiffness (Figure 3-14a) and physical pavement coring with material sampling for layer condition analysis (Figure 3-14b) are the standard, widely adopted practices.

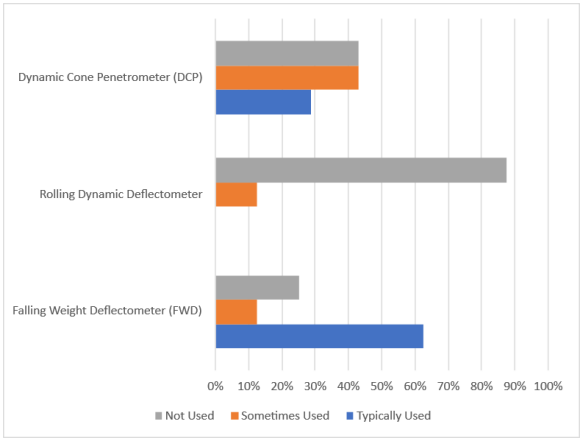

(a)Evaluation of stiffness condition

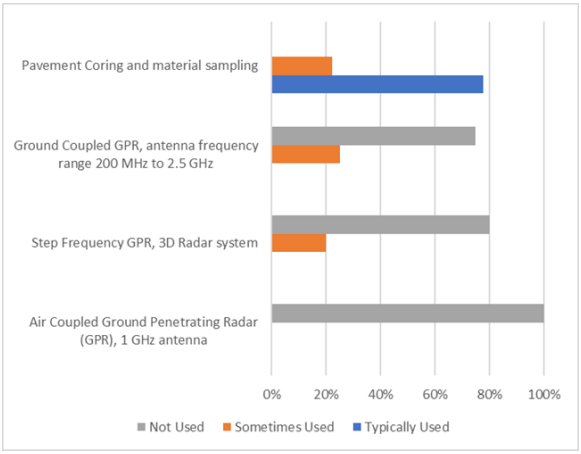

(b) Evaluation of layer condition

Figure 3-14 Evaluation of stiffness and layer condition

3.4 Summary

The nationwide practice survey paints a detailed picture of the current landscape surrounding the use of concrete overlays across transportation agencies in the United States. The field is marked by a wide range of practices, experiences, and interpretations. The following are the important aspects the survey reveals:

- Overlay definitions vary widely across agencies, leading to inconsistent terminology and communication challenges.
- CRCP and TWT overlays are not widely adopted, with usage concentrated among a few experienced professionals.
- The field shows a strong need for standardized terminology, design frameworks, and evaluation methods.
- Visual inspections for primary pavement condition assessment, FWD for stiffness condition assessment, and core and material sampling for layer condition assessment remain dominant evaluation tools, while advanced tech like GPR and LiDAR sees limited use.
- There's a gap in CRCP overlay design guidance for complex applications, especially intersections.
- Agencies express a desire for more performance-based data to inform overlay design and maintenance strategies.

CHAPTER 4
EVALUATION OF EXISTING PAVEMENT CONDITIONS

A comprehensive evaluation of existing pavement conditions is paramount in the design process for an overlay. The main goals of this chapter are:

- To propose criteria for selecting suitable projects.
- To establish a clear framework for evaluating pavements.
- To outline a typical plan and frequency for field testing.

By the end of this chapter, the designer/engineer will be able to carry out a well-defined framework for evaluating existing pavement conditions. The intention here is to be able to provide necessary inputs that would be required by design engineers to proceed with the proposed deflection-based design method.

4.1 Candidate Project Selection Criteria

Choosing the right projects is the first crucial step. You might ask, "What makes a project a good candidate for an overlay?" Deciding if a pavement is "good" or "bad" can be very subjective. Because of this, it's recommended that the engineer-in-charge has the final say in selecting candidate projects. Generally, any existing pavement (whether composite or asphalt) that has consistently underperformed and has an identified need for improvement should be considered a candidate.

"Underperformance" typically means the pavement has relatively low scores for its condition, ride quality, and overall distress. The condition score reflects surface distresses, while the ride score measures pavement roughness. Again, defining what counts as a "low score" can be subjective, especially considering the current limitations of the Pavement Management Information System (PMIS) scoring system. TxDOT is aware of these issues and has funded a two-year research project (Project 7218: "Revision for TxDOT's Pavement Management Information System (PMIS) Raters Manual") to address them. Three universities—Texas A&M (TTI), Texas Tech (TTU), and Texas State (TSU)—are working to make the PMIS rater manual and its scoring system more robust and reliable. Once this research project provides its findings, the engineer-in-charge should have more dependable numbers to base project selections on.

Until these updated guidelines are available, we recommend selecting projects based on PMIS score trends from the past three years. If a pavement's PMIS score falls into the "fair" or "poor" range (as defined in the current rater manual – see Table 4-1 for reference), it should be considered a candidate project. However, remember that practical factors like budget, time, and available resources will also guide the final decision.

Other factors to consider in project selection include:

- Existing Pavement Condition: This applies to all travel lanes, turn lanes, shoulders, and any other paved surfaces that might be used as future travel lanes.
- Alignment: Consider any changes to the road's vertical and horizontal alignment.
- Widening: Assess criteria and limitations for any potential widening of the pavement.
- Traffic Management: Plan for detours and how traffic will be handled during construction.
- Drainage: Evaluate final cross slope and drainage needs, especially at intersections.

Table 4-1 PMIS Score categories

Category	Distress Score (describes "distress")	Ride Score (describes "ride")	Condition Score (describes "condition")
Very Good	90 to 100	4.0 to 5.0	90 to 100
Good	80 to 89	3.0 to 3.9	70 to 89
Fair	70 to 79	2.0 to 2.9	50 to 69
Poor	60 to 69	1.0 to 1.9	35 to 49
Very Poor	1 to 59	0.1 to 0.9	1 to 34

4.2 Overview of Pavement Evaluation, Equipment and Tools

Once a candidate project is selected, the next step is to evaluate the pavement using the necessary equipment and tools. Our objective is to perform the required tests to gather data that will serve as input for the proposed overlay design method. Based on survey inputs and

recommendations from the Project Monitoring Committee (PMC) members, pavement evaluation is broadly divided into three categories, as illustrated in Figure 4-1.

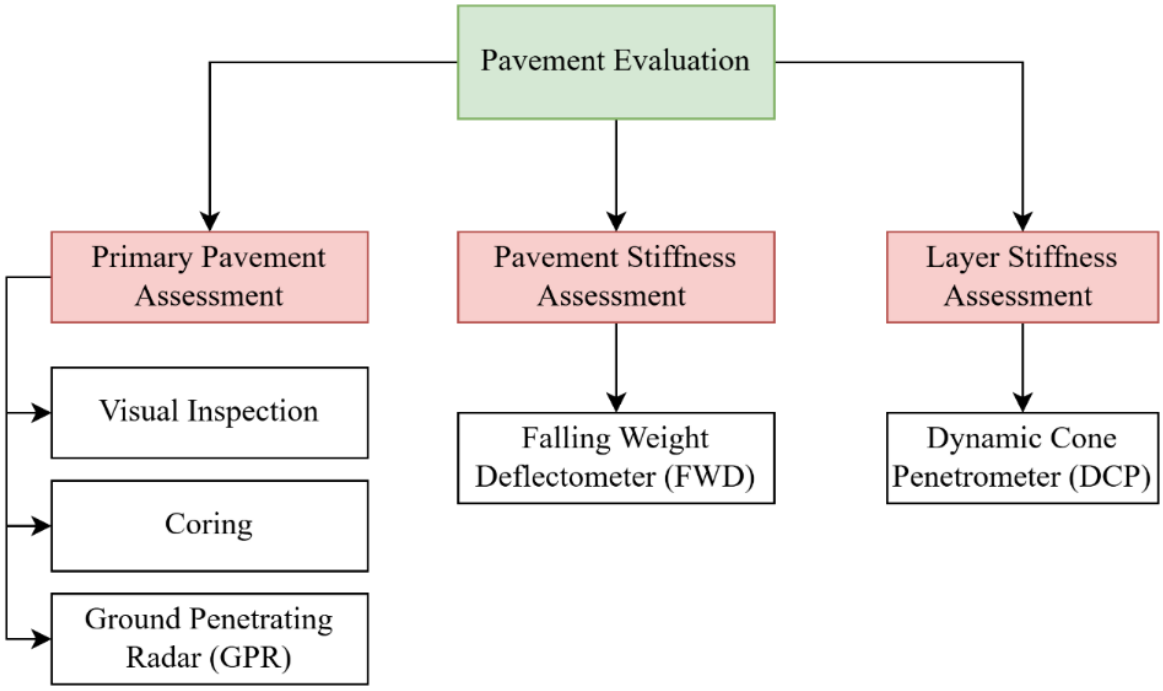

Figure 4-1 Pavement Evaluation Category

4.2.1 Primary Pavement Condition Assessment

The first category is the primary pavement assessment. This step involves a visual inspection of the pavement, followed by coring in specific areas of interest. If resources and time allow, Ground Penetrating Radar (GPR) can also be used for an initial assessment. Two key tasks in this step are:

1. To document the distresses, present in the existing pavement, with a particular focus on identifying and accounting for localized distresses.
2. To record the layer thicknesses of the existing pavement and the layers beneath it, ideally using GPR.

Visual Survey

Visual surveys are a fundamental part of this assessment. These surveys will be conducted following the procedures detailed in TxDOT's Pavement Manual, specifically Chapter 4 (Pavement Evaluation), Section 2 (Visual Pavement Condition Surveys). This manual provides guidance on identifying and categorizing various pavement distresses.

The primary aim of the visual survey in this context is to identify the type, extent, and severity of all visible distresses, including any previous repairs like patches or sealed cracks (Figure 4-2). This information is crucial for understanding the current pavement performance and for making

informed decisions about the overlay design. The TxDOT manual emphasizes the importance of decreasing subjectivity and variability in identifying these distresses by providing clear instructions for recording observations in an "orderly and consistent manner."

Figure 4-2 Visual Survey for distress

According to the manual, distresses are recorded systematically using metrics appropriate for each distress type, such as:

- Percent of an area affected (e.g., for raveling or block cracking).
- Linear feet per 100-ft station (e.g., for longitudinal cracking).
- Number of occurrences per station or per section (e.g., for failures or transverse cracks).

For project-level evaluations, such as those needed for overlay design, surveys are often conducted on foot. This allows for detailed mapping and a thorough characterization of distresses across the project length. A critical principle highlighted in the manual is that the root causes of this distress must be addressed in any comprehensive rehabilitation strategy. Simply applying an overlay without addressing underlying problems (like a weak base causing rutting, or active cracks) will likely lead to the distresses reappearing quickly in the new surface.

The TxDOT manual (Section 2.2) details various distress categories for flexible (asphalt) pavements. These include, but are not limited to:

1. Rutting: This longitudinal depression in the wheel path is a key load-associated distress. It's rated by area and depth (Shallow, Deep, Severe, Failure). Understanding its origin is vital, as the manual notes, "a thin overlay on top of a rut-susceptible or stripped mix would not be a suitable remedy." Such areas may require milling or more intensive repair before an overlay.
2. Alligator Cracking (Fatigue Cracking): These interconnected cracks in the wheel path indicate structural fatigue. The manual stresses that "Attempting to seal or place an overlay over these cracks without proper patching will result in rapid reappearance of the distress." Affected areas typically require removal and full-depth patching.
3. Failures: These are localized areas of severe distress, like large potholes or severely shoved areas. The manual states these "must be patched prior to resurfacing," even for light rehabilitation.
4. Patching: The presence and condition of existing patches indicate past maintenance. Improperly done patches can introduce roughness or become sources of new distress.
5. Longitudinal and Transverse Cracking: The type, location (wheel-path or not), width, and activity of these cracks are important. Their origin (load-associated or environmental) influences the corrective action needed before an overlay.
6. Block Cracking: While initially non-structural, climate-related distress, extensive or active block cracking may require sealing or other treatments before an overlay to prevent reflection.
7. Raveling and Flushing (Bleeding): These surface distresses affect texture and friction. Raveling indicates loss of aggregate, while flushing indicates excess asphalt. Both conditions need to be addressed during surface preparation for an overlay.

Table 4-2 shows the distress type found in asphalt along with its severity level and units it should be recorded while performing visual survey.

Table 4-2 Asphalt pavement distresses with its severity level and its unit of measurement for visual survey

S.No.	Distress Type	Severity/Criteria	Units Recorded
1	Rutting	Shallow (0.25–0.49 in.)	% Area
		Deep (0.50–0.99 in.)	% Area
		Severe (1.00–1.99 in.)	% Area
		Failure (≥2.00 in.)	% Area
2	Patching	Proper/Improper	% Surface Area
3	Failures	Number per 500-ft section	Count

4	Block Cracking		% Lane Area
5	Alligator (Fatigue) Cracking		% Wheel Path
6	Longitudinal Cracking	≥1/8-in., spalled, pumping/sealed	ft/100 ft
7	Transverse Cracking	≥1/8-in., spalled, pumping/sealed	count/100 ft
8	Raveling	Low, Medium, High	% Lane Area
9	Flushing (Bleeding)	Low, Medium, High	% Wheel Path

If the existing pavement is a composite structure (Section 2.3 of the manual), the visual survey will identify distresses specific to these pavement types. Key considerations for overlay include:

- Spalled Cracks and Failed Joints (for CPCD): These indicate deterioration at cracks or joints. Severe spalling may require repair before an overlay.
- Punchouts (primarily CRCP) or other Failures (CPCD): Punchouts are full-depth block failures. In CPCD, conditions like corner breaks or severe faulting are rated as failures. These often require full-depth concrete patching before an overlay.
- Shattered Slabs (CPCD): If slabs are extensively cracked and warrant complete replacement, a simple overlay is unlikely to be a viable long-term solution without slab replacement.
- Condition of Existing Patches (Asphalt or Concrete): Their performance and integrity need to be assessed.
- Apparent Joint Spacing (CPCD): These give insights into the slab's behavior and potential for movement that could affect an overlay.

Table 4-3 shows the distress type found in asphalt along with its severity level and units it should be recorded while performing visual survey.

Table 4-3 Composite pavement distresses and its severity level and unit of measurement for visual survey

S.No.	**Distress Type**	**Severity/Criteria**	**Units Recorded**
1	Spalled Cracks	CPCD ≥1-in. CRCP ≥3-in. wide	Count
2	Punchouts	≥12 in. dimension	Count

		severe spalling/faulting	
3	Asphalt Patches	Patches >10 ft counted as two	Count
4	Concrete Patches	Patches >10 ft counted per 10 ft	Count
5	Failures (CPCD)	Corner breaks, punchouts, Faulting, D-cracking, popouts	Count
6	Shattered Slabs (CPCD)	≥4 pieces, ≥5 failures/slab	Count
7	Slabs with Longitudinal Cracks	> half slab length, severe spalling/faulting	Count
8	Apparent Joint Spacing (CPCD)	≥0.5-in. wide across lane	ft/crack (joint)

This thorough visual assessment forms a critical input for the subsequent steps in the pavement evaluation and overlay design process. It is advised to refer to distress survey sheets published by FHWA in 2014 titled," *Distress identification manual for the Long-Term Pavement Performance Program (5th rev. ed.), Appendix A: Manual for distress surveys*". The sample distress survey sheet is attached in this report under Appendix A for reference.

Coring

Another essential component of the primary pavement condition assessment is coring, which allows us to obtain physical samples of the pavement layers. These samples are vital for detailed laboratory analysis, to confirm layer thicknesses, and to assess the material properties and conditions that cannot be fully determined from a surface survey alone. The general procedures for extracting core samples should follow those outlined in the TxDOT Pavement Manual, specifically Chapter 5 ("Destructive Evaluation of Pavement Structural Properties"), Section 5.3 ("Coring Procedure").

The number of cores to be taken is a project-level decision and should be sufficient to confidently determine the pavement layer thickness across the project area. As shown in Figure

4-3, cores should generally be taken through the full depth of the asphalt layer(s) and, if a stabilized base is present and a complete sample is desired, may optionally extend into this layer.

Figure 4-3 Coring operation with cored sample

Regarding core diameter, either 4-inch or 6-inch cores are standard. A 4-inch diameter core is typically adequate for visual inspection and some basic laboratory tests. However, if more advanced laboratory testing is warranted, such as the Hamburg Wheel Tracking Test or the Overlay Tester, it is recommended to obtain 6-inch diameter cores to meet the sample size requirements for these tests.

In summary, a primary objective of coring within this assessment is to confirm pavement layer thicknesses. To complement this targeted information and obtain a more continuous and comprehensive understanding of the pavement structure being evaluated, it is further recommended to use Ground Penetrating Radar (GPR) when available. GPR can provide a broader picture of layer variations between core locations.

Ground Penetrating Radar (GPR)

To achieve that broader picture of subsurface conditions and complement the discrete information obtained from coring, Ground Penetrating Radar (GPR) is a valuable non-destructive testing tool. GPR, illustrated in Figure 4-4, systems operate by sending electromagnetic waves into the pavement structure and detecting the reflected signals from layer interfaces or other anomalies.

Figure 4-4 GPR used for mapping the layer thickness

Systems using lower-frequency antennae are generally able to discern features deeper within the pavement structure and subgrade. For optimal results and improved resolution, the GPR systems are typically placed in direct contact with the pavement surface. This is often achieved by pushing the antenna on a buggy or by dragging it behind a van that houses the data acquisition system and other necessary electronics.

The Texas Department of Transportation (TxDOT) commonly utilizes GPR antennae with frequencies ranging from 200 MHz to 2.5 GHz. The maximum penetration depth of the GPR signal varies depending on the antenna frequency, the type of soil or material being investigated, and its degree of saturation. A key principle is that higher antenna frequencies provide lower penetration but offer higher resolution for near-surface layers. Conversely, lower frequencies penetrate deeper but provide poorer near-surface resolution.

4.2.2 Pavement Stiffness Assessment

Evaluating the structural stiffness of existing pavement is crucial element needed as a design input for the deflection-based design method.

Falling Weight Deflectometer (FWD)

The FWD is a trailer-mounted device, as shown in Figure 4-5. It operates by placing an 11.8-inch (300 mm) diameter load plate in firm contact with the pavement surface at each designated test location. Above this load plate, a load column carries a stack of weights. These weights are dropped from a predetermined height to impart an impact load to the pavement, simulating the effect of a passing dual truck tire set.

Figure 4-5 FWD, a trailer-mounted device

A series of seven geophones (deflection sensors) are mounted in line with the load plate, typically at 12-inch increments starting from the center of the plate. These geophones measure the surface deflection of the pavement in response to the impact load, generating a "deflection bowl." This deflection data provides insight into the pavement's structural response.

Measurements are generally acquired in the right wheel path of the outside lane. A recent upgrade (Figure 4-6) to the FWD includes an eighth geophone, typically mounted 12 inches from the load plate on the opposite side of sensor #2 (which is 12 inches from the load plate center). This eighth sensor is particularly useful for evaluating load transfer efficiency across joints and cracks in rigid pavements. For precise location documentation, GPS coordinates are automatically recorded and posted to the deflection data file for each test point.

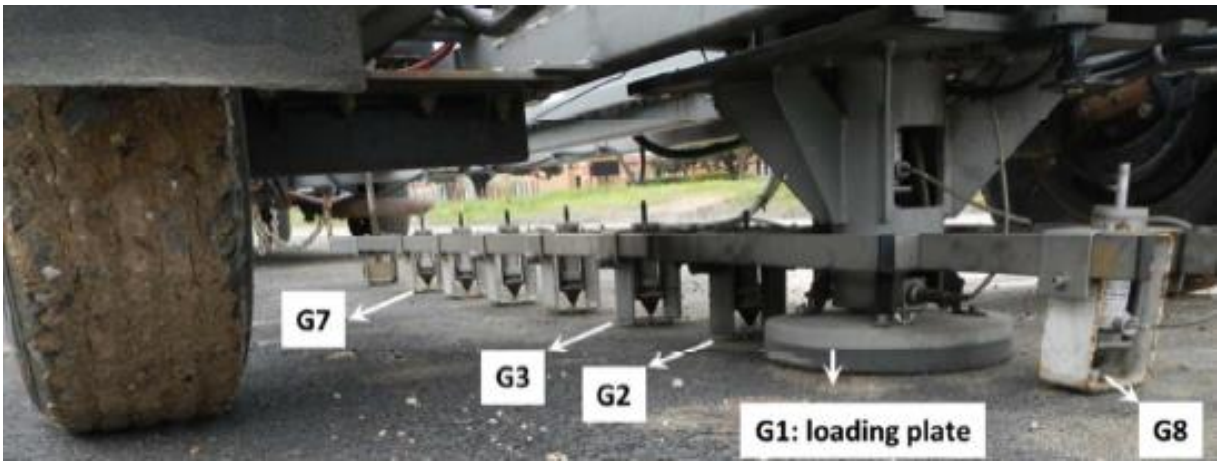

Figure 4-6 FWD sensor location with recent upgrade of eighth geophone.

Interpretation of the collected deflection data can range from simple comparisons of the normalized (for load) maximum measured deflections (typically the deflection at the center of the load plate) to much more rigorous analyses. The raw file generated after an FWD test (as

shown in Figure 4-7) includes several important pieces of information that should be carefully checked. Make sure the following details are recorded correctly:

- **Test date** – Confirms when the test was done.
- **Sensor location** – Check if the location of each sensor is listed accurately.
- **GPS data** – Ensure the GPS is working and capturing location properly.
- **Drop sequence** – The order of the loading drops should be clearly noted.
- **Temperature readings** – These are important for further analysis and should be recorded correctly.
- **Complete data** – Each test location must have both load and deflection values. If any of these are missing, the data may not be usable.

Carefully reviewing all this information early on helps ensure the data is reliable and ready for further analysis. Additionally, the data collected can be used to carry out back methods which includes using back calculation procedures to estimate the modulus values of individual pavement layers or evaluating deflection time-histories. Detailed discussion on the back calculation methodology for layer moduli in flexible pavements is found in Chapter 5, Section 4 ("FPS21 Modulus Inputs and Back calculation Methodology") of the relevant TxDOT manual. However, for layer stiffness assessment, DCP must be used. It is discussed next.

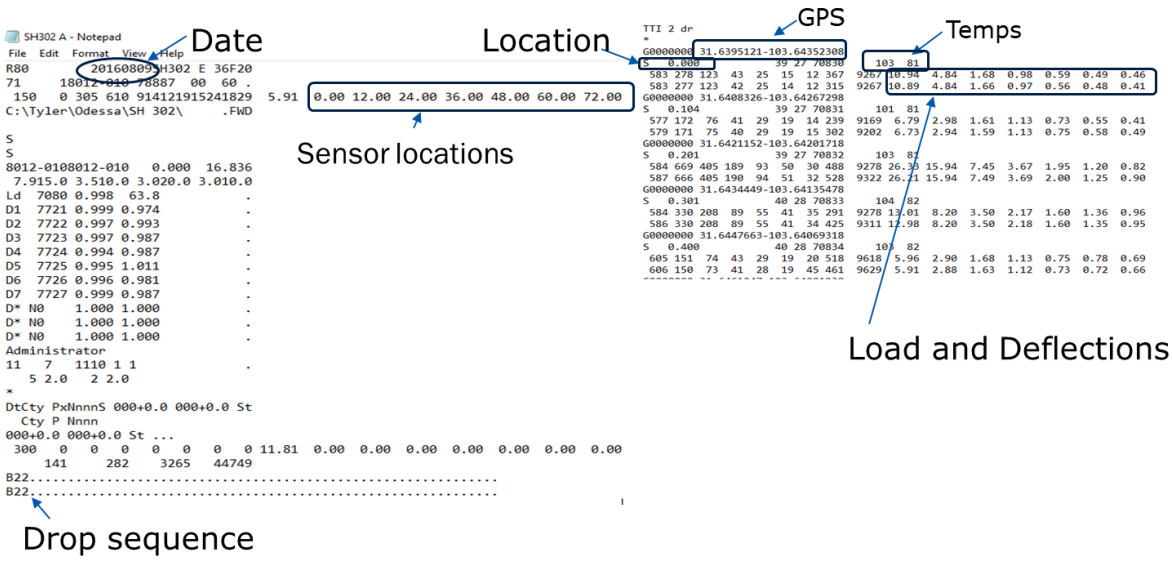

Figure 4-7 Contents of *.FWD file - Raw Data

4.2.3 Layer Stiffness Assessment

Determining layer stiffness will help to make informed design decisions for designers. This will stem from the need to select reliable deflection value as an input for design purpose. It is recommended to use Dynamic cone penetrometer for reasonable layer stiffness assessment.

Dynamic Cone Penetrometer (DCP)

The Dynamic Cone Penetrometer (DCP) is a portable field-testing device used to assess the in-situ strength and stiffness of unbound pavement layers and subgrade soils. The device and its use generally comply with ASTM D 6951.

The DCP, illustrated in Figure 4-8, consists of a two-piece rod. The lower rod is approximately 39 inches (1 meter) long and is fitted with a replaceable cone tip at the penetration end and an anvil at its upper end. The anvil includes a threaded or shear pin receptacle for attaching the upper rod. The upper rod carries a 17.6-lb sliding hammer and features a handle for steadying the device during testing. The hammer has a specified free-fall distance of 22.6 inches along the upper rod before striking the anvil.

Figure 4-8 DCP Testing

Figure 4-9 shows a typical plot of cumulative penetration depth versus cumulative blows generated using the collected data. A trend line is fitted to the data points for each distinct layer encountered. The penetration rate (PR), typically expressed in mm/blow (or inches/blow), is determined as the slope of this trend line. It's important to generate a separate trend line for each material layer, using only the data points measured within that specific layer. If pre-drilling

occurs, the first data point for the DCP test should correspond to the actual start depth after drilling, and the surface (zero depth) should not be included as a data point for that layer, as this would invalidate the penetration rate calculation.

Testing in flexible base materials containing larger aggregates can sometimes yield misleading results if the cone attempts to drive a large aggregate particle through the base material matrix rather than penetrating the matrix itself. Under such circumstances, it's advisable to halt testing at that location and either bore/drill down to a lower level to bypass the problematic zone or restart the test at an adjacent location.

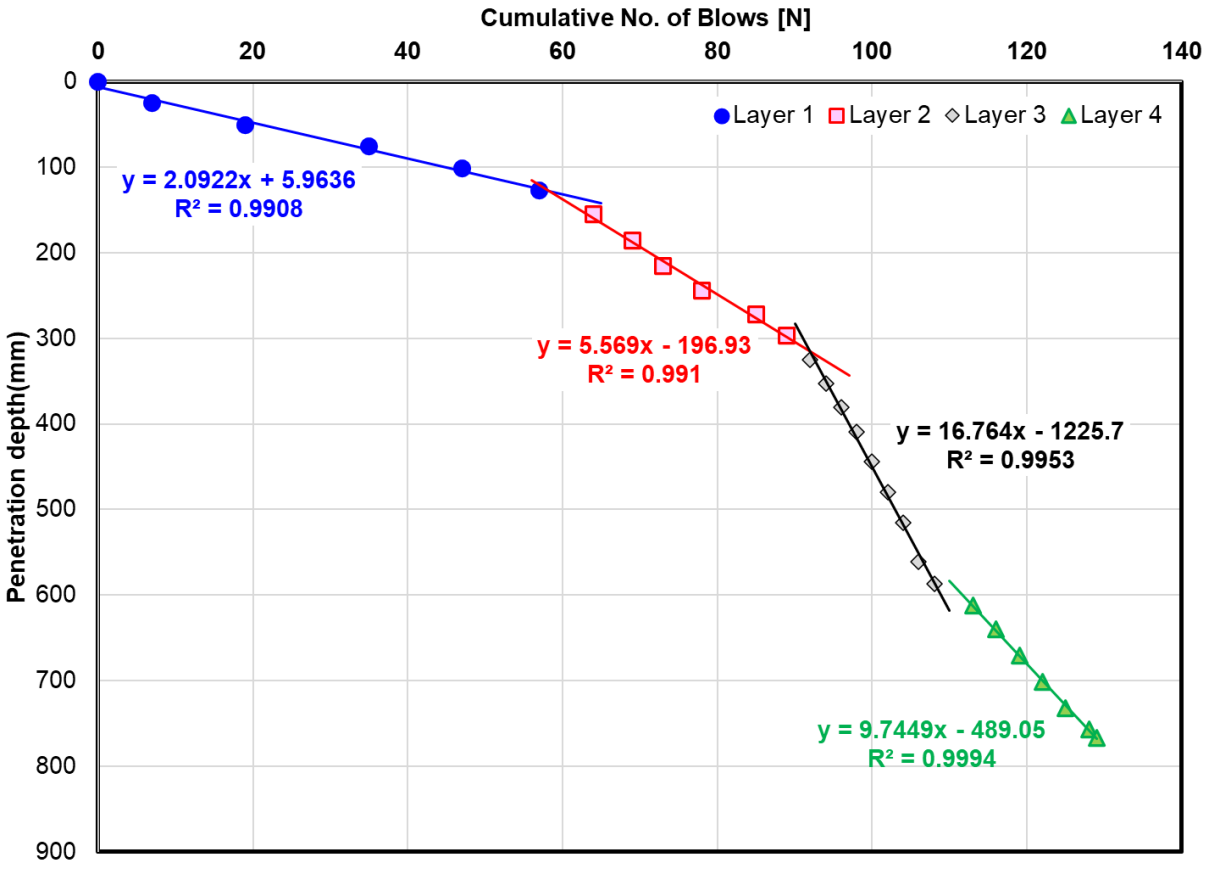

Figure 4-9 Typical plot of cumulative penetration depth versus cumulative blows

4.3 Field Testing Plan

In this section, we outline a detailed plan for conducting non-destructive and sampling-based field testing to evaluate existing pavement conditions in preparation for overlay design. As shown in Figure 4-10, this structured, phased approach ensures the reliability of the data collected and its effectiveness in informing design decisions under the deflection-based design method.

4.3.1 Phase 1: Project Background

- Gather Project Details:
  - Review control section information or control section job documentation to find relevant historical data.
  - Collect all available past maintenance records.
  - Obtain PMIS (Pavement Management Information System) data.
  - Compile any other available project-specific information.
- Collect Traffic Trends:
  - Gather historical and current traffic data. This information will be crucial later for determining the design input for traffic data (Design ESALs).

Calculating Design Traffic

The design traffic is calculated in million ESALs. For the preliminary calculation of design traffic, it is recommended to utilize TxDOT's web-based application ms2soft or RPDB(https://idatavisualizationlab.github.io/RPDB/general/traffic-data/) for quick reference to historical traffic data. Since both programs utilize the same data, it is recommended to make a selection based on user preference. For discussion in this section, we will stick to RPDB portal for obtaining our traffic data. To calculate the design traffic in million ESALs, we need the following inputs, which include:

A. $AADT_1$(one-directional)
   - *Initial Average Annual Daily Traffic in the design direction (vehicles per day) for the base year (the year the project opens to traffic).*

B. T = percentage of trucks in average daily traffic (ADT)
   - *Expressed as a decimal (e.g., 15% = 0.15)*

C. T_f = Truck Factor
   - *This factor converts the number of trucks into the number of 18,000 lb. equivalent single axle loads (ESALs). It accounts for the mix of truck classes and their respective axle loads and configurations.*

D. P = Design Period in years

E. G = Growth Rate
   - *This accounts for the projected increase in traffic over the design period; expressed as a decimal (e.g., 3% = 0.03).*

F. LF = Lane Factor
   - *This accounts for the distribution of traffic when multiple lanes exist in one direction.*
     i. *Use LF = 1, if 1 or 2 lanes*
     ii. *Use LF = 0.7, if 3 lanes*
     iii. *Use LF = 0.6, if 4 or more lanes*

Based on the above inputs the formula to be used for calculating cumulative design traffic is as follows:

$$\text{Cumulative Design Traffic (ESALs)} = \frac{AADT1\ X\ TT\ X\ TF\ X\ LF\ X\frac{(1+G)^P-1}{G}X365}{1{,}000{,}000}$$

4.3.2 Phase 2: Field Test

Conduct Visual Survey

- Systematically survey the entire project length.
- Identify and document all types of pavement distresses (e.g., cracking, faulting, spalling).
- Precisely locate any localized distress areas that require special attention or pre-overlay repairs.

Coring

- Perform coring at representative locations to determine the existing pavement thickness.
- Correlate coring locations with visual survey findings.

Ground Penetrating Radar (GPR) Survey (Optional)

- If the project budget and time allow, conduct a GPR survey to get a more continuous profile of pavement layer thicknesses and identify potential subsurface anomalies.

FWD Testing

To ensure the structural response of the pavement is properly captured.

- Data Review
    - Return to the office and thoroughly review the visual survey notes and coring data.
- Develop Optimized Testing Plan
    - Based on the collected data, create a strategic and optimized Falling Weight Deflectometer (FWD) testing plan. The goal is to accurately assess pavement stiffness and gather data for determining existing deflection values.
- Categorize FWD Testing Sections
    - Regular Sections:
        - Project length > 5 miles: Drop FWD points at 500 ft intervals.
        - Project length between 2 miles and 5 miles: Drop FWD points at 300 ft intervals.
        - Project length between 1 mile and 2 miles: Drop FWD points at 200 ft intervals.
        - Project length < 1 mile: Drop FWD points at 100 ft intervals.
    - Special Sections:
        - Intersections: Drop FWD points at every 50 ft.

        - Localized Distress Areas: Drop FWD points at every 20 ft or more frequently depending on the extent and nature of the distress.
- Conduct FWD Testing
    - Execute the FWD testing according to the prepared plan.
    - The outside lane must be tested at a minimum.
    - Test additional lanes when:
        - Pavement structure varies across lanes.
        - Surface distress appears more severe or different in the inner lanes.
        - The project area is small, and all lanes must be tested to meet the required number of drops.
- Dynamic Cone Penetrometer (DCP) Testing
    - During FWD testing, identify locations exhibiting high deflection and low deflection. Conduct DCP testing at these specific points.
    - Note any other additional points of interest observed during FWD testing and perform DCP tests there as well.
    - For special sections (intersections, localized distress), conduct as much DCP testing as feasible to thoroughly understand the subsurface conditions. The objective is to identify any underlying issues that need to be rectified before the overlay.
- Investigate High Deflection & Outliers
    - If FWD testing reveals areas with very high deflection, these locations must be studied thoroughly. Attempt to create a correlation between FWD deflection, DCP testing results, and subgrade modulus.
    - If there are outliers in the FWD testing data, further investigate the reason behind these anomalous readings (e.g., localized base failure, underground utility, poor drainage).

4.3.3 Phase 3: Laboratory Testing

- Laboratory testing is recommended only when localized, severe distresses are identified during the visual survey or field testing.
- The goal is to determine the root cause of the distress to ensure that it does not compromise the performance of the planned overlay.
- If deemed necessary based on field observations or DCP results, conduct laboratory tests such as:
    - Moisture content test
    - Atterberg limits
    - Shrink/swell testing (especially if problematic subgrade soils are suspected).

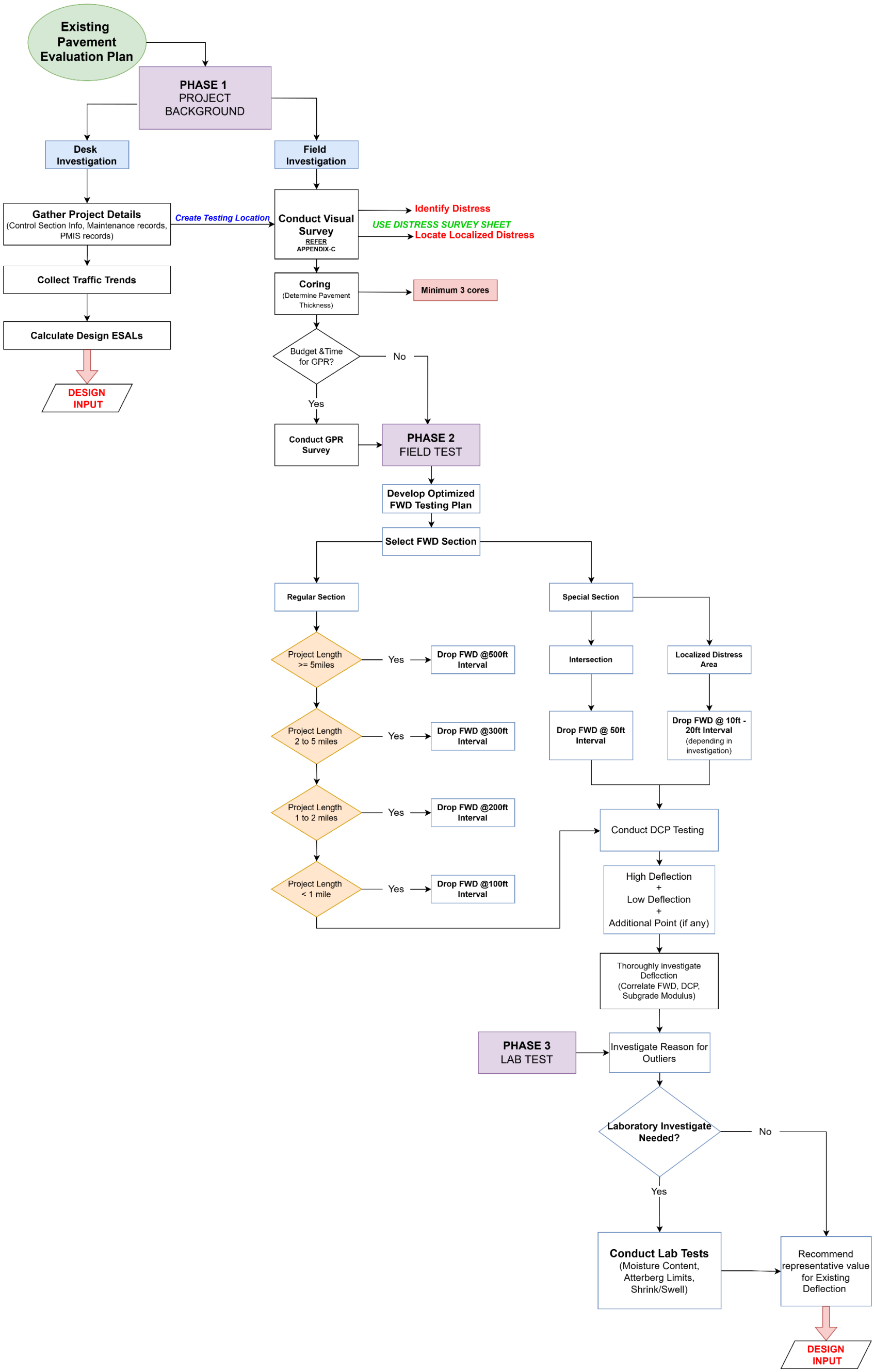

Figure 4-10 Decision Framework for Evaluating Existing Pavement for Deflection based design method

4.4 Summary

This chapter established a comprehensive and systematic framework for the evaluation of existing pavements, serving as a critical prerequisite for the proposed deflection-based overlay design. The central principle underpinning this chapter is that a successful and durable overlay cannot be designed in isolation; it must be engineered in direct response to the specific structural realities and deficiencies of the underlying pavement.

The methodology presented guides the design engineer through logical progression, beginning with a justifiable candidate selection process based on historical performance data and culminating in a detailed, multi-phased field investigation plan. By strategically integrating traditional visual surveys with non-destructive testing tools like the Falling Weight Deflectometer (FWD) and targeted diagnostic methods like the Dynamic Cone Penetrometer (DCP) and coring, this framework ensures a thorough understanding of the pavement system. This approach allows for the identification of not just the visible symptoms of distress but also their underlying root causes.

Ultimately, the rigorous process detailed in this chapter, from background data collection to structured field testing, is designed to produce reliable, defensible data. These data points, particularly the characterization of pavement stiffness and deflection response, are the essential inputs required for the deflection-based design method that will be detailed in the subsequent chapters. By following this framework, an engineer can move beyond subjective assessments and ensure that the overlay design is built upon a well-understood foundation, maximizing the potential for long-term performance

CHAPTER 5
DEFLECTION BASED CRCP SLAB THICKNESS DESIGN

In our previous chapters, we established groundwork for the deflection-based design method, now let's connect the dots. Throughout the preceding literature, we discussed at length the historical progression of slab thickness design and its current state. We noted that current approaches to overlay design primarily include the effective thickness method and the mechanistic method, while also presenting the significant limitations that have constrained their effectiveness. This led us to suggest that a promising path forward is likely to involve the deflection-based design method. We introduced this very method in the 'Research Approach' section of the Introduction. There, we briefly explained that the idea behind the deflection-based design method stems from both our field investigations and the lessons learned from the AASHO Road Test. We connected these two aspects to provide an initial understanding of their interplay. In this chapter, we will explore this method further and in detail.

A cornerstone for deflection-based design method is attributed to the field observations made and documented in rigid pavement database. The observation dictates that TxDOT over the years have recognized the profound impact of adequate slab support on reducing slab deflections and thereby enhancing pavement performance. Consequently, TxDOT mandated the use of stabilized bases in CRCP construction. This decision effectively prevented both pumping and the typical punchout failures often observed in CRCP, leading to numerous projects with stabilized bases significantly outperforming their original design lives. This crucial finding is reflected in the statewide deflection curve which shows the relationship between CRCP slab thickness and the CRCP deflection as shown in Figure 5-1. The development of this relationship involved a thorough methodological approach. Researchers selected a substantial and diverse array of 21 CRCP sections with varied thicknesses ranging from 6-inches to 15-inches. FWD tests were systematically conducted across these sections to capture deflection data. Each selected project, unique in its specific site conditions and construction characteristics, contributed to a rich dataset of deflection measurements. A critical step involved calculating the average deflection for each distinct project. Remarkably, this analysis revealed that CRCP sections of a certain thickness consistently exhibited a similar average deflection, irrespective of minor variations in other project parameters. When these average deflection values were plotted against their corresponding CRCP thicknesses, a power function (Equation 5-1) effectively characterized this relationship.

$$y = 252.85x^{-2.005} \qquad (Equation\ 5-1)$$

Where,

y = CRCP Deflection (in mils)

x = Slab Thickness (in inches)

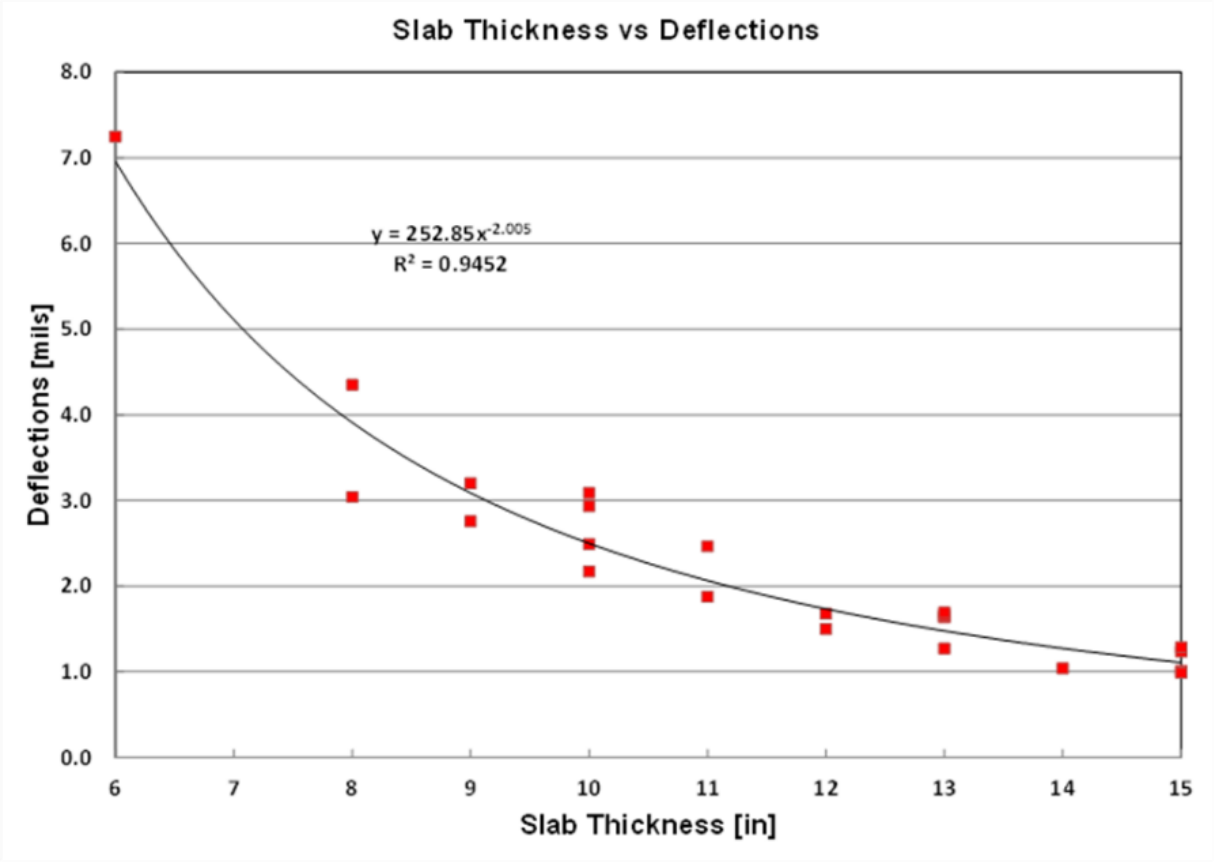

Figure 5-1 Statewide Deflection curve

The implications of this relationship are profound as demonstrated in Figure 5-2. For instance, a 6-inch CRCP typically yields an average deflection of approximately 7 mils. In contrast, a 10-inch CRCP exhibits a significantly lower average deflection of around 2.5 mils, while a 14-inch CRCP demonstrates a mere 1.27 mils of deflection. What makes this finding particularly profound is its consistency: whether a 1000-ft section of 6-inch CRCP is tested in Lubbock, Houston, or Tyler, FWD testing consistently yields an average deflection in the vicinity of 7 mils. This consistency provides a powerful diagnostic capability. It effectively establishes a benchmark, or a 'signature' deflection, for CRCP of a given thickness, which is fundamental to the proposed deflection-based design method. This signature deflection not only allows for an assessment of the pavement's current structural health but also provides a predictive benchmark for target deflections, indicative of anticipated future performance.

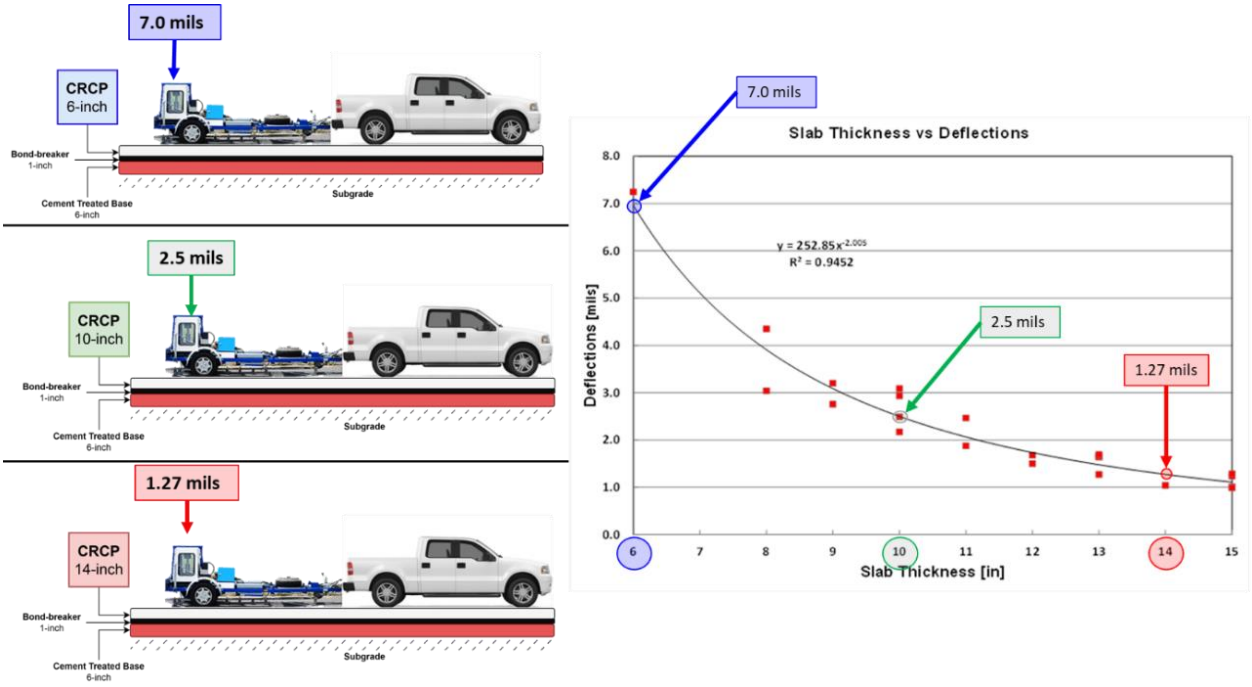

Figure 5-2 CRCP Deflection for 6-inch, 10-inch and 14-inch

Consider the practical application of this finding with a hypothetical scenario, illustrated in Figure 5-3. Imagine a CRCP section, originally constructed with a 10-inch thickness, which has subsequently been overlaid with a 4-inch Hot Mix Asphalt (HMA) layer due to ride deterioration. Over time, this overlaid system also begins to show signs of distress. An FWD assessment is conducted over a 1000-ft segment of this roadway, revealing an average deflection of 5.1 mils. According to the statewide deflection curve, a sound 10-inch CRCP (even with an HMA overlay, if the CRCP itself were structurally intact) should exhibit deflections closer to 2.5 mils. The measured 5.1 mils, however, is more characteristic of a 7-inch CRCP. This discrepancy provides critical insight: although the pavement system includes a nominal 10-inch concrete layer, its actual structural response is analogous to that of a much thinner 7-inch CRCP. Therefore, from a structural capacity perspective, if the pavement was originally designed to withstand traffic loads anticipated for a 10-inch CRCP, its current condition, as indicated by the elevated deflection, signifies an inability to meet these demands. This compromised state predisposes the pavement to accelerated deterioration and premature structural failure if subjected to its original design traffic. This example underscores the diagnostic power of the deflection-thickness relationship in quantifying the extent of structural degradation.

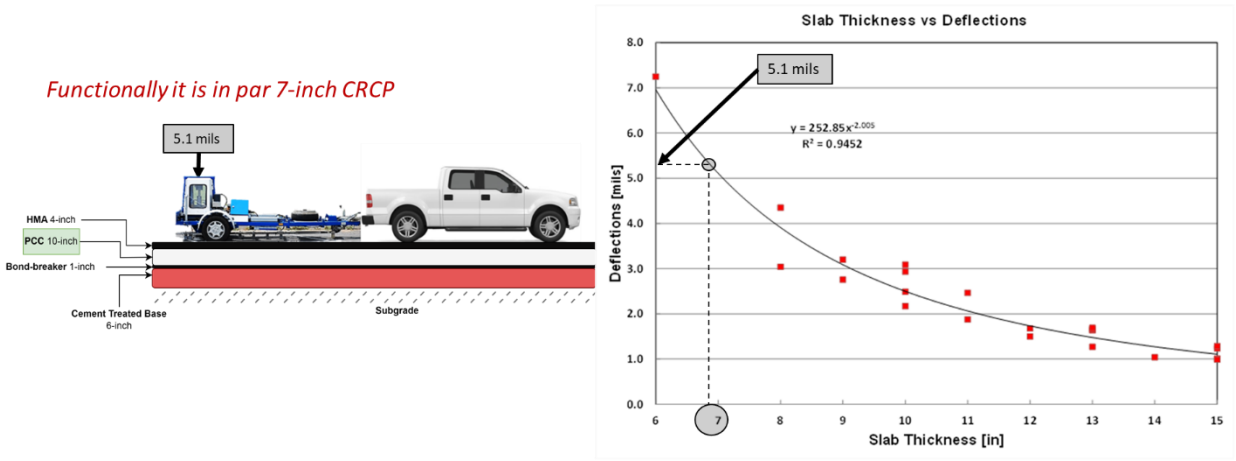

Figure 5-3 Deflection Analysis of a Deteriorated and Overlaid Pavement

To surmise, the premise for deflection-based pavement design is that if deflections on two new rigid pavements are equal, then their structural performances will be comparable to each other, regardless of the structural composition (slab thickness + base + subgrade) of the pavements. Let us see this in action with the example illustrated in Figure 5-4. Consider three distinct new CRCP structural designs:

- **Pavement A:** A 6-inch CRCP slab supported by a 1-inch bondbreaker and an 8-inch cement-treated base (CTB).
- **Pavement B:** A 10-inch CRCP slab, also with a 1-inch bondbreaker but overlying a 6-inch CTB.
- **Pavement C:** A substantially thicker 14-inch CRCP slab, placed directly over a 5-inch asphalt-stabilized base (ASB).

These three pavement structures, while clearly different in their layer thicknesses and base material types, offer an insightful comparison. If a finite element analysis, using a tool like ANSYS, were performed to model the response of these three distinct pavement configurations under a standard design load of 9000lb, the results would reveal a noteworthy convergence. The predicted surface deflections for each of these individual pavement structures would be remarkably similar, likely falling within a narrow range around approximately 3.1 mils. This underlines the concept that surface deflection can serve as a common denominator, a unifying metric for predicting and achieving equivalent long-term performance across a spectrum of viable structural designs (i.e., slab thickness, base type and thickness, subgrade preparation).

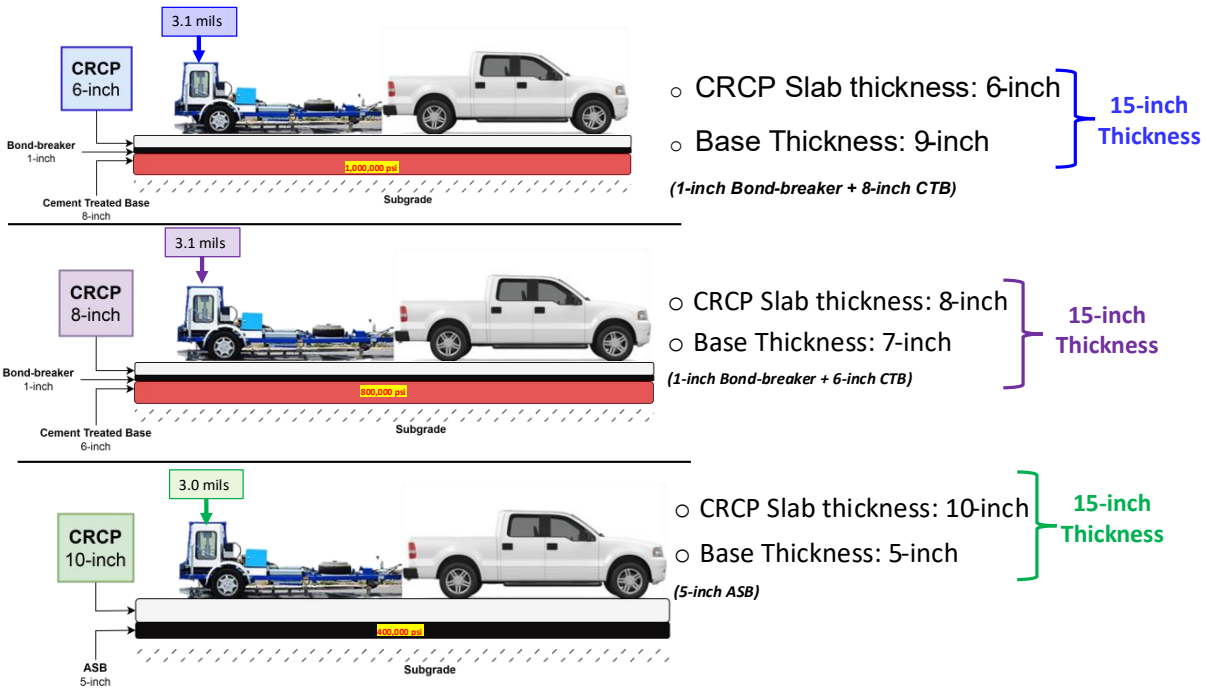

Figure 5-4 Comparison of deflection among different structural composition

Another component of a deflection-based design method involves integrating the influence of design traffic. Specifically, it becomes essential to establish a clear correlation between the anticipated design traffic, expressed in Equivalent Single Axle Loads (ESALs), and the required slab thickness necessary to accommodate that traffic. This link ensures that the chosen slab thickness and its corresponding slab deflection aligns with the pavement's intended service life under projected loading. The TxCRCP-ME program was used to develop this correlation following iterative simulation process.

For each specified ESAL input, the TxCRCP-ME program was utilized to determine the corresponding concrete slab thickness required to adequately sustain that level of traffic over the design period. This process of deriving design thicknesses for a spectrum of traffic levels using TxCRCP-ME is conceptually illustrated in Figure 5-5, which depicts typical program inputs and outputs.

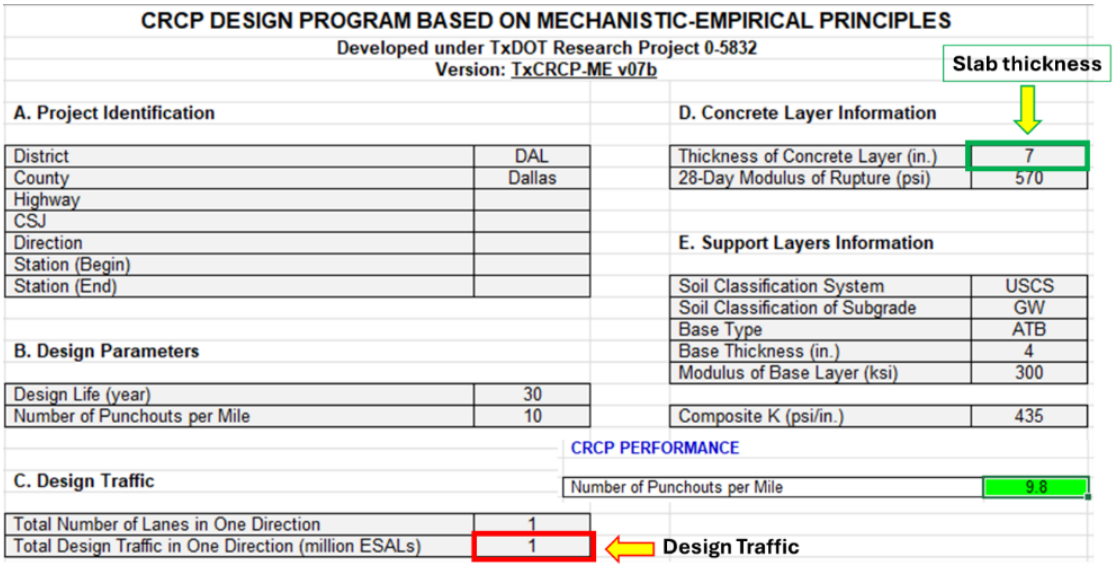

CRCP DESIGN PROGRAM BASED ON MECHANISTIC-EMPIRICAL PRINCIPLES

Developed under TxDOT Research Project 0-5832
Version: TxCRCP-ME v07b

Slab thickness

A. Project Identification

District	DAL
County	Dallas
Highway	
CSJ	
Direction	
Station (Begin)	
Station (End)	

B. Design Parameters

Design Life (year)	30
Number of Punchouts per Mile	10

C. Design Traffic

Total Number of Lanes in One Direction	1
Total Design Traffic in One Direction (million ESALs)	1

D. Concrete Layer Information

Thickness of Concrete Layer (in.)	7
28-Day Modulus of Rupture (psi)	570

E. Support Layers Information

Soil Classification System	USCS
Soil Classification of Subgrade	GW
Base Type	ATB
Base Thickness (in.)	4
Modulus of Base Layer (ksi)	300
Composite K (psi/in.)	435

CRCP PERFORMANCE

Number of Punchouts per Mile	9.8

Design Traffic

Figure 5-5 Deriving Design Slab Thicknesses for Varying Traffic Demands via TxCRCP-ME Simulations

Once sufficient data points were generated, this culminated in the development of the design graph presented in Figure 5-6, which explicitly illustrates the relationship between design traffic (ESALs) and the corresponding CRCP slab thickness as determined by the TxCRCP-ME program.

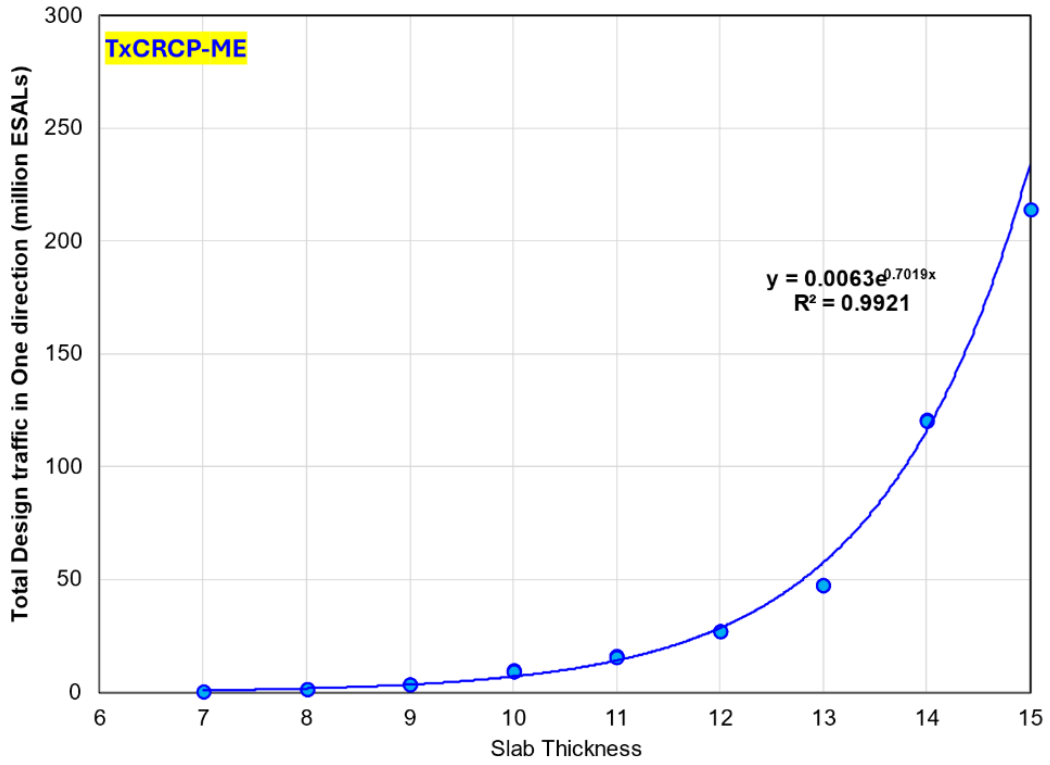

Figure 5-6 Relationship between design traffic and slab thickness using TxCRCP-ME

Let's trail back to the example illustrated in Figure 5-3. In this scenario, assume the pavement is a 40-year-old, 10-inch Continuously Reinforced Concrete Pavement (CRCP) with a 4-inch Hot Mix Asphalt (HMA) overlay. This pavement has exceeded its design life and requires long-term rehabilitation. For designing an overlay using a deflection-based method, one key input is the deflection of the existing composite pavement. This has been measured as an average deflection of 5.1 mils. As previously mentioned, this pavement is structurally equivalent to a new 7-inch CRCP. Additionally, the design traffic for this section over the next 30 years is estimated to be 50 million ESALs (Equivalent Single Axle Loads). Based on this design traffic, a brand-new CRCP constructed without any existing pavement (if designed using TxCRCP-ME, for example) would require a thickness of 13 inches. Falling Weight Deflectometer (FWD) testing on such a new 13-inch pavement would likely show a deflection of approximately 1.5 mils. Given that the current, existing pavement structurally performs like a 7-inch CRCP, it might seem that adding a 6-inch concrete overlay would make it function like the desired 13-inch slab. The goal of such an overlay would be to achieve a deflection of around 1.5 mils, as notionally shown in Figure 5-7, which illustrates an overlay thickness required to achieve this target deflection.

However, this simple addition may not be accurate. This is because there isn't a well-established relationship between the deflection measured on the existing pavement (which acts as a base) and the deflection of the new CRCP after the concrete overlay is placed. Therefore, it is crucial to determine this relationship. Establishing how base deflection correlates with the final CRCP deflection is essential for accurately designing the overlay.

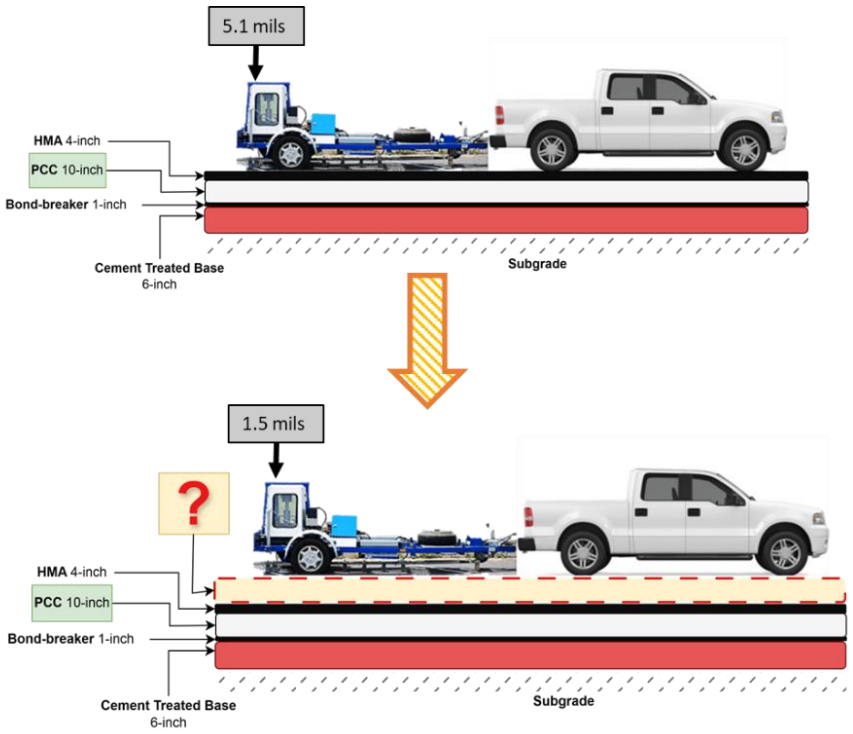

Figure 5-7 Conceptual overlay thickness on the existing pavement

5.1 Field Testing for Base Deflection and CRCP Deflection

This section provides a detailed account of the field testing conducted to gather the necessary data for developing the correlation data between base deflection and CRCP deflection. Field testing was conducted on two distinct project types: (1) new CRCP construction projects and (2) existing asphalt-overlaid rigid pavements. These two project types were selected because data from the new CRCP construction projects will provide the information required to establish the correlation between base deflection and CRCP deflection. Conversely, data from the asphalt-overlaid rigid pavements will help in understanding the inherent variability within pavement systems. This understanding will be valuable for validating the field data and addressing any inconsistencies observed in the dataset.

This section is organized into three main parts. First, the process of identifying and selecting test sections will be discussed. Next, the methodology employed in the field-testing program will be outlined. Finally, the section will conclude with an overview of each project and a presentation of the data collected.

5.1.1 Project Profiles and Testing Summaries

The identification and selection of test sections were conducted using resources available on the TxDOT website. Two types of projects were targeted for our study: the first involved identifying newly constructed CRCP projects with varying slab thicknesses, and the second focused on asphalt-overlaid rigid pavements.

For the first type, information on state-let construction projects was accessed through the "Plans Online" feature on the TxDOT website. This allowed us to compile a list of all projects proposing the construction of new CRCP within Texas over a three-year period (2020, 2021, and 2022). The goal was to track projects whose construction would align with the timeframe of this research. After compiling the list, we reached out to individual project contacts, primarily area engineers, to establish communication and determine suitable field tests for our needs. The aim was to secure 3 to 4 projects for each of the three slab thickness categories: 7-8 inches (low range), 9-12 inches (medium range), and 13-15 inches (high range). The methodology used for testing is detailed in the next section.

Table 5-1below shows the identified projects and the status of the test sections where testing was conducted. Additionally, Figure 5-1 shows the map of these test sections across Texas.

Table 5-1 Identified projects and the status of the testing

District	Highway	County	Point of Contact	Remarks
Dallas	-	Dallas	Amanda Miller	Section was too short to perform test
	-	Denton	Travis Campbell	No communication from Stacy Clack, TxDOT Engineer. Follow-up was done.

	-	Collin	Jennifer Vorster	No reply to the email
	-	Ellis	Juan Paredes	No reply to the email
Fort Worth	SH199	Tarrant	David Neeley	We performed the test
Houston	-	Brazoria	Maria Aponte	No reply to the email
	-	Galveston	David Lazaro	No reply from the contractor. Communicated from our end.
	-	Montgomery	Abraham Guzman	Replied to the email, but no further response
	-	Fort Bend	Carlos Zepeda	No reply to the email
Houston	-	Harris	Jamal Elahi	Project ended, so no further communication
Odessa	IH20	Midland	Fred Herrera	We performed the test
	-	Ector		No project identified
San Antonio	IH10	Guadalupe	Will Lockett	We performed the test
	-	Bexar		No project identified
Lubbock	Loop 88	Lubbock	Michael Whittie	We performed the test
	US69	Gaines	Seve Sisneros	We performed the test
	-	Lynn	-	No project identified
El Paso	-	West El Paso	Jonathan Concha	No reply to the email
	-	East El Paso	Rene Romero	The project ended, so no further communication
Bryan	IH45	Walker	Delmy Reyes	We performed the test
Paris	FM2642	Hunt	James Atkins	No reply from the contractor.
Atlanta	US59	Panola	Jacob Vise	We performed the test

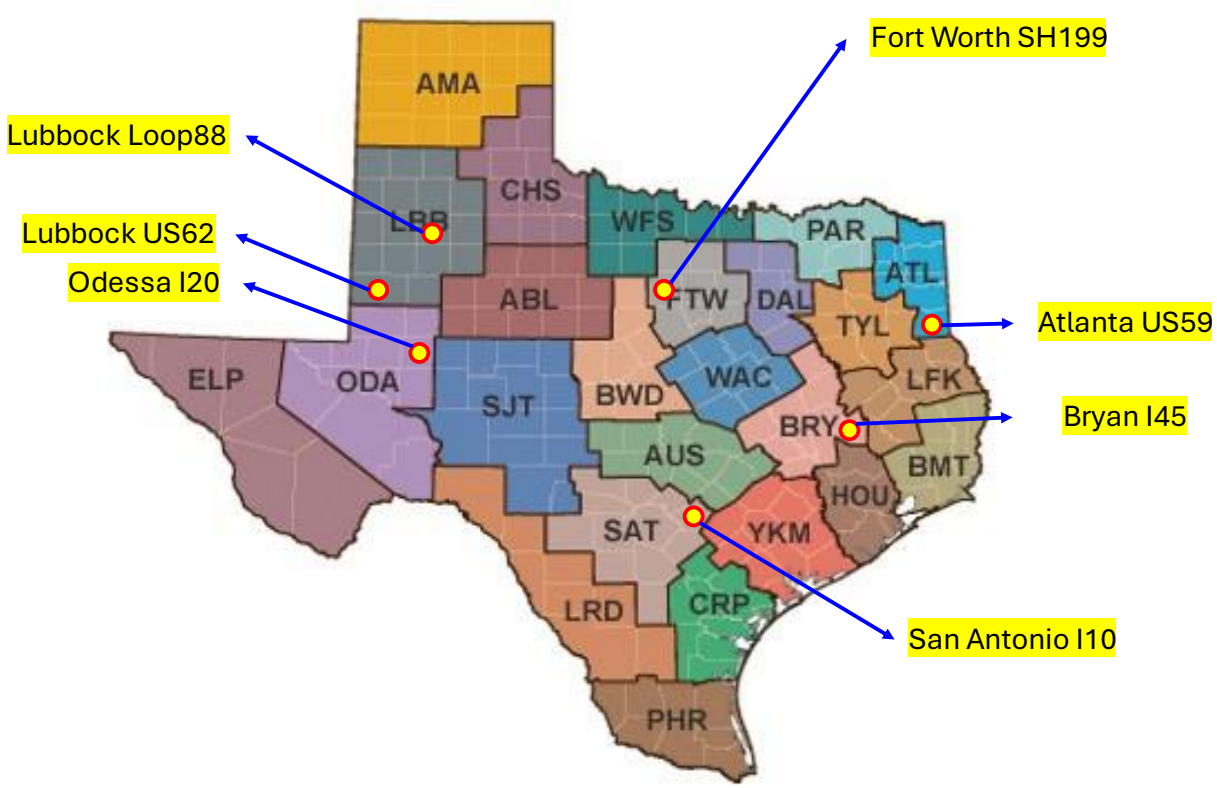

Figure 5-8 Location of test section selected for testing on New CRCP construction Projects

For the second type of project, which involved identifying asphalt-overlaid rigid pavements, we utilized PMIS data. Our effort was focused on locating pavements that were originally rigid but had an abrupt end to PMIS data collection. Further an inquiry was made to the district office in Houston for information on their asphalt overlaid section. The selected test sites and their corresponding map are shown in Figure 5-9.

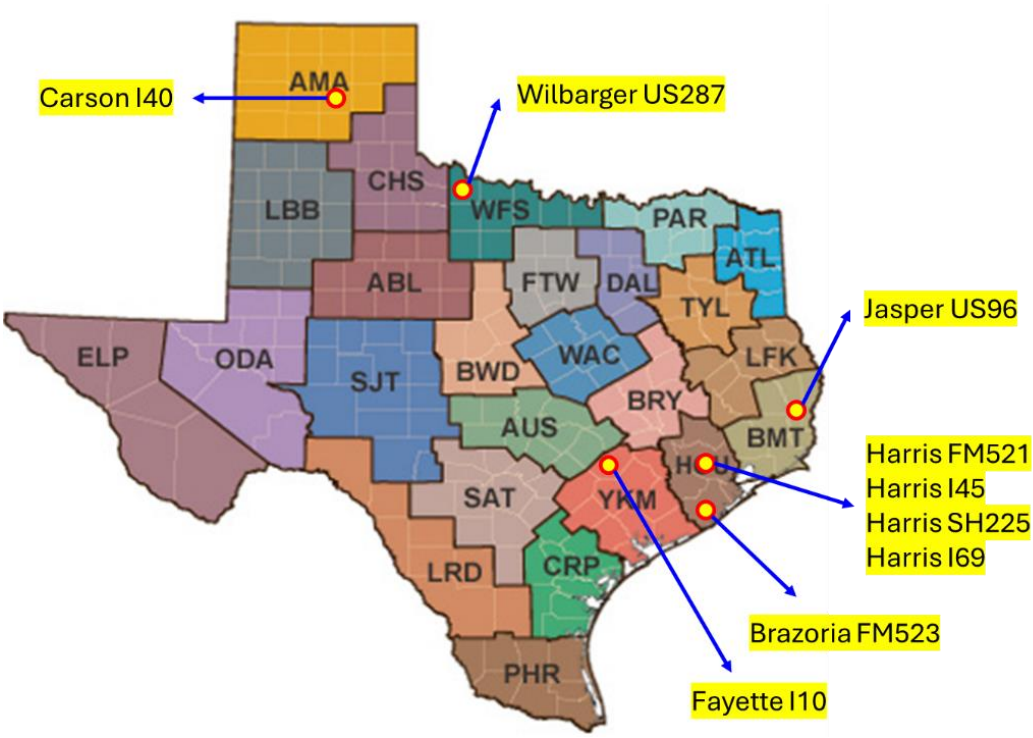

Figure 5-9 Location of test section selected for testing on Asphalt-overlaid rigid pavements

5.1.2 Methodology of field testing

The field-testing methodology for both types of selected projects is detailed below.

New CRCP Construction Projects

The primary objective of field testing for new CRCP construction projects was to obtain deflection data on both the newly constructed base layer and the CRCP itself. This data would then be used to develop correlations between the deflections observed on the base layer and those on the CRCP. The final selection of projects, as outlined in the earlier section, was based on three key factors:

- **Base Type:** To introduce variability in base types, efforts were made to identify projects that included both Asphalt Stabilized Base (ASB) and Cement Treated Base (CTB).
- **CRCP Slab Thickness:** While it was ideal to include all slab thicknesses in the testing, it was not feasible to test every thickness used in Texas. Therefore, three or four projects were selected from each of the following categories: lower end (7 to 8 inches), mid-range (9 to 12 inches), and high end (13 to 15 inches).
- **Section Geometry:** Ideally, the selected sections were on level terrain with a vertical grade of less than 2 percent. The length of the one-day placed section was at least 1,000 feet, and the total width was at least 20 feet to ensure accurate deflection measurements under interior loading conditions.

Another variable of interest was subgrade treatment (e.g., lime-treated vs. cement-treated). The modulus of the subgrade layer was evaluated using the Dynamic Cone Penetrometer (DCP) in each project, and the effects of subgrade treatment or subgrade type are analyzed during the data analysis phase.

The testing sequence for each selected project was as follows:

- **Selection of Alignments:** As illustrated in Figure 5-10, longitudinal alignments of 1,000 feet were chosen for testing. The test points along these alignments were carefully marked to ensure consistency in data collection.

Figure 5-10 Selection of 1000-feet length test section and recording of testing points

- **FWD Testing on ASB:** The Falling Weight Deflectometer (FWD) was deployed along the selected longitudinal alignments on the ASB/CTB base at 20-foot intervals, as shown in Figure 5-11. The FWD drops consisted of a seating drop, followed by loads of 6,000 lbs, 9,000 lbs, and 15,000 lbs, to capture a range of deflection data.

Figure 5-11 FWD testing on top of Base

- **DCP Testing:** To further assess the subgrade modulus and verify the quality of the deflection data, Dynamic Cone Penetrometer (DCP) testing was conducted every 100 feet along the selected 1,000-foot section where FWD testing was performed. As shown in Figure 5-12, a hole was first drilled into the constructed base to accommodate the DCP testing equipment as shown in Figure 5-13. This testing provided additional

insights into the subgrade conditions. In cases where further information on the soil was required, soil samples were collected to investigate any anomalies in the deflection data.

Figure 5-12 Drilling on the constructed base for DCP testing

Figure 5-13 DCP Testing performed in the drilled hole

- **FWD Testing on CRCP:** After the concrete was placed and cured for more than 10 days (but before the section was opened to traffic), FWD testing was conducted at the same locations as on the ASB layer, as shown in Figure 5-14. Ensuring that the FWD was positioned accurately within a few inches of the original ASB test locations was

critical for obtaining high-quality data. To achieve this, GPS technology equipped with real-time kinematic (RTK) positioning was used to provide precise location information. Access to the Receiving Agency's RTK Network was secured to set up the nearest base station to the project site, ensuring the necessary level of accuracy in the test points.

Figure 5-14 FWD testing on CRCP

Asphalt-Overlaid rigid pavements

The methodology for selecting and testing asphalt-overlaid rigid pavements followed a process similar to that used for new CRCP construction projects. The final selection of highway segments was based on the following criteria:

- **Asphalt Overlay Thickness:** Test sections with both thin overlays (2 inches or less) and thick overlays (greater than 2 inches) were identified for inclusion.
- **Type of Rigid Pavement:** Both CRCP (Continuously Reinforced Concrete Pavement) and CPCD (Continuously Reinforced Concrete Design) pavements that had undergone asphalt overlay were selected.
- **Thickness of Rigid Pavement Layer:** The selected test sections were categorized into three groups: thin (less than 9 inches), medium (9 to 11 inches), and thick (greater than 11 inches).
- **Section Geometry:** Efforts were made to select sections that were at least 1,000 feet in length, on level terrain, and with a vertical grade of less than 2 percent.

The actual number of selected locations depended on the existing hot mix asphalt (HMA) overlay on the CPCD/CRCP sections.

The testing sequence for each selected project involved the following steps:

- **Selection of Alignments:** As illustrated in Figure 5-15, longitudinal alignments of 1,000 feet were chosen for testing.

Figure 5-15 Selection of 1000feet of testing and marking of the test location

- **FWD Testing on HMA over CPCD/CRCP:** Figure 5-16 shows the use of the FWD machine on the HMA overlay along the selected longitudinal alignments, with tests conducted at 20-foot intervals. The FWD drops included a seating drop, followed by loads of 6,000 lbs, 9,000 lbs, and 15,000 lbs.

Figure 5-16 FWD testing on asphalt overlaid rigid pavements

- **Additional Testing:** At selected locations where further information was required, cores of the asphalt overlay, concrete, and base layers were taken, and Dynamic Cone Penetrometer (DCP) testing was conducted, as shown in Figure 5-17.

Figure 5-17 Coring and DCP test on the points of interest

5.1.3 Project Overview and Presentation of Data

Based on the list of identified and selected test sites, testing was conducted in alignment with the methodology described in the earlier section. In this section, two objectives will be addressed: first, to introduce the details of each project, and second, to present the FWD testing data and subgrade modulus, which will be utilized in Chapter 3.

New CRCP Construction Projects

Testing was performed based on the availability of projects and their schedules that matched our timeframe. A total of nine projects were identified under the new CRCP construction category, as shown in Table 5-2. The table below outlines the projects categorized by CRCP thickness, along with information on location, CSJ, respective thickness, base type, and the status of testing.

The projects are categorized as follows:

- Low Range (7-8 inches CRCP)
    - Loop88 Lubbock
    - US59 Panola
    - SH199 Tarrant
- Medium Range (9-12 inches CRCP)
    - US62 Gaines
- High Range (13-15 inches CRCP)
    - IH20 Midland

- IH10 Guadalupe
- IH45 Walker

Table 5-2 Detailed on selected new CRCP construction project

S.No.	State-let-Construction Year	District	County	Highway	CSJ	CRCP Thickness (inches)	Base Type	Status
1	2021	LBB	Lubbock	Loop88	1502-01-029	8	4" ASB + Density Controlled	CRCP Deflection pending
2	2020	ATL	Panola	US59	0063-10-015	8	1" Bond Breaker + 6" CTB + 8" CTS	Completed
3	2020	FWT	Tarrant	SH199	0171-04-050	8	4" ASB + 8" LTS	Completed
6	2022	LBB	Gaines	US62	0228-02-049	10	4" ASB + Density Controlled	Completed
7	2021	ODA	Midland	I20	0005-14-084	13	1" Bond Breaker + 6" CTB	Completed
8	2021	SAT	Guadalupe	I10	0025-03-097	13	5" ASB + Density Controlled	Completed
9	2021	BRY	Walker	I45	0675-07-097	15	1" Bond Breaker + 6" CTB + 8" LTS	Completed

There are six different base profiles, as shown in Figure 5-18. These profiles have been assigned specific nomenclature that will be useful in interpreting the data in the next chapter. Detailed information on each individual project will be presented in the following sections.

- BM 1 – 1” Bond Breaker + 6” CTB + 8” LTS + Subgrade
- BM 2 - 1” Bond Breaker + 6” CTB + 8” CTS + Subgrade
- BM 3 - 1” Bond Breaker + 6” CTB + Subgrade
- BM 4 - 4” ASB + 8” LTS + Subgrade
- BM 5 – 5” ASB + Subgrade
- BM 6 – 4” ASB + Subgrade

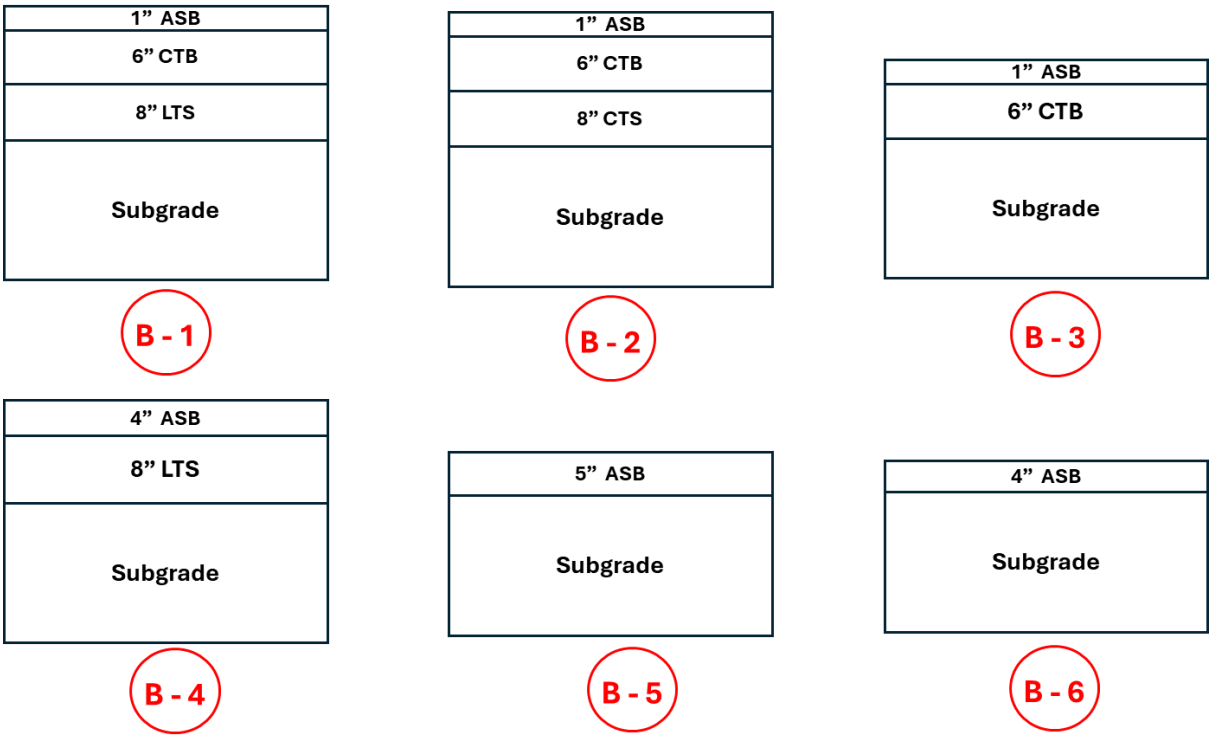

Figure 5-18 Different Type of Base encountered within selected test projects

SH199 Tarrant (8-inches)

The test section in question falls under both the Low Range and Medium Range categories, as it comprises 8-inch and 10-inch CRCP. This section will focus on the 8-inch portion, with details on the 10-inch section to be discussed later. The test section is located at SH199 in Tarrant County, within the Fort Worth district. Figure 5-19 illustrates the start and end points of CSJ 0171-04-50. The pavement base structure consists of a 4-inch layer of Hot Mix Asphalt (HMA) over an 8-inch Lime Treated Subgrade (LTS). The Falling Weight Deflectometer (FWD) test was conducted over a selected 1,000-foot section to measure deflections.

FWD Test Results:

- **Base Deflection:**
  - The deflection of the base layer ranged from a maximum of 33 mils to a minimum of 3.5 mils.
- **CRCP Deflection**
  - The deflection measured on the CRCP ranged from 3 mils to 0.65 mils. The notably low deflection values in some parts of the section were attributed to refusal encountered during the Dynamic Cone Penetrometer (DCP) test.

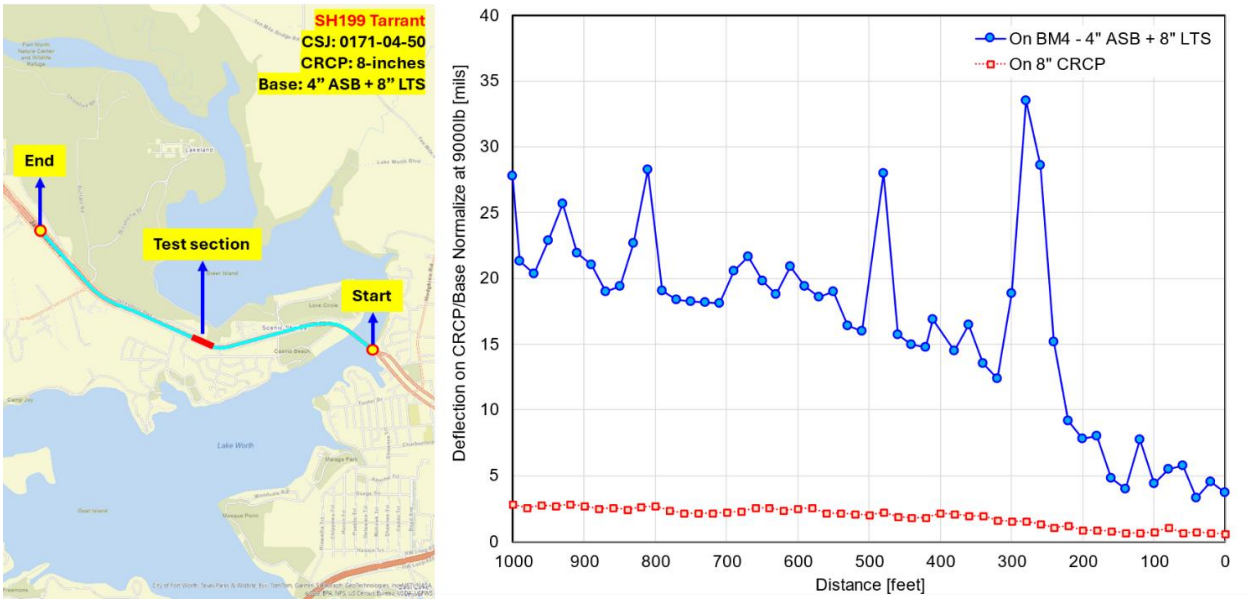

Figure 5-19 Map and FWD testing results of SH199 Tarrant (8-inches)

Subgrade Modulus:

- As seen in Figure 5-20, the subgrade modulus was measured at 100-foot intervals along the test section using the DCP method. A total of 11 points were tested, with three points showing refusal, indicating extremely high subgrade stiffness.
- The effective subgrade modulus ranged from 9.51 ksi to 20.58 ksi, reflecting variability in subgrade conditions along the test section.

To ensure the accuracy of the analysis, the low deflection values observed in the latter 300 feet of the test section, likely influenced by the extremely stiff subgrade, were excluded from the final field measurement data. This exclusion helps to prevent any potential bias in the interpretation of the overall deflection behavior across the test section.

On 8" CRCP	3.16	2.96	2.98	2.45	2.76	2.21	2.37	1.73	1.00	0.84	0.65
On 4" HMA Ty B	27.81	21.94	28.26	18.12	20.93	15.99	16.87	18.83	7.83	4.39	3.72
Depth (in)	1913	1914	1915	1916	1917	1918	1919	1920	1921	1922	1923
4" HMAC TY "B" PG64-22 + Prime Coat (EC-30) + 8" LTS											
1–31	19.61 / 10.7	19.20 / 11.4	19.81 / 10.87	27.06 / 15.42 / 8.13 / 15.6	17.92 / 9.4 / 8.2	21.87 / 16.5 / 7.65 / 22.5	17.81 / 9.63 / 24.53 / 16.27	29.21 / 18.73 / 11.65 / 24.16	24.15 / 13.03 / 35.94 / REFUSAL	25.58 / REFUSAL	25.04 / REFUSAL
Effective Modulus (ksi)	11.66	12.24	11.89	10.98	9.51	10.88	20.58	18.89	22.01	25.58	25.04

Figure 5-20 Subgrade Modulus profile for SH199 Tarrant (8-inches)

Loop 88 Lubbock (8-inches)

The second test section represents the Low Range category, as it comprises 8-inch CRCP. This test section is located on Loop 88 in Lubbock County, within the Lubbock district. Figure 5-21 provides a visual representation of the start and end points of CSJ 1502-01-030. The pavement base structure consists of a 4-inch layer of Hot Mix Asphalt (HMA) placed over a density-controlled subgrade. The Falling Weight Deflectometer (FWD) test was conducted over a selected 1,000-foot section to measure deflections and determine the subgrade modulus at 11 different points along the section. However, it is important to note that the FWD test on the CRCP is currently in the construction phase and has yet to be completed. Once the testing is finished, the report will be updated accordingly.

FWD Test Results

Base Deflection

- The deflection of the base layer ranged from a maximum of 45.2 mils to a minimum of 16.68 mils.

CRCP Deflection

- The deflection of the CRCP layer ranged from a maximum of 3.00 mils to a minimum of 1.87 mils.

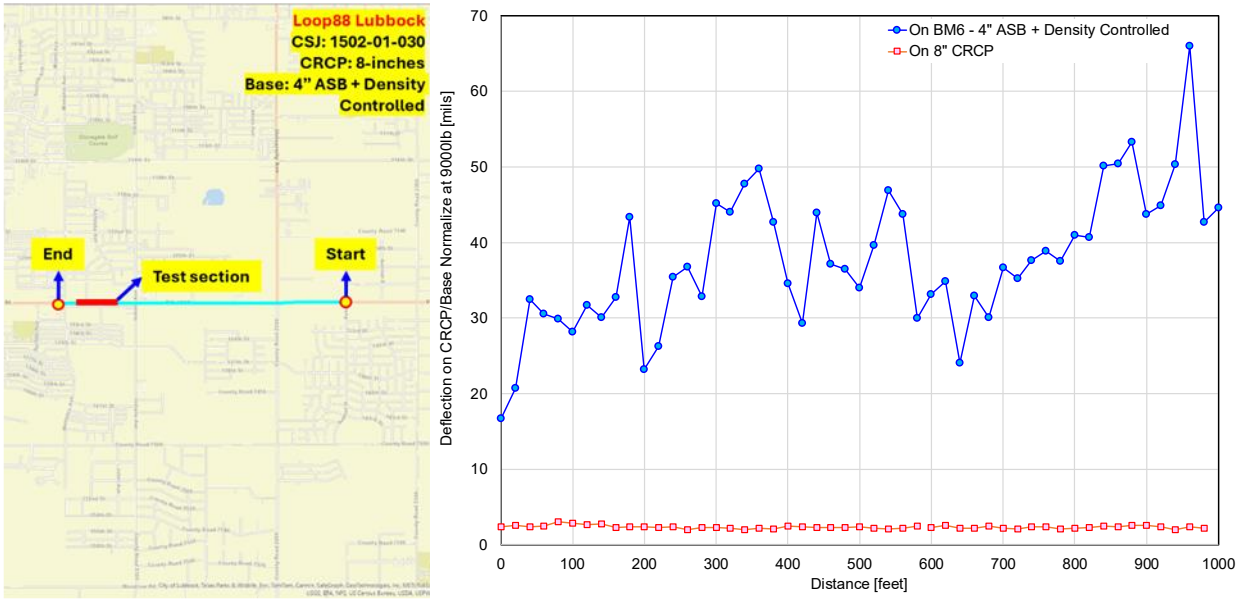

Figure 5-21 Map and FWD testing results of Loop88 Lubbock (8-inches)

Subgrade Modulus

- No refusal was encountered.
- Figure 5-22 shows an effective subgrade modulus ranged between 13.94 ksi to 21.63 ksi. This range indicates a moderately stiff subgrade, providing adequate support.

On 8" CRCP	2.39	3	2.32	2.26	2.06	2.29	2.27	2.5	2.07	2.52	2.15
On 4" HMA Ty B	16.68	28.14	23.16	45.2	34.56	33.99	33.18	36.68	41.02	43.76	44.64
Station No.	13503	13504	13505	13506	13507	13508	13509	13510	13511	13512	13513
Depth (in)	*4" HMAC TY "C" + Prime Coat (EC-30)*										
1–31	24.33	20.84	14.97	11.27	15.31	13.21	15.77	11.18	15.46	14.90	12.06
	12.61	15.35		18.95	21.66	23.86	23.42	17.1	22.56	21.45	21.3
	19.74	25.80		24.55				28.99	28.97		13.64
Effective Modulus (ksi)	18.57	21.52	14.97	16.65	17.46	15.86	17.96	16.15	21.63	17.47	13.94

Figure 5-22 Subgrade Modulus profile for Loop88 (8-inches)

US59 Panola (8-inches)

The third test section under consideration is also categorized under the Low Range category, featuring an 8-inch CRCP. This section is located on US59 in Panola County, within the Atlanta district. Figure 5-23 provides a detailed map showing the start and end points of CSJ 0063-10-015. The pavement base structure consists of a 1-inch bond breaker, a 6-inch Cement Treated Base (CTB), and an 8-inch Cement Treated Subgrade (CTS). The Falling Weight Deflectometer (FWD) test was conducted over a selected 1,000-foot section to measure deflections and determine the subgrade modulus at 11 different points along the section. However, it is important to note that the FWD test on the CRCP could only be conducted for an 800 foot length because the construction of the first 200 feet was postponed due to a change in the paving plan.

FWD Test Results

Base Deflection

- The deflection of the base layer ranged from a maximum of 21.98 mils to a minimum of 8.18 mils.

CRCP Deflection

- The deflection of the CRCP layer ranged from a maximum of 2.77 mils to a minimum of 1.87 mils.

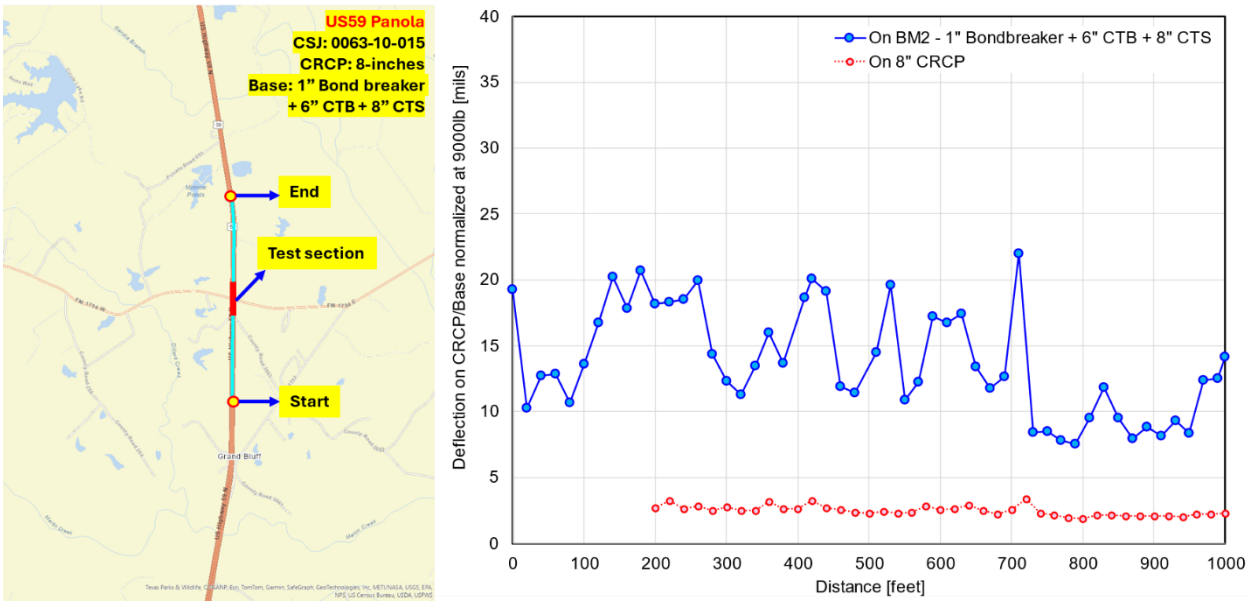

Figure 5-23 Map and FWD testing results of US59 Panola(8-inches)

Subgrade Modulus

- No refusal was encountered.

- Figure 5-24 shows the effective subgrade modulus ranged between 10.72 ksi to 28.95 ksi. This range indicates a moderately stiff subgrade, providing adequate support.

On 8" CRCP	-	-	2.69	2.77	2.61	2.29	2.59	2.55	1.87	2.09	2.29
On 1" HMA	19.25	13.59	18.21	12.34	18.67	14.48	16.74	21.98	9.50	8.18	14.13
Depth (in)	867	866	865	864	863	862	861	860	859	858	857
1" HMAC + Prime MC-30 + 6" CTB + 8" CTS											
1	30.13	26.73	26.65	37	21.24	12.45	26.14	42.06	44.62	55.29	48.34
2						8.79	13.45				
3				17.34				6.97			
4						16.48	8.94		13.95	11.74	10
5	19.91	22.51	12.69	26.84	14.63			11.02			
6						23.34					
7				38.31							
Effective Modulus (ksi)	20.87	22.91	13.94	28.95	16.16	16.36	10.72	15.34	20.34	18.06	15.72

Figure 5-24 Subgrade Modulus profile for US59 Panola (8-inches)

US69 Gaines (10-inches)

The fifth test section under consideration is also categorized under the Medium Range category, featuring a 10-inch CRCP. This section is located on US62 in Gaines County, within the Lubbock district. Figure 5-25 provides a detailed map indicating the start and end points of CSJ 0228-02-049. The pavement base structure consists of a 4-inch Asphalt Stabilized Base (ASB) over a density-controlled subgrade. The Falling Weight Deflectometer (FWD) test was conducted over a selected 1,000-foot section to measure deflections and determine the subgrade modulus at 11 different points along the section.

FWD Test Results

Base Deflection

- The deflection of the base layer ranged from a maximum of 40.62 mils to a minimum of 20 mils.

CRCP Deflection

- The deflection of the CRCP layer ranged from a maximum of 2.1 mils to a minimum of 2.87 mils.

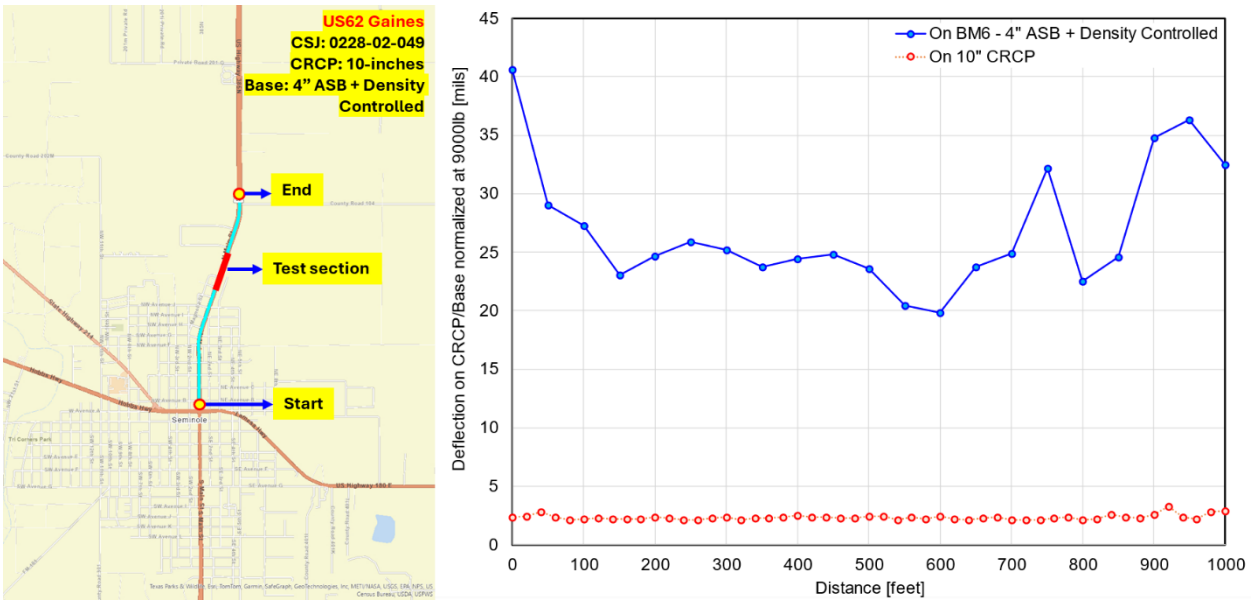

Figure 5-25 Map and FWD testing results of US69 Gaines(10-inches)

Subgrade Modulus

- No refusal was encountered.
- Figure 5-26 shows the effective subgrade modulus ranged between 9.38 ksi to 24.34 ksi. This range indicates a moderately stiff subgrade, providing adequate support.
- Two specific points showed effective subgrade modulus values of 10.16 ksi and 9.38 ksi, with a layer which had subgrade modulus as low as 8 mils.

On 10" CRCP	2.39	2.19	2.34	2.34	2.48	2.43	2.4	2.12	2.1	2.62	2.87
On 4" ASB	40.62	27.27	24.68	25.19	24.45	23.6	19.89	24.882	22.53	34.76	32.46
Depth (in)	81+00	82+00	83+00	84+00	85+00	86+00	87+00	88+00	89+00	90+00	91+00
4" Type C HMA + Density Controlled											
1 2 3 4 5 6 7 8 9 10 11 12 13 14 15 16 17 18 19 20 21 22 23 24 25 26 27 28 29 30 31 32 33 34 35 36	15.82 12.45 8.28	15.26 19.8	17.76 43.75 28.18 13.15	9.2 16.1 27.6 34.7	14.92 27.27 31.79 12.92	14.45 25.16 24.12 16.67	16.04 27.62 14.89	19.79 21.51 16.52 44.05	23.71 27.49 25.05 14.44	8.18 21.04 14.76 9.63	6.23 10.49 11.4 8.27
Effective Modulus (ksi)	**10.16**	**18.52**	**24.34**	**11.76**	**18.79**	**21.98**	**19.08**	**21.09**	**21.65**	**16.05**	**9.38**

Figure 5-26 Subgrade Modulus profile for US69 Gaines (10-inches)

I20 Midland (13-inches)

The seventh test section under consideration is also categorized under the High Range category, featuring a 13-inch CRCP. This section is located on IH20 in Midland County, within the Odessa district. Figure 5-27 provides a detailed map indicating the start and end points of CSJ 0005-14-084. The pavement base structure consists of a 1-inch bond breaker placed over a 6-inch Cement Treated Base (CTB). The Falling Weight Deflectometer (FWD) test was conducted over a selected 1,000-foot section to measure deflections and assess the subgrade modulus at 11 different points along the section.

FWD Test Results

Base Deflection

- The deflection of the base layer varied significantly, ranging from a maximum of 31.2 mils to a minimum of 8.07 mils.

CRCP Deflection

- The deflection of the CRCP layer ranged from 2.26 mils to 1.33 mils. These relatively low deflection values indicate that the CRCP is performing effectively.

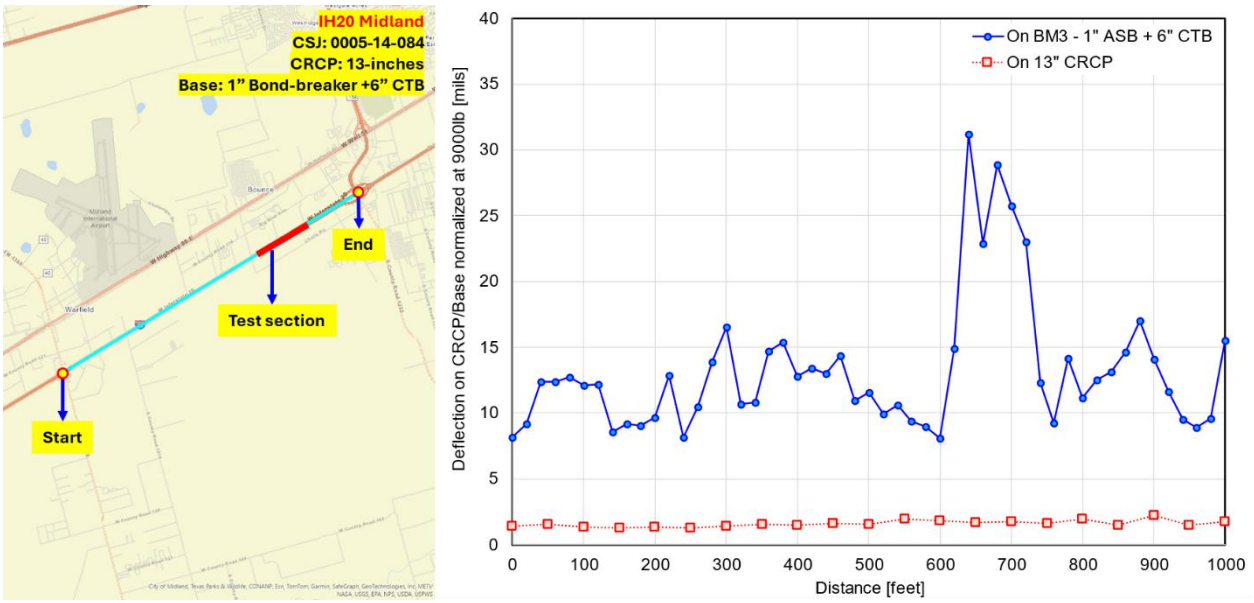

Figure 5-27 Map and FWD testing results of IH20 Midland(13-inches)

Subgrade Modulus

- Refusal was encountered at five out of the 11 test points as shown in Figure 5-28. This suggests areas of exceptionally high subgrade stiffness, which can significantly impact the deflection measurements.
- The effective subgrade modulus ranged between 19.79 ksi to 82.72 ksi. This range indicates a very stiffer subgrade, providing adequate support.
- To avoid any potential bias, deflection data from points where refusal was encountered have been excluded from the final analysis.

On 13" CRCP	1.4	1.33	1.34	1.42	1.47	1.56	1.8	1.74	1.94	2.26	1.76
On 1" TOM-C	8.99	12.09	9.64	16.56	12.81	11.58	8.07	25.72	11.15	14.08	15.54
Depth (in)	1007	1008	1009	1010	1011	1012	1013	1014	1015	1016	1017
1" TOM-C + 6" CTB											
1 2 3 4 5 6 7 8 9 10 11 12 13 14 15 16 17 18 19 20 21 22 23 24 25 26 27 28 29 30 31 32 33 34 35 36	34.14 / 18.1	49.42 / 21.18	60.29 / 28.29 / 16.41	72.59 / REFUSAL	42.17 / 116.19 / REFUSAL	78.32 / REFUSAL	68.81 / REFUSAL	49.34 / 27.06 / 15.66	82.72 / REFUSAL	49.34 / 27.06 / 15.66 / 18.39	66.68 / 45.39 / 32.44 / 12.54
Effective Modulus (ksi)	19.79	24.28	30.59	72.59	67.07	78.32	68.81	26.50	82.72	33.70	31.89

Figure 5-28 Subgrade Modulus profile for IH20 Midland (13-inches)

I10 Guadalupe (13-inches)

The eighth test section under consideration is also categorized under the High Range category, featuring a 13-inch CRCP. This section is located on IH10 in Guadalupe County, within the San Antonio district. Figure 5-29 provides a detailed map showing the start and end points of CSJ 0025-03-097. The pavement base structure consists of a 5-inch Asphalt Stabilized Base (ASB) placed over a density-controlled subgrade. The Falling Weight Deflectometer (FWD) test was conducted over a selected 1,000-foot section to measure deflections and assess the subgrade modulus at 11 different points along the section.

FWD Test Results

Base Deflection

- The base layer deflection ranged from a maximum of 17.69 mils to a minimum of 11.46 mils.

CRCP Deflection

- The deflection of the CRCP layer was relatively consistent, ranging from a maximum of 1.81 mils to a minimum of 1.48 mils.

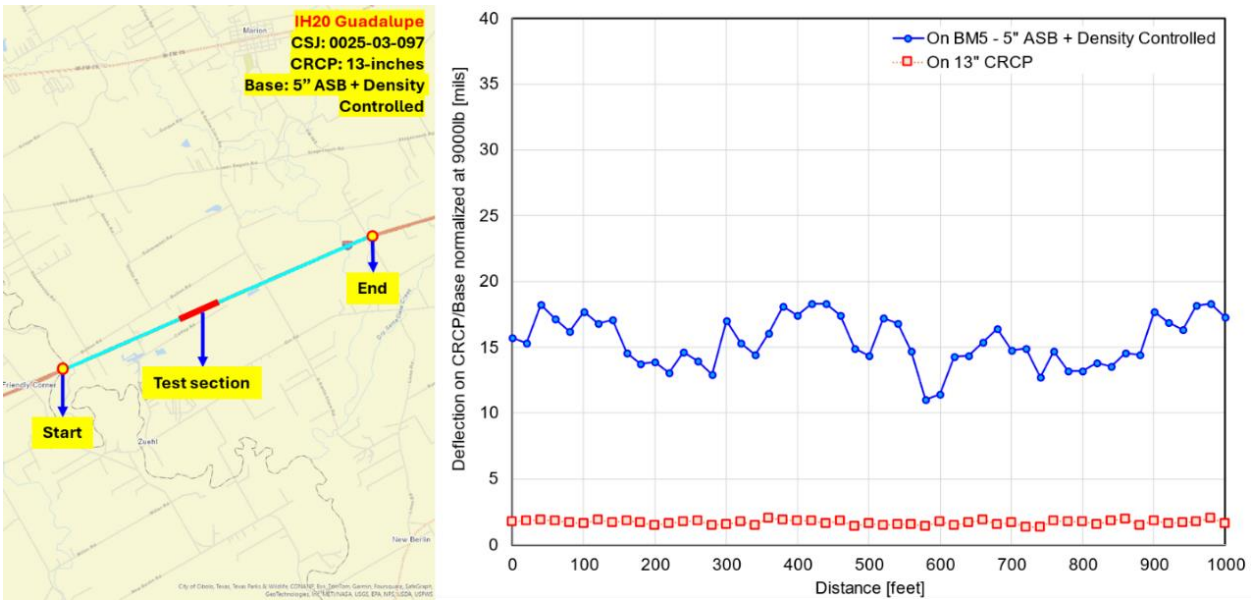

Figure 5-29 Map and FWD testing results of IH20 Guadalupe(13-inches)

Subgrade Modulus

- No refusal encountered.
- Figure 5-30 shows the effective subgrade modulus values range from 11.46 ksi to 17.68 ksi, indicating a moderately stiff subgrade layer.

On 13" CRCP	1.73	1.60	1.48	1.55	1.81	1.63	1.75	1.69	1.74	1.80	1.63
On 5" HMA Ty B	15.70	17.68	13.91	17.04	17.41	14.37	11.46	14.80	13.17	17.69	17.28
Depth (in)	1855	1856	1857	1858	1859	1860	1861	1862	1863	1864	1865
13" CRCP +5" HMA Type - B + Prime Coat + Density Controlled											
1	56.83	20.17	51.01	36	53.84	50.8	84.9	30.91	66.22	66.22	54.57
2											
3											
4											
5											
6											
7	28.17		37.46		27.1	30.08	29.98				36.55
8											
9											
10		22.65			39.16	42.62			24.62		
11											
12											
13											
14											
15											
16	12.79			16.25				16.55	26.13		
17											
18											
19											
20		12.71	16.24		15.02	17.6	20.52				16.56
21											
22											
23											
24								14.46	14.5		
25											
26											
27	18.86										
28											
29											
30											
31											
Effective Modulus (ksi)	24.92	16.06	30.31	23.21	22.72	25.96	27.63	23.43	31.19	24.57	25.76

Figure 5-30 Subgrade Modulus profile for IH10 Guadalupe (13-inches)

I45 Walker (15-inches)

This section is located on IH45 in Walker County, within the Bryan district. Figure 5-31 provides a visual representation of the start and end points of CSJ 0675-07-097. The pavement base structure consists of a 1-inch bond breaker placed over a 6-inch Cement Treated Base (CTB) and an 8-inch Lime Treated Subgrade (LTS). The FWD test was conducted over a selected 1,000-foot section to measure deflections and assess the subgrade modulus at 11 different points along the section. However, it is important to note that the FWD testing on the CRCP is still in the construction phase and has yet to be completed. Once testing is finished, the report will be updated accordingly.

FWD Test Results

Base Deflection

- The deflection of the base layer ranged from a maximum of 12.86 mils to a minimum of 5.31 mils. This relatively low deflection suggests that the base structure, supported by the 6-inch CTB and 8-inch LTS, provides robust support.

CRCP Deflection

- The deflection of the CRCP layer was relatively consistent, ranging from a maximum of 1.27 mils to a minimum of 0.87 mils, an average of 1.08 mils.

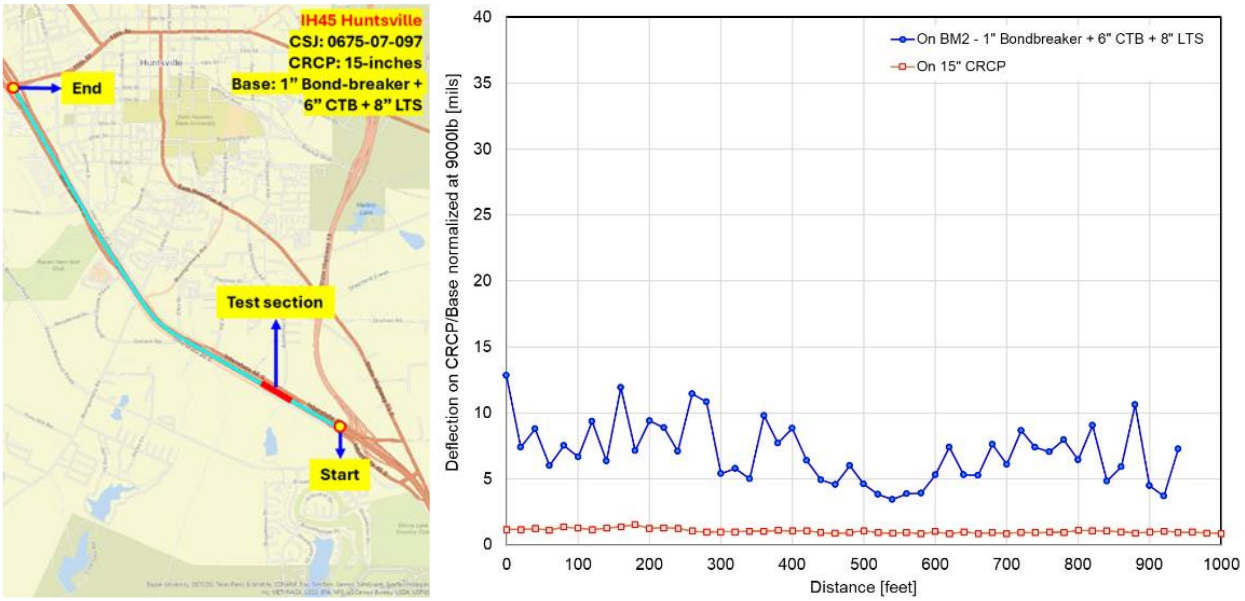

Figure 5-31 Map and FWD testing results of IH45 Walker(15-inches)

Subgrade Modulus

- No refusal encountered.
- Figure 5-32 shows the effective subgrade modulus values ranged from 16.42 ksi to 47.75 ksi, indicating a stiffer subgrade layer.

On 15" CRCP	1.16	1.27	1.26	0.99	1.05	1.09	1.01	0.87	1.11	0.98	
On 1" Tom-C	12.86	6.66	9.40	5.38	8.83	4.63	5.31	6.11	6.46	4.49	
Depth (in)	1704	1705	1706	1707	1708	1709	1710	1711	1712	1713	1714
15" CRCP + 1" TOM-C + 6"CTB + 8" CTS											
1 2 3 4 5 6 7 8 9 10 11 12 13 14 15 16 17 18 19 20 21 22 23 24 25 26 27 28 29 30 31 32 33 34 35	34.83	46.72	52.93	60.28	29.52	59.75	43.65	50.9	123.99	58.99	40.58
	12.35	20.48	11.75	13.09	11.29	22.56	28.75	27.6	34.39	27.54	28.13
	11.07	12.87	6.3	17.18	17.99	55.75					
	21.91	9.45	22.47	30.4	13.86	28.36					
Effective Modulus (ksi)	16.42	20.34	21.13	25.10	18.17	36.54	31.29	30.93	47.75	32.08	30.01

Figure 5-32 Subgrade Modulus profile for IH45 Walker (15-inches)

Asphalt overlaid rigid pavements

Table 5-3 presents the list of projects identified with asphalt-overlaid rigid pavements. The testing was conducted based on the availability of the projects and ongoing communication with area engineers. A total of nine projects were identified under this category. Among these, three sections fall under the category of HMA over CPCD/JRCP, while the remaining six sections involve HMA over CRCP. Testing and data collection were successfully completed for all identified projects, with the exception of the I-69 Frontage Road in Harris County, Houston district. This section underwent milling in preparation for an additional layer of asphalt overlay. Despite this, the milled surface provided an opportunity for preliminary testing. A follow-up round of FWD testing is planned once the asphalt overlay is completed later this year.

Table 5-3 List of Project identified with asphalt-overlaid rigid pavements

S. No.	District	County	Highway	CS	Pavement Structure	Status
1	BMT	Jasper	US96	0064-08	1.5" ASB + 9 CPJR + 8" CTB + 8" Select Materials	Completed
2	HOU	Harris	SH225	0502-01	1" TOM + 8" JRCP + 6" CSB + 6" LTS	Completed
3	HOU	Harris	I69	0027-13	1" TOM + 9" JRCP + 6" ASB + 6" LTS	Waiting for asphalt overlay
4	AMA	Carson	IH40	0275-04	3.5" ASB + 8" CRCP + LTS	Completed
5	YKM	Fayette	IH10	0535-07	5" ASB + 8" CRCP + Cement Treated Materials	Completed
6	WFS	Wilbarger	US287	0043-07	5" ASB + 8" CRCP + 4" CTB	Completed
7	HOU	Harris	FM521	0111-01	1.5" HMA + 8" CRCP +1"Bond Breaker + 6" CTB + 6" LTS	Completed

8	HOU	Harris	I45	0500-03	2" HMA + 6" CRCP + 6" CTB + 6" LTS	Completed
9	HOU	Brazoria	FM523	1003-01	1" HMA + 8" CRCP +1"Bond Breaker + 6" CTB + 6" LTS	Completed

US96 Jasper

The first test section for the asphalt overlaid rigid pavement that will be discussed was conducted on US96 in Jasper County. According to the details from the CS, this section features a pavement structure that includes a 1.5-inch asphalt overlay, a 9-inch JRCP, 8-inch CTB, and an 8-inch Select Materials. Testing was conducted on the outside lane in the northbound direction for 1000-ft length. This in the test section due to the unavailability of the coring equipment, we resort to drilling the test points and perform DCP testing.

FWD Test Results

- Figure 5-33 shows the deflection values for this test section, ranged from 1.83 mils to 3.79 mils, with an average deflection of 2.72 mils.

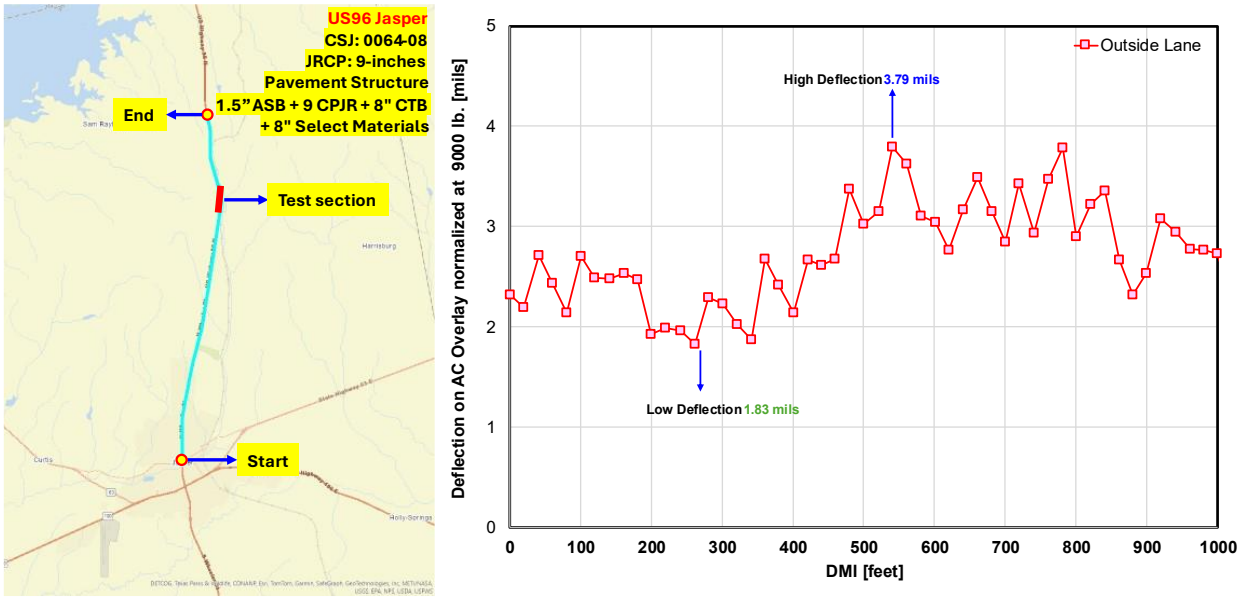

Figure 5-33 Map and FWD testing results of US96 Jasper

Subgrade Modulus

- The effective subgrade modulus was noted to be 21.40 mils and 29.38 mils for high and low deflections respectively as shown in Figure 5-34. It is important to note that both modulus ranges from moderate stiffness to high stiffness indicating this might be the reason for the difference in the deflection. However, it is important to note that the

variation in thickness does make a difference which will be more evident in other tested sections.

Depth (in)	High Deflection 3.79 mils	Low Deflection 1.83 mils
	Pavement Structure	
	1.5" HMA + 9 CPJR + 8" CTB + 8" Select Materials	
1 2 3 4 5 6 7	22.06	10.91
8 9 10 11 12 13 14	33.3	19.3
15 16 17 18 19 20 21 22 23 24 25 26 27 28 29 30 31 32 33 34 35 36		40.02
Effective Modulus (ksi)	21.40	29.38

Figure 5-34 Subgrade Modulus profile for US96 Jasper

SH225 Harris

The second test section is located on the frontage road of SH225 in Harris County, within the Houston district. This section features a pavement structure with a 1-inch Thin Overlay Mix (TOM) asphalt overlay. The existing pavement beneath the overlay consists of 8 inches of Jointed Reinforced Concrete Pavement (JRCP), 6 inches of Cement Stabilized Base (CSB), and 6 inches of Lime Treated Subgrade (LTS). Testing was conducted on the outside lane in the northbound direction over a 1,000-foot stretch.

FWD Test Results

As illustrated in Figure 5-35, the average deflection measured across this section was 4.95 mils, with a maximum deflection of 7.86 mils and a minimum deflection of 3.26 mils. It is important to note that the higher deflection was influenced by the proximity of the JRCP joint to the FWD drop location. To mitigate this bias, a deflection value of 5.44 mils was selected at a mid-slab location to investigate the cause of the observed thickness variation.

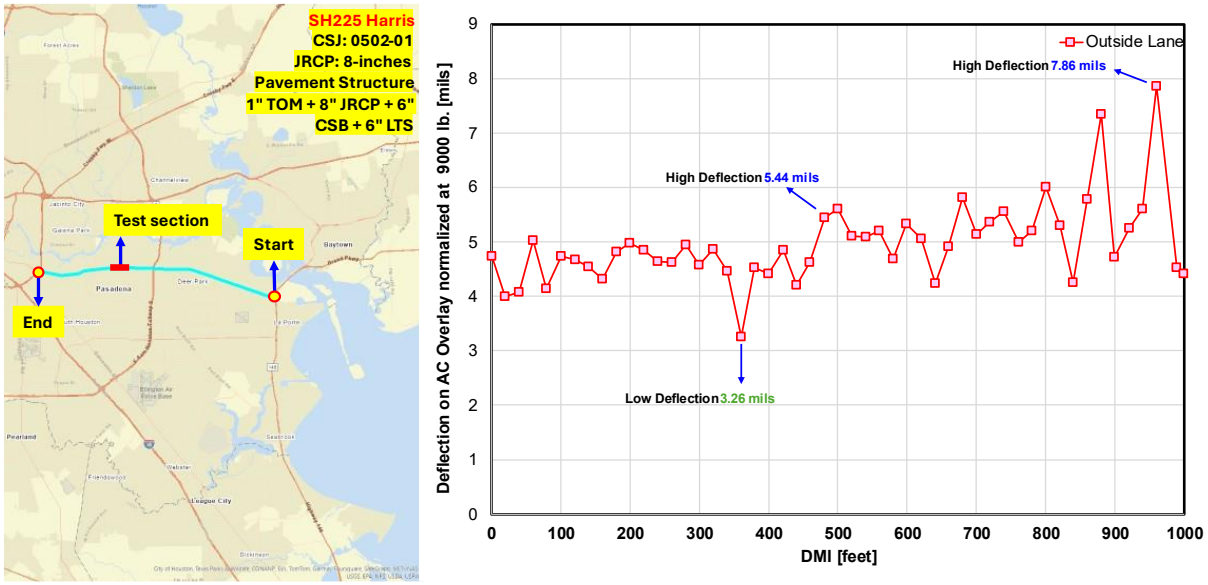

Figure 5-35 Map and FWD testing results of SH225 Harris

Core Analysis

Concrete cores were extracted from the locations with the highest and lowest deflections as shown in Figure 5-36.

- The core analysis revealed that the area with the higher deflection had a CRCP thickness of 8.5 inches. Additionally, the bond breaker in this area was found to be deteriorated, which likely contributed to the increased deflection. The Cement Treated Base (CTB) in this area measured 5 inches in thickness.
- In contrast, the location with the lower deflection had an asphalt overlay thickness of 1 inch and a CRCP thickness of 8 inches. The CTB in this area was intact and measured 4.5 inches, which contributed to the lower deflection observed.

High Deflection

Low Deflection

Figure 5-36 Concrete cores from SH225 Harris

Subgrade Modulus

The effective subgrade modulus was measured at two cored locations, yielding values of 11.28 ksi and 13.58 ksi, as shown in Figure 5-37. These measurements indicate that the subgrade modulus at both locations is relatively comparable. However, one notable difference is that the top 6 inches at the point with lower deflection exhibited a higher subgrade modulus. This suggests that the reduced deflection is not solely due to a single factor, but rather a combination of factors, including the thickness of the pavement layers, the integrity and bonding of these layers, and the subgrade modulus near the slab.

This observation highlights the importance of considering the subgrade modulus as a contributing factor when interpreting field data. The interaction between the pavement layers and the subgrade, particularly the stiffness of the subgrade near the slab, plays a significant role in influencing deflection outcomes.

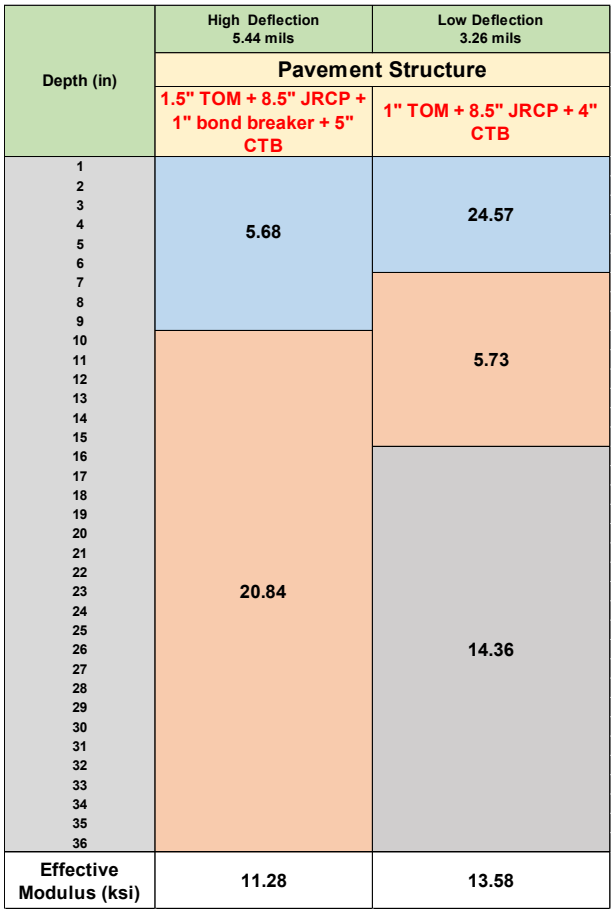

Figure 5-37 Subgrade Modulus profile for SH225 Harris

I69 Harris

The I-69 Frontage Road in Harris County, Houston district is the third section with 9-inch JRCP as shown in Figure 5-38. As mentioned earlier this section undergoes milling in preparation for an additional layer of asphalt overlay. Taking this as an opportunity, we performed FWD testing on presently milled surface. A follow-up round of FWD testing is planned once the asphalt overlay is completed later this year. This will help us compare before and after scenarios and measure the difference between the deflection that is being recorded.

The FWD test showed that it ranged between 2.16mils to 4.48 mils with an average of 3.05mils

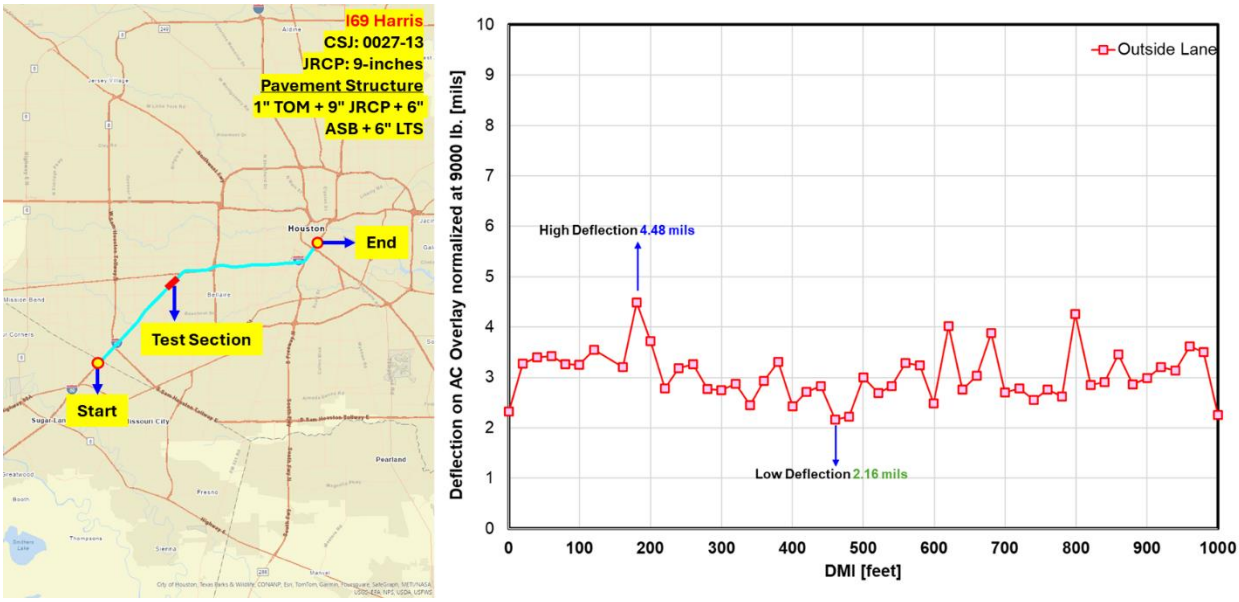

Figure 5-38 Map and FWD testing on IH69 Harris

I40 Carson

The fourth test section for asphalt overlaid rigid pavement was conducted on IH40 in Carson County, within the Amarillo district. This section, as specified by the CSJ, features a pavement structure that includes a 3.5-inch asphalt overlay, an 8-inch CRCP, and a Lime Treated Subgrade (LTS). The testing was performed on the outside lane in the westbound direction, covering a 1,000-foot stretch.

FWD Test Results

Figure 5-39 shows the deflection values for this test section ranged from 2.84 mils to 7.15 mils, with an average deflection of 3.55 mils. Since the Coring operation was not available due to

maintenance issue drilling was performed to conduct the DCP testing.

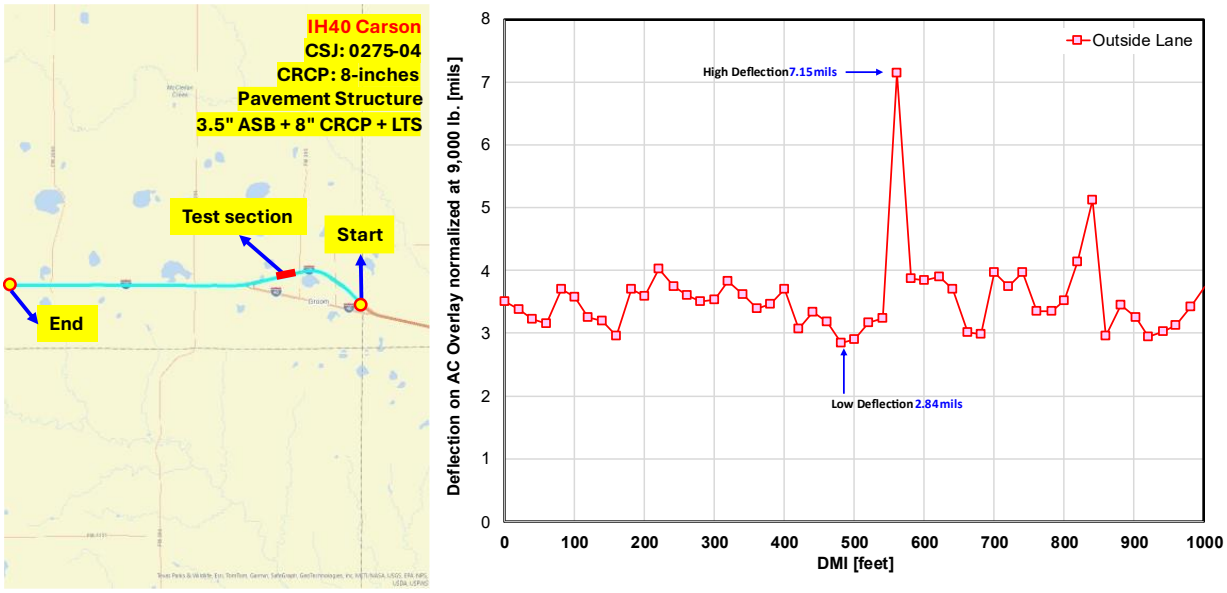

Figure 5-39 Map and FWD testing on IH40 Carson

Subgrade Modulus

The effective subgrade modulus was measured at two cored locations, yielding values of 19.74 ksi and 22.67 ksi as seen in Figure 5-40. These measurements indicate that the subgrade modulus at both locations is comparable. However, a noticeable difference in deflection was observed between the two points. Upon further investigation, the difference in deflection was attributed to the presence of a nearby crack, which was observed in the area with the higher

deflection. Based on field observations, it was concluded that this crack is the primary cause of the discrepancy in deflection measurements.

Depth (in)	High Deflection 7.15 mils	Low Deflection 2.84 mils
	Pavement Structure	
	3.5" ASB+8" CRCP + LTS	
1 2 3 4 5 6 7 8 9 10	8.96	10.68
11 12 13 14 15 16	16.09	17.42
17 18 19 20 21 22 23 24 25 26 27 28 29 30 31 32 33 34 35 36	26.78	29.13
Effective Modulus (ksi)	19.74	22.67

Figure 5-40 Subgrade Modulus profile for IH40 Carson

IH10 Fayette

The fifth test section was conducted on IH10 in Fayette County, within the Yoakum district. This section, as specified by the CSJ, features a pavement structure that includes a 5-inch asphalt overlay, an 8-inch CRCP, and a Cement Treated Materials (LTS). The testing was performed on the inside lane in the eastbound direction, covering a 1,000-foot stretch.

FWD Test Results

Figure 5-41 shows the deflection values for this test section, ranged from 2.37 mils to 4.09 mils, with an average deflection of 3.23 mils.

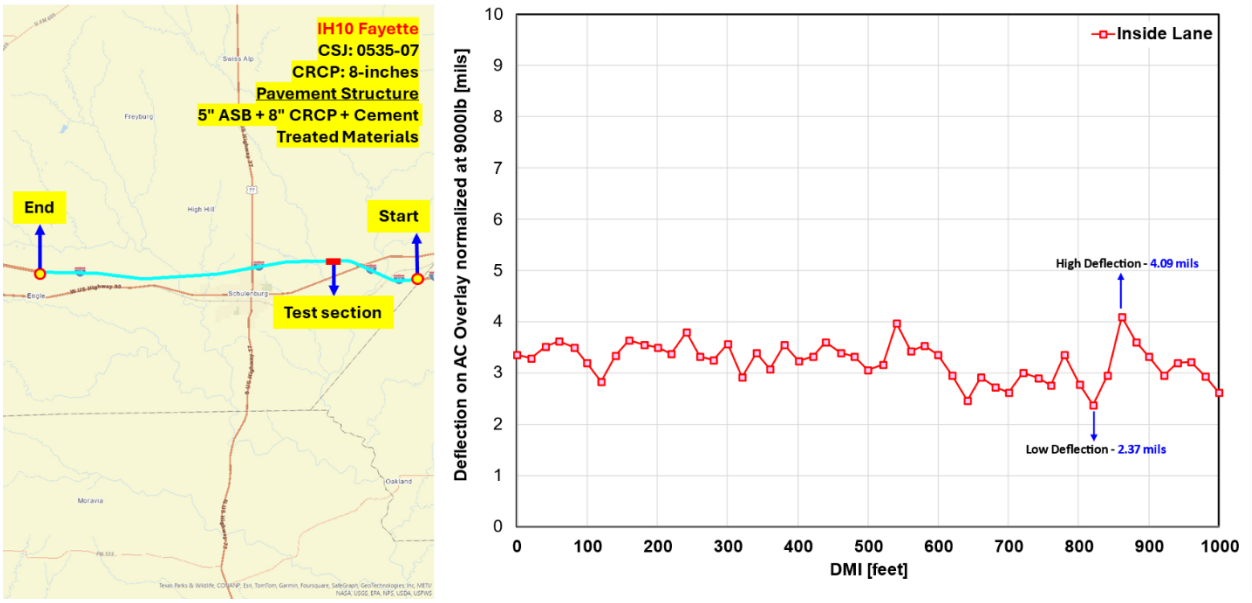

Figure 5-41 Map and FWD testing on IH10 Fayette

Subgrade Modulus

Figure 5-42 shows the effective subgrade modulus was measured at two points: the high deflection point had a modulus of 16.59 ksi, while the low deflection point had a higher modulus of 24.49 ksi. This inverse relationship suggests that areas with higher deflection are supported by a less stiff subgrade, whereas areas with lower deflection benefit from a stiffer subgrade.

Depth (in)	High Deflection 4.09 mils	Low Deflection 2.37 mils
	Pavement Structure	
	5" ASB+8" CRCP + Cement Treated Materials	
1 2 3 4 5	16.79	25.95
6 7 8 9 10	7.95	20.86
11 12 13 14 15 16	20.64	25.1
17 18 19 20 21 22 23 24 25 26 27 28 29 30 31 32 33 34 35 36	17.64	
Effective Modulus (ksi)	**16.59**	**24.49**

Figure 5-42 Subgrade Modulus profile for IH10 Fayette

US287 Wilbarger

The sixth test section was conducted on US287 in Wilbarger County, within the Wichita Falls district. This section, as specified by the CSJ, features a pavement structure that includes a 5-inch asphalt overlay, an 8-inch CRCP, and a 4-inch Cement Treated Base (CTB). The testing was performed on the outside lane in the northbound direction, covering a 1,000-foot stretch.

FWD Test Results

Figure 5-43 shows the deflection values for this test section ranged from 3.12 mils to 4.35 mils, with an average deflection of 3.58 mils. Interestingly all the deflection are in closer range indicating not much discrepancy.

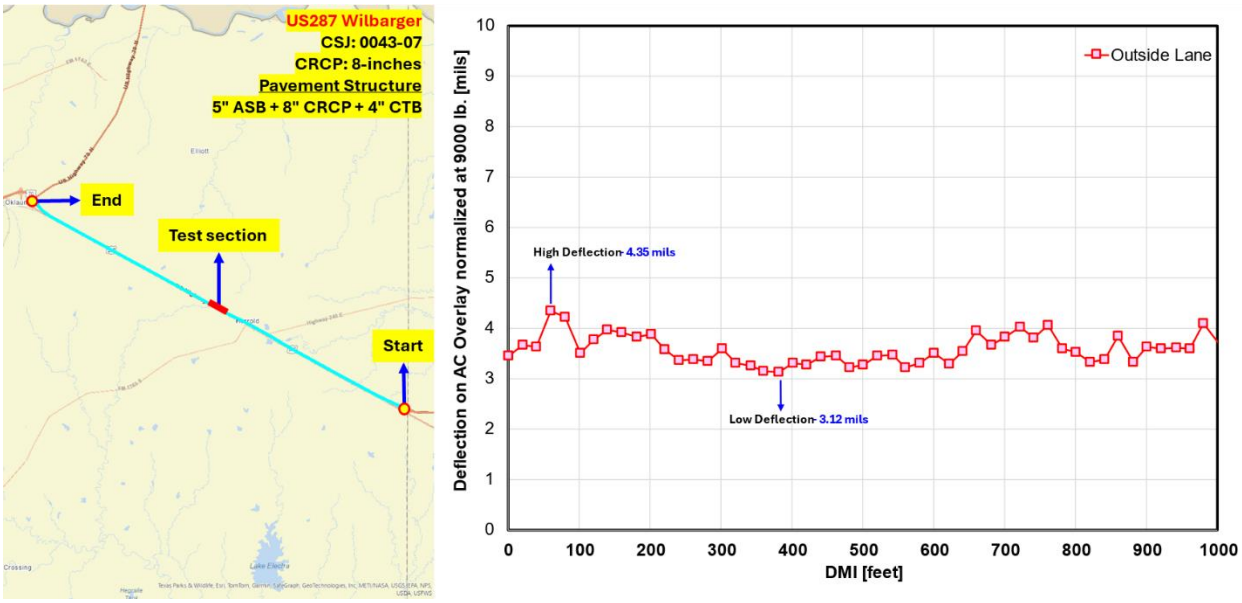

Figure 5-43 Map and FWD testing on US287 Wilbarger

Subgrade Modulus

Figure 5-44 shows the higher deflection has a lower subgrade modulus whereas the lower deflection has a higher subgrade modulus. However, they are in a range of 24.60 ksi to 29.30 ksi indicating that they are comparable to each other. Moreover, the reason for the lower deflection is contributed by the thickness of CRCP which when cored showed the thickness of 8.5-inch.

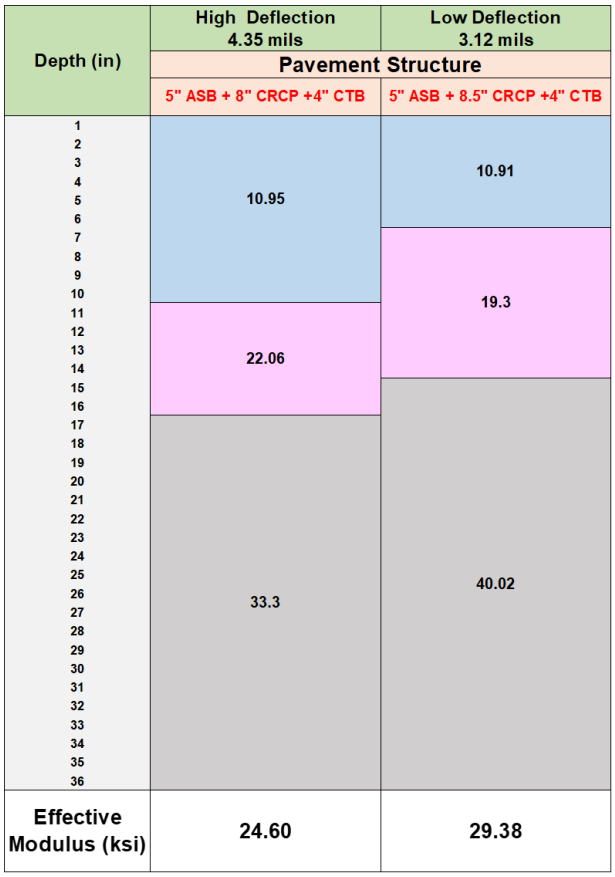

Figure 5-44 Subgrade Modulus profile for US287 Wilbarger

FM521 Harris

The seventh test section for the asphalt overlaid rigid pavement was conducted on FM521 in Harris County. According to the CSJ, this section features a pavement structure that includes a 1.5-inch asphalt overlay, an 8-inch CRCP, a 1-inch bond breaker, a 6-inch Cement Treated Base (CTB), and a 6-inch Lime Treated Subgrade (LTS). Testing was conducted on the outside lane in the southbound direction for 640-ft length due to traffic constraints.

FWD Test Results

Figure 5-45 shows the deflection values for this test section ranged between 3.39 mils to 22.43 mils, with an average deflection of 4.38 mils. This variation in deflection suggests differences in the underlying pavement structure.

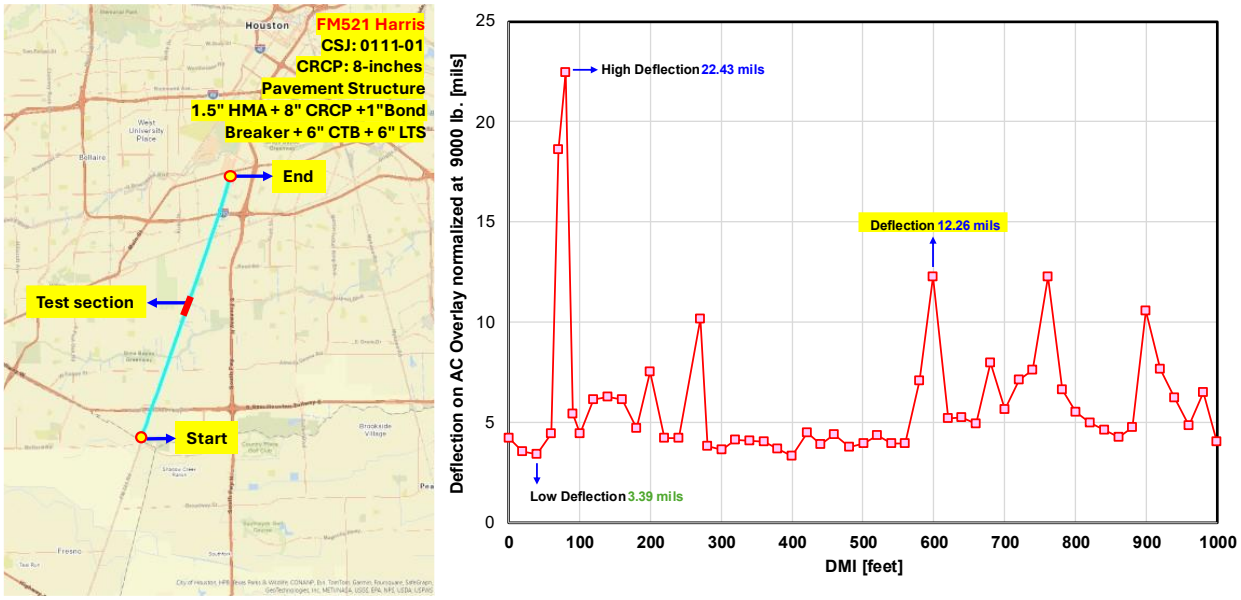

Figure 5-45 Map and FWD testing on FM521 Harris

Core Analysis

To better understand the cause of the variability in deflection, concrete cores were extracted from the locations with the highest and lowest deflections as shown in Figure 5-46.

- The core analysis revealed that the area with the higher deflection had a CRCP thickness of 8.5 inches, with a CTB thickness of 8 inches. It was surprising that even with this thicker slab and base it recorded higher deflection making us curious about its actual cause. Further investigation revealed the reason was the cavity that was beneath the concrete slab and CTB layer as shown in Figure 5-47.
- Since the high deflection arose due to bias led by cavity present, we cored another point with the next high deflection, 12.26 mils. As shown in Figure 5-48 the concrete core had a CRCP thickness of 8.25-inch with 5-inch CTB. Same as earlier cases, the bond breaker between the layers seems to deteriorate with void present measuring high deflections.
- In contrast, the location with the lower deflection had an asphalt overlay of 1.5 inches and a CRCP thickness of 8 inches. Additionally, the CTB in this area was intact and measured 6 inches.

High Deflection

Low Deflection

Figure 5-46 Concrete cores from FM521 Harris

Figure 5-47 Cavity as observed in high deflection test point

Figure 5-48 Concrete core taken in 12.26mils deflection

Subgrade Modulus

Figure 5-49 shows the effective subgrade modulus was quite low for all three points, measuring between 5.16 ksi to 8.96 ksi. These similar subgrade modulus values suggest that the subgrade beneath both the high and low deflection areas is consistent, indicating that thickness of base subbase and concrete is the one driving the deflection.

Depth (in)	High Deflection 22.43 mils	Deflection 12.26 mils	Low Deflection 3.39 mils
	Pavement Structure		
	1.5" HMA + 8.5" CRCP + 1" Bondbreaker + 8"CTB	1.75" HMA + 8.25" CRCP + 1" Bondbreaker + 5"CTB	1.5" HMA + 8" CRCP + 1" Bondbreaker + 6"CTB
1 2 3 4 5 6 7 8 9 10 11 12 13 14 15 16 17 18 19 20 21 22 23 24 25 26 27 28 29 30 31 32 33 34 35 36	8.96	8.73	4.38
			8.43
Effective Modulus (ksi)	8.96	8.73	5.16

Figure 5-49 Subgrade Modulus profile for FM521 Harris

I45 Harris

The eighth test section for the asphalt overlaid rigid pavement was conducted on I45 Frontage Road in Harris County. According to the CSJ, this section features a pavement structure that includes a 2-inch asphalt overlay, a 6-inch CRCP, a 6-inch Cement Treated Base (CTB), and a 6-inch Lime Treated Subgrade (LTS). Testing was conducted on the inside lane in the Northbound direction for 800-ft length due to traffic constraints.

FWD Test Results

Figure 5-50 shows the deflection values for this test section ranged between 4.55 mils to 10.17 mils, with an average deflection of 6.21 mils.

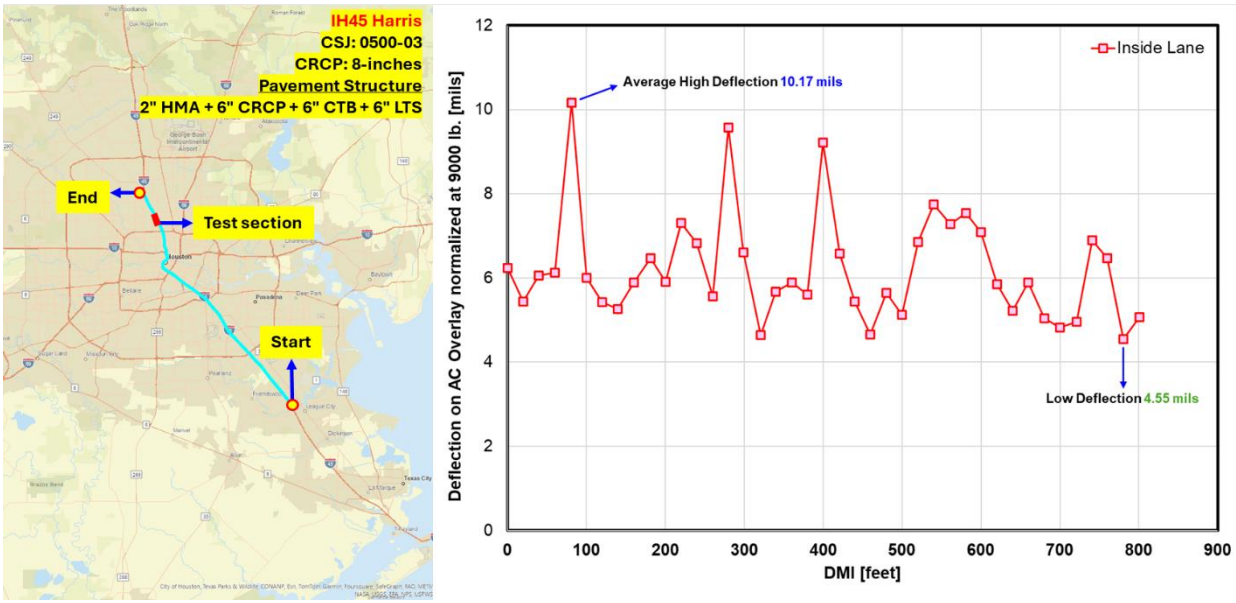

Figure 5-50 Map and FWD testing on IH45 Harris

Core Analysis

Concrete cores were extracted from the locations with the highest and lowest deflections as shown in Figure 5-51.

- The core analysis revealed that the area with the higher deflection had a CRCP thickness of 6.5 inches, with a CTB thickness of 4 inches.
- In contrast, the location with the lower deflection had a CRCP thickness of 7 inches. Additionally, the CTB in this area was intact and measured 5 inches.
- This points us again to the direction that grading issues in thinner slabs does make a substantial difference in the deflection measured.

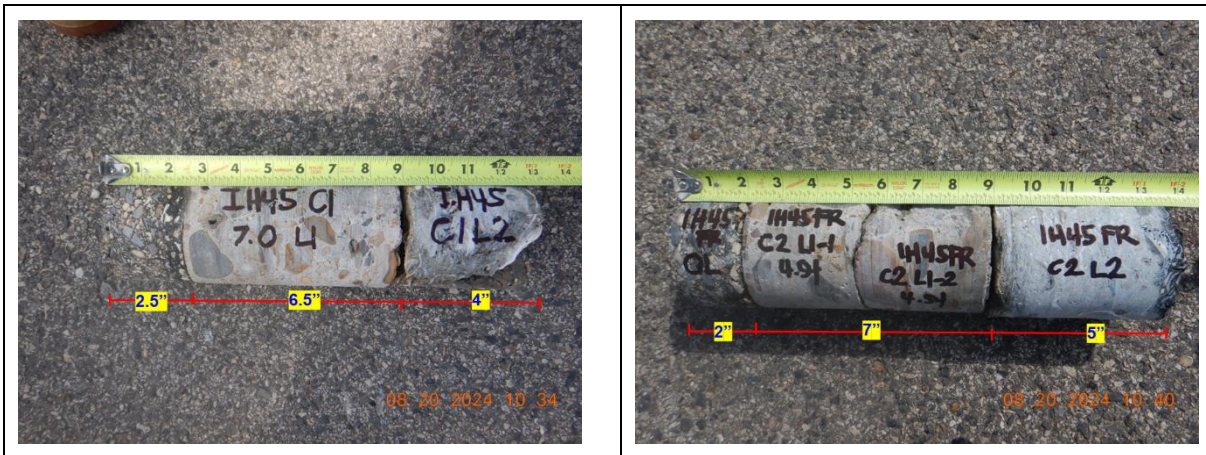

High Deflection	Low Deflection

Figure 5-51 Concrete cores from I45 Harris

Subgrade Modulus

Figure 5-52 shows the effective subgrade modulus was moderately stiff, measuring 13.95 ksi and 19.93 ksi for high and low deflection. The combination of thicker slab with high subgrade modulus is the probable reason for the low deflection measured.

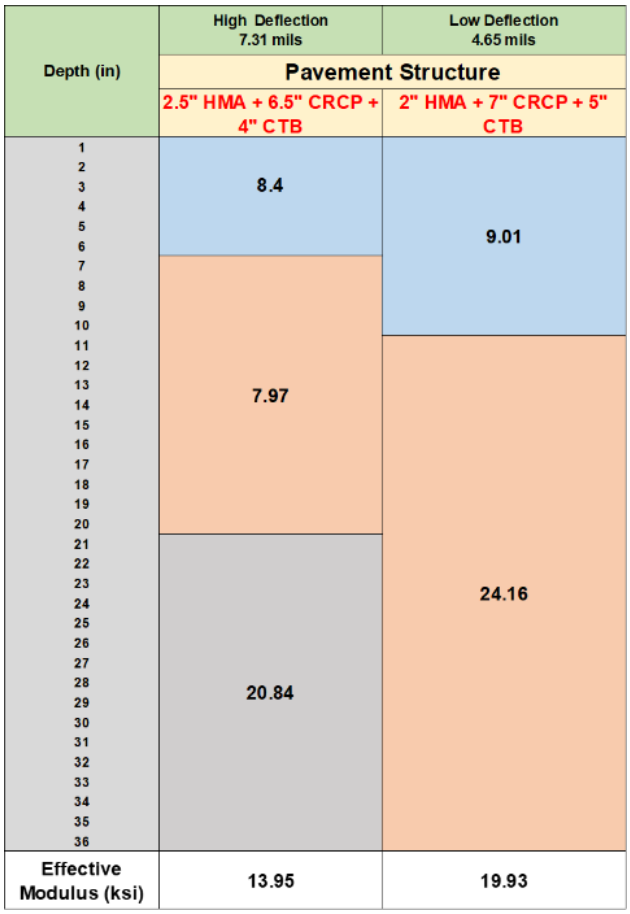

Figure 5-52 Subgrade Modulus Profile for I45 Frontage Road Harris

FM523 Brazoria

The final test section for the asphalt overlaid rigid pavement was conducted on FM523 in Brazoria County. According to the CSJ, this section features a pavement structure that includes a 3-inch asphalt overlay, an 8-inch CRCP, a 1-inch bond breaker, a 6-inch Cement Treated Base (CTB), and a 6-inch Lime Treated Subgrade (LTS). Testing was conducted on the outside lane in the southbound direction for 640-ft length due to traffic constraints.

FWD Test Results

Figure 5-53 shows the deflection values for this test section ranged from 3.65 mils to 5.31 mils, with an average deflection of 4.38 mils. This variation in deflection suggests differences in the underlying pavement structure.

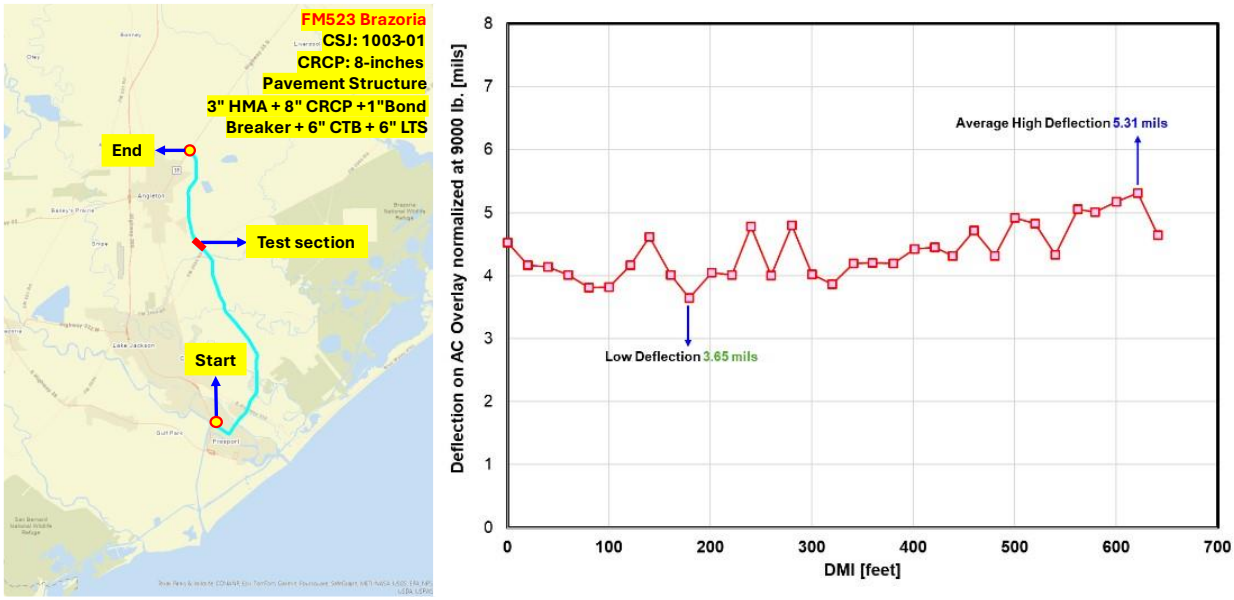

Figure 5-53 Map and FWD testing on FM523 Brazoria

Core Analysis

To better understand the cause of the variability in deflection, concrete cores were extracted from the locations with the highest and lowest deflections as shown in Figure 5-54:

- The core analysis revealed that the area with the higher deflection had a CRCP thickness of 7.5 inches, with a CTB thickness of 4 inches. This thinner CRCP and CTB likely contributed to the higher deflection observed in this area.
- In contrast, the location with the lower deflection had a thicker asphalt overlay of 3.5 inches and a CRCP thickness of 8.5 inches. Additionally, the CTB in this area was intact and measured 5 inches. The greater thickness of both the asphalt and concrete layers likely contributed to the reduced deflection at this location.

	
High Deflection – 5.31 mils	Low Deflection – 3.65 mils

Figure 5-54 Concrete cores from FM523 Brazoria

Subgrade Modulus

Figure 5-55 shows the effective subgrade modulus was relatively low, measuring 9.28 ksi and 11.60 ksi at the two cored locations. These similar subgrade modulus values suggest that the subgrade beneath both the high and low deflection areas is consistent, reinforcing the conclusion that the deflection variability is primarily due to differences in pavement layer thickness rather than subgrade conditions.

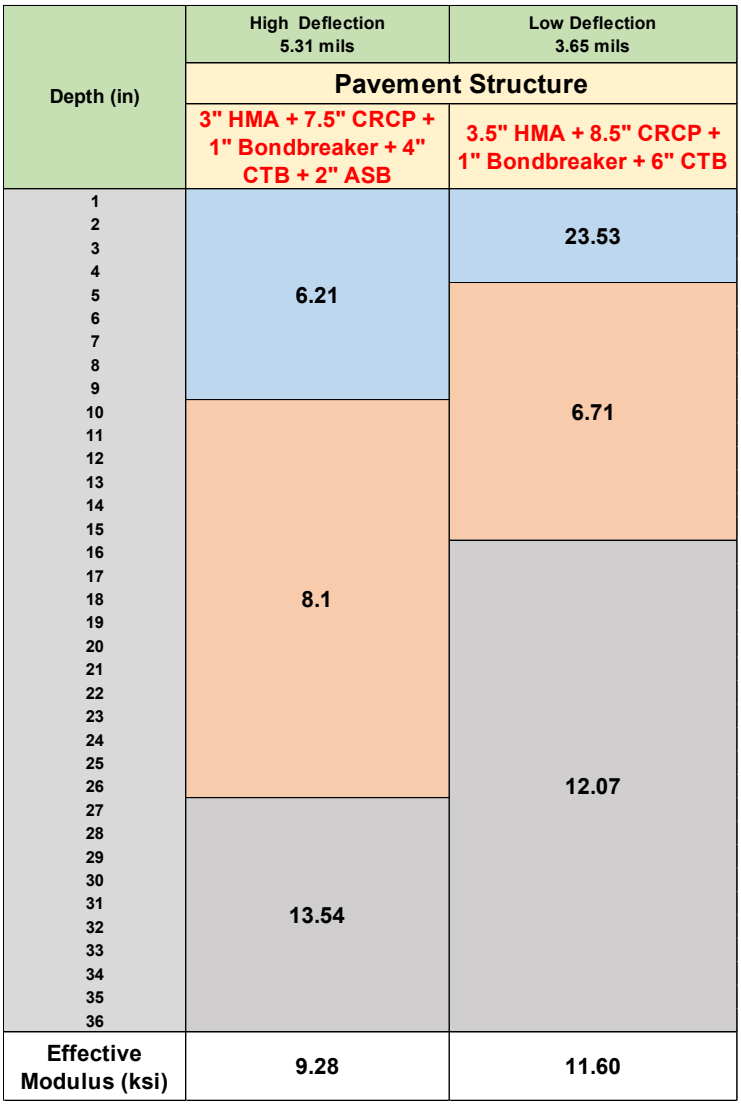

Figure 5-55 Subgrade Modulus profile for FM523 Brazoria

5.2 Data Analysis

5.2.1 Subgrade Modulus and Deflection Relationships

Figure 5-56 illustrates the relationship between deflection on different base layers and their respective effective subgrade modulus. As previously categorized, the six distinct base types can be grouped into two categories, as outlined in table 5-4 below:

Table 5-4 Types of base layer observed during field testing

ID	Pavement Detail	Group
BM 1	1” Bond Breaker + 6” CTB + 8” LTS + Subgrade	Group A
BM2	1” Bond Breaker + 6” CTB + 8” CTS + Subgrade	
BM 3	1” Bond Breaker + 6” CTB + Subgrade	
BM 4	4” ASB + 8” LTS + Subgrade	Group B
BM 5	5” ASB + Subgrade	
BM 6	4” ASB + Subgrade	

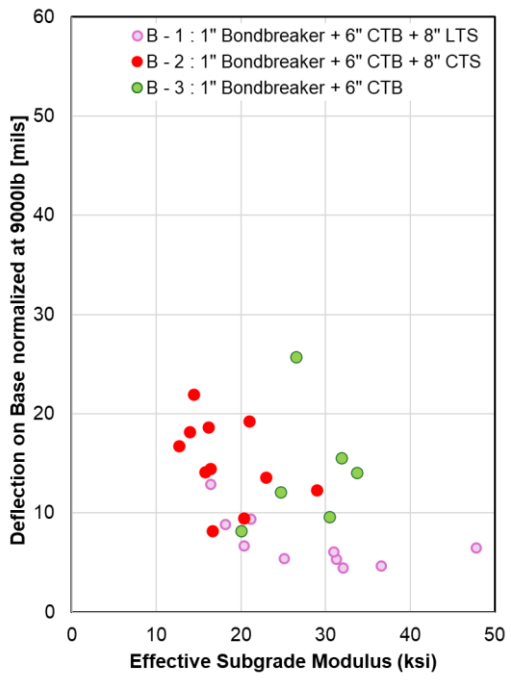

Base Type - Group A

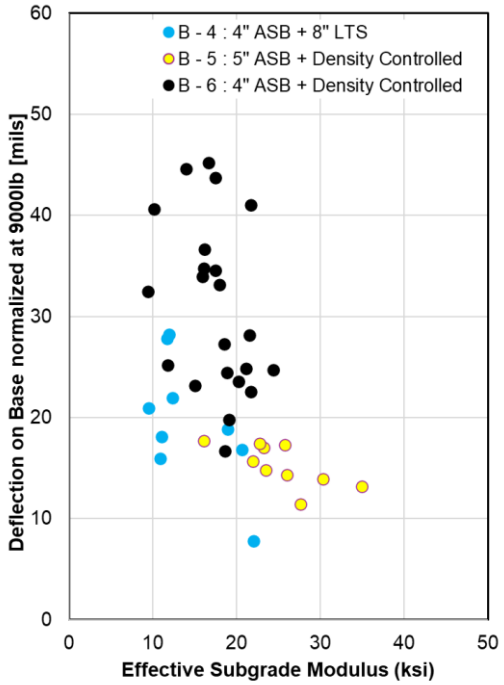

Base Type - Group B

Figure 5-56 Relationship between deflection on different Base Type and Effective Subgrade Modulus

These groups are based on the stiffness characteristics of the base layers. Group A consists of bases that include a bond breaker combined with Cement-Treated Base (CTB), while Group B includes bases that utilize Asphalt-Stabilized Base (ASB) or Hot Mix Asphalt (HMA). The rationale behind this grouping is the assumption that a bond breaker with CTB will create a stiffer base compared to those that use ASB/HMA. This assumption is supported by the data collected from field experiments.

As shown in the graph, bases with a 1-inch bond breaker and 6-inch CTB demonstrated greater stiffness, with deflection values ranging from 5 mils to 26 mils, averaging 11.96 mils (rounded to 12 mils) with a standard deviation of 5.64 mils. In contrast, the ASB/HMA-based layers showed more variability, with deflection values ranging from 7.83 mils to 45.20 mils, an average of 24.65 mils (rounded to 25 mils), and a standard deviation of 9.81 mils.

It is important to note that the effective subgrade modulus in both groups ranged between 10 mils to 30 mils. This variability in deflection can be attributed to two main factors: the variability in the thickness of the base layers being tested and the inherent stiffness of the layers themselves.

This observation highlights the significant influence that the type of base layer has on deflection after CRCP is overlaid, emphasizing the need to consider this factor when examining the relationship between CRCP deflection on different slab thickness and effective subgrade modulus as well as base layer deflection. This will be further discussed and elaborated on in the subsequent sections.

5.2.2 Relationship between different CRCP slab thickness and Effective Subgrade Modulus

The relationship between CRCP slab thickness, deflection, and effective subgrade modulus as depicted in Figure 5-57. The data gathered from seven projects, categorized into three slab thickness ranges—low (7 to 8 inches), medium (9 to 12 inches), and high (13 to 15 inches) reveals interesting trends.

For low range CRCP, the slope is much steeper, indicating a significant decline. In technical terms, for every 10 ksi increase in effective subgrade modulus, the deflection on the CRCP slab decreases by approximately 0.75 mils. This steep negative slope suggests that thinner slabs are highly sensitive to changes in subgrade stiffness. The R^2 value of 0.3512 is the highest among the three groups, indicating a relationship, albeit not super strong between deflection and subgrade modulus for thinner CRCP slabs. This implies that the effective subgrade modulus has a substantial influence on deflection in this range. Similarly, for medium range CRCP, the slope is moderately negative, indicating a noticeable decline. Statistically, this means that for every 10 ksi increase in effective subgrade modulus, the deflection on the CRCP slab decreases by approximately 0.266 mils. The R^2 value of 0.3472, while still modest, suggests a stronger relationship between deflection and subgrade modulus compared to the high range CRCP, meaning the subgrade modulus plays a significant role in influencing deflection in this thickness range.

However, the slope for the high range CRCP is nearly flat, with a very gentle negative incline. This means that for every 10 ksi increase in effective subgrade modulus, the deflection on the CRCP slab decreases by approximately 0.045 mils. This suggests that there is minimal influence of effective subgrade modulus on the deflection for thicker slabs. The low R^2 value of 0.0072 indicates that the relationship between deflection and subgrade modulus in this range is weak, meaning the effective subgrade modulus has little to no practical impact on deflection for thicker CRCP slabs.

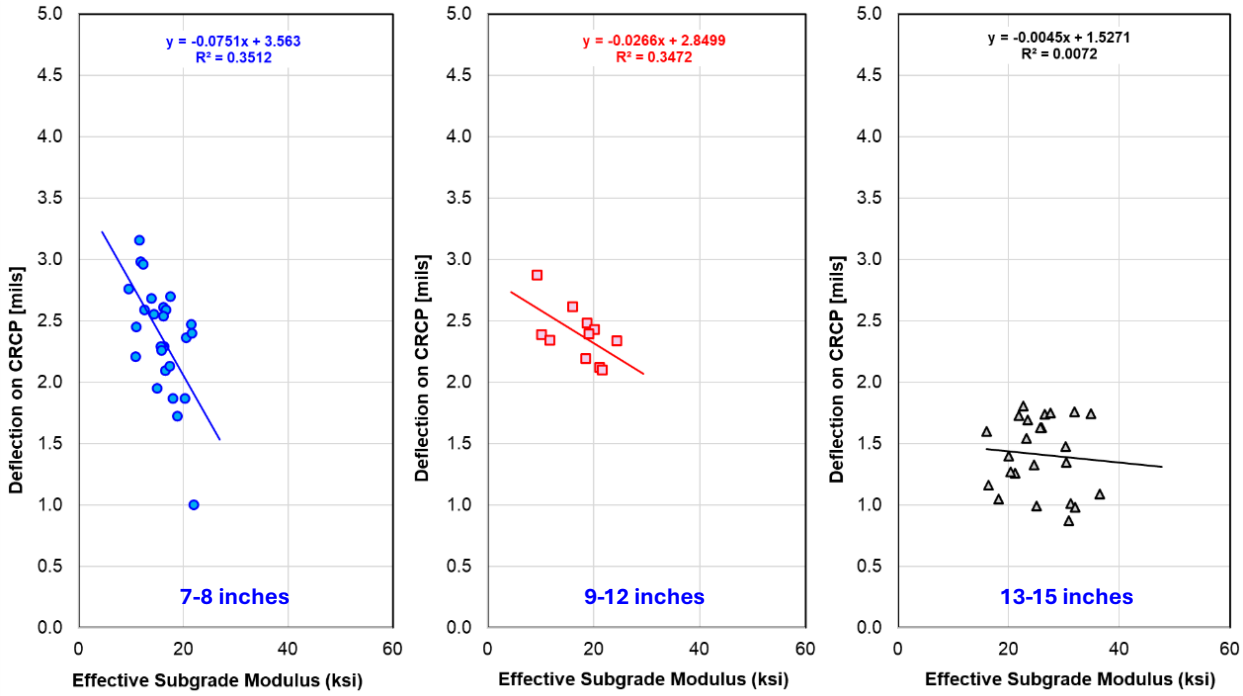

Figure 5-57 Relationship between deflection on different CRCP Thickness and Effective Subgrade Modulus

In summary, the slope of thinner slabs is approximately 17 times steeper than thicker slabs and 3 times steeper compared to medium thickness slabs. This comparison illustrates that thinner CRCP slabs are much more affected by the underlying subgrade conditions than thicker slabs. As slab thickness increases, the sensitivity to subgrade stiffness decreases significantly.

5.3.3 Base Deflection and CRCP Deflection Relationships

In Figure 5-58, the graph illustrates the relationship between deflection on the CRCP layer and the base layer for three different CRCP slab thickness categories: low range (7-8 inches), medium range (9-12 inches), and high range (13-15 inches). For the low range CRCP (7-8 inches), the slope of 0.0661 with an R^2 value of 0.55 indicates a moderately strong relationship between the deflection on the base layer and the deflection on the CRCP layer. The wider spread of deflections, ranging from 1 mil to 3.2 mils, suggests that thinner slabs are more susceptible to variations in the base layer's characteristics. This variability is likely influenced by the type of base used, which has a more pronounced effect on thinner slabs. Likewise, in the

medium range CRCP (9-12 inches), the slope is much flatter at 0.0159, with an R^2 value of 0.193, indicating a weaker relationship between the base and CRCP deflections. The deflections are more concentrated within a narrower range, from 2 mils to just below 3 mils. This suggests that as the slab thickness increases, the influence of the base layer variability on deflection diminishes. In regards of the high range CRCP (13-15 inches), the slope of 0.0223 with an R^2 value of 0.3148 shows a slightly stronger relationship than the medium range but still indicates a relatively weak influence of the base layer on deflection. The deflections are tightly clustered between 1.2 mils and 2 mils, reinforcing the observation that thicker slabs are less affected by base layer variations.

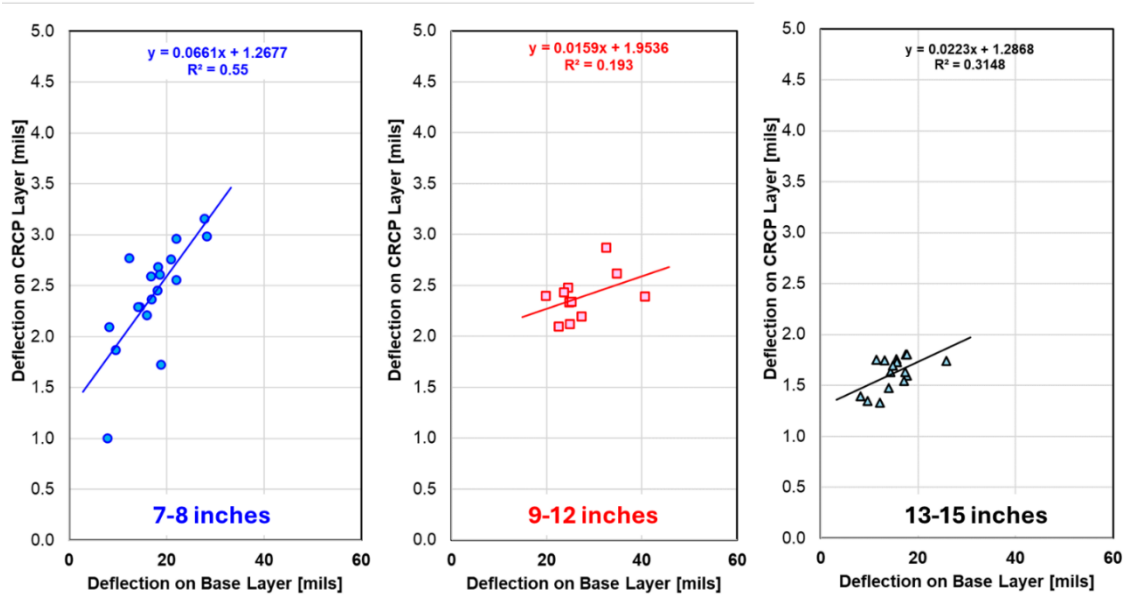

Figure 5-58 Relationship between deflection on different CRCP Thickness and their respective Base Type

One key factor influencing deflection, particularly in thinner slabs, is the variability in slab thickness during construction. Field observations, such as those made at the Panola US59 site, highlight this issue as shown in Figure 5-59. For instance, after conducting FWD testing and subsequent DCP testing at a location with a high deflection of 3.37 mils, it was found that the CRCP slab thickness varied to 9 inches instead of the intended 8 inches. This variability was attributed to grading issues during construction, leading to inconsistent slab thicknesses that significantly impact deflection measurements. This observation underscores the importance of consistent slab thickness in deflection-based design, particularly for thinner CRCP slabs, where even slight variations can lead to substantial differences in deflection.

Figure 5-59 Inconsistency in Slab thickness as observed in Panola US59

To summarize, though the graph provides a foundational understanding of the relationship between deflection on the CRCP layer and the base layer, it does not fully address the need to interpolate all the necessary curves. Given the data collected and the insights gained, the next logical step is to conduct a mechanistic analysis of the CRCP system using the Finite Element Method (FEM). This analysis will be discussed in detail in the following chapter, where we will explore how these relationships can be further refined and applied to develop a comprehensive deflection-based design methodology.

5.3 Mechanistic Analysis

Based on the field measurements a thorough literature review on performing mechanistic analysis of CRCP Systems was conducted. The primary objective was to analyze the deflections within the pavement structure and compare the results with field measurement data obtained through FWD testing. The finite element method (FEM) was employed as the primary mechanistic tool, with ANSYS, a widely used commercial software, serving as the platform for simulation. The ultimate goal was to establish a robust correlation between the simulated deflection data and the field measurements, enabling accurate predictions of deflections in scenarios where FWD testing was not feasible.

To refine the model and ensure that the simulated data closely matched the field measurements, a systematic recalibration process was undertaken. The study was structured into six key phases:

1. Literature Review
2. Developing an FE model
3. Validating the FE model
4. Recalibration of the FE model
5. Identification of Grey areas

This structured approach ensures a comprehensive analysis and contributes to the ongoing refinement and validation of mechanistic models for this research. The details of each phase will be discussed henceforth.

5.3.1 Literature Review

This phase includes a thorough review of existing research, and methodologies related to mechanistic analysis of CRCP systems. The primary objective was to identify and critically assess the studies that have previously attempted to simulate FWD testing using ANSYS or similar Finite element analysis (FEA) tools. Table 5-5 shows the list of research papers and their respective key findings which are relevant to identify key factors that must be addressed to enhance the reliability and validity of our mechanistic modeling approach:

Table 5-5 List of Research papers with their main findings

S.No.	Authors	Main Findings
1	Stolle (1991)	Modeled dynamic response of pavements to impact loading, providing a foundational approach for understanding pavement behavior under dynamic loads.
2	Shoukry et al. (1996)	Used DYNA3D to develop a 3D FE pavement structure model and imposed a dynamic load. Concluded that the bond strength between layers influenced FWD test results, though the model lacked validation against field measurements.

3	Hadi and Bodhinayake (2003)	Modeled a 3D pavement structure subjected to static and cyclic loadings in ABAQUS, considering linear and nonlinear material properties. Found that static load assumptions led to higher-than-expected deflections, while cyclic loading and nonlinear materials provided better results.
4	Kuo and Chou (2004)	Developed a 3D FE model for flexible pavements using ABAQUS. The model can simulate the behavior of a flexible pavement under wheel loading and predict pavement response accurately.
5	Al-Qadi et al. (2008)	Recommended the integration of dynamic load models into 3D FE models, highlighting the close alignment of dynamic analysis results with field measurements.
6	Uddin and Garza (2010)	Developed a 3D-FE model of a flexible pavement, imposed dynamic load, and found that damping resulted in smaller peak deflections. Identified the limitations of using infinite elements for pavement models.
7	Zhou et al. (2010)	Compared FWD and Benkelman Beam methods in evaluating pavement structure capacity, identifying the advantages and limitations of each method.
8	Tarefder and Ahmed (2014)	Used FEM to perform dynamic and static analysis of FWD deflection basin. Found that the deflection basins generated by dynamic and static analyses were similar to the measured deflection basin, with static analysis yielding closer results.
9	Melaku and Qiu (2015)	Designed a 3D FE analysis tool for pavement issues, revealing significant insights into vertical deflection, stress-strain, and shear stress responses under vehicle loads.
10	Uddin et al. (2017)	Developed 3D-FE modeling and dynamic response analysis of asphalt pavements subjected to FWD impact loads, improving the accuracy of pavement performance predictions.
11	Li et al. (2017)	Conducted finite element modeling and parametric analysis of viscoelastic and nonlinear pavement responses under

		dynamic FWD loading, providing a more detailed understanding of pavement behavior.
12	Arimilli et al. (2018)	Compared conventional pavement with alternative cold recycled technologies, finding good alignment with KENPAVE and IITPAVE but lower values for ANSYS.
13	Elbagalati et al. (2018)	Developed the pavement structural health index based on FWD testing, contributing to a more comprehensive assessment of pavement conditions.
14	Hamim et al. (2018)	Concluded that ANSYS, an FE program, is the most adaptable and versatile tool for simulating the FWD test and establishing the deflection basin.
15	Rosyidia et al. (2020)	Developed pavement structure models using various computer programs and highlighted ANSYS's capability in simulating the FWD test.

The key takeaways from the literature review are:

i. **ANSYS in FWD Simulation**: As noted by Hamim et al. (2018) and Rosyidia et al. (2020), ANSYS is a highly adaptable and versatile tool for simulating FWD test. Its ability to accurately model the deflection basin and its flexibility in handing various pavement materials make it a preferred choice for mechanistic analysis of CRCP systems.

ii. **Nonlinear material properties:** Studies such as those by Hadi and Bodhinayake(2003) and Li et. Al. (2017) reveal that nonlinear material properties significantly affect pavement deflections. Static load assumptions often lead to overestimated deflections, whereas more sophisticated models incorporating viscoelastic behaviors yield results that are more consistent with real-world observations

iii. **Dynamic Load Modeling:** Several studies, such as those by Stolle (1991), Al-Qadi et al. (2008), and Uddin et al. (2017), emphasize the importance of incorporating dynamic load models into finite element analysis (FEA) for accurately simulating the pavement response under FWD testing. Dynamic analysis provides results that closely align with field measurements, highlighting its critical role in reliable pavement modeling.

5.3.2 Developing an FE model

This second phase includes constructing a finite element model that accurately represents the CRCP system. To achieve these following five steps were adopted:

a. ANSYS Implementation
b. Selection of Geometry model
c. Assigning layer properties
d. Meshing the model
e. Assigning the load condition

However, before diving into the five steps it is crucial to fully understand the basis of FE modeling. For that it is essential to revisit the mathematical models that laid the foundation for this field. Historically, pavement modeling has been categorized into three primary mathematical models: Plate Theory, Layered Theory, and Finite Element Analysis (FEA), as illustrated in Figure 5-60. With advancements in research and computational capabilities, these mathematical models have evolved into sophisticated software tools, significantly enhancing the accuracy and reliability of pavement analysis. Despite these advancements, the foundational principles remain unchanged. In this section, we will explore the underlying mathematical models and their significance in pavement design. This exploration will guide us to the first step on developing an FE model which is to select the correct model geometry of pavement structures that simulates the FWD test.

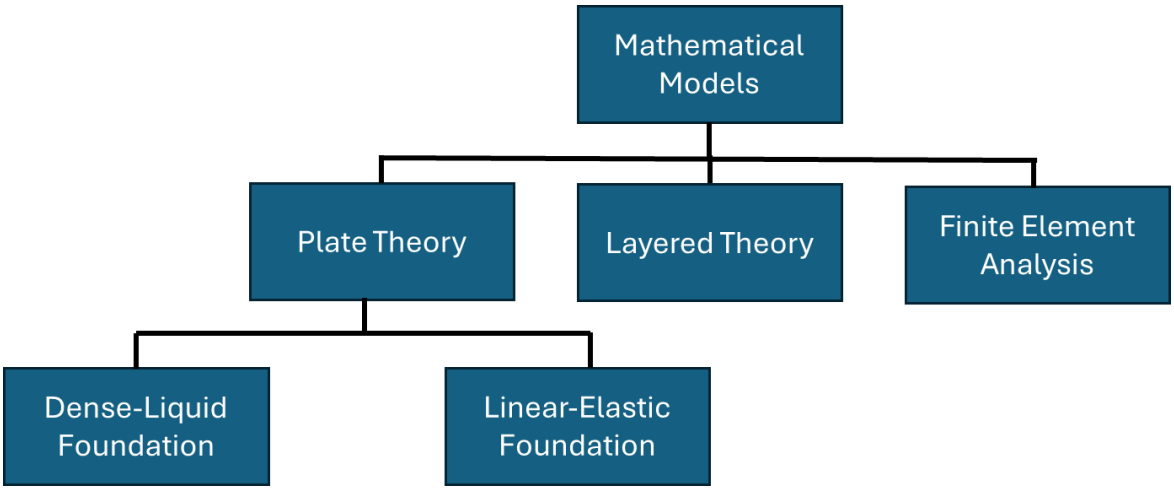

Figure 5-60 Mathematical models for pavement design

Plate Theory

Plate theory is used to analyze how pavement structures behave under the load, such as during a FWD test. The theory typically assumes that the foundation supporting the pavement is either a dense liquid or a linear-elastic material.

Dense-Liquid Foundation: Most of the solutions in highway engineering assume that the foundation acts like a dense liquid, often described using the Winkler-Zimmerman model. This model suggests that when a load is applied to the pavement, the foundation responds with an equal and opposite force proportional to the deflection (movement) of the pavement. This

reaction is defined by a modulus of reaction (k). The dense-liquid model is often visualized as a bed of springs or a liquid that gets denser as the load increases. This model was first developed by Westergaard in 1926, who created formulas for different load placements, such as at the corner, edge, or center of a concrete slab. Later, other researchers, like Kelley and Spangler, refined these formulas to account for additional factors like curling stresses and load transfer at joints. These equations are widely used because they are relatively simple to solve for specific conditions.

Linear-Elastic Foundation: On the other hand, the linear-elastic foundation assumes that the pavement's foundation behaves like an elastic material, which is more realistic than the dense-liquid assumption. This model considers the foundation's elastic properties, like modulus of elasticity and Poisson's ratio, which can be measured in the lab. However, this approach was less commonly used in highway and airport engineering because the math involved was more complex, and the Westergaard equation’s popularity overshadowed it.

Layered theory

Layered theory is a method used to analyze pavement structures by considering each layer's unique properties. Before the advent of modern computers, solving boundary-value problems for pavements with multiple layers was nearly impossible due to the complexity involved. However, with the development of computational techniques, it became feasible to solve these problems, allowing for a more detailed understanding of how stress and strain are distributed throughout a pavement structure. Donald M Burmister (1943) was a pioneer in this field, providing solutions for pavements with two layers resting on an elastic foundation. He assumed that the layers were fully continuous, meaning there was no slippage between them. This assumption implies that the strain at the bottom of one layer is equal to the strain at the top of the next layer, although the stress levels may differ depending on each layer's modulus of elasticity.

Later, researchers like Hank and Scrivner, as well as Peattie and Jones, expanded Burmister's work to include three-layered pavements. They explored different continuity conditions between layers—ranging from full continuity (no slippage) to zero continuity (complete slippage). Their findings showed that stress levels could vary significantly depending on the continuity condition and the relative stiffness of the layers. However, in most real-world pavements, full continuity is likely, making this assumption realistic for practical applications.

There are numerous commercial tools that have been developed based on layered theory. Among them WinJULEA is a windows-based program developed by the U.S. Army Engineer Research and Development Center (ERDC) which is designed for multi-layer linear elastic analysis of pavements. We have used this software for comparing and validating our results with ANSYS and field data. The actual reason for this use pertains to check the difference on the results that stems from using an analytical method and numerical method. In this case, both plate theory and layered theory fall under the category of analytical methods and Finite element method using ANSYS falls under numerical method.

Finite Element Analysis:

With advancements in research and computational capabilities, Finite Element Analysis (FEA) emerged as a pivotal tool in pavement design, offering a sophisticated approach to solving complex numerical problems that are difficult to address with traditional analytical methods. FEA works by breaking down a structure into smaller, simpler parts called elements, which are connected at points known as nodes. This process, called discretization, transforms a complex geometry into a mesh of these elements. Each element's behavior under load is described by a stiffness matrix, which defines how much the element will deform when subjected to forces. These individual stiffness matrices are then assembled into a global stiffness matrix that represents the entire structure. By applying boundary conditions and loads, the global stiffness matrix is used to solve the displacements at each node in the mesh. Once the displacements are known, other important quantities such as stresses and strains can be calculated. FEA is widely used across various engineering disciplines to analyze and optimize designs, from automotive components to aerospace structures, providing critical insights into how a structure will perform under real-world conditions. Thus, to conduct mechanistic analysis of CRCP system we have implemented ANSYS, a widely used commercial software, serving as the platform for simulation.

ANSYS Implementation

Key considerations for determining geometry include the setup of the FWD test, and the type of geometry analysis and model needs discussion. Here in this section, we will first discuss setup of the FWD test followed by the type of geometry analysis and type of model that would suit our purpose.

Setup of the FWD test

The FWD test simulates the impact load exerted by a moving vehicle on a pavement surface. In this test, a weight is dropped onto a circular load plate placed on the pavement, simulating the load exerted by a moving vehicle. This impact generates a deflection basin in the pavement, which is measured by a series of sensors, known as geophones, positioned at specific intervals from the load plate as shown in Figure 5-61. Typically, seven sensors are utilized, spaced one foot apart, with one sensor located directly beneath the point of loading. The deflections are measured in mils (thousandths of an inch). The load levels typically range from 1,500 to 27,000 pounds. The drop sequence involves varying load levels, which are usually normalized to 9,000 pounds.

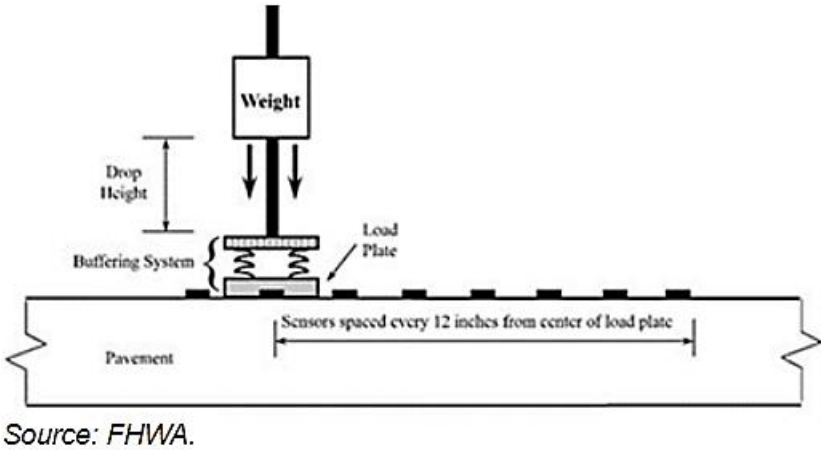

Figure 5-61 Schematic of an FWD sensor configuration

Selection of Geometry Analysis

Based on the literature review, transient dynamic analysis has been identified as a superior method for simulating FWD testing. However, in this study, both static structural analysis and transient dynamic analysis were employed in ANSYS to simulate the FWD test. These methods were selected to compare the deflection values generated by the FE model with those obtained from field measurements, thereby assessing the accuracy and reliability of the simulations.

Static Structural Analysis is used to determine how displacement, stress, strain, and force in a structure or component respond to imposed loads. This method does not consider the effects of inertia (the resistance to changes in motion) or damping (the reduction of motion over time). It assumes that loading and the resulting responses change slowly over time. In ANSYS, thin models typically perform better with a direct solver, while more complex, bulky models work better with an iterative solver. The general equation used in this type of analysis is:

$$[K]\{u\} = \{F\} \qquad (Equation\ 5-1)$$

Where [K] represents the stiffness matrix {u} is the displacement vector, and {F} denotes the load vector. ANSYS automatically selects the appropriate solver based on the analysis type and model geometry.

Transient Dynamic Analysis (also known as time-history analysis) is used to determine how structures respond dynamically to time-dependent loads. Unlike static analysis, this method accounts for both inertia and damping effects. It can be used to calculate how displacement, strain, stress, and force change over time under various types of loads, including static, transient (short-term), and harmonic (cyclical).

$$[M]\{\ddot{u}\} + [C]\{\dot{u}\} + [K]\{u\} = \{F(t)\} \qquad (Equation\ 5-2)$$

Where [M], [C], and [K] represent the mass, damping, and stiffness matrices, respectively, and {ü}, {u̇}, and {u} are vectors for acceleration, velocity, and displacement. {F(t)} denotes the

time-dependent load vector. ANSYS solves this equation at specific time intervals using methods like Newmark time-integration and the Hilber-Hughes-Taylor (HHT) method.

Selection of Geometry model

Different types of FE models can be used for pavement structures, including 2D plane strain, axisymmetric, and 3D models. Each type has its own advantages and limitations:

1. **2D Plane Strain Models**: These models are often chosen for their computational efficiency and short processing time. However, their accuracy is lower because they only represent the load as a line load rather than as a more realistic elliptical or rectangular load distribution.
2. **Axisymmetric Models**: These models are developed in a 2D space but represent a 3D structure by rotating the 2D profile around a vertical axis. Axisymmetric models are suitable for simulating circular loads, such as those applied in the FWD test. This model type has a balance between computational efficiency and the ability to simulate realistic load conditions, but it is limited to scenarios involving single circular loads and cannot account for conditions such as cracks or joints in the pavement.
3. **3D Models**: These are the most comprehensive and accurate but also the most computationally demanding. 3D models can account for complex pavement conditions, such as multiple wheel loads, pavement distress, and dynamic loading, making them suitable for detailed analyses.

When translating theoretical concepts into a finite element (FE) model, careful consideration must be given to the model's geometry and boundary conditions. While theoretical models often assume infinite horizontal extent, practical FE models require a finite domain. The horizontal extent should be sufficiently large to minimize edge effects on the area of interest, and the vertical extent must be deep enough to accurately capture stress distribution, typically until the stress becomes negligible. After a thorough literature review, we selected an axisymmetric model with horizontal and vertical extents of 33.33 times the load radius, as supported by the findings in the literature (see Table 5-6). Similarly, for the boundary condition as shown in Figure 5-62 roller support was assigned on vertical left and vertical right allowing vertical movement but restraining the horizontal movement. The bottom of the model was assigned fixed support where both horizontal and vertical movement was not allowed. Also, the connection between two adjacent layers is assumed to be fully bonded with no gap replicating no slip between two connected layers.

Table 5-6 Literature Review on Vertical and Horizontal extent for Model Geometry

Author	Vertical Boundary	Horizontal Boundary	Model Details
Duncan et al. (1968) ; Huang, Y.H. (2004)	50 times the load radius	12 times the load radius	Recommended for axisymmetric models
Kim, M., & Tutumluer, E. (2006)	20 times the load radius	20 times the load radius	Used in general-purpose FE program.
Kim et al. (2009)	140 times the load radius	20 times the load radius	Analyzed the nonlinear behavior of pavement foundations using both 2D and 3D models.
Tarefder and Ahmed (2014), Hamim et. Al. (2018)	33.33 times the load radius	10 times the load radius	Developed a 2D axisymmetric FE model for FWD deflection basins.

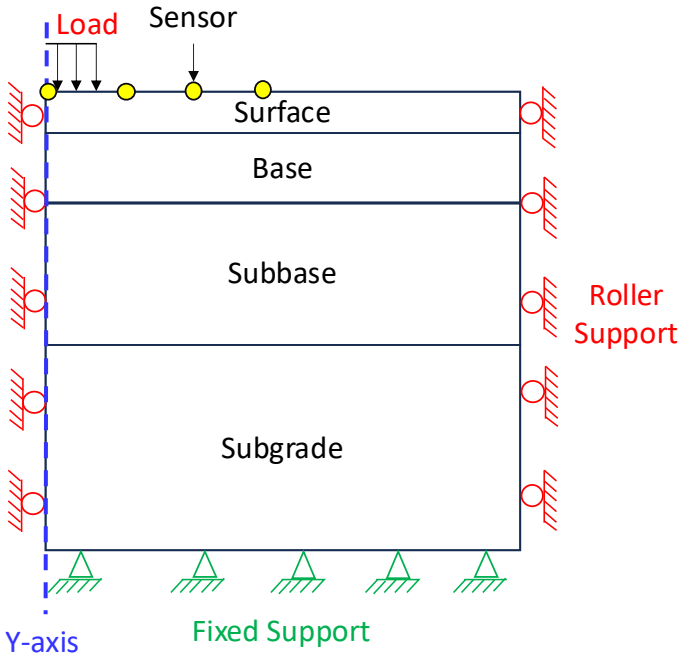

Figure 5-62 Schematic of boundary condition

To conclude, the decision to use an axisymmetric model for this analysis is based on two key factors:

1. **Appropriateness for FWD Testing**: FWD testing involves a circular load, which aligns well with the capabilities of axisymmetric models to simulate single circular loads. The

model effectively replicates the load's impact without needing to account for complex conditions like cracks or joints. Furthermore, it is capable of performing a dynamic analysis which is a suitable method for simulating FWD testing.

2. **Computational Efficiency**: The axisymmetric model offers a balanced approach, providing a realistic representation of a 3D structure by rotating a 2D profile around a vertical axis. This allows the model to handle 3D problems with greater computational efficiency compared to fully 3D models.

Representation of Soil Subgrade

In this research project, we are faced with the challenge of how we should go about deciding the true representation of soil support or say subgrade in FWD simulation. One may argue that this decision shouldn't be wearisome as we have always relied on Westergaard's explanation of modulus of subgrade reaction(*k*) to represent the soil support. This is evident from the TxDOT standpoint as it dictates the use of 300psi/in for all of its design. However, the true challenge comes when we make an attempt to calculate the *k*-value in the field and represent it for the purpose of simulation in ANSYS. Few questions that arise are: *How do we even perform the field test? Is it even feasible? Does it really make sense and is it practical in practice?* These are the questions which will be answered subsequently in this section.

The concept of a subgrade reaction modulus(*k*) originates from the Winkler foundation model (1867), which idealizes the soil as a bed of independent linear springs. In pavement engineering, this idea was first applied rigorously by H.M. Westergaard in the 1920s. In 1926, Westergaard published a pioneering theoretical analysis treating a concrete pavement slab as an elastic plate resting on a spring-like subgrade characterized by a constant *k*-value(Hudson, 1963). This *k* was defined as the pressure sustained per unit deflection of the subgrade, with units of pressure per length (psi/in). Westergaard's work introduced related concepts such as the radius of relative stiffness, which combines the concrete's elastic modulus (E of the slab) and thickness with the subgrade *k*-value to determine pavement response(Hudson, 1963). Over the next few decades, Westergaard refined his equations (notably in 1933, 1939, 1947), and others like F.T. Sheets and L. Teller contributed empirical adjustments, but the *k*-value remained a central parameter for characterizing subgrade support in rigid pavement analysis. Yet with all this refinement, there existed inherent limitations and doubts surrounding the modulus of subgrade reaction. These were the concerns that were not merely external critiques but were, in fact, voiced by Westergaard himself. His reluctance to fully endorse *k* as an absolute measure of soil support is evident in his early works, where he suggested that minor variations in *k* should not significantly impact slab stress predictions. This perspective was later echoed by Karl Terzaghi (1955), who outright questioned whether the level of precision engineers sought in determining *k* was even necessary in practice. A fundamental contradiction in Westergaard's approach was that his analysis required a *k*-value for slab design, yet the most reliable way to determine *k* was by back-calculating it from an existing slab (Anastasios M. Ioannides &

Tingle, 2024). This created a vicious cycle: one needed a pavement slab to determine *k*, but *k* was required to design the slab in the first place.

Recognizing this paradox, Westergaard himself avoided recommending the plate load test(PLT) the test most commonly used to determine *k* as a reliable means to characterize subgrade stiffness. Instead, he favored back-calculating *k* from field deflections of existing pavements, a preference that was later reinforced by the limitations exposed in the Teller and Sutherland (1943) experiments. The PLT itself was adopted out of wartime urgency rather than engineering rigor. The Ioannides and Tingle (2024) paper reveals that the 30-inch diameter plate which is a critical element of the test, was hastily standardized by the U.S. Army Corps of Engineers (USACE) during World War II to meet the urgent need for rapid airfield construction. There was little time to validate whether this plate size accurately represented the true subgrade response, and internal debates within the USACE revealed significant skepticism about its applicability. Teller and Sutherland (1943), who conducted extensive PLT studies, concluded that *k* values derived from smaller plates were drastically different from those obtained using larger plates, making the test highly sensitive to plate size and soil conditions. This sensitivity directly contradicted one of Westergaard's key assumptions that *k* was a constant for a given soil.

Adding to these concerns, Terzaghi's 1955 paper directly challenged the theoretical foundations of the modulus of subgrade reaction. He argued that the pressure-displacement relationship in real soils was nonlinear, whereas the PLT (and, by extension, the use of *k* in pavement design) was based on the assumption that soil behavior remained linear under load. Moreover, Terzaghi demonstrated that the distribution of subgrade reaction beneath a loaded area was far from uniform, meaning that *k* was not a true soil property but a highly variable parameter dependent on test conditions, soil moisture, and loading conditions. These limitations, along with historical records from pavement engineering pioneers, illustrate that the use of *k* as a universal subgrade descriptor has always been fraught with uncertainty. However, the question remains: *Should pavement engineers continue to rely on k?* , knowing its inherent limitations, or *should they seek alternative methods that better capture the true mechanical behavior of subgrade soils?* This sort of applies in our research as well. Well, if we are to seek alternative, the question may arise: *What will work?* The hint to answer this question may be found if we are to compare: the 1993 AASHTO Guide (largely empirical) and the 2008 MEPDG (Mechanistic-Empirical Design Guide). The 1993 AASHTO Guide requires a *k* for rigid pavement design, whereas the newer MEPDG uses M_R for subgrade in all designs.

In retrospect, it does make sense to use M_R as this is something we could evaluate in the field using Dynamic Cone Penetrometer (DCP) testing method. The DCP test effectively evaluates subgrade strength, clearly indicating whether the underlying soil, located beneath the pavement layers (base and subbase), has sufficient strength to support the pavement structure. Given its recognized utility, we rely on the DCP test data for our simulation purposes. However, determining how to translate this subgrade assessment into a numerical input for ANSYS

simulation presents another challenge. In regard to ANSYS, it provides two primary methods to input these values: using the modulus of subgrade reaction (*k*-value) within a Winkler foundation approach or using the modulus of elasticity (E-value) based on the theory of elasticity. Although the DCP test directly provides a penetration index (typically expressed in mm/blow), it does not explicitly measure either *k* or E values. Therefore, we need to use empirical correlations to convert DCP data into practical design parameters. Typically, this conversion involves a two-step correlation process:

STEP 1 - Correlate DCP penetration rate to CBR, and

STEP 2 - Correlate CBR to E or *k*.

Extensive studies conducted by military and highway agencies have established reliable equations for the first step. One widely cited relationship, developed by the U.S. Army Corps of Engineers is:

$$CBR(\%) = \left(\frac{292}{DCP^{1.12}}\right) \qquad (Equation\ 5-3)$$

This equation, initially proposed by Webster et al. (1992), is incorporated in ASTM standards and many DOT manuals, with modifications for specific soil classes. For example, ASTM D6951 recommends separate formulas for lean clays (CL) and fat clays (CH), as these soil types do not fit the general correlation. Once an estimated CBR value is obtained from the DCP data, it can be converted to a resilient modulus (M_R) using correlations such as those developed by Heukelom & Klomp or the UK's Transport Research Laboratory. Common relationships include:

$$M_R(psi) = 1500 * CBR$$

(an early approximation frequently used for highway subgrades).

$$M_R(psi) = 2555 * (CBR)^{0.64}$$

(a more accurate, non-linear correlation identified by Powell et al., 1984, suitable for CBR values ranging from 5 to 100).

These relationships yield typical values; for instance, a CBR of 10 would correspond to an M_R around 15,000 psi (approximately 100 MPa). Subsequently, the resilient modulus (or static E) can be related to a *k*-value. The AASHTO and PCA methods assume a standard 30-inch plate, using a formula:

$$k\left(\frac{psi}{in}\right) = \frac{M_R}{19.4} \qquad (Equation\ 5-4)$$

In practice, agencies often combine these steps into a single correlation directly from DCP to *k*. For instance, the American Concrete Pavement Association (ACPA) software WinPAS utilizes:

$$k(pci) = 53.4\ X\ (CBR)^{0.5719} \quad \text{(Equation 5-5)}$$

Applying this formula, a DCP penetration rate indicating CBR ≈ 10 results in $k \approx 134$ pci. The FAA has similarly published DCP-based design methods within its Unified Facilities Criteria, where DCP results estimate CBR profiles by depth, and subsequently, a weighted or relevant CBR is converted to a *k*-value for rigid pavement design. An older FAA correlation described by Tuleubekov & Brill (2014) is:

$$k = \left(\frac{CBR\ X\ 1500}{26}\right)^{0.778} pci \quad \text{(Equation 5-6)}$$

This correlation tends to be conservative, especially for soils with low CBR values. Therefore, based on the above discussion, M_R for subgrade is used to represent soil subgrade in case of Mechanistic Analysis.

Assigning layer properties

The material properties for the Finite Element (FE) model were assigned using appropriate values for elastic modulus and Poisson's ratio, as detailed in Table 5-7. The modulus of elasticity values was selected based on widely accepted practices in the simulation community. For static analysis, these values are sufficient. However, for dynamic analysis, a damping factor must be included. In this study, a damping ratio of 0.02 was assumed, which meets the requirements for dynamic analysis in ANSYS.

Table 5-7 Layer properties used for ANSYS

Material	**Modulus of Elasticity (psi)**	**Poisson's Ratio**
Concrete	5,000,000	0.15
Asphalt	100,000 – 1,000,000	0.35
Subgrade	Varies from 5ksi to 90ksi	0.3

Meshing the model

The meshing of the model depends on the desired accuracy for the simulation. A finer mesh size generally leads to more accurate results. For our model, we aimed for high accuracy, so a standard mesh size of 1.5 inches was selected. Among different metrics, the aspect ratio was used to assess the quality of the mesh. Typically, the aspect ratio ranges from 1 to 2. An aspect ratio of 1 indicates that the element is perfectly square, which is ideal because it means the element's length and width are equal, reducing the likelihood of numerical inaccuracies during simulations.

For our 2D axisymmetric model, there are a total of 17,689 elements and 56,003 nodes. Of these, 16,891 elements, accounting for 95% of the total element count, have an aspect ratio of 1. This result indicates that our selection of a 1.5-inch mesh size is appropriate for our model's performance.

Assigning the load condition

To enhance the accuracy of the predicted pavement response, the FE model was utilized to simulate the conditions experienced during field loading. For the static load condition, a constant load magnitude of 9000-lb was assumed throughout the FWD test. For dynamic load condition, an impulse load peaking at 9000-lb was applied to a 12-inch loading plate for approximately 25 milliseconds. The FE model assigned a pressure of 79.5 psi to the loading area.

5.3.3 Validating the FE model

This section discusses a critical phase in the process for developing mechanistic analysis validating the model to ensure its accuracy and reliability. As previously mentioned, this validation involves comparing the FE model results with field deflection data, using WinJulea for preliminary analysis, and later comparing these results with static analysis performed in ANSYS. The primary goal here is to ensure that the FE model accurately reflects the behavior observed in the field.

WinJulea Results

WinJulea was used for each combination of subgrade modulus and base/subbase stiffness, we measured the respective deflections across three different slab thickness categories: 7-8 inches, 9-12 inches, and 13-15 inches. The deflection values obtained from WinJulea for each scenario are summarized in Table 5-8. The rationale behind selecting these stiffness values is to capture the influence of a wide range of stiffness conditions on deflection, particularly under varying subgrade modulus values (10 ksi, 20 ksi, and 30 ksi).

Table 5-8 WinJulea deflections with varying subgrade modulus and stiffness of Base and Subbase

Stiffness	**1,000,000 psi (High)**			**100,000 psi (Low)**		
Effective Subgrade Modulus	**10 ksi**	**20 ksi**	**30 ksi**	**10 ksi**	**20 ksi**	**30 ksi**
Deflection(mils) (7-8 inches slab)	6.06	3.88	3.00	7.89	5.02	3.86
Deflection(mils) (9-12 inches slab)	5.26	3.37	2.61	6.49	4.13	3.18
Deflection(mils) (13-15 inches slab)	4.38	2.81	2.18	5.12	3.27	2.53

Figure 5-63 presents the above data graphically. The first observation from this analysis is that none of the predicted deflection values from WinJulea align closely with the measured deflection data from the field. This discrepancy indicates that the WinJulea software, which relies on layered theory, has limitations in accurately capturing the complex behavior of CRCP systems under real-world conditions. This reinforces the need for static analysis using ANSYS, which may provide a more accurate representation of the pavement's structural response.

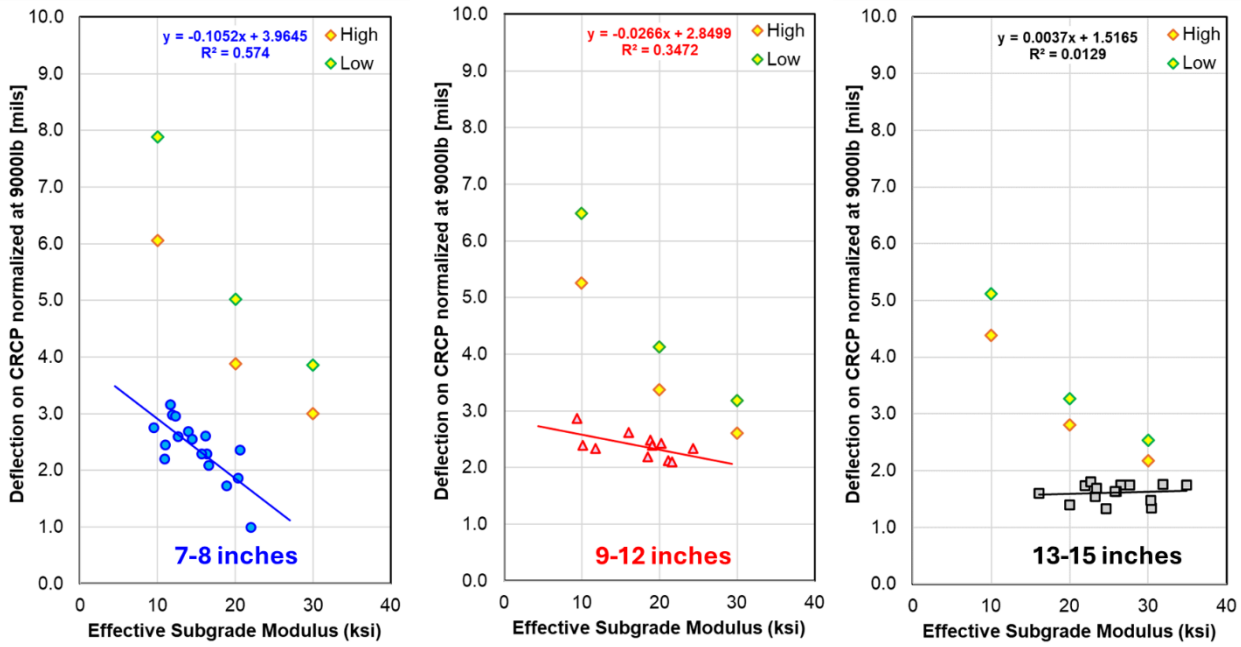

Figure 5-63 Graphical representation comparing WinJulea deflection with real field data

Static Analysis Results

The deflection values obtained from the FE model using static analysis are summarized in Table 5-9. Compared to the results from WinJulea, the deflections obtained through static analysis show significant improvement in accuracy. This is inferred since the deflection obtained from Static comes closer to field data. The reduction compared to WinJulea shows the reduction ranges 31% in an average.

Table 5-9 Static Analysis deflections with varying subgrade modulus and stiffness of Base and Subbase

Effective Subgrade Modulus	**High Stiffness 1,000,000 psi**			**Low Stiffness 100,000 psi**		
	10 ksi	**20 ksi**	**30 ksi**	**10 ksi**	**20 ksi**	**30 ksi**
Low Range CRCP	3.88	2.78	2.26	5.70	3.91	3.12

Medium Range CRCP	3.10	2.28	1.88	4.31	3.03	2.45
High Range CRCP	2.37	1.77	1.47	3.08	2.22	1.82

Figure 5-64 shows the graphs with deflection predicted from Static Analysis with the measured deflection data from the field. Although the static analysis has provided improved results, it is evident that deflection issues persist, as it fails to capture the field observations. Thus, to mitigate this discrepancy, dynamic behavior of CRCP under real-world FWD loading should be studied. Said that, it is necessary to perform a dynamic analysis and recalibrate our model. The dynamic analysis will assess whether the application of dynamic loads can further refine the model and improve the alignment between the FE model results and field observations.

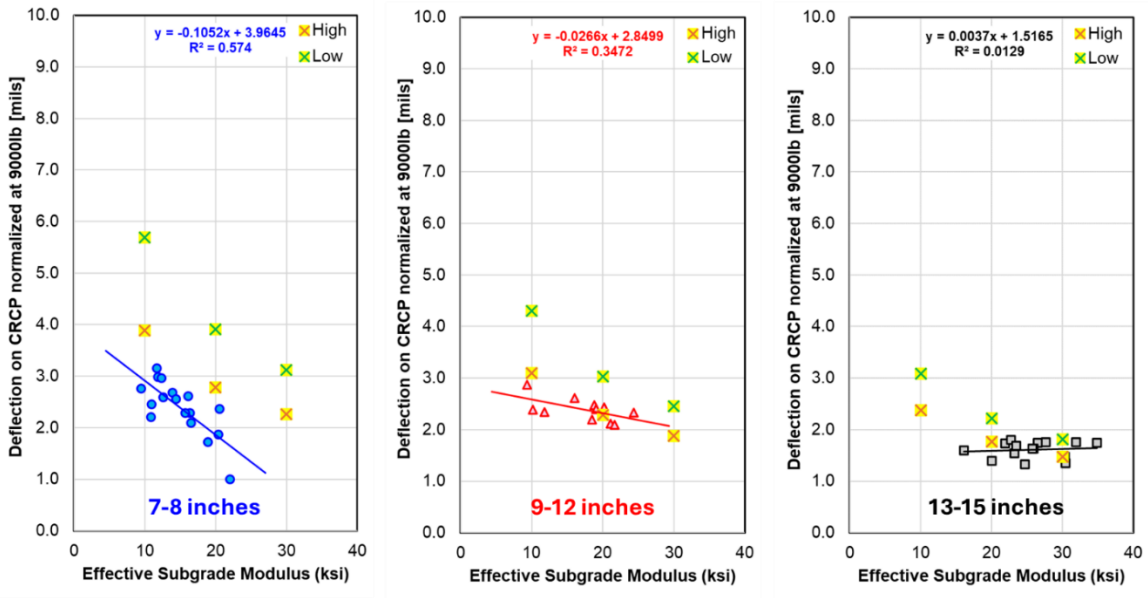

Figure 5-64 Graphical representation comparing Static Analysis deflection with real field data

Recalibration of the FE model

After running both WinJulea and static analysis, it became clear that neither model provided the deflection range required for our specific case. As a result, dynamic analysis was introduced to address this issue. The deflection values obtained from the FE model using dynamic analysis are summarized in Table 5-10. The inclusion of dynamic analysis has proven beneficial in refining and recalibrating the deflection values, bringing them closer to what is observed in real field data.

The observed deflection for the 7–8-inch slabs as shown in Figure 5-65 is slightly lower than what was predicted by ANSYS. Yet again, as mentioned earlier this discrepancy can be attributed to the slab thickness that arises from improper grading during construction. Contractors often attempt to correct grading errors by laying thicker slabs, which leads to lower-than-expected deflection measurements. The medium range slabs exhibit a more consistent

deflection pattern. Most of the field measured value does fall into the envelope of higher stiffness and lower stiffness curves. For the high range slabs, the deflection values are the lowest among all categories, which is expected given the increased thickness of the slab. This reduced deflection is indicative of the slab's ability to distribute loads more effectively, minimizing the influence of subgrade stiffness. In general, using dynamic analysis reduces the deflection by 51% in average compared to WinJulea and almost 29% in average compared to Static Analysis.

Table 5-10 Dynamic Analysis deflections with varying subgrade modulus and stiffness of Base and Subbase

Effective Subgrade Modulus	**High Stiffness 1,000,000 psi**			**Low Stiffness 100,000 psi**		
	10 ksi	**20 ksi**	**30 ksi**	**10 ksi**	**20 ksi**	**30 ksi**
Low Range CRCP	2.64	2.03	1.69	3.76	2.81	2.30
Medium Range CRCP	2.15	1.68	1.41	2.88	2.19	1.81
High Range CRCP	1.61	1.29	1.09	2.05	1.60	1.34

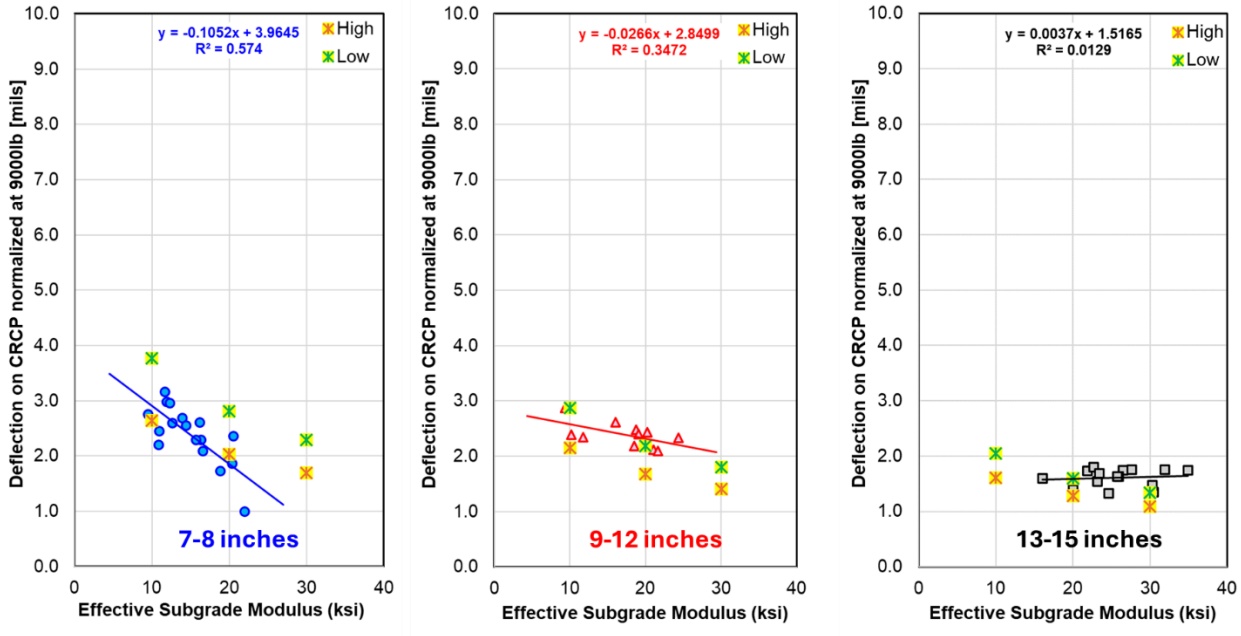

Figure 5-65 Graphical representation comparing Dynamic Analysis deflection with real field data

5.3.4 Identification of Grey areas

In conclusion, the introduction of dynamic analysis has significantly enhanced the accuracy of the FE model by bringing deflections closer to what is observed in the field. However, there remain certain grey areas in the application of ANSYS as a finite element modeling (FEM) tool that needs to be acknowledged and addressed.

- Accurately simulating field conditions with an FE model is inherently challenging. The process involves defining input parameters that best approximate real-world conditions, but it's important to recognize that these models can only approximate, not replicate, the complexities of actual field data. The accuracy of the model is heavily dependent on the precision of the input parameters and the assumptions made during the modeling process.
- For developing the deflection-based design, we assume lower stiffness for the base and subbase layers. This assumption is made to accommodate the highest possible deflection values measured during dynamic analysis. By considering lower stiffness, the model will capture the worst-case scenario in terms of deflection, ensuring that the design is conservative and robust.

5.4 Development of Design Curves

This section outlines the development of comprehensive design curves. We will begin by establishing the fundamental relationship between deflections in the base layer and the overlying CRCP slab using our recalibrated Finite Element (FE) model in ANSYS. This correlation is key to understanding the deflection interactions within the pavement structure.

Next, we will integrate these findings into a practical design tool. We'll introduce a flowchart that connects traffic data, a statewide deflection curve, and our newly developed correlation curves to create a design nomograph. This nomograph will provide a rational and straightforward method for determining allowable deflections. To further enhance usability, we will then present a standalone design program developed in Python, offering a user-friendly interface for applying our methodology.

Finally, we'll validate our approach through a series of case studies and sensitivity analyses, comparing its performance against existing overlay design methods. This comprehensive evaluation will allow us to summarize the key findings and contributions to proposed design methodology.

5.4.1 Developing Correlations between Base Layer Deflection and CRCP Layer Deflection

In our previous analysis of field data, we identified an initial relationship between CRCP and base layer deflections. However, the limited range of slab thicknesses in our field tests necessitated a more robust approach. To bridge these gaps, we turned to our calibrated ANSYS FE model to systematically investigate CRCP behavior across a wider spectrum of design parameters.

A primary objective was to establish correlation curves for CRCP slab thicknesses ranging from 4 to 15 inches. To ensure our design curves are conservative and account for field variability, we focused on a "worst-case scenario" for the pavement structure. Our field data indicated that a 4-inch Hot Mix Asphalt (HMA) base exhibits the greatest deflection sensitivity; therefore, this was selected as the basis for our model. As illustrated in Figure 5-66, our model consists of this 4-inch HMA base over a subgrade with a modulus ranging from a very weak 5 ksi to a very strong 1000 ksi. This wide range of subgrade stiffness ensures our resulting deflection curves are applicable to diverse site conditions.

To generate the necessary data, we conducted a two-phase dynamic analysis in ANSYS:

1. **Base Layer Analysis:** First, we modeled the 4-inch HMA base (with a conservative modulus of 100 ksi) directly on the subgrade, omitting the concrete slab. We performed a dynamic analysis by applying a load and ran this simulation for 14 different subgrade moduli to determine the baseline deflections of the base layer.
2. **CRCP System Analysis:** Following the base layer analysis, we added the CRCP slab to the model. We then systematically ran the dynamic analysis for 13 different slab

thicknesses (from 4 to 15 inches) for each of the subgrade conditions. This second phase resulted in a total of 182 simulation runs (14 subgrade conditions x 13 slab thicknesses).

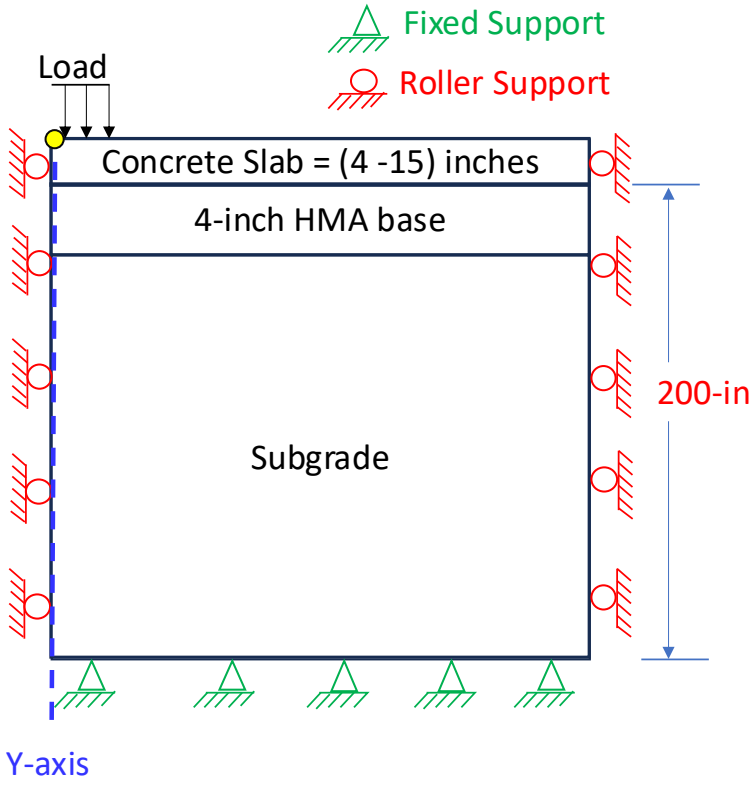

Figure 5-66 Geometry model of the pavement structure

The comprehensive dataset generated from these simulations is presented in Figure 5-67. This table establishes the critical correlations between base deflection and the corresponding CRCP deflection for various slab thicknesses, providing the foundational data for the design tools developed in the subsequent sections.

STEP as e La e r Ana s is

STEP CRCP La e r Ana s is

S.No.	Subgrade Modulus (E)	Base Deflection	4-inches	5-inches	6-inches	7-inches	8-inches	9-inches	10-inches	11-inches	12-inches	13-inches	14-inches	15-inches
	(psi)	mils	mils											
1	5000	50.53	11.51	8.88	7.07	5.78	4.84	4.14	3.60	3.15	2.78	2.46	2.19	1.95
2	7500	38.26	9.66	7.57	6.10	5.04	4.26	3.67	3.20	2.82	2.50	2.23	1.99	1.79
3	10000	31.23	8.41	6.65	5.42	4.51	3.83	3.31	2.90	2.57	2.29	2.05	1.84	1.66
4	15000	23.19	6.78	5.43	4.48	3.77	3.23	2.81	2.47	2.20	1.97	1.78	1.61	1.46
5	20000	18.67	5.76	4.65	3.85	3.27	2.82	2.46	2.18	1.94	1.75	1.58	1.44	1.31
6	25000	15.75	5.04	4.09	3.41	2.90	2.51	2.20	1.95	1.75	1.58	1.43	1.31	1.19
7	30000	13.69	4.51	3.67	3.07	2.63	2.28	2.01	1.78	1.60	1.45	1.31	1.20	1.10
8	35000	12.17	4.11	3.35	2.80	2.40	2.09	1.85	1.65	1.48	1.34	1.22	1.12	1.03
9	40000	11.00	3.78	3.09	2.60	2.22	1.94	1.71	1.53	1.38	1.25	1.14	1.05	0.97
10	50000	9.29	3.29	2.70	2.27	1.95	1.71	1.51	1.35	1.22	1.11	1.02	0.94	0.87
11	70000	7.24	2.67	2.20	1.86	1.60	1.41	1.25	1.12	1.02	0.93	0.86	0.79	0.74
12	90000	6.09	2.30	1.89	1.60	1.38	1.22	1.09	0.98	0.89	0.82	0.75	0.70	0.65
13	100000	5.66	2.16	1.78	1.50	1.30	1.15	1.02	0.92	0.84	0.77	0.71	0.66	0.62
14	1000000	2.07	0.84	0.68	0.57	0.49	0.44	0.39	0.36	0.33	0.31	0.29	0.27	0.26

STEP a se La er Ana sis

- 14 simulation runs (14 subgrade conditions).

STEP CRCP S ste Ana sis

- 168 simulation runs (14 subgrade conditions x 12 slab thicknesses).

Figure 5-67 Correlations between CRCP Slab Deflections and Base Deflections

Figure 5-68 shows the relationship between Base Deflections layer (existing pavement deflections) and CRCP Deflection layer. It was graphed using y-axis as a base layer and x-axis as a CRCP deflection layer. So, what was done is each layer thickness value was used to create line and later linear equation line was drawn to figuratively get a straight curve with distinction of each of the line.

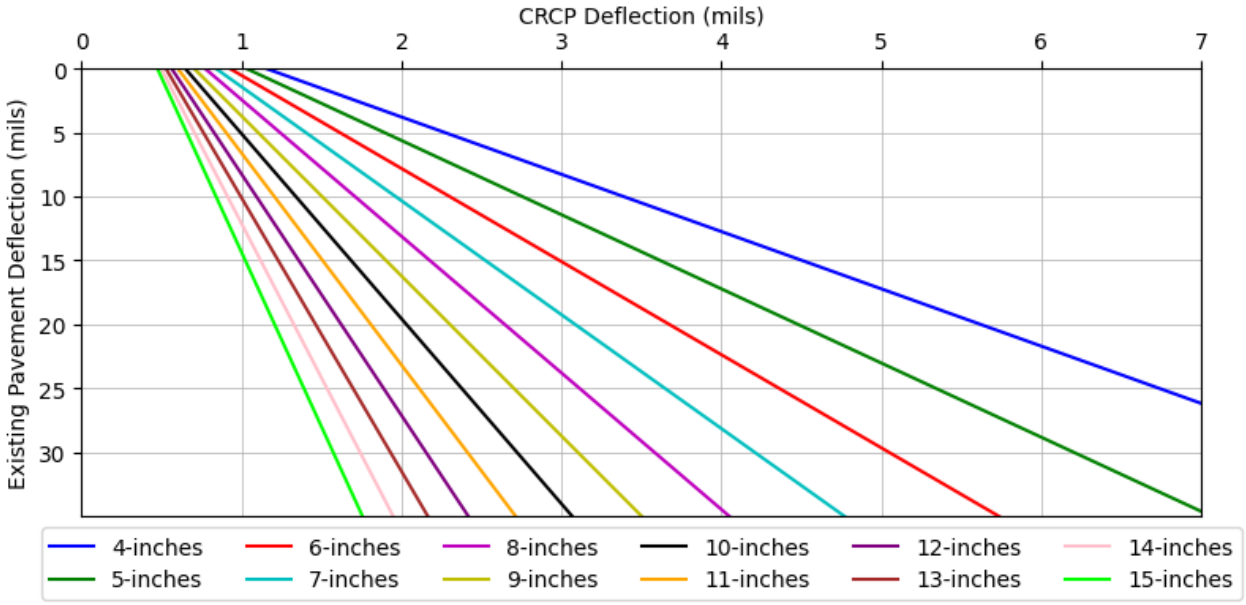

Figure 5-68 Correlations between CRCP slab deflections and existing pavement deflections

5.4.2 Flowchart & Nomograph

The proposed design methodology is summarized in the flowchart presented in Figure 5-69. This five-step process provides a systematic framework for determining the required CRCP thickness. To facilitate this process, a design nomograph (Figure 5-70) has been developed, which graphically integrates design traffic, statewide deflection data, and the deflection correlation curves established in the previous section.

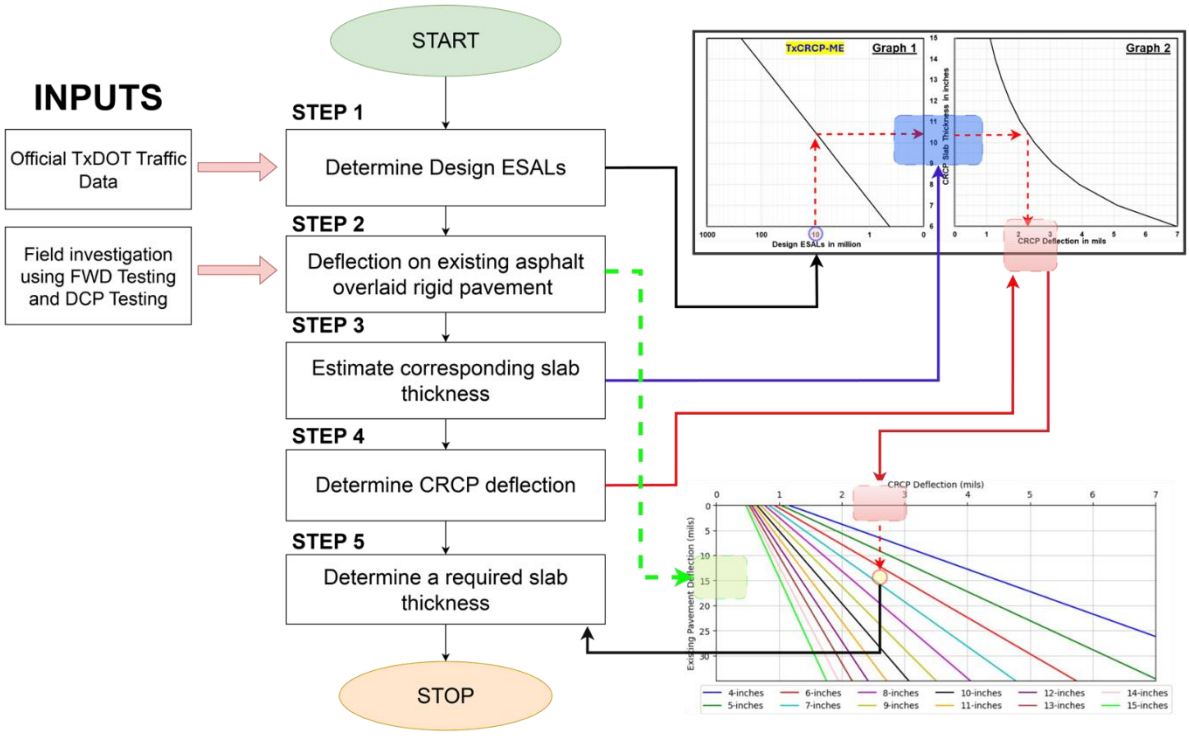

Figure 5-69 Flowchart for Proposed Design

The nomograph consists of three linked graphs:

- Graph 1: Relates design traffic (ESALs) to CRCP slab thickness based on the TxCRCP-ME and is presented in logarithmic scale (Figure 5-70).

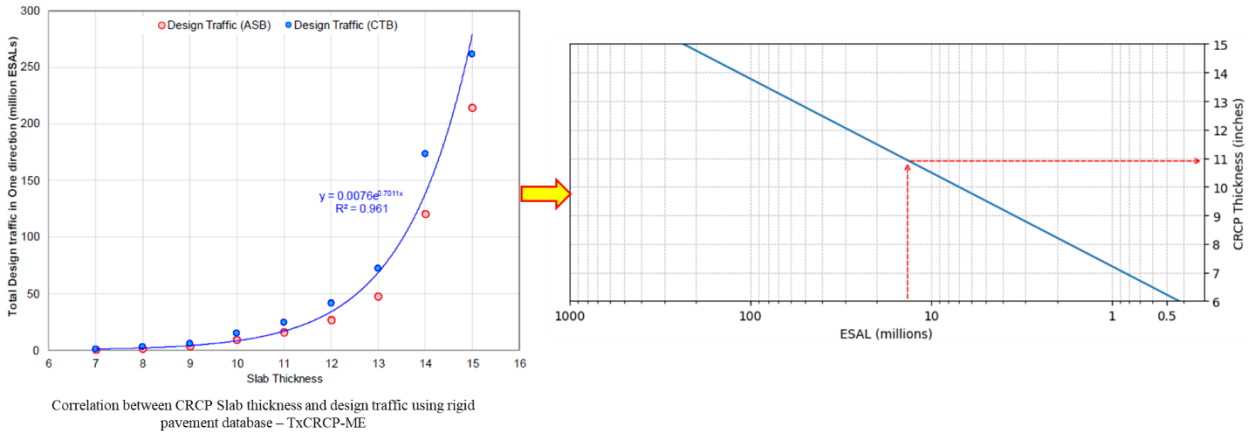

Correlation between CRCP Slab thickness and design traffic using rigid pavement database – TxCRCP-ME

Figure 5-70 Relation between Slab thickness

- Graph 2: Uses a statewide deflection curve to determine the maximum allowable CRCP deflection corresponding to the preliminary slab thickness (Figure 5-71).

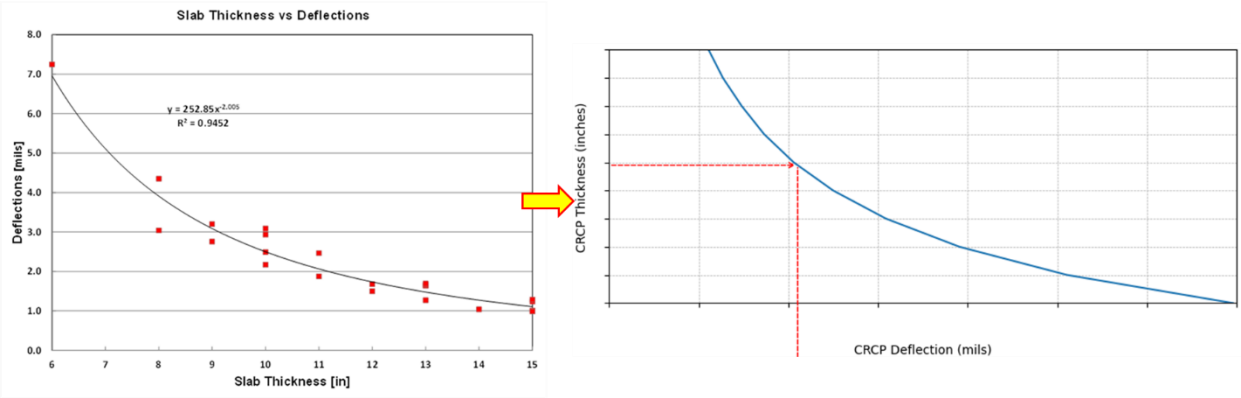

Figure 5-71Statewide deflection curve

- Graph 3: Utilizes the correlation curves (from Figure 5-68) to determine the final required CRCP slab thickness based on the allowable CRCP deflection and the actual measured deflection of the existing base.

The following steps provide a practical guide for using the design nomograph (Figure 5-72) to determine the required CRCP slab thickness.

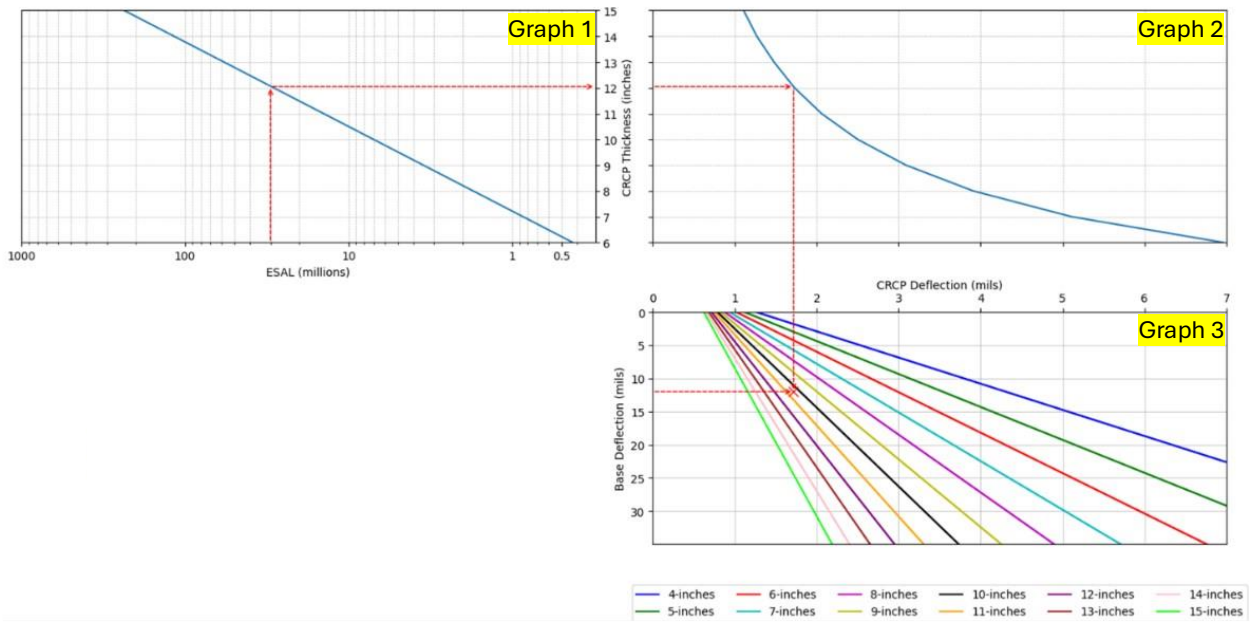

Figure 5-72 Proposed Nomograph for deflection-based design method

Step 1: Determine Preliminary Slab Thickness from Design Traffic (Graph 1)

- **Input:** Begin with the design traffic in Equivalent Single Axle Loads (ESALs) for the project, which can be obtained from sources like the MS2soft TxDOT software platform or the RPDB website.
- **Action:** Locate your design traffic value on the horizontal axis of Graph 1. Draw a vertical line up to intersect the design curve. From this intersection point, draw a horizontal line to the right to find the corresponding preliminary CRCP slab thickness on the vertical axis.

Step 2: Determine Allowable CRCP Deflection (Graph 2)

- **Input:** Use the preliminary CRCP slab thickness determined in Step 1.
- **Action:** Locate this thickness value on the vertical axis of Graph 2. Draw a horizontal line to the right until it intersects the statewide deflection curve. From that point of intersection, draw a vertical line down to the horizontal axis to read the corresponding maximum allowable CRCP deflection.

Step 3: Determine Required CRCP Slab Thickness (Graph 3)

- **Inputs:** This final step requires two inputs:
  - The allowable CRCP deflection is determined in Step 2.
  - The average measured base layer deflection from Falling Weight Deflectometer (FWD) field testing.
- **Action:**
  - Locate the allowable CRCP deflection (from Step 2) on the horizontal axis of Graph 3 and project a vertical line downwards.

- Locate the measured base deflection on the vertical axis of Graph 3 and project a horizontal line to the right.
- The point where these two lines intersect determines the required CRCP slab thickness. The required thickness is given by the correlation curve on or immediately above the intersection point. For example, if the lines intersect in the region between the 13-inch and 14-inch curves, a 14-inch slab thickness would be selected.

This graphical approach provides a direct and rational method for selecting an appropriate CRCP slab thickness that accounts for both future traffic demands and existing pavement conditions.

5.4.3 Standalone Design Program

A Python-based application with a graphical user interface (GUI) was developed using Tkinter and matplotlib to aid as a design tool for this research. The tool integrates design input parameters, traffic loading projections, and structural response relationships into a set of interconnected nomographs, offering users a clear, interactive way to visualize design decisions.

The tool is designed to estimate the appropriate CRCP overlay thickness based on projected traffic loads (expressed in ESALs) and to evaluate whether the structural support provided by the base layer is sufficient to accommodate deflection demands. Figure 5-73 shows the user interface of the program developed.

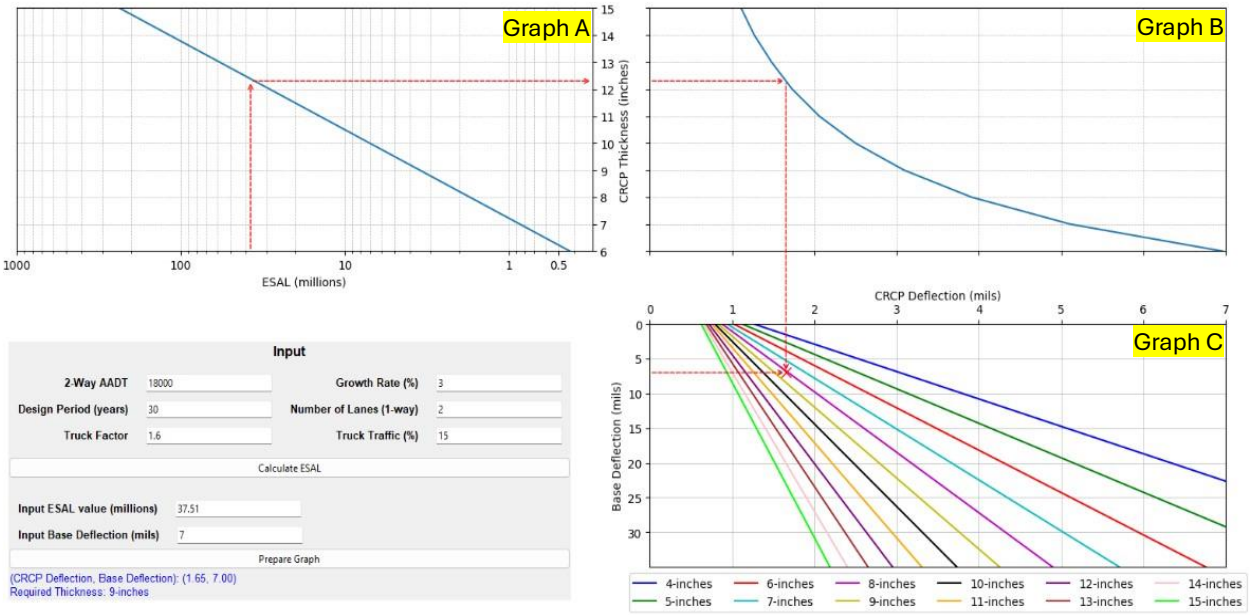

Figure 5-73 Proposed Design Program

Key Functional Components:

1. Input Section

Users provide essential traffic and structural input values through a set of fields:

- Traffic Inputs: 2-way AADT, growth rate, design period, truck factor, and truck percentage.
- Structural Input: Base deflection (in mils).

These inputs are used to calculate the cumulative ESALs over the design period using a formula that incorporates growth rates and lane distribution factors.

2. Plot Layout (Nomograph Panels)

The interface contains three active plots arranged in a 2×2 grid:

- **Graph A – ESAL vs CRCP Thickness:**
  - Displays the logarithmic relationship between cumulative ESALs and CRCP thickness. A red arrow dynamically traces the user's input ESAL value to the corresponding pavement thickness.
- **Graph B – CRCP Thickness vs CRCP Deflection:**
  - Illustrates how deflection decreases with increasing CRCP thickness. This plot translates the selected CRCP thickness into a corresponding deflection value.
- **Graph C – CRCP Deflection vs Base Deflection:**
  - Shows a family of curves representing different CRCP overlay thicknesses. Each curve plots the base deflection response as a function of CRCP deflection, based on empirical E-based data. The tool uses linear regression to draw these lines.

Once the user enters ESAL and base deflection values:

- The program interpolates the CRCP thickness from Graph A and the corresponding CRCP deflection from Graph B.
- In Graph C, it then plots a red arrow from the origin to the input deflection point.
- It automatically identifies the minimum CRCP thickness curve in Graph C that lies above the point (indicating sufficient structural capacity).
- The corresponding thickness is displayed in a label as the "Required Thickness."

The charts update interactively with every valid input, and tooltips, tick labels, and color-coded lines help guide user interpretation.

This tool streamlines the design process for CRCP overlays, especially in evaluating traffic demand, structural performance, and required thickness using a practical and engineer-friendly interface.

5.4.4 Case Study and Comparison with current design method

Unbonded Overlay

This section presents a case study to validate the proposed deflection-based design methodology for unbonded concrete (UBCO) overlays. The selected test section, US 287-2, located near Electra in the Wichita Falls district, provides an exemplary case of an in-service unbonded overlay. The location of this test section is illustrated in Figure 5-74. The primary objective of

this analysis is to evaluate the performance of the existing overlay and compare the overlay thickness determined by the current Unbonded TxDOT design method and the proposed deflection-based approach.

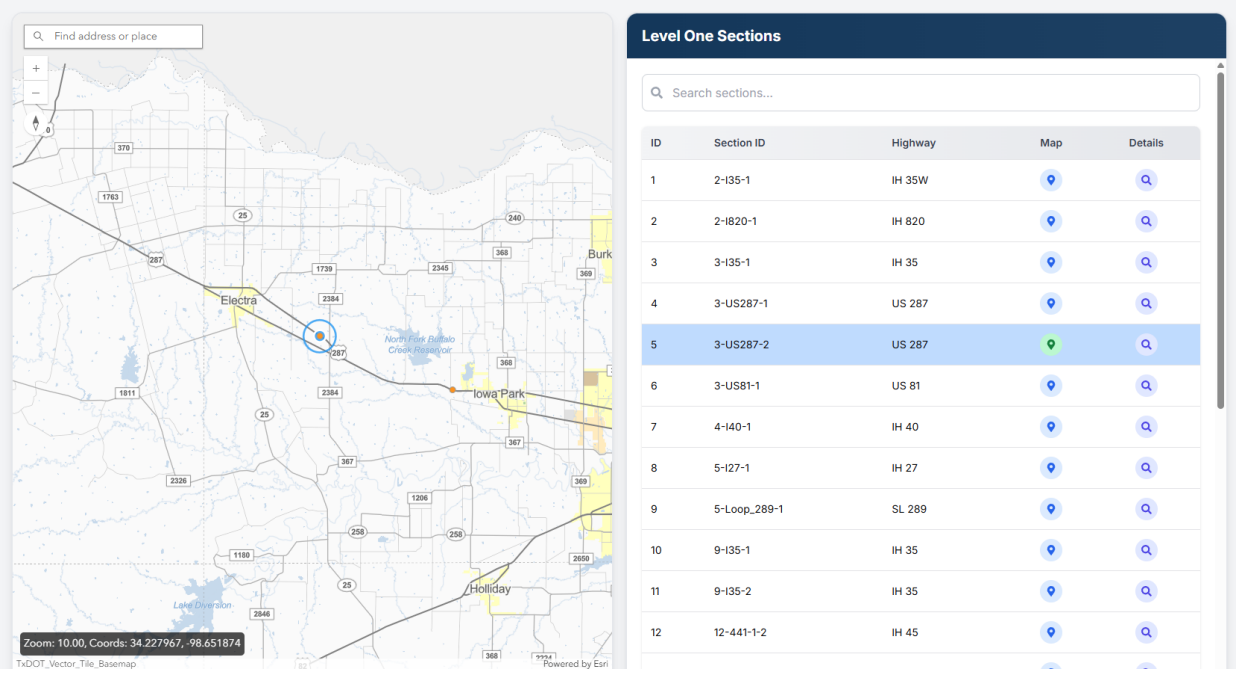

Figure 5-74 Section 3-US287-2 in Wichita Falls

The pavement at section US 287-2 consists of a composite system. Coring samples, as shown in Figure 5-75, reveal an original 8-inch CRCP that was subsequently overlaid with a 2-inch layer of HMA, which now serves as a separation layer. A 10-inch CRCP was then placed as the unbonded overlay. The total thickness of this composite pavement system is 20 inches.

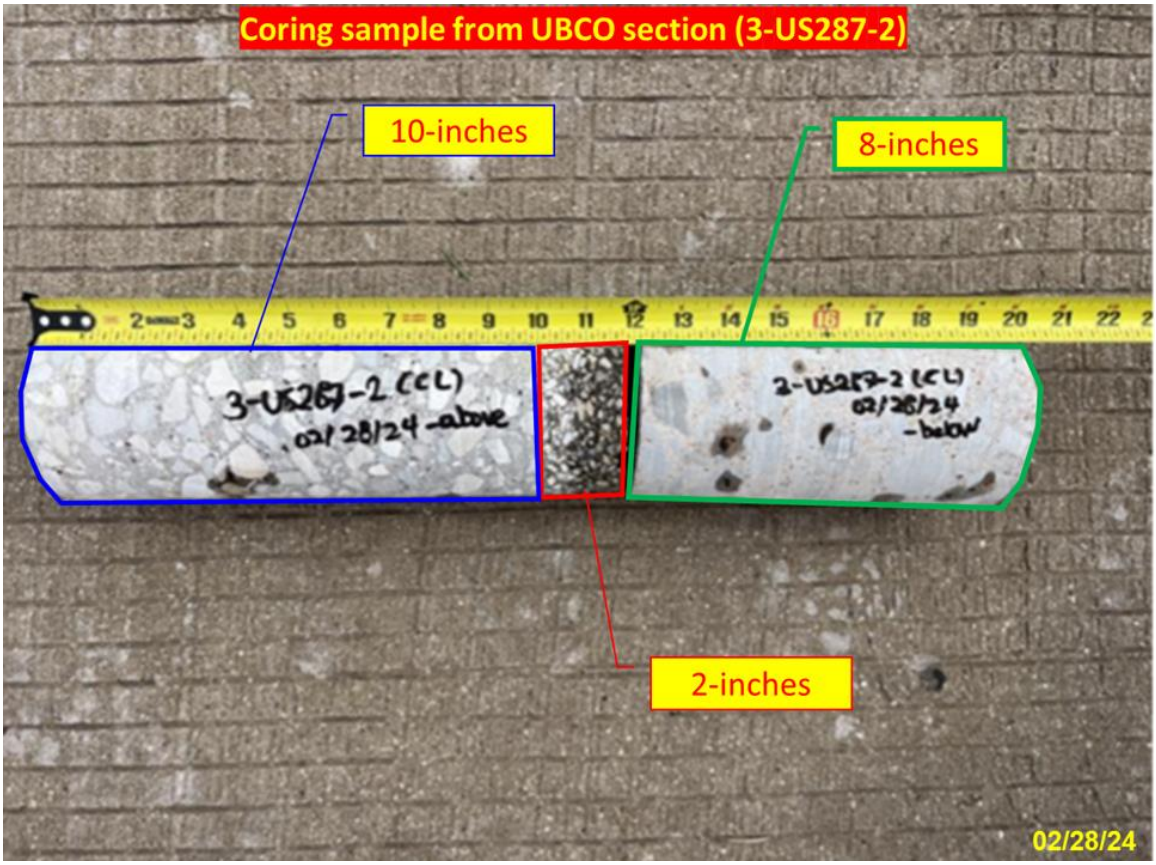

Figure 5-75 Coring sample: Existing slab of 8-inches + 2-inches HMA + 10-inches overlay

To assess the structural capacity of the existing pavement, FWD testing was conducted. The resulting deflection data, presented in Figure 5-76, indicates an average deflection of 1.5 mils for the entire 20-inch composite system. For comparative purposes, the statewide deflection curve for a new 10-inch concrete pavement suggests an expected deflection of approximately 2.5 mils. The measured deflection of 1.5 mils is significantly lower, indicating that the composite system exhibits a structural response equivalent to a much thicker, monolithic slab, conceptually, a 13-inch slab. This superior performance, along with the absence of significant distress, suggests that the existing 10-inch overlay may be over-designed for the historical traffic it has sustained.

An initial back-calculation was attempted to reconcile the existing 10-inch overlay with the underlying 8-inch slab using the existing design equation. However, the analysis, which considered a hypothetical worst-case scenario, yielded inconsistent results, suggesting a required existing slab thickness of 9.22 inches to justify the 10-inch overlay.

$$D_{ol} = \sqrt{(D_f)^2 - (D_{eff})^2}$$

Let us consider, $F_{jcu} = 0.90$ (the worst-case scenario)

$$D_{ol} = \sqrt{(13)^2 - (0.9\,XD_{existing})^2}$$

$$(13)^2 - (10)^2 = (0.9\,XD_{existing})^2$$
$$169 - 100 = (0.9\,XD_{existing})^2$$
$D_{existing}$ is 9.22 inches.
However, Existing slab thickness $(D) = 8$

This discrepancy highlights the potential inaccuracies that can arise from design methods that rely on nominal layer thicknesses rather than direct, in-situ structural response and measurements.

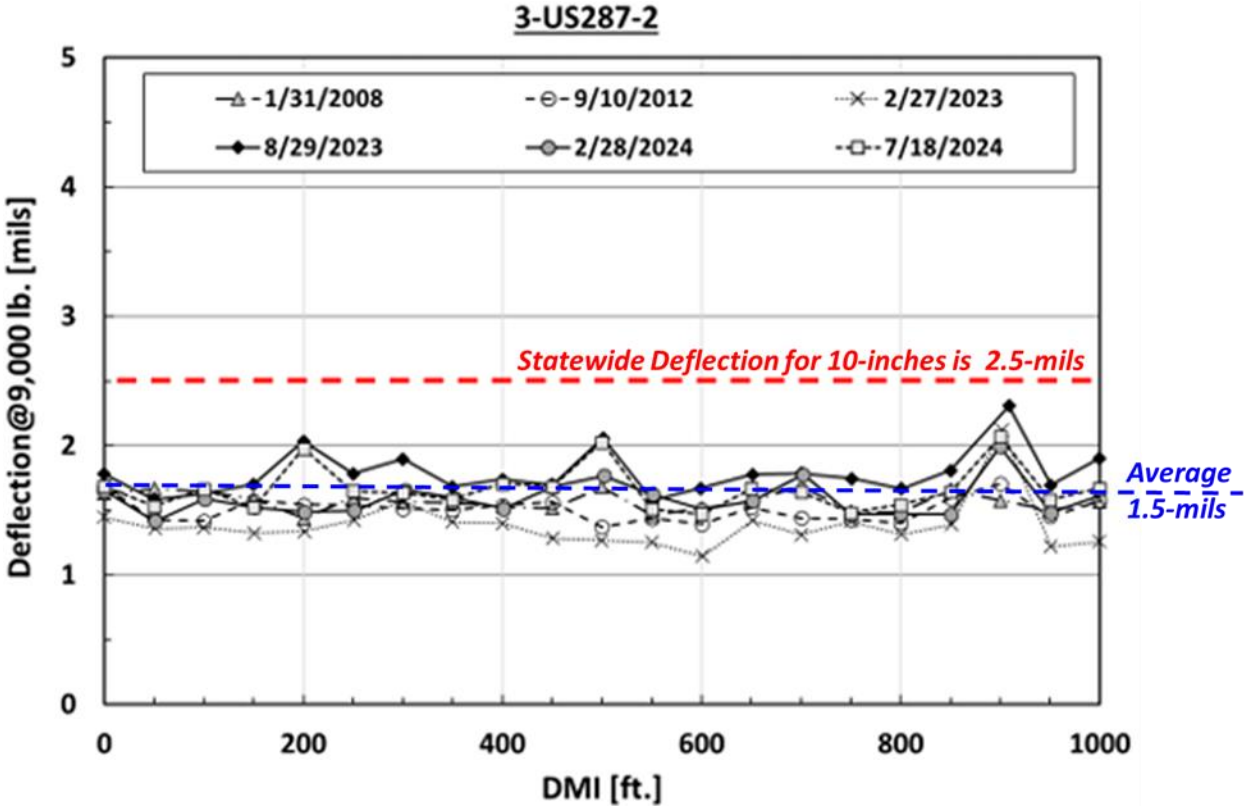

Figure 5-76 Deflection data on the composite pavement

To provide a comprehensive evaluation, a comparative analysis was performed to determine the required overlay thickness to sustain the projected traffic for the next 30 years.

Traffic Projection

The current Average Annual Daily Traffic (AADT) for this section in 2023 is 17,812 vehicles, with a truck traffic percentage of 18.3%. As detailed in the traffic projection analysis shown in Figure 5-77, the cumulative 80-kip equivalent single axle loads (ESALs) for a 30-year design life are estimated to be approximately 34 million.

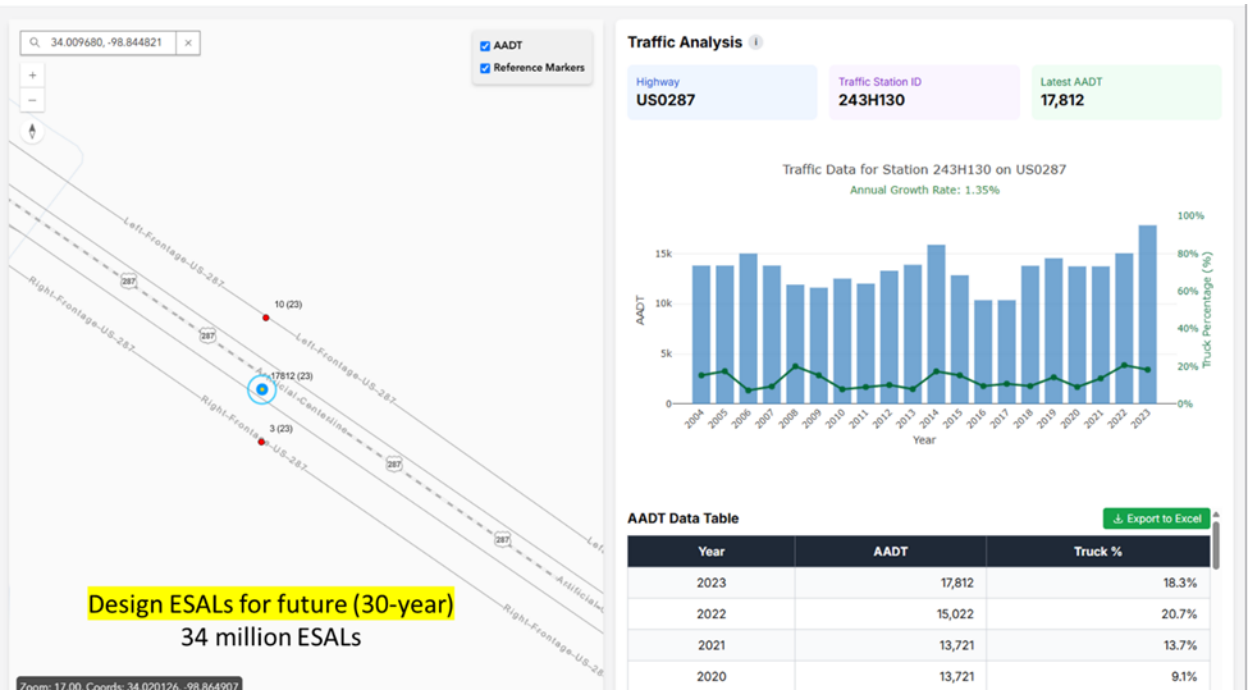

Figure 5-77 Traffic prediction for next 30-years

The current TxDOT design procedure for unbonded overlays is based on the following formula, which relates the required overlay thickness $\boldsymbol{D_{ol}}$ to the thickness required to carry future traffic $\boldsymbol{D_f}$ and the effective thickness of the existing slab $\boldsymbol{D_{exist}}$:

$$\boldsymbol{D_{ol}} = \sqrt{(\boldsymbol{D_f})^2 - (F_{jcu} * \boldsymbol{D_{exist}})^2}$$

Where F_{jcu} is a factor accounting for the condition of the existing pavement. For this analysis, a conservative approach is taken.

$$F_{jcu} = 0.90$$

Existing slab thickness $(D) = 8$

$$D_{eff} = 8 * 0.90 = 7.2\ inches$$

Slab thickness to carry future traffic $(D_f) = 13\ inches$

Design ESALs for future (30-year) = 34 million ESALs

$$\boldsymbol{D_{ol}} = \sqrt{(\mathbf{13})^2 - (\mathbf{7.6})^2} = \mathbf{10.54 = 11\text{-inches}}$$

Whereas using nomograph for the proposed design method we get as shown in Figure 5-78

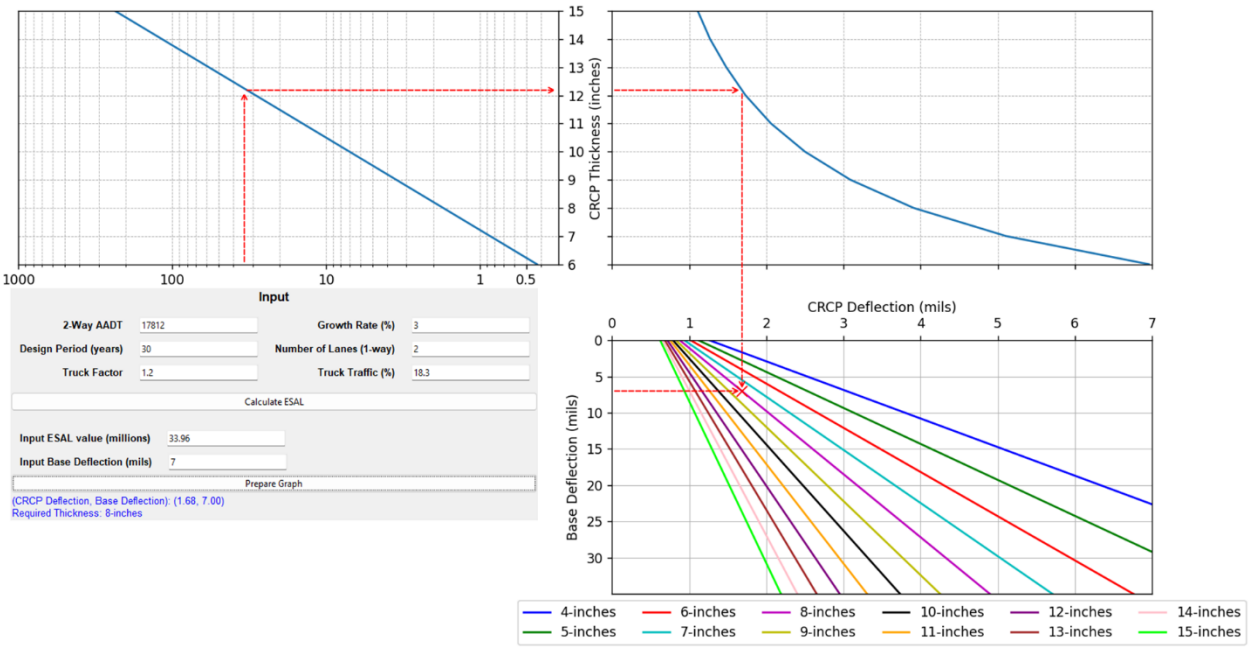

Figure 5-78 Proposed Design Method with existing deflection of 7mils gives us an overlay thickness of 8-inches

The proposed design method utilizes the measured surface deflection of the existing pavement prior to the overlay as the primary input parameter. This approach directly captures the in-situ structural capacity and support conditions of the existing slab.

The deflection on the original 8-inch CRCP over the 2-inch HMA separation layer is the critical input. Based on statewide deflection data, an 8-inch concrete pavement typically exhibits a maximum deflection of approximately 4 mils. Even under worst-case assumptions where significant deterioration has occurred, the deflection would unlikely exceed 7 mils on average.

Using the nomograph developed for the proposed design method (Figure 5-72), these deflection values are used to determine the required overlay thickness for the 34 million ESAL design traffic:

- For a measured deflection of 7 mils or 10mils, the proposed method requires an overlay thickness of 8 inches or 10 inches respectively.
- For a measured deflection of 4 mils (representing a pavement in good condition), the required overlay thickness is only 6 inches.

The comparative analysis, summarized in Figure 5-79, reveals a stark contrast between the design methodologies. The conventional TxDOT method stipulates an 11-inch unbonded overlay for the future traffic demand. In contrast, the proposed deflection-based method, leveraging direct structural response measurements, indicates a required overlay thickness of between 6 and 8 inches.

Even when considering a conservative deflection value of 7 mils for the existing pavement, the proposed method yields an 8-inch overlay, a 3-inch (or 27%) reduction in thickness compared to the TxDOT design. This case study demonstrates that the current TxDOT unbonded overlay design approach, which is rooted in theoretical calculations and potentially erroneous assumptions about the effective strength of existing layers, tends to be overly conservative.

S.No.	Input Deflection	US287	
		Current TxDOT UBCO Design	Proposed Design Method 30 year: 34 million ESALs
1	4-mils	11-inches	6
2	7-mils		8
3	10-mils		10

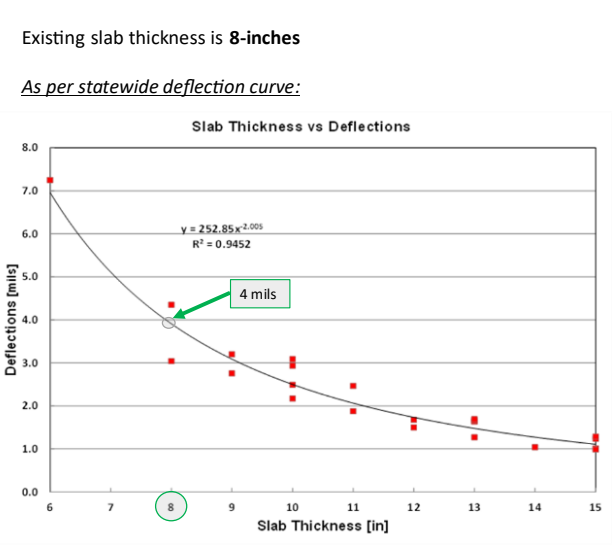

Figure 5-79 Comparison between existing TxDOT UBCO Design with Proposed Deflection based Design Method

Whitetopping

This section details a comparative case study designed to validate the proposed deflection-based design methodology for whitetopping applications. The study focuses on two deteriorated flexible pavement intersections in Texas, which are candidates for rehabilitation with a concrete overlay, as depicted in Figure 5-80.

The two locations selected for this case study are the intersections at US 281 and SH 72 at IH 37. Both sites exhibit significant pavement distress typical of high-stress locations on flexible pavements. A foundational step in pavement design is the characterization of traffic loading, which serves as a primary input for the conventional TxDOT design method.

The traffic data for the year 2023 are as follows:

- **US 281:** Average Annual Daily Traffic (AADT) of 18,408 with 12.5% truck traffic.
- **SH 72 at IH 37:** AADT of 7,056 with 18.3% truck traffic.

The current TxDOT whitetopping design procedure requires the traffic input to be expressed in terms of trucks per day per lane. This value was derived assuming a 50% directional distribution

and a lane distribution factor consistent with a multi-lane highway. The resulting design traffic values are:

- **US 281:** 743 trucks per day per lane
- **SH 72 at IH 37:** 427 trucks per day per lane

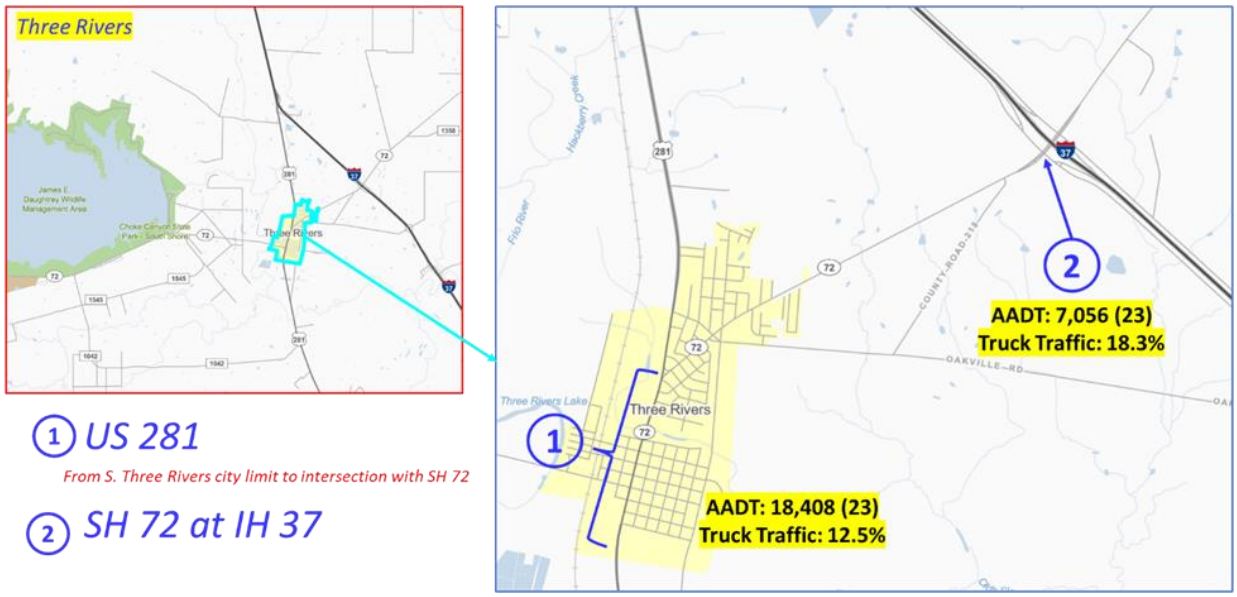

Figure 5-80 Whitetopping Project

The TxDOT whitetopping design guide primarily relies on the traffic level (trucks per day per lane) to determine the necessary concrete overlay thickness referencing back to Table 1-1 in Chapter I. Based on this approach:

- An overlay thickness of 7.0 inches is required for the US 281 intersection.
- An overlay thickness of 6.0 inches is required for the SH 72 at IH 37 intersection.

In contrast, the proposed method integrates both traffic loading and the structural response of the existing pavement, quantified by its maximum surface deflection under a standard FWD load. The central premise is that the overlay thickness should be contingent upon the level of support provided by the foundation it is placed on. A stiffer foundation (lower deflection) requires a thinner overlay to achieve the same service life, and vice versa.

The comparison in table 5-11 clearly illustrates the advantages of the proposed deflection-based design. For the US 281 intersection, while the TxDOT method prescribes a fixed 7.0-inch overlay, the proposed method allows for a reduction to 6.0 or even 5.0 inches or 4.0 inches if the existing pavement is in fair to good condition (i.e., exhibiting deflections of 10 or 7 or 3 mils, respectively). Similarly, for the SH 72 intersection, the proposed method could justify a 4.0 or 5.0-inch overlay, representing a significant thickness difference compared to the prescribed 6.0-inch thickness.

Table 5-11 Comparison between existing TxDOT Whitetopping Design with Proposed Deflection based Design Method

S.No.	Input Deflection	US281 Intersection		SH72 at IH37 Intersection	
		Current TxDOT Whitetopping Design (10 yr: 743 trucks/day/lane) (inches)	**Deflection Based Design Method** (10 yr: 5.3 million ESALs) (inches)	**Current TxDOT Whitetopping Design** (10 yr: 427 trucks/day/lane) (inches)	**Deflection Based Design Method** (10 yr: 3.2 million ESALs) (inches)
1	**3-mils**	7	4	6	4
2	**7-mils**		4		4
3	**10-mils**		5		5
4	**15-mils**		7		6
5	**20-mils**		8		7

5.5 Summary of Design Findings

The key finding is the development of a practical, deflection-based design method for CRCP overlays, grounded in both extensive field testing and mechanistic analysis. A foundation to the proposed deflection-based design method is a "Statewide Deflection Curve," which shows that any new, structurally sound CRCP has a predictable "signature" deflection based on its thickness. This curve acts as a powerful diagnostic tool, allowing an engineer to measure an existing pavement's deflection and determine its "structurally equivalent" new thickness, providing a direct assessment of its remaining structural life.

The core principle of the design, that different pavement structures with the same deflection will perform similarly, was validated through mechanistic modeling. This confirms that deflection can be used as a universal design target. The initial real-world data for this method came from a rigorous field-testing program on seven new CRCP projects, where deflections were measured on the base layer before paving and on the new concrete slab after establishing the critical link between the two. The field testing revealed that stiffer bases, like Cement Treated Base, yield significantly lower deflections (averaging ~12 mils) than more flexible bases like asphalt (averaging ~25 mils). It also confirmed that thinner CRCP slabs are highly sensitive to the underlying subgrade conditions, while thicker slabs are largely unaffected. Because the field data had a limited scope, a calibrated ANSYS computer model was used to simulate a much wider range of conditions. This modeling determined that a dynamic analysis was essential to accurately replicate FWD loading, as simpler methods consistently overpredicted deflections compared to real-world measurements. This calibrated

model successfully generated a comprehensive set of correlation curves that form the engine of the new design method.

Finally, for design engineers, two practical tools were created: a graphical Design Nomograph and a user-friendly, Python-based Design Program. Both tools seamlessly integrate design traffic, the statewide deflection curve, and the new correlation data, translating complex findings into a straightforward and reliable process for determining the required overlay thickness.

CHAPTER 6
CRCP REINFORCEMENT AT INTERSECTIONS

Reinforcement design for CRCP whitetopping at intersections lacks sufficient reference material primarily because most of the whitetopping projects at intersections are jointed concrete pavement (CPCD) except for rigid pavements built specifically to address shoving and rutting in asphalt pavement from stop-and-go traffic, where approach legs have longer lengths and departure legs have shorter length, presenting a challenge for designers. Current practice often applies standard CRCP reinforcement designs to intersections without accounting for their unique conditions. This approach has led to issues such as steel overcrowding at intersections. Additionally, the overuse of reinforcement at intersections results in unnecessary costs for the agency. To address this issue of overcrowding of steel this chapter aims to understand and propose reinforcement designs for CRCP whitetopping at intersections. This work focuses on two primary objectives.

First, we explore the potential for formulating a design equation specific to CRCP whitetopping at intersections, building on our understanding of CRCP behavior. Second, we address the problem of steel congestion by evaluating whether the amount of required reinforcement could be reduced. One proposed alternative is to incorporate saw cuts at intersections, similar to those used in CPCD. Saw cuts are cost-effective, offer improved aesthetics, and provide a more uniform cracking (in a stricter sense, discontinuity in the concrete) pattern that aligns with user expectations, especially in stop-and-go traffic conditions at intersections. Riders would likely prefer intersections with straight, patterned cuts over random cracks for appearance.

It is also worth noting that CRCP at intersections is generally much shorter in length than general CRCP sections. This raises an argument that the required reinforcement could be reduced due to the smaller restraints needed to control concrete volume changes. However, a counterpoint to this argument is that the limited size of CRCP overlays at intersections may render cost savings negligible, potentially making reductions in steel reinforcement unjustifiable.

6.1 Overview of CRCP Behavior

There are two components that play a major role in CRCP structural responses, i.e., environmental factors and external load factors. These factors act individually or in combination, resulting in concrete tensile stresses within the concrete. Environmental factors, such as temperature and moisture variations, cause volume changes in the concrete. However, these volume changes need to be either accommodated as in CPCD or restrained as in CRCP so that they do not cause undesired pavement responses and performance. This is where we introduce reinforcement within the CRCP system with the purpose of restraining these volume changes. In CRCP, tensile stresses in the concrete from restrained volume changes are relieved in the form of transverse cracking. In a generic sense, “transverse cracking” is an essential part

of CRCP behavior. One may even argue that it is of utmost need for CRCP to have transverse cracks to function properly, since they not only relieve concrete stresses, but they also provide "flexibility" to the pavement system as seen in CRCP slabs accommodate any irregularities in the layers underneath, as long as they are not excessive. But these transverse cracks do come with a caveat, which is that the "structural continuities" are maintained at transverse cracks in such a way that wheel load stresses near the transverse cracks are not that much different from those away from the cracks. In other words, transverse cracks should be maintained sufficiently tight throughout the pavement design life so that the loading condition near the transverse cracks is close to so-called Westergaard's interior condition. Thus, it is a fundamental precept in the reinforcement design of CRCP that the longitudinal steel amount should be large enough, so that "structural continuity" is maintained at transverse cracks.

6.2 Factors Influencing Reinforcement Design

The question on how we decide the optimum percentage of longitudinal steel requires comprehensive investigation of CRCP behavior. In literature, there has been mention of different factors that affect the CRCP behavior: length of the slab, subbase friction, temperature seasonal/daily variation, moisture variation, coarse aggregate type, slab thickness, slab grade, and subgrade. Table 6-1 summarizes the different factors and their effects on CRCP behavior.

Table 6-1 Different factors and their effects on CRCP behavior

Factor	Effect
Length of the slab	Movement increases with slab length up to 1,000-1,250 ft. Beyond this, additional length does not significantly contribute to end movement.
Subbase friction	Higher subbase friction resists movement. Stabilized subbases create greater restraint compared to untreated or granular subbases.
Temperature seasonal/daily variation	Temperature fluctuations directly influence CRCP movement through thermal expansion and contraction.
Moisture variation	Moisture fluctuations directly influence CRCP movement through shrinkage and swelling.
Coarse aggregate type	Aggregates with higher thermal coefficients (e.g., siliceous river gravel) produce larger slab movement compared to limestone.

Slab thickness	Thicker slabs exhibit greater axial and flexural forces due to increased cross-sectional area.
Slab grade	End movement decreases as slab grade increases. Higher grades cause reduced horizontal forces driving the movement.
Subgrade	Consolidation or volume changes in subgrade materials could alter local slab behavior.

6.2.1 Slab Length

Research shows that slab movement diminishes significantly once we move approximately 600 feet away from the free end. A pivotal study by McCullough and Sewell in 1964, titled "Parameters Influencing Terminal Movement on Continuously Reinforced Concrete Pavement," found that for slabs shorter than 1,000 feet, both ends contribute to terminal movement. However, for slabs exceeding 1,000 feet in length, only the first 600 feet from each end exhibit movement, while the interior portion of the slab remains stationary due to subbase friction. More exhausted field experimentation conducted in TxDOT research study 0-6326 revealed similar results. However, intersections are usually of shorter length, implying that only the middle portion of the pavement is restrained from slab movements while the majority undergoes slab movements, which reduces concrete stresses from environmental loading. Obviously, this condition is quite different from normal CRCP sections, where the majority of the sections are under severe restraints on concrete volume changes and remain quite stationary, which results in transverse cracking pattern rather consistent throughout the section, except for near free ends. Accordingly, larger slab movements or concrete strains due to shorter length in whitetopping at intersections and resulting smaller concrete stresses is an advantage when it comes to required longitudinal steel amount since the amount of longitudinal steel that will provide a structural equilibrium with lower concrete stresses will be less. This is consistent with the lower amount of longitudinal steel (about 0.15 ~ 0.20 percent) in 60-ft long JRCP (jointed reinforced concrete pavement).

6.2.2 Subbase Friction

Further, the extent of the restrained zone, whether it extends 600 feet, 400 feet, or 300 feet, depends significantly on the surface texture and type of the asphalt base layer. For instance, a coarse-textured base, such as a rough HMA Type B mix or ASB, provides greater restraint and limits movement, whereas a smooth HMA Type D mix allows for more extensive movement.

The role of subbase friction in controlling CRCP movement was explored in detail in the 2012 study titled "Rational Use of Terminal Anchorages in Portland Cement Concrete Pavements." Table 6-2, which is referenced from the report highlights the Waco project on IH-

35 used polyethylene sheeting to minimize subbase friction. This approach resulted in a notably higher daily movement rate compared to other projects. These findings underscore the critical importance of subbase friction in restraining CRCP movement and its influence on reinforcement requirements especially at the intersections. Since the subbase friction on asphalt stabilized base course is proportional to the slab movement up to 0.06-in slab movements, it would be 600-ft before full frictional resistance is materialized, assuming $5x10^{-6}$ /ºF of concrete CTE and 20 ºF temperature daily variations in concrete. In other words, if the total length of the intersection is less than 1,200-ft, concrete stresses due to environmental loading in the whitetopping intersection due to subbase friction would be less than those in regular CRCP sections, potentially lowering the required steel amount.

Table 6-2 Summary of results from research 0-6326

Project Location	**Aggregate Type**	**Pavement Length (miles)**	**Subbase Type**	**Construction Year**	**Daily Movement Rate (mils/°F)**	**Seasonal Movement Rate (mils/°F)**
El Paso (Spur 601)	Limestone	0.8	3 in. ASB	2009	0.56	9.59
Wichita Falls (US 82)	Limestone	0.5	3 in. ASB	2009	0.56	9.69
Linden (US 59)	Siliceous river gravel	>1.00	4 in. ASB	2009	0.51	4.53
Houston (US 290)	Limestone	1.05	1 in. ASB + 6 in. CSB	1995	0.4	2.63
Texarkana (LP 151)	Siliceous river gravel	0.45	4 in. ASB	2004	0.61	3.56
Lubbock 1 (US 82)	Siliceous river gravel	0.45	4 in. ASB	2009	0.33	-
Lubbock 2 (Loop 289)	Limestone	0.45	1 in. ASB + 6 in. CSB	2010	0.07	0.51
Waco (IH 35)	Limestone	0.06	4 in. ASB + two layers of polyethylene plastic sheet	2008	6.83	-

In summary, a fully restrained CRCP section, where the concrete is prevented from moving longitudinally, the concrete experiences its maximum potential stress due to temperature and

moisture variations. On the other hand, if the concrete is allowed to move due to less degree of restraint, concrete stresses will become less, potentially justifying less amount of longitudinal steel needed at whitetopping intersections. The behavior of CRCP whitetopping intersection from environmental loading is, accordingly, somewhere between regular CRCP and JRCP, and the required reinforcement could be less than the value for regular CRCP but more than that for JRCP.

6.3 Review of Existing Design Models

The percentage of longitudinal steel in CRCP is a critical factor in the design process, directly impacting the pavement's behavior and long-term performance, as well as project cost. While there is no single universally accepted method for determining the optimum percentage, there are methods which provide insights into the considerations and approaches used to arrive at a suitable value. The saga of calculating steel reinforcement in concrete pavement began as early as 1924 with the introduction of the Subgrade Drag Theory, which addressed the effects of subgrade friction on reinforcement design. Later, in 1933, C.P. Vetter provided a significant advancement by analyzing stresses in continuously reinforced concrete structures caused by variations in temperature and moisture. His work offered a foundational understanding of how one can calculate the percentage of steel reinforcement in concrete structures to address environmental loading, called temperature steel. Subsequently, the AASHTO Design Guides over different periods of time introduced, refined, and standardized a mechanistic framework for developing reinforcement design especially tailored for CRCP. Likewise, numerous contributions from organizations like ACI, WRI, PCA, etc. have formulated reinforcement design for slabs-on-ground and developed recommendations.

This section briefly discusses the available reinforcement design details for CRCP. We will attempt to investigate early available resources and explore how the methods conceived gave way to calculate the required longitudinal and transverse steel. With this we will draw an insight into how we could possibly use it to recommend the required reinforcement detail for whitetopping intersection and unbonded overlays.

6.3.1 Subgrade Drag Theory

In 1932, R.D. Bradbury from the Wire Reinforcement Institute (WRI) published a research paper titled *"Proper Use of Reinforcing Steel in Concrete Pavement."* This paper discussed and proposed the use of subgrade drag theory to determine the required percentage of steel reinforcement in concrete pavements. In the paper, he made a distinction between two types of reinforcement: distributed reinforcement and accessory reinforcement. According to Bradbury, distributed reinforcement was not intended to prevent the formation of initial cracks or fissures. Instead, it was designed to hold fissures tightly together, thereby delaying the appearance of visible cracks. He viewed distributed reinforcement as essential for providing complete strengthening of the entire slab. Similarly, he defined accessory reinforcement as reinforcement

meant to strengthen specific areas of the pavement, such as edges, joints, or localized sections of the slab that required additional support.

Bradbury's approach to design did not aim to produce a balanced reinforced beam section. Instead, his method relied on using a safe bending strength value for the plain concrete section. The goal was to provide adequate slab thickness to resist transverse bending forces, based on the safe fatigue value for the modulus of rupture, without relying on steel to increase the direct moment of resistance of the section. The primary purpose of the steel reinforcement, as he proposed, was to provide just enough steel to keep the crack openings caused by lateral contraction forces as small as possible.

To achieve this, Bradbury applied Subgrade Drag Theory. This calculation involved determining the amount of steel necessary to resist the force of subgrade friction acting on a given unit of the slab. For example, as shown in figure 6-1, he considered a slab of length (L) and thickness (h) undergoing volume changes due to a temperature drop. The decrease in concrete temperature causes the slab to shrink, generating shear stress at the interface between the concrete slab and the subgrade, represented as frictional stress.

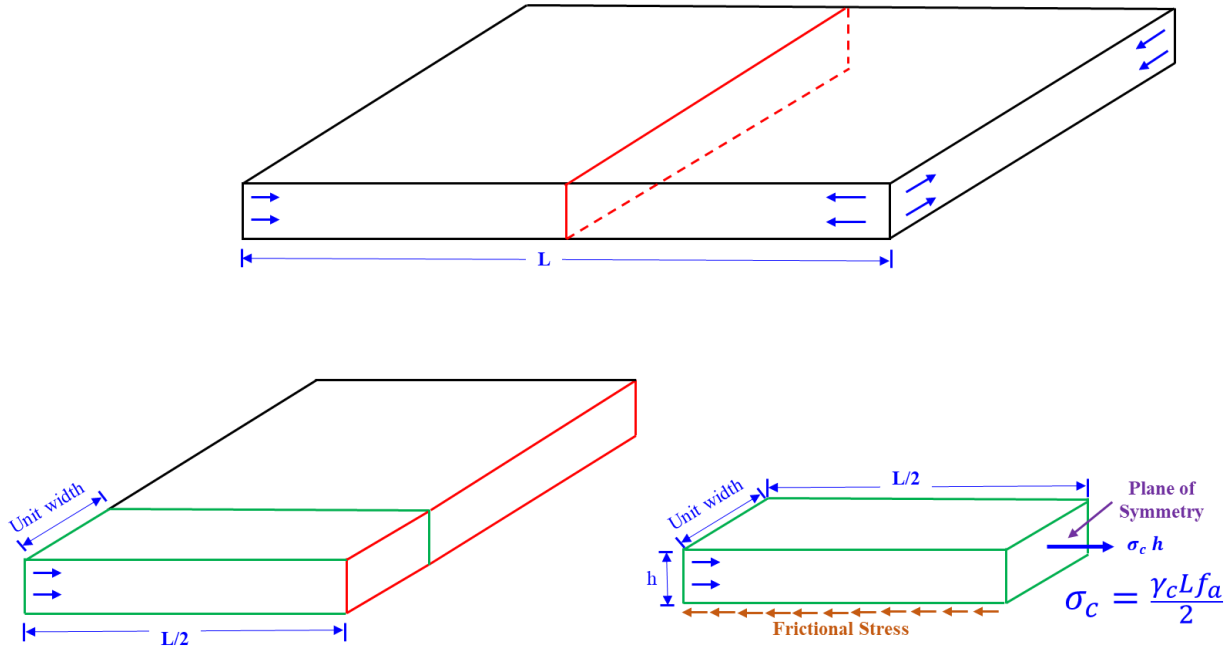

Figure 6-1 Illustration to accompany formula based on subgrade drag theory

Using equilibrium, the tensile stress in the concrete(σ_c) is equal to the frictional stress developed by the subgrade:

σ_c*h= weight of concrete per unit length * frictional coefficient (f_a)

Substituting weight of concrete:

$$weightofconcrete = Volumeofconcrete(V_c) * densityofconcrete(\gamma_c)$$

weight of concrete=Volume of concrete (V_c)*density of concrete (γ_c)

$$= h * 1 * \frac{L}{2} * \gamma_c * f_a$$

Solving for σ_c,

$$\sigma_c = \frac{\gamma_c L f_a}{2} \quad \text{(Equation 6-1)}$$

So, the total force exerted on the face of the concrete (F_c) is

$$F_c = \sigma_c * Area(A_c)$$

Substituting $A_c = h * 1$ (area per unit width):

$$F_c = \frac{\gamma_c L f_a}{2} * \mathrm{h} * 1$$

$$F_c = \frac{\gamma_c h L f_a}{2} \quad \text{(Equation 6-2)}$$

This force exerted by the concrete (F_c) must be in equilibrium with the force provided by the steel reinforcement (F_s):

$$F_s = F_c$$

Substituting

$$f_s A_s = \frac{\gamma_c h L f_a}{2}$$

Solving for the area of steel reinforcement (A_s)

$$A_s = \frac{\gamma_c h L f_a}{2 f_s} \quad \text{(Equation 6-3)}$$

Bradbury's work provided a systematic approach to reinforcement design, emphasizing crack control rather than relying on steel to improve bending strength. His application of subgrade drag theory remains a foundational concept in modern concrete pavement design, influencing practices for both distributed and accessory reinforcement. However, there are few assumptions or limitations which make subgrade drag theory not fully applicable for reinforcement purposes. The assumptions are:

- There are no temperature variations through the slab depth. (Or slab displacements are in uni-axial direction only).
  - Numerous research has shown this is not true.
- Concrete and subbase are in full contact all the time.

- At slab edges, the slab is found to experience upward curling in the morning and downward curling in the afternoon. This means the concrete and subbase are not in contact all the time.

- Subbase frictional stress is elastic (no frictional energy loss).
  - Numerous research has shown this is not true.

In addition to these limitations, the design criteria for the selection of required steel amount are to keep the steel stresses below a certain level – normally ¾ of steel yield stress, not to keep the crack widths sufficiently tight enough, which further limits the viability of the subgrade drag theory in reinforcement design of CRCP.

6.3.2 Vetter's Formula

C.P. Vetter's 1933 research paper, *"Stresses in Reinforced Concrete Due to Volume Changes,"* provides a foundational analysis of the stresses that occur in continuous reinforced concrete structures due to variations in temperature and moisture. His work established critical formulas and design principles to predict and manage these stresses, offering a systematic approach to reinforcement design for crack control.

In his work, Vetter investigated the concrete stresses caused by drying shrinkage and temperature variations separately. He found each stress induces tension in the concrete and proposed formula for reinforcement design such that it does not prevent cracks but controls their size and spacing to enhance durability and functionality. His analysis showed shrinkage alone requires lower reinforcement ratios compared to temperature stresses. Table 6-3 presents the design formula for reinforcement he proposed for different design conditions.

Table 6-3 Design formulas proposed by CP Vetter for different design condition

TABLE 1.—Special Arrangement of Important Design Formulas

Item	Design condition	Shrinkage only, Equation (11)	Temperature drop only, Equation (12)	Indoor structures, shrinkage, and temperature drop, Equation (13)	Outdoor structures, swelling, and temperature drop, Equation (14)
(a)	Minimum reinforcement	$p=\frac{S'_c}{S_s}$	$p=\frac{S'_c}{S_s-n\,S'_c}$	$p=\frac{S'_c}{S_s-n\,S'_c}$	$p=\frac{S'_c}{S_s-w\,E_s-n\,S'_c}$
(b)	Maximum temperature drop for minimum reinforcement	.....	$T=\frac{S_s+n\,S'_c}{2\,\epsilon\,E_s}$	$T=\frac{S_s+n\,S'_c}{2\,\epsilon\,E_s}$	$T=\frac{S_s+n\,S'_c+w\,E_s}{2\,\epsilon\,E_s}$
(c)	Reinforcement for greater temperature drop	.....	$p=\frac{S'_c}{2\,(S_s-T\,\epsilon\,E_s)}$	$p=\frac{S'_c}{2\,(S_s-T\,\epsilon\,E_s)}$	$p=\frac{S'_c}{2\,(S_s-T\,\epsilon\,E_s)}$
(d)	Critical volume change	$z_1=\frac{S'_c}{E_c}\left(\frac{1}{2\,pn}+1\right)$	$\epsilon t_1=\frac{S'_c}{E_c}\left(\frac{1}{2\,pn}+1\right)$	$\epsilon t_1+z_1=\frac{S'_c}{E_c}\left(\frac{1}{2\,pn}+1\right)$	$\epsilon t_1-w_1=\frac{S'_c}{E_c}\left(\frac{1}{2\,pn}+1\right)$
(e)	Distance between cracks	$L=\frac{(S'_c)^2}{np^2qu\,(z\,E_c-S'_c)}$	$L=\frac{(S'_c)^2}{np^2qu\,(\epsilon t\,E_c-S'_c)}$	$L=\frac{(S'_c)^2}{np^2qu\,[(\epsilon t+z)\,E_c-S'_c]}$	$L=\frac{(S'_c)^2}{np^2qu\,[(\epsilon t-w)\,E_c-S'_c]}$
(f)	Minimum distance between cracks	$L_{\text{min.}}=\frac{2\,S'_c}{pqu}$	$L_{\text{min.}}=\frac{2\,S'_c}{pqu}$	$L_{\text{min.}}=\frac{2\,S'_c}{pqu}$	$L_{\text{min.}}=\frac{2\,S'_c}{pqu}$

The formula for calculating the required minimum percentage of longitudinal steel reinforcement (p) is given by:

$$p = \frac{S_c'}{S_s - nS_c'} X\ 100 \qquad \text{(Equation 6-4)}$$

where:

S_c' = Concrete tensile strength (psi): The stress the concrete can withstand before cracking.

S_s = Yield strength of steel (psi): The stress at which the steel begins to deform plastically.

$n = \frac{E_s}{E_c}$ = the ratio of modulus of elasticity of steel to concrete

Let us assume that:

$$S_c' = Ranges\ (300\ psi\ to\ 700\ psi)$$

$$S_s = 60{,}000\ \text{ps}i$$

$$E_s = 29{,}000{,}000\ \text{ps}i$$

$$E_c = 5{,}000{,}000\ \text{psi}$$

Then, for $S_c' = 300\ psi$

$$p = \frac{300}{60{,}000 - \frac{29{,}000{,}000}{5{,}000{,}000}300} X\ 100$$

p = 0.52%

And, for $S_c' = 700\ psi$

$$p = \frac{700}{60{,}000 - \frac{29{,}000{,}000}{5{,}000{,}000}700} X\ 100$$

p = 1.26%

For typical conditions, Vetter suggested reinforcement ratios between 0.52% to as high as 1.26%, ensuring crack control for durability. Research has recognized that the Vetter equation is inclined to propose greater reinforcement ratios than what is required. Part of the reason contributed to the subbase frictional resistance, which was not included in the analysis.

Vetter's concept for developing the percentage of reinforcement in CRCP had significant influence on 1991 study by Won, Hankins, and McCullough, titled "Mechanistic Analysis of Continuously Reinforced Concrete Pavements Considering Material Characteristics, Variability, and Fatigue." They utilized C.P. Vetter's work as a foundational basis for determining the percentage of longitudinal steel reinforcement in CRCP. While the study acknowledges the limitations of Vetter's formulas, it expands upon his concepts and integrates more contemporary factors, including probabilistic approaches and fatigue considerations.

6.3.3 AASHTO Guide

Throughout the revisions of AASHTO Guide for Design of Pavement Structure there has been improvement and refining of the proposed longitudinal steel reinforcement design. The 1972 AASHO Interim Guide for Design of Pavement Structures recommends the following formula for longitudinal steel (Figure 6-2):

$$p = (1.3 - 0.2F)\frac{S_c'}{f_s} X\ 100$$

where:

p = Required steel percentage (%)

F = friction factor of subbase

S_c' = tensile strength of concrete(psi)

f_s = allowable working stress in steel (psi)

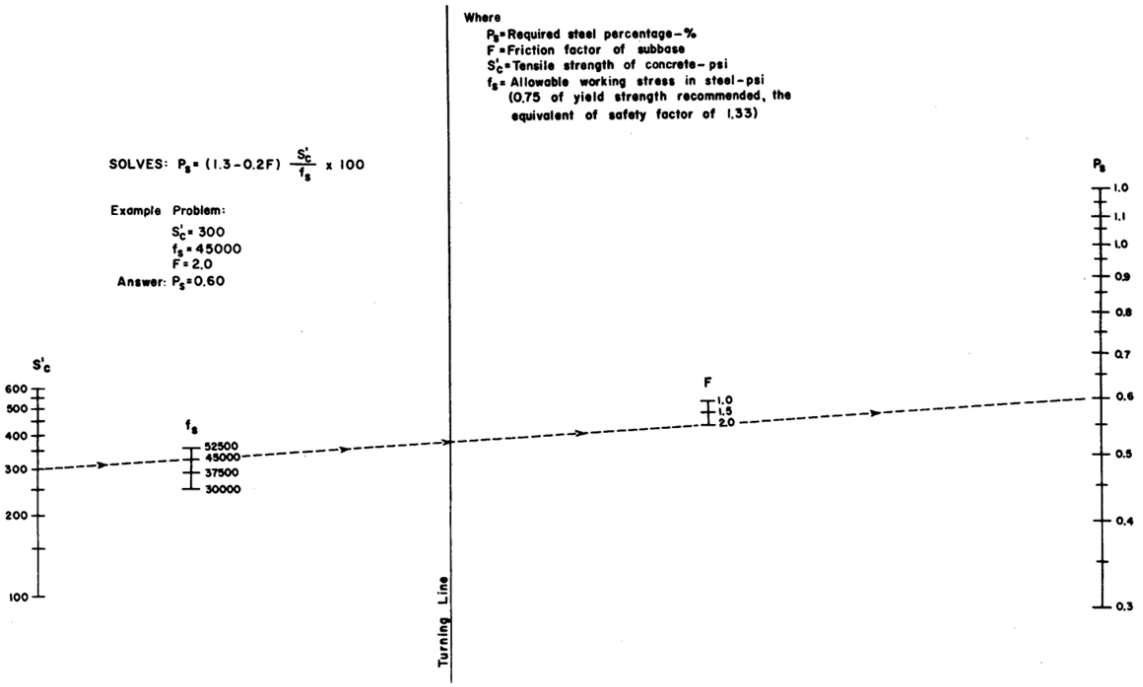

Figure 34. Longitudinal steel for CRCP (8).

Figure 6-2 Nomograph for calculating longitudinal reinforcement for AASHO 1973

The Guide does point out that for concrete with conventional coarse aggregates, longitudinal steel should not be less than 0.4%, as lower percentages compromise load transfer at cracks. In colder regions, the minimum should be increased to 0.5%.

The 1986 and 1993 AASHTO Guide for Design of Pavement Structures recommended a different formula for deriving the required reinforcement. These Guides incorporated empirical

data and established limiting criteria for design. Figure 6-3 illustrates the conceptual framework that determines the percentage of steel based on crack spacing, crack width, and steel stresses:

- As the percentage of steel increases, crack spacing decreases.
- Optimal crack spacing is considered to be between 3.5 and 8 feet, which determines the maximum and minimum steel percentages, respectively.
- For crack width, a recommended limit of 0.04 inches is used to ensure durability and performance.
- Steel stress must remain below the yield stress of 62 ksi to maintain tight cracks and avoid overstressing the reinforcement.

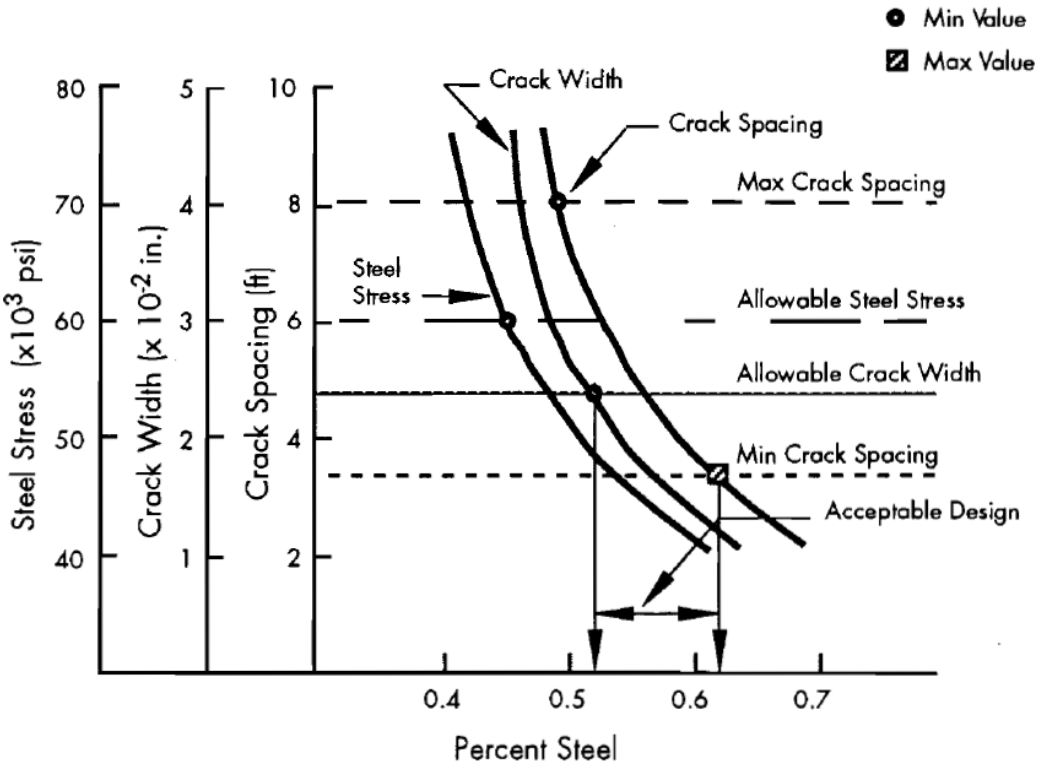

Figure 6-3 Conceptual illustration for selecting percent longitudinal steel using AASHTO Guideline

Based on this concept, the following formula were developed from regression analysis of the results from computer program developed at the University of Texas at Austin.:

$$\text{Crack Spacing } (\bar{X}) = \frac{1.32\left(1+\frac{f_t}{1000}\right)^{6.70} * \left(1+\frac{\alpha_s}{2\alpha_c}\right)^{1.15} * (1+\emptyset)^{2.19}}{\left(1+\frac{\sigma_w}{1000}\right)^{5.20} * (1+P)^{4.60} * (1+1000Z)^{1.79}}$$

$$\text{Crack Width } (CW) = \frac{0.00932\left(1+\frac{f_t}{1000}\right)^{6.53} * (1+\emptyset)^{2.20}}{\left(1+\frac{\sigma_w}{1000}\right)^{4.91} * (1+P)^{4.55}}$$

$$\text{Steel Stress } (\sigma_s) = \frac{47{,}300\left(1+\frac{DT_D}{100}\right)^{0.425} * \left(1+\frac{f_t}{1000}\right)^{4.09}}{\left(1+\frac{\sigma_W}{1000}\right)^{3.14} * (1+P)^{2.74} * (1+1000Z)^{0.494}}$$

where:

f_t = concrete indirect tensile strength

Z = concrete shrinkage at 28 days

α_c = concrete thermal coefficient

$\emptyset$ = reinforcing bar or wire diameter

α_s = steel thermal coefficient

DT_D = design temperature drop

σ_W = wheel load tensile stress

6.3.4 Reinforcing Slabs-on-ground

As mentioned earlier, different organizations have contributed towards the procedure for determining the required steel percentage for slabs-on-ground. Among them, ACI stands out as it provides extensive guidelines on concrete design and construction, including pavements; however, like any other procedures it does not offer specific guidance on steel design for CRCP. Primarily the ACI references worth looking into are as follows:

- ACI 318-14 Building Code Requirements for Structural Concrete
- ACI 325 for concrete pavements
- ACI 360R slabs-on-ground design

Table 6-4 shows that in ACI 318-14, it proposes 0.002(0.2%) as a minimum reinforcement ratio for shrinkage and temperature control.

Table 6-4 Minimum ratios of deformed shrinkage and temperature reinforcement area to gross concrete area (ACI314-14 Table24.4.3.2)

Reinforcement type	f_y, **psi**	**Minimum reinforcement ratio**	
Deformed bars	< 60,000	0.0020	
Deformed bars or welded wire reinforcement	≥ 60,000	Greater of:	$\frac{0.0018 \times 60{,}000}{f_y}$
			0.0014

Further, ACI Committee 325 highlights that similar pavement thickness design methods are used for plain and reinforced pavements, as reinforcement does not significantly affect load-

carrying capacity. It points out that the primary role of steel reinforcement in pavements is to control crack openings and maintain aggregate interlock if cracks form. Also, economic considerations, such as initial construction and life-cycle costs, are emphasized in pavement design. While Appendix A of the Committee 325 report details procedures for determining pavement thickness, including stress ratios and fatigue life, it focuses on the concrete slab rather than steel reinforcement.

ACI 360R slabs-on-ground design somehow does a better job of providing information on reinforcement design details. It is important to highlight that ACI itself refers to other organization works like U.S. Army Corps of Engineers (USACE), the National Academy of Science, and the Department of Housing and Urban Development (HUD), Portland Cement Association (PCA), Wire Reinforcement Institute (WRI), Concrete Reinforcing Steel Institute (CRSI), Post-Tensioning Institute (PTI), as well as several universities and consulting engineers. Thus, we will look into different steel reinforcement procedures proposed by different organizations. Irrespective of which procedure one uses they are usually based on the three key considerations: Shrinkage Control, Temperature Control and Moment Capacity. Depending on the purpose, designers can select which procedure works for them. Table 6-5 summarizes different steel design procedures and respective formulas along with its intended application.

Table 6-5 Different Steel area design procedure

Steel area Design Procedures	**Formulas**	**Application**
Confirmed Capacity Procedure	$A_s = \frac{4.4\ x\ MOR\ x\ t}{f_y(SF)}$	This ensures a minimum moment capacity based on the slab's working stress and geometry. The slab thickness is typically pre-determined through other design procedures.
Temperature Procedure	$A_s = \frac{f_r\ x\ 12t}{2(f_s - T\ \alpha_c E_s)}$	This formula ensures that reinforcement is sufficient to control crack widths due to thermal stresses.
Equivalent Strength Procedure	$A_s = \frac{36\sqrt{f_c' t}}{f_s}$	This formula ensures high steel percentages for applications like highways and runways, where crack frequency must be minimized.
Crack Restraint Procedure	$A_s = \frac{9360t}{f_y}$	This is derived from the relationship between concrete shrinkage and steel's ability to counteract that shrinkage. The method applies

		to sensitive environments, ensuring minimal microcracking.

where:

f_y= yield stress of the reinforcement(psi)

t = thickness of the slab in inches

MOR = modulus of rupture of concrete (psi)

SF = safety factor (normally taken as 2)

f_r = tensile strength of concrete (psi) (calculated at 0.4 x MOR)

f_s= working stress in reinforcement (psi)

T = range of temperature the slab is expected to be subjected to (°F)

E_s = modulus of elasticity of steel (psi)

f_c'= compressive strength of the concrete (psi)

α_c = concrete thermal coefficient (in/in/°F)

Since the procedure is based on either of three key considerations, Table 6-6 summarizes the procedure versus considerations they would suffice. Among them, equivalent strength procedure is considered most favorable as it can be used for heavy duty applications like highways, truck ramps, and airport runways. Importantly, it balances concrete's tensile strength and reinforcement yield stress. While it primarily focuses on reducing cracks (shrinkage and temperature-related), it also inherently improves moment capacity. However, it cannot be directly used for steel design in our case as it is not intended for CRCP.

Table 6-6 Different procedure versus considerations they would suffice

Procedure	**Shrinkage Control**	**Temperature Control**	**Moment Capacity**
Confirmed Capacity Procedure	✗	✗	✓
Temperature Procedure	✗	✓	✗
Equivalent Strength Procedure	✓	✓	✓
Crack Restraint Procedure	✓	✓	✗

Development of New Reinforcement Strategies

6.4 Evidence-based approach

It is evident that designing steel for CRCP Whitetopping at intersections presents numerous challenges. It would be an oversimplification to suggest that we can create a definitive formula for calculating the steel required for such applications. While it may be possible to account for factors like shrinkage, temperature, and moment capacity in a formula, incorporating the complex interactions among concrete, steel, subbase friction and environmental loading remains a significant challenge. Additionally, the initial conditions of concrete placement, such as concrete setting temperature, weather condition, and curing effectiveness, play a critical role in the cracking behavior at early ages. This is why it is often difficult, if not impossible, to predict with certainty cracking characteristics such as crack spacing and its distribution, even though numerous research studies attempted do so. This difficulty stems from, as discussed earlier, interactions among various factors, and more importantly, concrete tensile stresses near the slab surface from environmental loading are rather uniform except within about 1-ft or 2-ft from transverse cracks, resulting in transverse cracks occurring at which the local strength is lower than other areas, i.e., where there are "defects" in the concrete, defined by whatever causes the lowest ultimate concrete tensile strain capacity such as microcracks at the interface between coarse aggregate surface and surrounding mortar. Determining where the "defects" are located is almost impossible. Fortunately, cracking characteristics of CRCP, as long as they are not quite unusual, do not appear to have substantial effects on CRCP performance, if those cracks are kept sufficiently tight by adequate amount of longitudinal steel. The key here is what is "adequate" or optimum amount of longitudinal steel. As discussed earlier, determining the exact percentage of steel based on formula or mechanistic analyses required for CRCP including whitetopping is therefore a highly impractical endeavor. Instead, an evidence-based approach offers a more reliable path forward. With past field data and empirical observations, we can better address the uncertainties and complexities inherent in steel design for CRCP applications, including whitetopping.

6.4.1 Route US40, West of Vandalia, Illinois

The first CRCP project in Illinois was constructed between 1947 and 1948 on Route US 40, west of Vandalia. This experimental project covered a length of 5.5 miles and was divided into eight test sections. The test sections varied in pavement thickness and longitudinal steel content:

- Pavement Thickness: Four sections were 7 inches thick, and the other four were 8 inches thick.
- Steel Percentages: Each thickness group had one section with each of the following steel percentages: 0.3%, 0.5%, 0.7%, and 1.0%.

The longitudinal reinforcement consisted of round deformed bars, placed continuously through each test section. A comprehensive performance review was provided in a report titled *"A Twenty-Year Report on the Illinois Continuously Reinforced Pavement"* by John E. Burke and Jagat S. Dhamrait. The findings are summarized below:

0.3% Steel:

- **Performance:** This steel content was inadequate for long-term performance. Sections with 0.3% steel experienced significant issues, including:
  - Excessive crack widths.
  - Pronounced spalling at transverse cracks.
  - Pumping at construction joints, leading to pavement distress.
- **Condition Over Time:** By 1967, the sections were nearing a "slightly rough" category according to roughness index readings.
- **Conclusion:** After 20 years, these sections were considered unlikely to provide satisfactory performance for much longer.

0.5% Steel:

- **Performance:** This section performed better than the 0.3% section but still showed some issues:
  - Isolated failures were observed, particularly in the 7-inch-thick pavement sections.
  - Construction joints exhibited signs of pumping and required patching.
- **Conclusion:** Although this steel content could be considered the minimum for acceptable performance, a higher percentage was recommended for better long-term results.

0.7% and 1.0% Steel:

- **Performance:** These sections demonstrated the best results:
  - Minimal spalling, even at construction joints.
  - Crack openings remained narrow over time, preserving structural integrity.
- **Maintenance:** Required little to no maintenance beyond routine joint and crack sealing.
- **Condition Over Time:** By 1967, these sections maintained "smooth" or "very smooth" ratings according to roughness index measurements.

The US 40 Vandalia test section provides valuable insights into the impact of longitudinal steel content on the performance of CRCP. The findings suggest that a steel content of 0.7% or higher is crucial for long-term performance, minimizing crack widths, spalling, and pumping. Additionally, the inclusion of a center joint and a subbase can further enhance the pavement's service life. Figure 6-4 shows the condition of the 1.0 % section in 2002, after 54 years of service. It is noted that crack spacing is quite small, smaller than the minimum value suggested by the AASHTO Guide; however, this section survived more than 50 years of harsh environmental conditions in Illinois. On the other hand, cracks in sections with lower steel amounts were rather large, as shown in Figure 6-5. The findings indicate that the optimum steel percentages are somewhere between 0.5 % and 1.0 % in Illinois.

Figure 6-4 Condition of the 1.0 % section in 2002 Route US40, West of Vandalia, Illinois

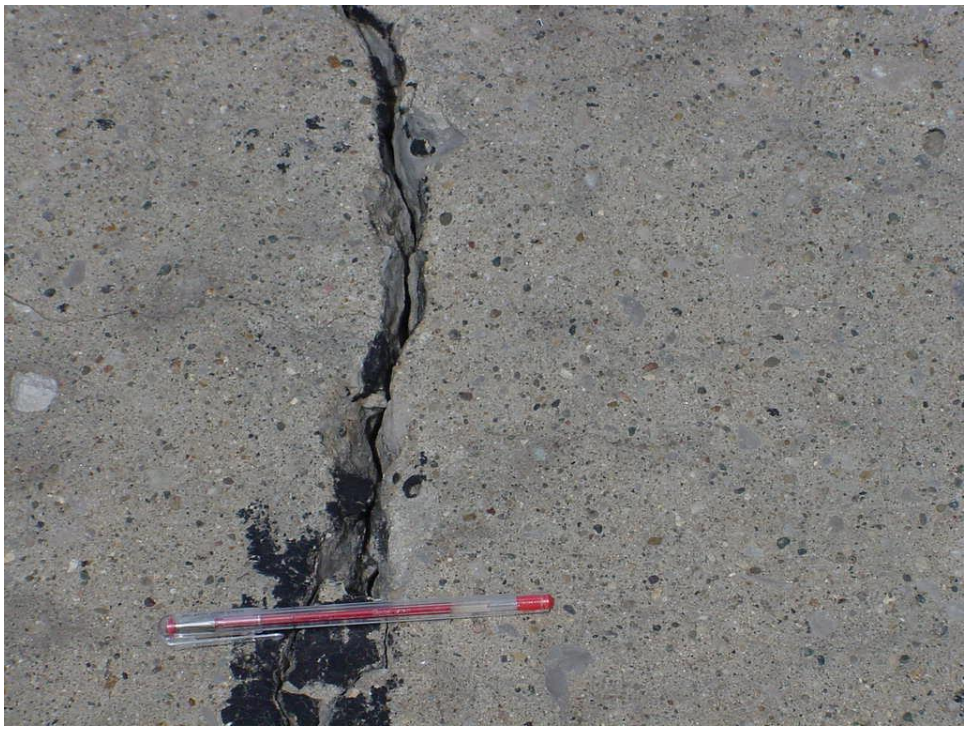

Figure 6-5 Condition of the lower steel section in 2002 Route US40, West of Vandalia, Illinois

6.4.2 Beltway 8 (BW 8) and IH45, Texas

TxDOT research 0-6274 titled *"Project Level Performance Database for Rigid Pavements in Texas, II"* presents the detailed performance evaluation of two experimental sections in Texas. Figure 6-6 shows the test layout for BW8 and IH45 sections, respectively. The main objective for both projects was to investigate the effect of varying steel percentages and aggregate types on the performance of CRCP.

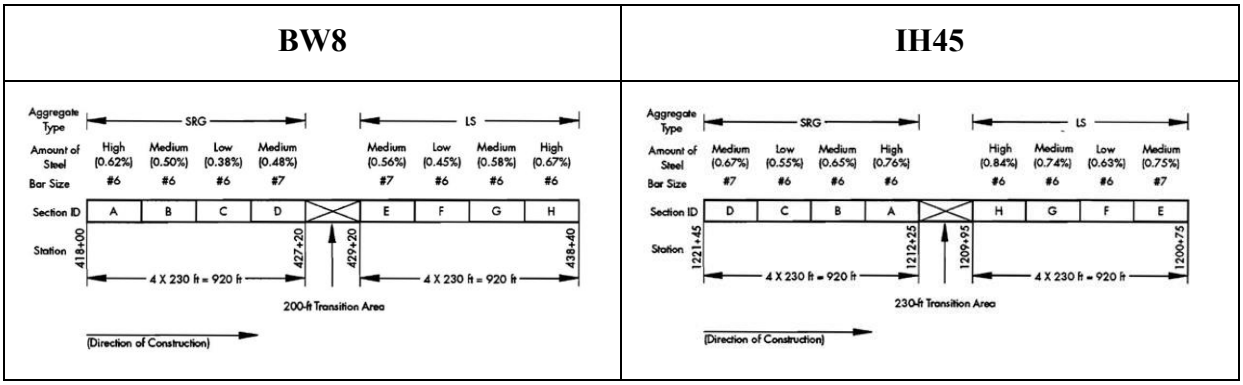

Figure 6-6 Layout of Test Sections for BW8 and IH45

The BW 8 section, built with a 10-inch slab thickness, featured steel percentages ranging from 0.38% to 0.67% and utilized single-layer longitudinal reinforcement with #6 and #7 bars. It was constructed on November 24-25, 1989, at the frontage road of beltway 8 eastbound, near Antoine Road. It consisted of two sets of coarse aggregate types: Siliceous River Gravel (SRG) and Limestone (LS). At the writing of this report, this pavement is 35 years old.

As shown in Figure 6-7a, the performance evaluation after 20 years revealed that the higher percentage of steel 0.67% with limestone aggregate recorded crack spacing of 6.2 ft whereas, lower percentage of steel 0.38% with SRG recorded crack spacing of 8.0 ft. The LS sections in BW 8 outperformed SRG sections, exhibiting no spalling and requiring no maintenance over the last 35 years. In contrast, as shown in Figure 6-7b, severe spalling occurred in SRG sections, although higher steel percentages mitigated these distresses by better restraining concrete movements at transverse cracks.

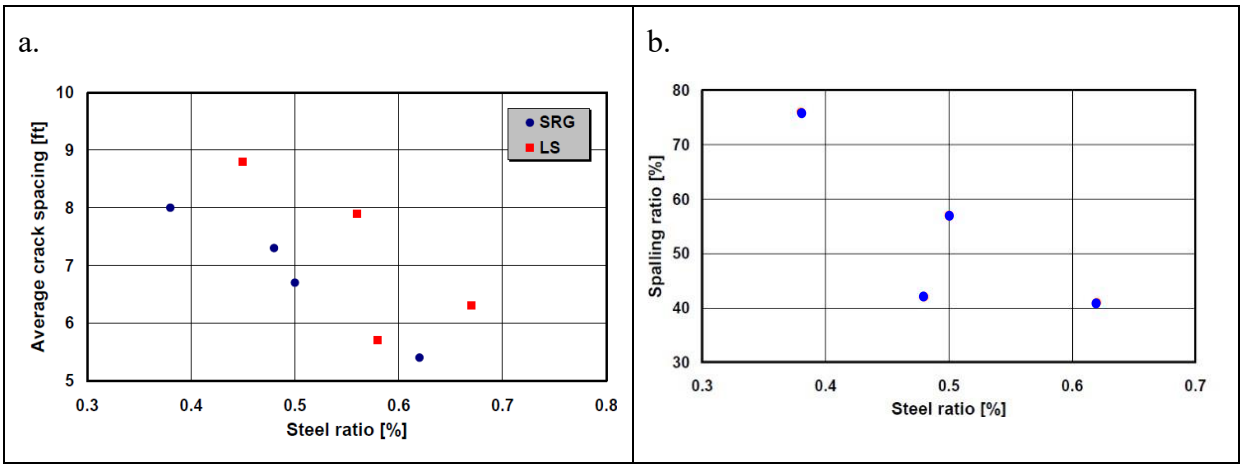

Figure 6-7a. Correlation between Crack Spacing and steel ratio for two different aggregate types and 7b. Relationship between Spalling (%) and Steel ratio (%) on BW8

Similarly, IH45 section, built with a 15-inch slab thickness, featured steel percentages ranging from 0.45% to 0.75% and utilized double-layer longitudinal reinforcement with #6 and #7 bars. It was constructed on January 14-21, 1990, at the main lanes of IH 45 northbound, just north of Spring Creek. It consisted of two sets of coarse aggregate types: SRG and LS.

As shown in Figure 6-8a, the performance evaluation revealed that the higher percentage of steel 0.84% with limestone aggregate recorded crack spacing of 4 ft whereas, lower percentage of steel 0.55% with SRG recorded crack spacing of 4.6 ft. However, the impact of steel percentage on spalling was less pronounced compared to BW 8. As shown in Figure 6-8b, the thicker slab and double-layer reinforcement in IH 45 likely played a dominant role in reducing spalling and maintaining structural performance. LS sections in IH 45 remained spalling-free, whereas SRG sections experienced spalling after 14 years of service, which required repairs with flex-patch materials.

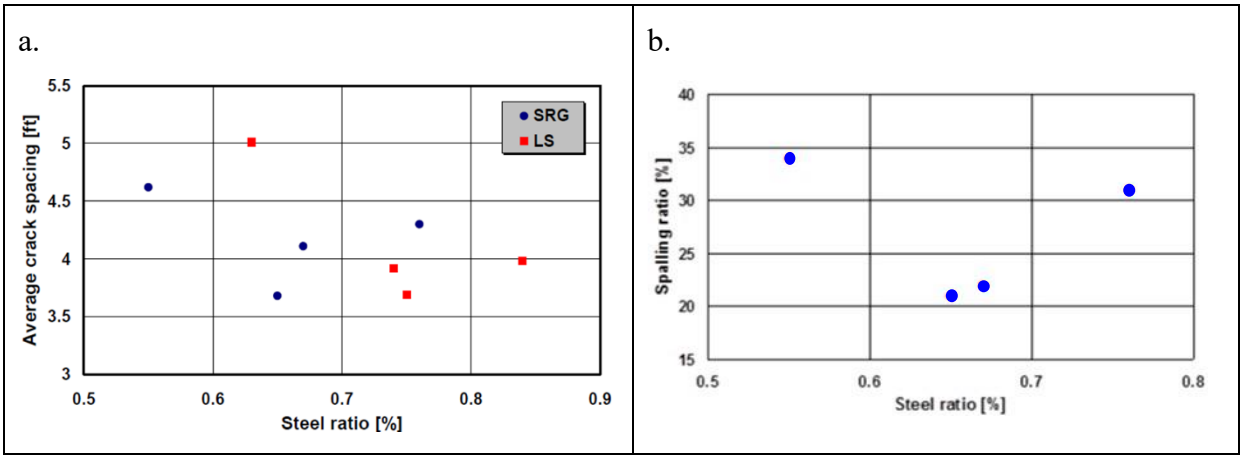

Figure 6-8a. Correlation between Crack Spacing and steel ratio for two different aggregate type and b. Relationship between Spalling (%) and Steel ratio (%) on IH45

Overall, sections with higher steel percentages consistently outperformed those with lower percentages in both test sites. They exhibited better crack control, reduced spalling, and enhanced long-term performance, especially in LS sections under heavy traffic. Annual average daily traffic (AADT) on IH 45 section was about 200,000 in 2023. These findings emphasize the importance of selecting adequate steel percentages and coarse aggregate types to ensure long-term performance and minimize maintenance needs in CRCP pavements. However, the interpretation of IH 45 section data is somewhat complicated due to the use of 2-mat steel. Currently, a research study is underway to further analyze CRCP behavior affected by 2-mat steel.

Even though the selection of the optimum steel percentages poses a challenge, most agencies in the US use a value between 0.5 % and 0.8 %. Table 6-7 provides a summary of steel percentage requirements for different states along with pavement thickness and their performance overview.

Table 6-7 List of state with their respective requirements for Steel percentage

State	Steel Percentage	Pavement Thickness	Performance Overview
California	0.5% - 0.7%	8 to 12 inches	Early sections performed well; modern CRCP is used for heavy truck traffic with minimal maintenance. Effective designs have adopted CRCP for overlays.
Georgia	0.70%	11 to 12 inches	CRCP is used on high-traffic highways with minimal maintenance. Some overlays on jointed pavements have performed satisfactorily.
Illinois	0.6% - 0.8%	7 to 14 inches	Extended life CRCP with 30–40-year designs have been successful. CRCP outperformed jointed concrete pavement in longevity and traffic capacity.
Indiana	0.7% - 1.0%	8 to 12 inches	Early sections in the 1930s were experimental. Modern designs with 0.7% steel have resumed after a hiatus, focusing on high-traffic routes.
Louisiana	0.6% - 0.8%	8 to 14 inches	Mixed performance due to subgrade issues; modern designs focus on improved

			construction techniques and thicker CRCP for longevity.
North Dakota	0.6% - 0.7%	8 to 12 inches	CRCP preferred for its low maintenance costs. Used successfully over expansive soils with granular bases.
Oklahoma	0.70%	8 to 12 inches	CRCP is the standard for interstates. Long-lasting sections with rehabilitation required for only 25% of pavements after decades.
Oregon	0.6% - 0.7%	8 to 11 inches	Long lifespan with minimal maintenance. Modern CRCP incorporates widened slabs for truck lanes and overlays.
South Dakota	0.66% - 0.69%	8 to 12 inches	Issues like Y-cracking and early spalling addressed with improved aggregate size and steel limits. High reliability over expansive soils.
Texas	0.5% - 0.7%	6 to 13 inches	Largest inventory of CRCP in the U.S. Very low punchout rates and long-lasting performance with research-driven enhancements.
Virginia	0.6% - 0.7%	8 to 13 inches	Significant improvements in recent designs. Earlier issues resolved with stricter construction standards. Smooth and durable with minimal maintenance.

Based on the general practice in the US, we can infer steel percentage between 0.6%-0.7% as an ideal pick for CRCP. However, CRCP whitetopping at intersections presents unique challenges that warrant careful consideration. As previously discussed, the shorter slab lengths typical of intersections result in less restraint on concrete volume changes and, consequently, reduce concrete stresses. This observation might suggest that reducing steel percentages could be a cost-effective option for agencies. Yet, while this intuition may appear promising, it comes with some levels of risks.

Evidence from earlier studies, including the pivotal 1991 research, highlights those factors such as environmental conditions during and immediately after construction, as well as concrete properties, play an important role in CRCP performance. Reducing steel percentages too much could compromise the performance of CRCP whitetopping, potentially leading to

premature failures. The repercussions of such failures costly repairs, commuter disruptions, and negative publicity for agencies like TxDOT underscore the importance of making technically sound decisions in this regard.

This brings us to the central question: *Does lowering steel percentages provide significant cost savings for the agency, and if so, are these savings worth the potential risks?* Beyond cost, there are other considerations that merit attention:

1. **Aesthetic and Functional Design:** Regardless of whether we choose to lower the steel percentage or not, could incorporating design elements such as saw cuts enhance the ride quality and aesthetic appeal of intersections for commuters, particularly in stop-and-go traffic conditions? Saw cuts have been shown to improve functionality and appearance by providing a uniform cracking pattern.
2. **Cost-Benefit Analysis of Saw Cuts:** *What would be the additional costs of implementing saw-cuts?* and *would these additional costs be justified by the potential benefits, such as mitigating random cracking?*

These critical questions surrounding cost savings, functionality, and reliability of CRCP whitetopping at intersections form the basis of the next section.

6.5 Cost vs. Reliability Trade-offs

This section presents comparative analysis of design alternatives, examining the trade-offs between steel percentages, and the associated reliability of CRCP system. The findings aim to provide a balanced perspective, enabling agencies to make decisions that align with both fiscal responsibility and long-term pavement performance.

6.5.1 Cost Estimation for a CRCP Whitetopping Intersection

To explore the cost implications of varying steel percentages, we use a hypothetical case study based on an intersection in Whitewright, Texas. It is important to note that several assumptions have been made for this analysis, and while there may be deviations from general practice, the objective is to evaluate the potential impact of altering steel percentages on overall costs and reliability.

Figure 6-9 shows the project layout in Whitewright, Texas. As shown in the figure, the intersection connects three projects with different control sections (CS): CS 0410-02 (US 69 to the north and SH 160 to the south), CS 0202-13 (US 69 to the east), and CS 0510-02 (SH 11 to the west).

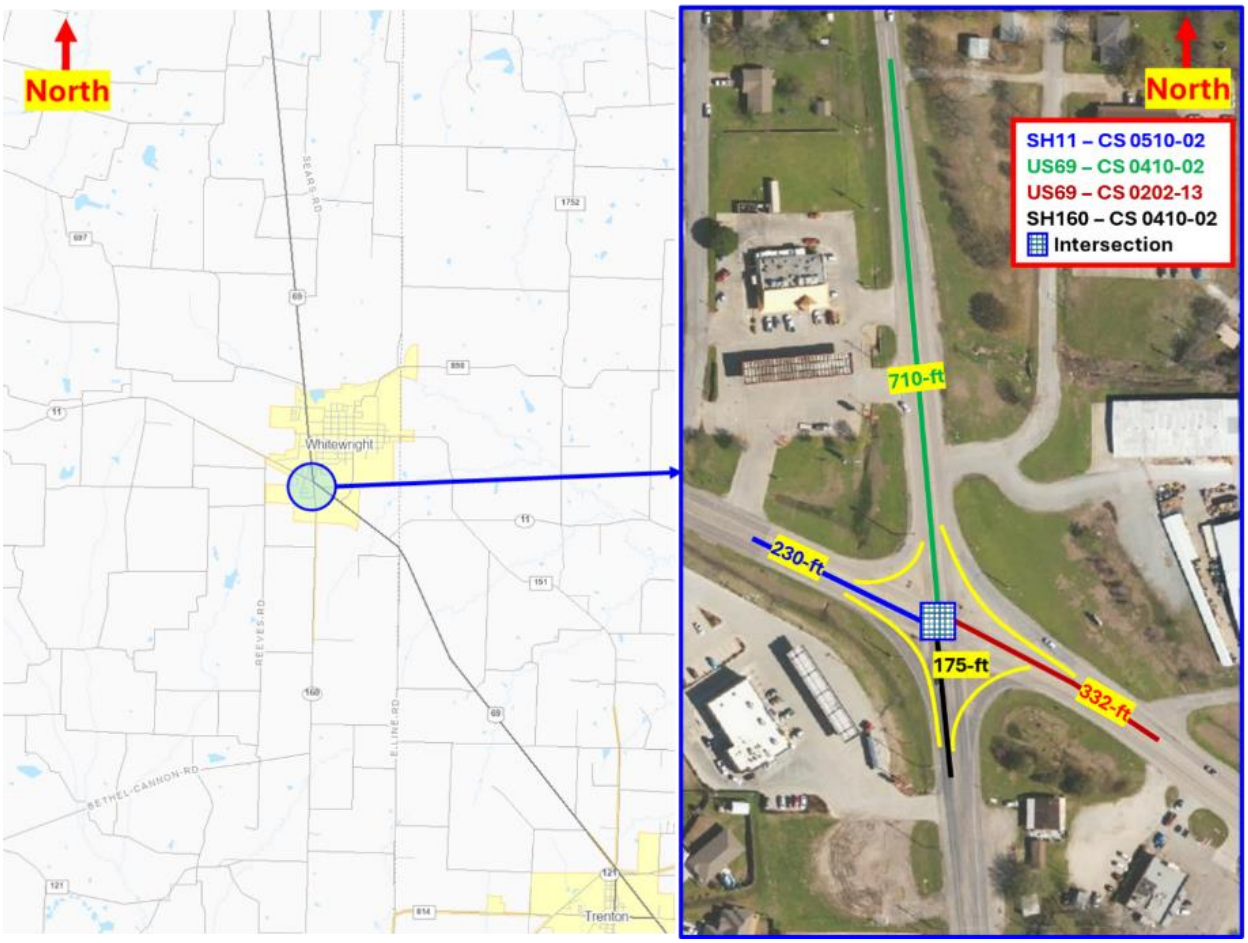

Figure 6-9 Map showing location of Intersection located in Whitewright, Texas

Figure 6-10 shows the proposed area for the CRCP Whitetopping with a total area of 7159 SY and proposed thickness of 8-inches for the design traffic of 11.19 million ESALs for 20years.

Figure 6-10 Proposed area for CRCP Whitetopping at Whitewright Intersection, Texas

The estimated costs for constructing the CRCP Whitetopping intersection are shown in Table 6-8, based on TxDOT's average low bid unit prices. Notably, items such as steel reinforcement and saw-cutting are included within Item 530-6001 (Intersections - Concrete). This bundling simplifies cost reporting but complicates a detailed analysis of individual contributions such as steel percentages.

Table 6-8 Typical Cost breakdown for CRCP Whitetopping Intersection

ESTIMATE SUMMARY						Remarks
Item No.	**Description**	**Unit**	**Total**		**Amount**	
			Qty.	**Cost**		
100	Prep ROW	STA	4			
110	Excavation (Roadway)	CY	333	$ 31.29	$ 10,419.57	Considered for general work
168	Vegetative Watering	MG	5	$ 206.24	$ 1,031.20	
275 6001	Cement	TON	50	$ 261.35	$ 13,067.50	
275	Cement treated (Existing Material)	SY	1800	$ 5.00	$ 9,000.00	
529	Concrete curb and gutter	LF	1864	$ 45.00	$ 83,880.00	
530 6001	Intersections(concrete)	SY	7159	$ 102.89	$ 736,589.51	Price includes Reinforcement labor and cost
531	Concrete Sidewalk	SY	200	$ 130.00	$ 26,000.00	
531	Concrete Sidewalk (Wheelchair Ramp)	EA	4	$ 3,500.00	$ 14,000.00	
624	Ground Boxes	EA	2	$ 2,000.00	$ 4,000.00	
644	Small Roadside Sign Assemblies	EA	4	$ 1,000.00	$ 4,000.00	
662	Work Zone Pavement Markings Removal	LF	500	$ 1.00	$ 500.00	
666	Retro reflectorized Pavement Markings TY I	LF	1200	$ 2.00	$ 2,400.00	
672	Raised Pavement Markers	EA	50	$ 10.00	$ 500.00	
677	Eliminating Existing Pavement Markings and Markers	LF	500	$ 5.00	$ 2,500.00	
688	Pedestrian Detectors and Vehicle Loop Detectors	LF	120	$ 20.00	$ 2,400.00	

500	Mobilization	LS	1	$ 87,676.95	$ 87,676.95	Contingency costs (10%)
502	Barricades, sign, and Traffic Handling	LS	1	$ 87,676.95	$ 87,676.95	Contingency costs (10%)
Total Cost	Before Contingency	$876,769.51				
	After Contingency	$1,052,123.41				

6.5.2 Analysis of Varying Steel Percentages

To evaluate the impact of steel percentages on project cost, we calculated the material cost for different reinforcement levels, assuming that all the other costs such as mobilization, labor, traffic control, and other prep work will remain the same. The unit cost for the steel and concrete unit weight selected for the analysis are as follows:

- Steel Price: $1,500/ton for #6 bars. (current average price in the market)
- Concrete Weight: 150 lb./ft³.

Steps for calculation

Concrete Volume and Weight:

- Area of the slab = 7159 SY = 7159 x 9 ft^2 = 64,431 ft^2
- Thickness of the slab = 8-inches = 0.667-ft
- Volume = 64,431 x 0.667 = 42,954 ft^3
  - Total concrete weight = 42,954 × 150 = 6,443,100 lb.

The material costs of steel at varying steel percentages are shown in Table 6-9.

Table 6-9 Weight and cost of steel at varying steel percentages

Concrete weight (lb.)	Steel Percentage	Steel Weight (lb.)	Steel Weight (tons)	Cost of steel (per ton)	Total Cost of Steel
6443100	0.30%	19329	10	$1,500	$15,000
	0.40%	25772	13		$19,500
	0.50%	32216	16		$24,000
	0.60%	38659	19		$28,500
	0.70%	45102	23		$34,500

	0.80%	51545	26		$39,000
	0.90%	57988	29		$43,500

The results indicate that variations in steel percentages contribute marginally to overall project costs. For example, Figure 6-11 shows increasing steel content from 0.3% to 0.7% results in an additional cost of only **$19,500** for the entire project. This emphasizes that reducing steel percentages yields only marginal cost savings while potentially compromising pavement performance.

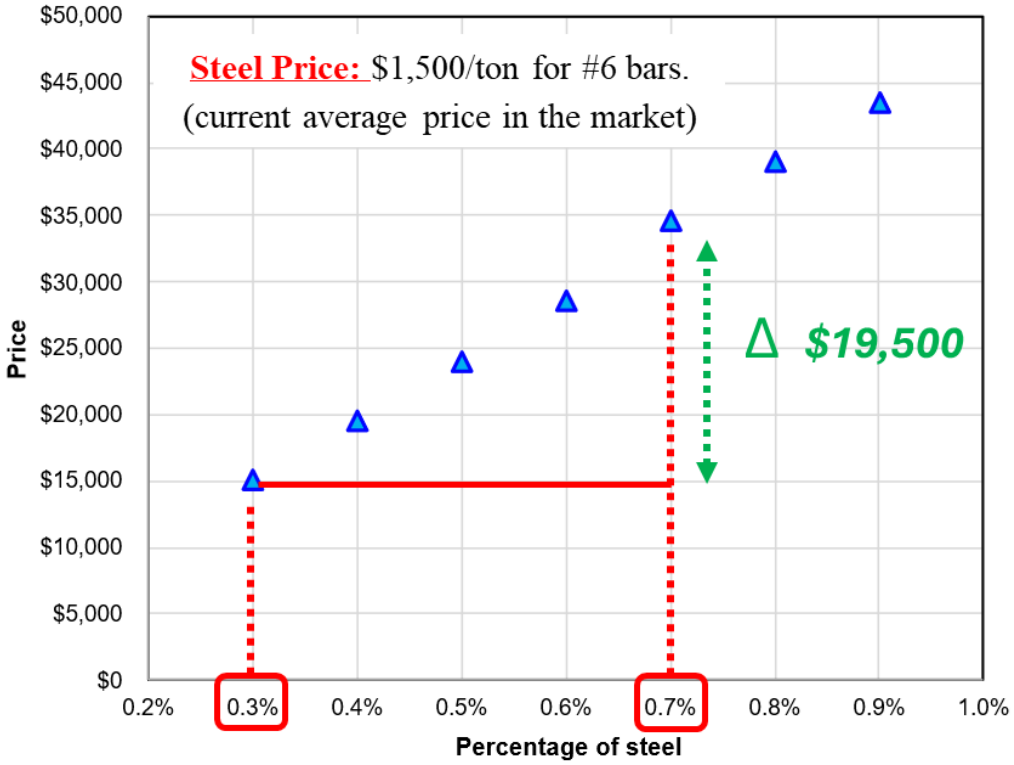

Figure 6-11 Marginal Increase in the price

6.5.3 Saw-Cutting in CRCP Whitetopping

In general, saw-cutting is not incorporated in CRCP construction, except at longitudinal warping joints. However, other counties such as Belgium implemented saw-cutting in their CRCP in the form of active crack control. Also, in Texas, early-entry saw-cuts were made on US 290 in Hempstead and Cypress in the Houston District in the early 1990s to investigate its viability to control spalling in CRCP with SRG as coarse aggregate. It was a one-inch-deep saw-cut made within a few hours of concrete placement. Overall, its performance has been quite good, with no severe spalling occurring. It appears that early-age cracks occurred along the saw-cuts, relieving concrete stress in other areas thereby reducing the spalling potential. For this analysis:

- **Saw-Cutting Specifications:** Cuts will be shallow (1.5 inches deep), dividing the area into 6x6-foot sections.
- **Linear Feet of Cuts:** The total area of 64,431 ft^2, divided into 6x6-foot sections, results in 1,789 sections. Each section requires cuts along with its length and width, with interior cuts shared among adjacent sections. The total saw-cut length is approximately 15,000 linear feet.
- **Cost Estimate:** At an estimated cost of $0.60 per linear foot, the total saw-cutting expense is $9,000. Adding a 10% contingency, the cost rises to $10,000.

The estimated cost of saw-cutting for the intersection, including a contingency, is approximately $10,000. This expense is negligible compared to the total project cost of over $1,052,000. The benefits of saw cuts, such as mitigating random cracking and enhancing pavement aesthetic, are considered to outweigh this small additional cost.

While reducing steel percentages may seem appealing for cost savings, it poses some unknown risks. Based on evidence presented and the cost analysis in this chapter, we recommend adhering to TxDOT's existing CRCP reinforcement requirement. These designs have consistently delivered reliable performance, as demonstrated by CRCP's excellent performance in Texas. Attempting to reduce steel percentages for marginal cost savings is not justified when weighed against the potential risks to long-term pavement performance and reliability.

6.6 Summary

In summary, there are challenges and opportunities associated with reinforcement design of CRCP whitetopping at intersections. The findings are as follows:

- CRCP whitetopping at intersections operates under unique conditions, including shorter slab lengths and varying restraint forces that are different from regular CRCPs. These conditions suggest the possibility of reducing steel reinforcement percentages. However, based on evidence from field studies and cost analyses, reducing steel percentages below 0.6%-0.7% risks compromising pavement performance and long-term reliability.
- In the case of intersection box, it is recommended to use the low-COTE steel design.
- Marginal cost savings from lower steel content are outweighed by the potential risks of lower reliability of the pavement system and potential increased maintenance cost.
- Saw-cutting has emerged as a practical and cost-effective strategy for enhancing the aesthetic and functional design of CRCP intersections. By promoting a uniform cracking pattern, saw cuts mitigate random cracking, reduce maintenance requirements, and improve aesthetics of pavement surface for commuters at stop-and-go traffic conditions. Thus, it is strongly recommended.

Based on the above findings, it is recommended that the current reinforcement design in TxDOT CRCP Design Standards be utilized for CRCP whitetopping intersections. However, it

is recommended to introduce and develop new whitetopping standard for thinner section steel layouts which are not currently included in the existing CRCP standard.

CHAPTER 7
CONCLUSION AND RECOMMENDATIONS

7.1 Need for a New Approach

Despite the investment of billions of dollars, American roads face an unprecedented and ever-growing maintenance backlog. This compounding issue creates a dire situation where agencies struggle to keep pace with deteriorating infrastructure. The Texas Department of Transportation (TxDOT) currently dedicates a substantial portion of its budget, approximately 45 cents of every dollar, to maintenance and replacement, a figure that is projected to rise. While asphalt overlays are a common rehabilitation strategy, they are often insufficient for addressing underlying structural issues, highlighting the need for more robust, long-term solutions like concrete overlays.

However, for a concrete overlay strategy to be sustainable, its design methodology must ensure that the fix is not just temporary but durable and reliable for years to come. This research identified a critical void in current TxDOT practice. The existing design methods for whitetopping and unbonded overlays are referenced from national guides like the ACPA method and AASHTO 93, which, as this report has detailed, suffer from significant limitations and rudimentary assumptions. Furthermore, a formal design procedure for CRCP whitetopping and unbonded CRCP overlays does not currently exist within TxDOT, leaving a significant gap in the engineer's toolkit.

7.2 A Critical Review of the State of Pavement Design

To address this gap, this research first looked to the past to learn from foundational principles. The AASHO Road Test, a watershed moment in pavement engineering, provided three timeless lessons: (1) preventing pumping is key to preventing distress, (2) good slab support leads to better performance, and (3) a pavement's deflection profile is a powerful predictor of its future performance.

Unfortunately, these critical lessons have been diluted over time. The AASHTO 1993 design guide, for instance, diminished the importance of slab support while introducing abstract concepts like reliability factors and coefficients for joints and drainage that obscured the physical realities of pavement behavior. Modern tools like the AASHTOWare Pavement ME Design (MEPDG) have introduced another layer of complexity, relying on sophisticated computational models whose assumptions often conflict with real-world field data. The entire Mechanistic-Empirical framework hinges on "transfer functions" to predict pavement life; yet these functions have been shown to be poorly calibrated and unreliable—the system's "Achilles' heel."

This review confirmed that modern design has largely abandoned deflection as a key design criterion, despite its proven reliability. The result is a significant divergence between idealized design models and the practical realities of construction and field performance, reinforcing the need for a new methodology rooted in measurable, evidence-based principles.

7.3 Summary of Research Findings

This research project sought to fill the identified voids by developing a new, deflection-based design methodology. The key findings and contributions from each phase of the work are summarized below.

7.3.1 Findings from the Nationwide Survey

A nationwide survey of transportation agencies revealed a field characterized by inconsistency and a reliance on traditional methods. Key findings include:

- There is a significant lack of uniform, nationwide definitions for common overlay types, making it difficult to compare design methods and performance data.
- CRCP and TWT overlays are not widely used, with deep knowledge concentrated among a small number of veteran professionals, indicating a potential industry-wide knowledge gap.
- Agencies overwhelmingly rely on traditional evaluation methods: visual inspection, Falling Weight Deflectometer (FWD) for stiffness, and physical coring for layer analysis. Advanced tools like GPR see limited use in routine decision-making.

Overall, there is a clear demand for more standardized design frameworks and more comprehensive performance data to create reliable, data-driven overlay designs.

7.3.2 A New Framework for Pavement Evaluation

To ensure the proposed design method is built on a solid foundation, a comprehensive framework for evaluating existing pavement conditions was developed.

- This framework provides a structured, objective process for selecting candidate projects based on PMIS score trends and other engineering criteria.
- It outlines a logical workflow where visual surveys identify problem areas, coring verifies layer structure, and the FWD assesses the structural response, ensuring a complete picture of the pavement's condition.
- Critically, the framework mandates the identification of the root causes of distress, ensuring that pre-overlay repairs are effective and preventing the premature failure of the new overlay.
- The entire evaluation process is specifically designed to gather the critical deflection and stiffness data required as direct inputs for the new design method.

7.3.3 The Deflection-Based Design Methodology

The core contribution of this research is a new, deflection-based design method for CRCP overlays, built upon the following key discoveries:

- A "Signature Deflection" for New Pavements:
    - Extensive field testing established a "Statewide Deflection Curve," which demonstrates that a new, structurally sound CRCP of a given thickness has a predictable and repeatable deflection. This curve serves as a powerful diagnostic

benchmark to determine the "structurally equivalent" thickness of an existing pavement.

- Validation of the Core Design Principle:
    - Mechanistic modeling confirmed that different pavement structures will have comparable long-term performance if they are designed to have the same surface deflection, validating deflection as a universal design target.
- Quantification of the Base-to-Overlay Relationship:
    - Through rigorous field testing, the direct correlation between the deflection of a base layer before paving and the final deflection of the new CRCP overlay after paving was established. This testing also confirmed that stiffer bases lead to significantly lower deflections and that thinner CRCP slabs are far more sensitive to subgrade conditions than thicker slabs.
- Development of a Robust, Calibrated Model:
    - An advanced ANSYS computer model using dynamic analysis was essential for simulating FWD loading accurately and expanding upon the field data. This calibrated model generated the comprehensive set of correlation curves that form the engine of the new design method.
- Creation of Practical, User-Friendly Design Tools:
    - The research culminated in two tools to make the methodology accessible:
        - A Design Nomograph: A graphical chart that allows engineers to visually and systematically determine the required overlay thickness.
        - A Python-Based Design Program: A standalone software tool that automates the entire design process, providing instant solutions from user inputs.

7.4 Recommendations for Practice

Based on the comprehensive findings of this research, the following recommendations are made for TxDOT and the broader pavement engineering community:

- Adopt the Proposed Deflection-Based Design Methodology:
    - This research has demonstrated that the deflection-based method is a rational, evidence-based, and practical approach for designing CRCP overlays. Its adoption would provide a standardized and reliable procedure where one currently does not exist.
- Maintain Adequate Steel Reinforcement in Intersections:
    - While the unique conditions at intersections might suggest that steel percentages in CRCP could be reduced, this research concludes that the marginal cost savings are outweighed by the significant risk to long-term performance and reliability. It is recommended that steel percentages not be reduced below the 0.6%–0.7% range. In the case of intersection box, it is recommended to use the low-COTE steel design.

- Implement Saw-Cutting at CRCP Intersections:
    - Saw-cutting has emerged as a practical and cost-effective strategy for controlling the cracking pattern at CRCP intersections. This practice mitigates random cracking, which improves aesthetics and reduces future maintenance needs. Its implementation is strongly recommended for all new CRCP intersection projects.

7.5 Final Conclusion

This research was initiated to address a critical gap in pavement rehabilitation strategy at a time when maintenance demands are at an all-time high. By returning to the foundational principles of pavement engineering and leveraging evidence-based approach, this project has developed a complete, data-driven methodology for designing CRCP overlays. From the nationwide survey that contextualized the problem to the development of a user-friendly design program, this work provides a tangible path forward. The adoption of this deflection-based approach offers TxDOT a more rational and sustainable way to engineer concrete overlays, ensuring that future investments in our roadway infrastructure are both durable and cost-effective.

BIBLIOGRPAHY

AASHO. (1962). *The AASHO Road Test* (Issue 1061, p. 438). National Academy of Sciences-National Research Council.

American Concrete Institute (ACI). (2002). *Guide for design of jointed concrete pavements for streets and local roads* (ACI 325.12R-02). American Concrete Institute

American Concrete Institute (ACI). (2006). *Design of slabs-on-ground (ACI 360R-06)*. American Concrete Institute.

Anastasios M. Ioannides, & Tingle, J. S. (2024). Secrets of Plate Load Test.pdf. *Secrets of the Plate Load Test (1941-1955)*. 13th International Conference on Concrete Pavements.

Al-Qadi, I. L., H. Wang, P. J. Yoo, and S. H. Dessouky. 2008. "Dynamic analysis and in situ validation of perpetual pavement response to vehicular loading." Transp. Res. Rec. 2087 (1): 29 39. https://doi.org/10.3141/2087-04.

Arimilli, S., M. N. Nagabhushana, and P. K. Jain. 2018. "Comparative mechanistic-empirical analysis for the design of alternative cold recycled asphalt technologies with the conventional pavement." Road Mater. Pavement Des. 19 (7): 1595–1616. https://doi.org/10.1080/14680629.2017.1338187.

American Concrete Institute (ACI). (2014). *Building code requirements for structural concrete and commentary* (ACI 318-14). American Concrete Institute

Bellis, R., Osborne, B., & Davis, S. L. (2019, May). *Repair Priorities—2019*. Tranportation for America & Taxpayers for Common Sense. https://t4america.org/wp-content/uploads/2019/05/Repair-Priorities-2019.pdf

Burnham, T. (2005). *Forensic Investigation Report For MnROAD Ultrathin Whitetopping Test Cells 93, 94 and 95* (p. 115). Minnesota Department of Transportation. http://www.lrrb.org/PDF/2005-45

Burke, J. E., & Dhamrait, J. S. (1967). *A twenty-year report on the Illinois continuously reinforced pavement*. Illinois Division of Highways.

Bradbury, R. D. (1932). Proper use of reinforcing steel in concrete pavements. *Wire Reinforcement Institute.*

Choi, P., Ryu, S., Zhou, W., Saraf, S., Yeon, J., Ha, S., & Won, M. (2014). *Project level performance database for rigid pavements in Texas, II* (Research Report No. 0-6274-2). Texas Tech University, Center for Multidisciplinary Research in Transportation.

DM, B. (1945). The general theory of stresses and displacements in layered soil systems. III. J Appl Phys, 16, 126-127.

Elbagalati, O., Elseifi, M., Gaspard, K., & Zhang, Z. (2018). Development of the pavement structural health index based on falling weight deflectometer testing. International Journal of Pavement Engineering, 19(1), 1-8.

Federal Highway Administration (FHWA). (2021). *Tech brief: Continuously reinforced concrete (CRC) roundabouts*. FHWA-HIF-20-081.

Ferrebee, E. (2001). *Design and construction of concrete roundabouts*. American Concrete Pavement Association (ACPA)

Federal Highway Administration. (2016). *Guide to continuously reinforced concrete pavements: From design to performance*. Washington, DC: Federal Highway Administration.

M.N.S. Hadi, B.C. Bodhinayake, Non-linear finite element analysis of flexible pavements, Adv. Eng. Softw. 34 (2003) 657–662, https://doi.org/10.1016/S0965-9978(03)00109-1.

National Ready Mixed Concrete Association (NRMCA). (2015). *Concrete pavement intersections: Design considerations and benefits*. NRMCA.

Hamim, A., N. I. M. Yusoff, H. Ceylan, S. A. P. Rosyidi, and A. El-Shafie. 2018. "Comparative study on using static and dynamic finite element models to develop FWD measurement on flexible pavement structures." Constr. Build. Mater. 176 (Jul): 583–592. https://doi.org/10.1016/j.conbuildmat.2018.05.082.

Hu, X., A. N. Faruk, J. Zhang, M. I. Souliman, and L. F. Walubita. 2017."Effects of tire inclination (turning traffic) and dynamic loading on the pavement stress–strain responses using 3-D finite element modeling." Int. J. Pavement Res. Technol. 10 (4): 304–314. https://doi.org/10.1016/j.ijprt.2017.04.005.

Huang, Y. H. 2004. Pavement analysis and design. 2nd ed. Upper Saddle River, NJ: Prentice Hall.

Hudson, W. R. (1963). *Comparison of Concrete Pavement Load-Stresses at AASHO Road Test With Previous Work* (62–2; 42nd Annual Meeting of the Highway Research Board). https://library.ctr.utexas.edu/digitized/texasarchive/thdresearch/ny-62-2.pdf#:~:text=In%201926%20Dr,in%20slabs%20of%20uniform%20thickness

J.M. Duncan, C.L. Monismith, E.L. Wilson, Finite element analysis of pavements, Highw. Res. Rec. 228 (1968) 18–33.

Jaiswal, H., Ryu, S., Choi, P., Choi, S., Jayawickrama, P., Senadheera, S., Yeon, J., & Won, M. C. (2012). *Rational use of terminal anchorages in Portland cement concrete pavements*. Research Report No. 0-6326-1. Texas Tech University.

Innovative ways to reinforce slabs-on-ground: Formulas for success. *Wire Reinforcement Institute*.

Kim, M., & Tutumluer, E. (2006). "Modeling Nonlinear, Stress-Dependent Pavement Foundation Behavior Using a General-Purpose Finite Element Program." Geotechnical Special Publication, 154, 29-36.

Kim, M., E. Tutumluer, and J. Kwon. 2009. "Nonlinear pavement foundation modeling for three-dimensional finite-element analysis of flexible pavements." Int. J. Geomech. 9 (5): 195–208. https://doi.org/10.1061/(ASCE)1532-3641(2009)9:5(195).

L. Zhou, Q. Wu, J. Ling, Comparison of FWD and Benkelman Beam in evaluation of pavement structure capacity, Geotech. Spec. Publ. 203 (2010) 405–411, https://doi.org/10.1061/41104(377)51.

Lee, Y.-H., & Darter, M. I. (1994). Development of performance prediction models for Illinois continuously reinforced concrete pavements. *Transportation Research Record, 1505*, 75–86.

M. Li, H. Wang, G. Xu, P. Xie, Finite element modeling and parametric analysis of viscoelastic and nonlinear pavement responses under dynamic FWD loading, Constr. Build. Mater. 141 (2017) 23–25, https://doi.org/10.1016/j. conbuildmat.2017.02.096.

McGhee, K. H. (1994). *NCHRP - Synthesis of Highway Practice 204—Portand Cement Concrete Resurfacing* (NCHRP 204; p. 77). Transporation Research Board, National Research Council. https://onlinepubs.trb.org/Onlinepubs/nchrp/nchrp_syn_204.pdf

Melaku, S., and H. Qiu. 2015. "Finite element analysis of pavement design using ANSYS finite element code." In Proc., 2nd Int. Conf. on Civil Engineering, Energy and Environment, 64–69. Hubei, China: Wuhan Univ. of Technology.

McCullough, B. F., Ma, J. C. M., & Noble, C. S. (1979). *Limiting criteria for the design of CRCP*. Research Report No. FHWA/TX-79/177-17. Center for Highway Research, The University of Texas at Austin

Nullens, A. (2013). *Concrete roundabouts: Design and construction aspects*. EUPAVE.

Noble, C. S., McCullough, B. F., & Ma, J. C. M. (1976). Nomographs for the design of steel reinforcement in continuously reinforced concrete pavement. *Transportation Research Record*, (756).

National Research Council, Transportation Research Board, Committee on Rigid Pavement Design. (1977). *Design of terminals for rigid pavements to control end movements: State of the art*. Special Report 173. National Academy of Sciences

R.A. Tarefder, M.U. Ahmed, Modeling of the FWD deflection basin to evaluate airport pavements, Int. J. Geomech. 14 (2014) 205–213, https://doi.org/10.1061/(ASCE)GM.1943-5622.0000305.

Rosyidia, S. A. P., A. Hamimb, A. M. Taibb, N. A. A. Jamaludinc, Z. A. Memond, N. I. Md, and M. R. H. Yusoffb. 2020. "Determination of deflection basin using pavement modelling computer programs and finite element method." Jurnal Teknologi 82 (4): 55–63. https://doi.org/10.11113/jt.v82.14376

Shoukry, S. N., Martinelli, D. R., & Selezneva, O. I. (1996, November). Dynamic considerations in pavement layers moduli evaluation using falling weight deflectometer. In Nondestructive Evaluation of Bridges and Highways (Vol. 2946, pp. 109-120). SPIE.

Stolle, D. F. E. (1991). Modelling of dynamic response of pavements to impact loading. Computers and Geotechnics, 11(1), 83-94.

Shelby, M. D., & McCullough, B. F. (1960). Experience in Texas with continuously-reinforced concrete pavement. *Highway Research Board Bulletin 274*. National Academy of Sciences - National Research Council.

Tayabji, S., & Plei, M. (2019). *Optimized design details for continuously reinforced concrete pavements*. FHWA-HIF-19-066. Federal Highway Administration

Uddin, W., & Garza, S. (2010). 3D-FE simulation study of structural response analysis for pavement-subgrade systems subjected to dynamic loads. In Pavements and materials: Testing and modeling in multiple length scales (pp. 170-181).

Uddin, W., Nanagiri, Y., & Garza, S. (2017). 3D-FE Modeling and dynamic response analysis of asphalt pavements subjected to FWD impact loads. In Bearing Capacity of Roads, Railways and Airfields (pp. 1317-1325). CRC Press.

Vetter, C. P. (1933). Stresses in reinforced concrete due to volume changes. *Transactions of the American Society of Civil Engineers, 98*(2), 1039–1053.

Woolley, W. R. (1960s). Design of continuously reinforced concrete pavement. *Highway Research Board Proceedings*. Truscon Steel Division, Republic Steel Corporation.

Won, M., Hankins, K., & McCullough, B. F. (1991). *Mechanistic analysis of continuously reinforced concrete pavements considering material characteristics, variability, and fatigue*. Center for Transportation Research, The University of Texas at Austin.

Wu, W., & McCullough, B. F. (1992). *Terminal movement in continuously reinforced concrete pavements*. Research Report No. FHWA/TX-92+1169-4. Center for Transportation Research, The University of Texas at Austin.

Zhou, W., Choi, P., Ryu, S., & Won, M. C. (2013). *Pilot Implementation of Whitetopping: Final Report*. Texas Department of Transportation. www.ntis.gov.

APPENDIX - A

Case Study - US 69 at SH 11 Intersection (Whitewright, Texas)

Project Background

The intersection investigated is located in Whitewright, Texas which falls in Grayson County of Paris District. As shown in Figure A-1, the intersection connects three control sections (CS): CS 0410-02 (US 69 to the north and SH 160 to the south), CS 0202-13 (US 69 to the east), and CS 0510-02 (SH 11 to the west). The primary objective of this case study is to evaluate the existing pavement conditions at the intersection (Figure A-2) and utilize the collected data to compare slab thickness designs from various existing concrete overlay design methods with a proposed design method. The investigation of the existing intersection was conducted using testing like Ground Penetrating Radar (GPR), Falling Weight Deflectometer (FWD), and Dynamic Cone Penetrometer (DCP) testing.

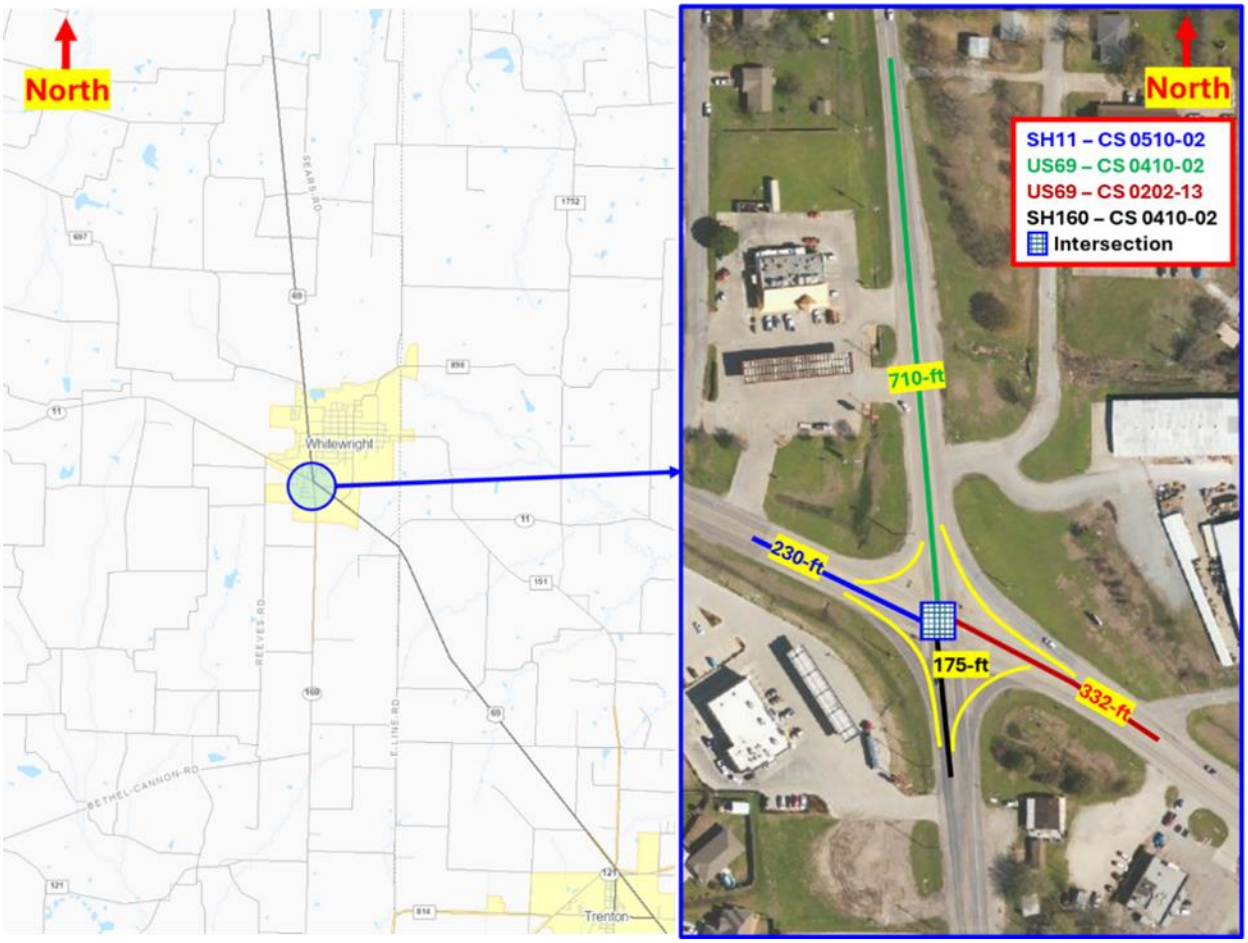

Figure A- 1 Map showing location of Intersection located in Whitewright, Texas

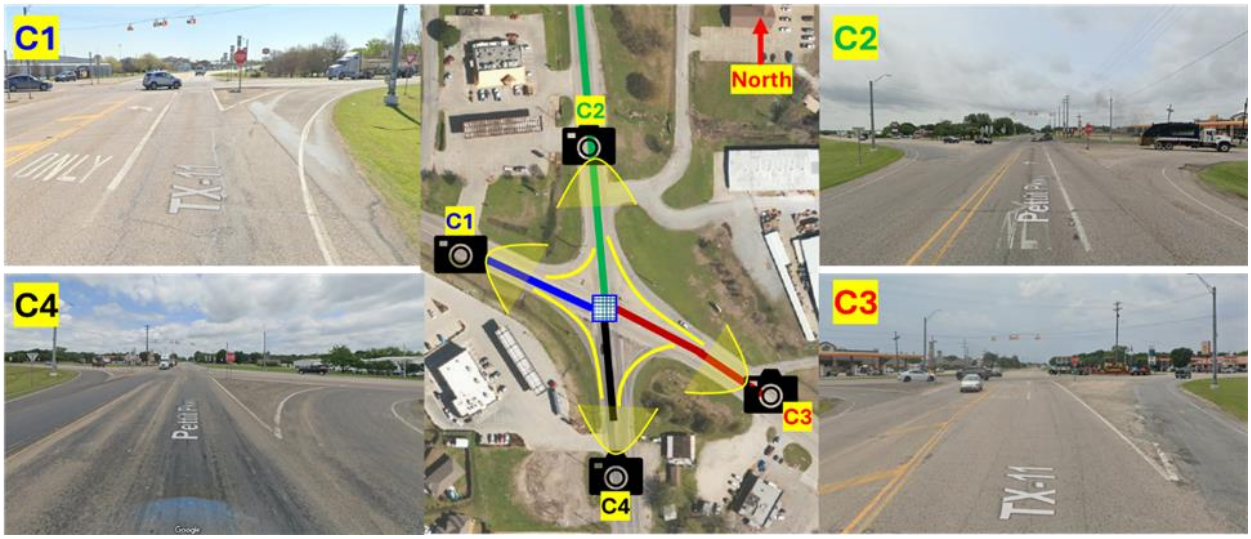

Figure A- 2 Existing Condition of Pavement under investigation

Traffic Data

The intersection located at Whitewright, Texas, serves as an illustrative example to demonstrate the calculation of cumulative design traffic in million ESALs. Figure A-3 highlights the traffic map with current Average Annual Daily Traffic (AADT) data for various directional flows at this intersection. When determining design traffic, it is prudent to adopt conservative values, selecting the highest recorded directional traffic for enhanced reliability in pavement design calculations.

The intersection includes the following directional traffic movements:

- US69 North to SH160 South
- SH160 South to US69 North
- SH11 West to US69 East
- US69 East to SH11 West

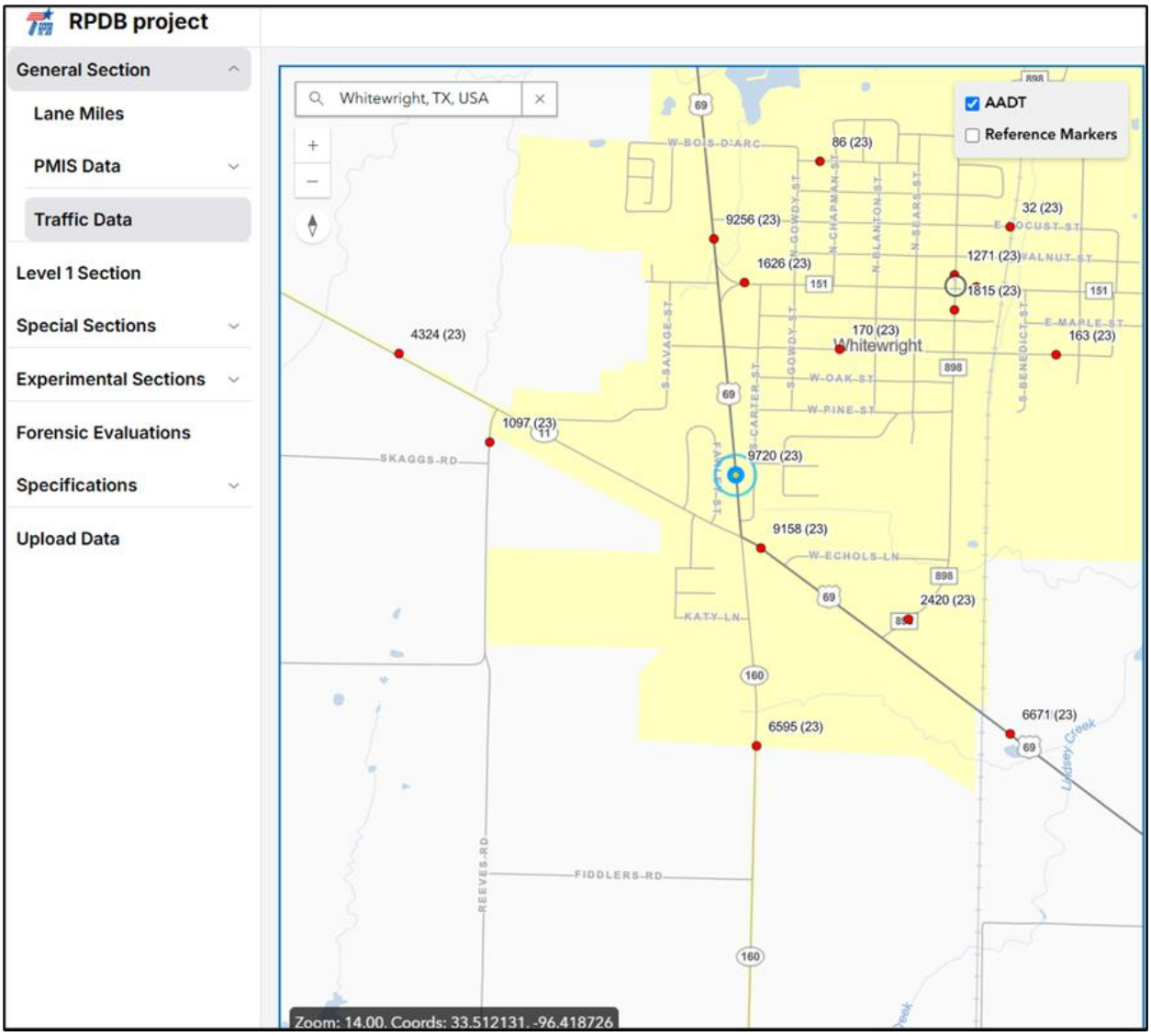

Figure A- 3 Traffic data at the Intersection

Based on recent traffic data (Figure A-3), Table A-1 presents directional AADT and selected values. The highest directional traffic volumes were selected to ensure conservative and robust pavement design:

Table A- 1 Traffic data calculation for each Direction

S.No.	Direction	AADT (2023)	Selected AADT	$AADT_1$	Total $AADT_1$	Truck Traffic	Selected Truck Traffic
1	US69 North to SH160 South	9720	9720	4860	9439	10.9%	13%

2	SH160 South to US69 North	6595					
3	SH11 West to US69 East	9158	9158	4579		13%	
4	US69 East to SH11 West	4324					

The final recommended design inputs based on the above analysis are:

- $AADT_1$ = 9439 vehicles/day (*combined conservative estimate*)
- T = 13% (*0.13 in decimal*)
- T_f = 1.2 (*typical for rural highways*)
    - *For rural highways, 1.2 is common. For urban interstates, 1.5–1.8 might be used.*
- P = 30 years
- G = 3% (*0.03 in decimal, assumed based on historical trends*)
- LF = 1 (as the intersection has only one lane per direction)

Using these inputs, the cumulative design traffic in million ESALs is calculated as follows:

$$\text{Cumulative Design Traffic (ESALs)} = \frac{9439\ X\ 0.13\ X\ 1.2\ X\ 1\ X \frac{(1+0.03)^{30}-1}{0.03} X 365}{1{,}000{,}000}$$

Plugging the values into the formula:

Cumulative Design Traffic (ESALs) = 25.59 million ESALs

This calculated cumulative design traffic (approximately 25.59 million ESALs) provides a robust and conservative basis for subsequent input design at the Whitewright intersection.

Field Testing

FWD Testing

The FWD test was conducted in all four directions, as well as on the ramp, as shown in Figure A-4. A total of 40 locations were investigated. Based on the FWD test results, points of interest included six locations which recorded higher and lower deflections. DCP testing was then conducted at these locations to calculate the subgrade modulus. Figure A-5 to Figure A-12

present all measured and calculated FWD testing data for each drop in every direction, including the ramp.

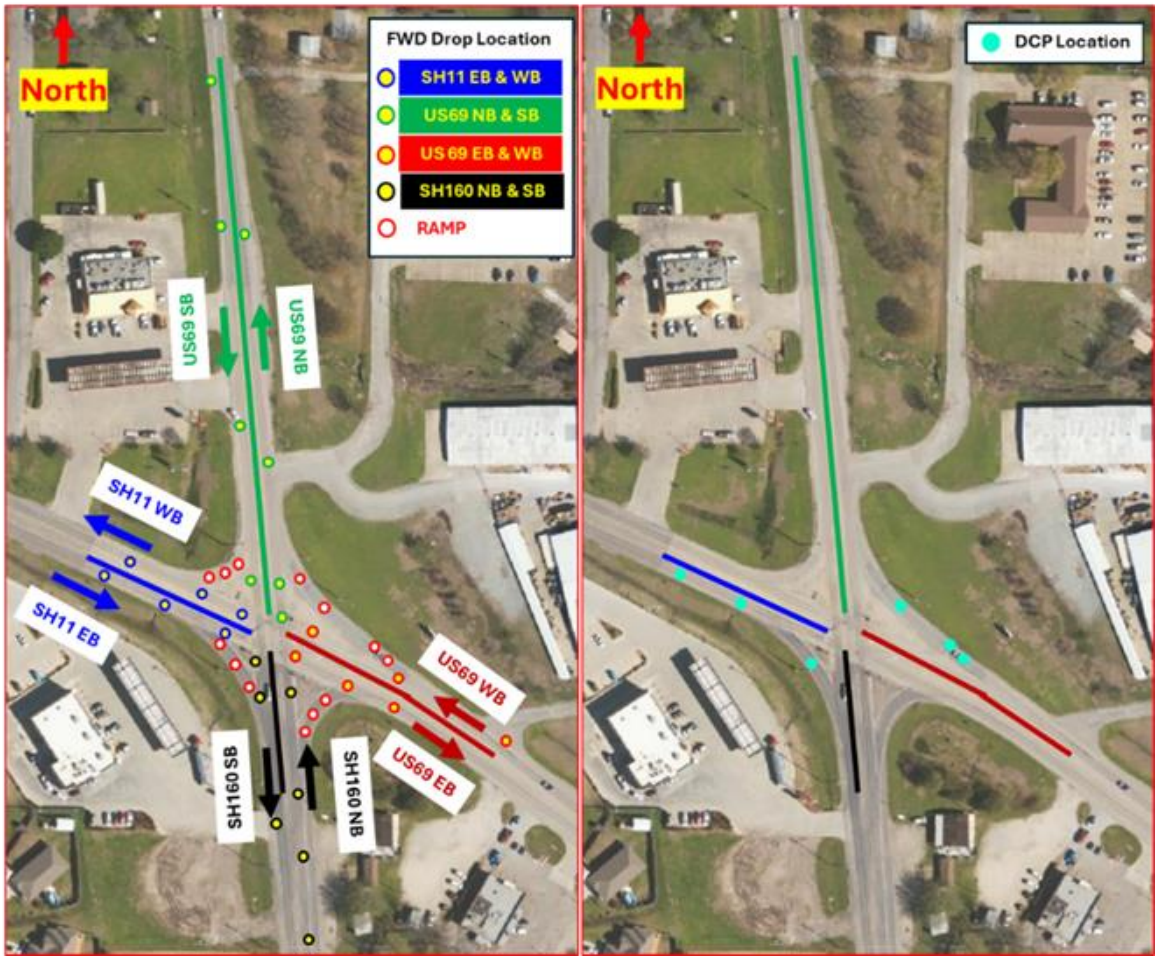

Figure A- 4Traffic data at the Intersection

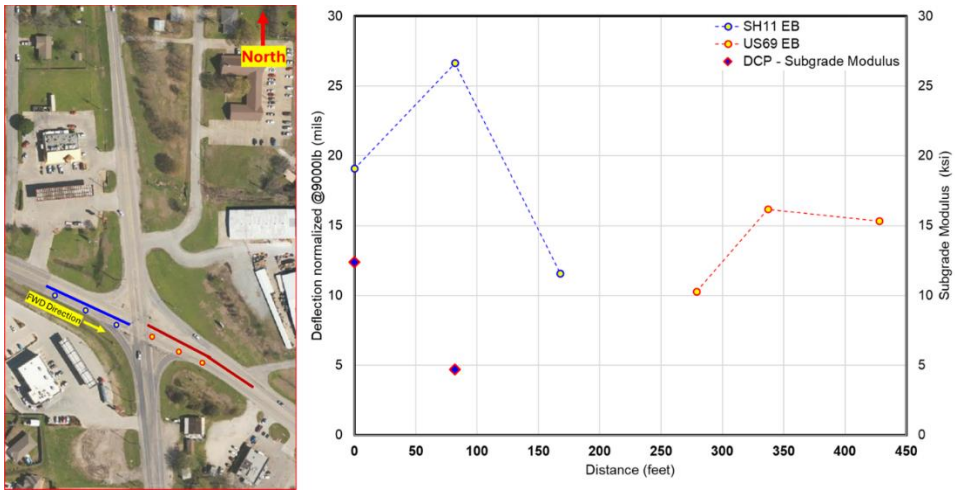

Figure A- 5 SH11 EB and US69EB Main Lane FWD Testing

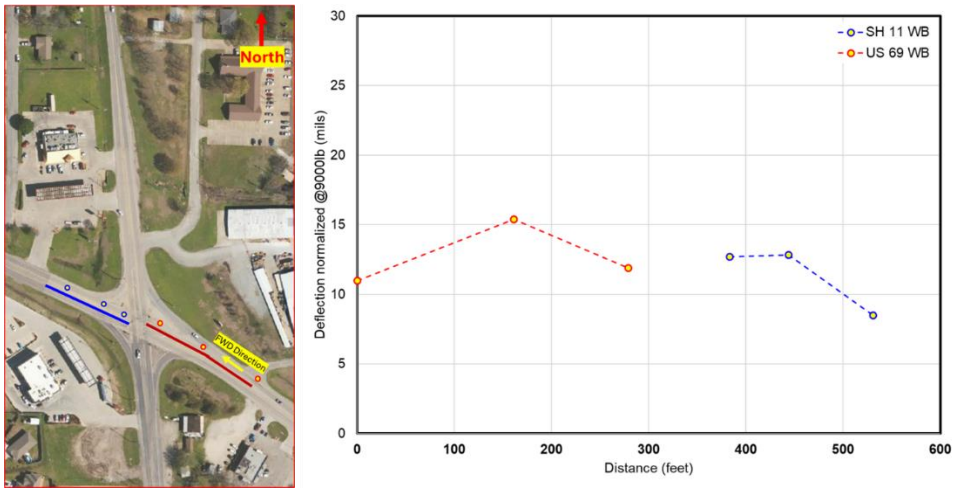

Figure A- 6 SH11 WB and US69WB Main Lane FWD Testing

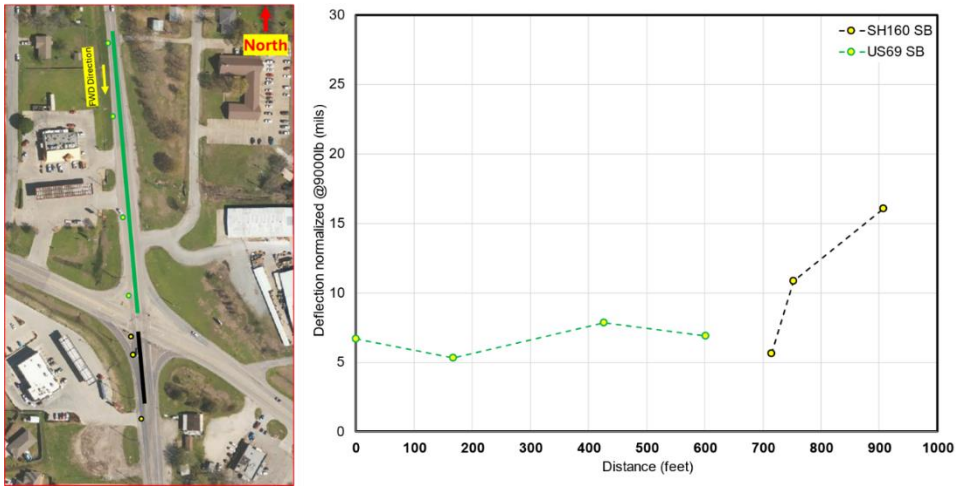

Figure A- 7 US69SB and SH160SB Main Lane FWD Testing

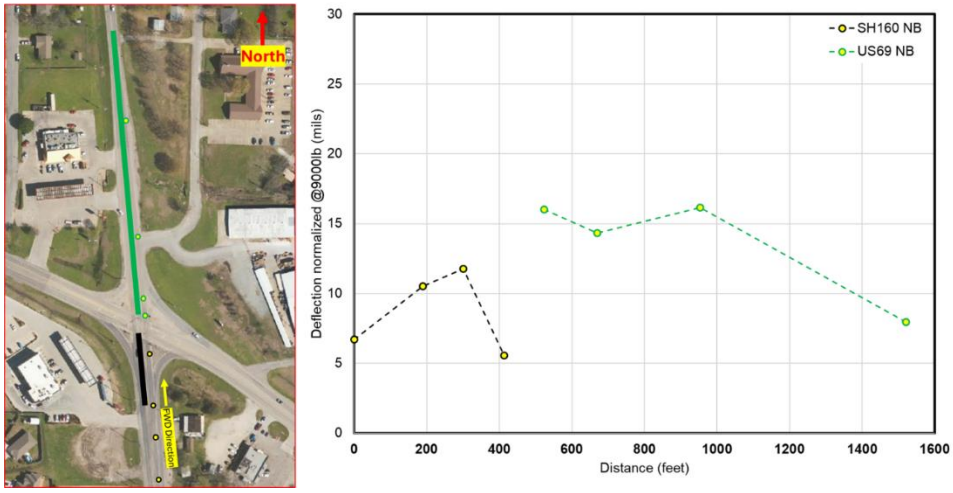

Figure A- 8 SH160 NB and US69 NB Main Lane FWD Testing

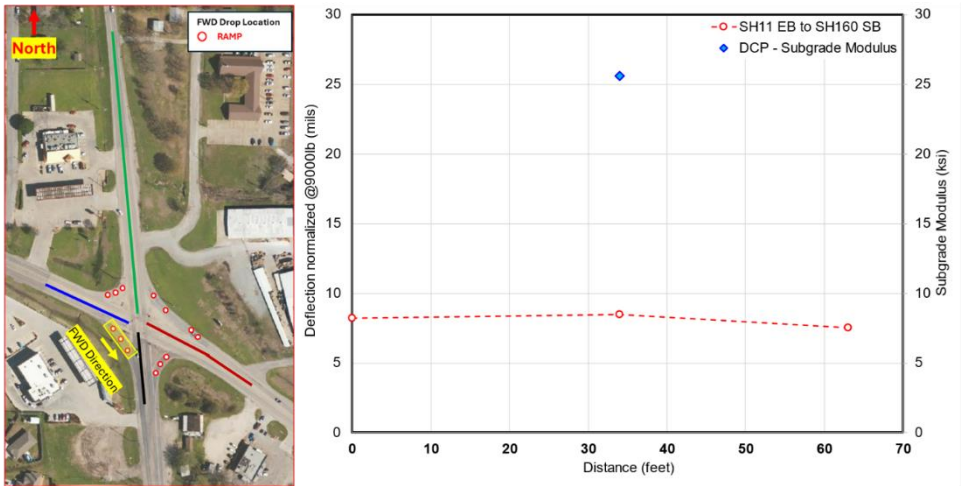

Figure A- 9 FWD Testing of Ramp from SH11EB to SH160 SB

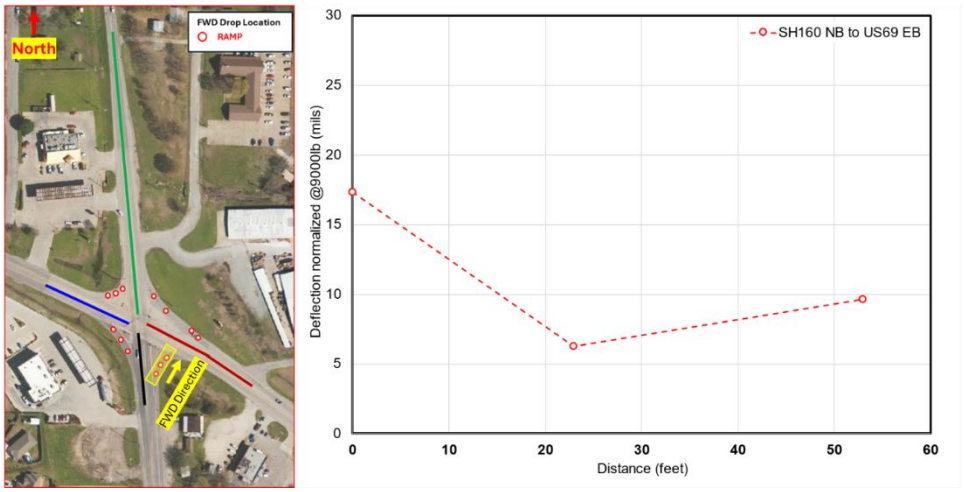

Figure A- 10 FWD Testing from Ramp SH160 to US69 EB

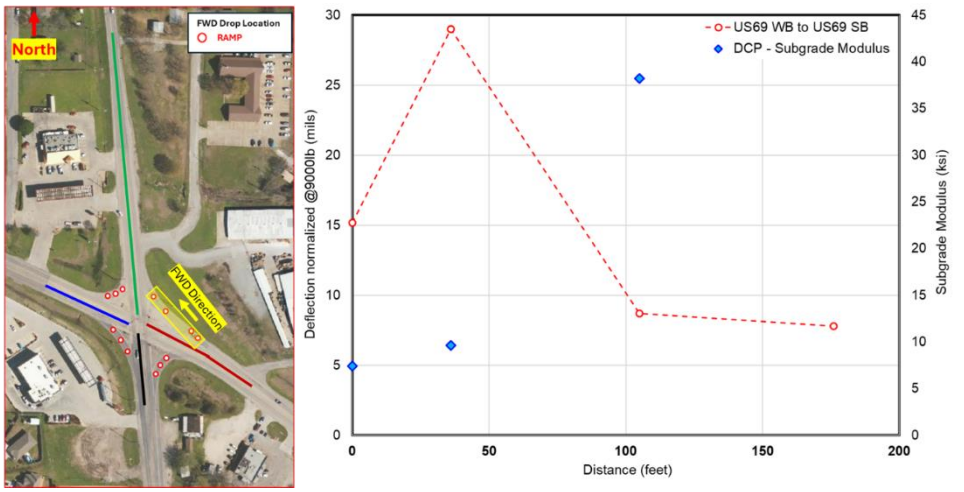

Figure A- 11 FWD Testing from Ramp US69 WB to US 69 SB

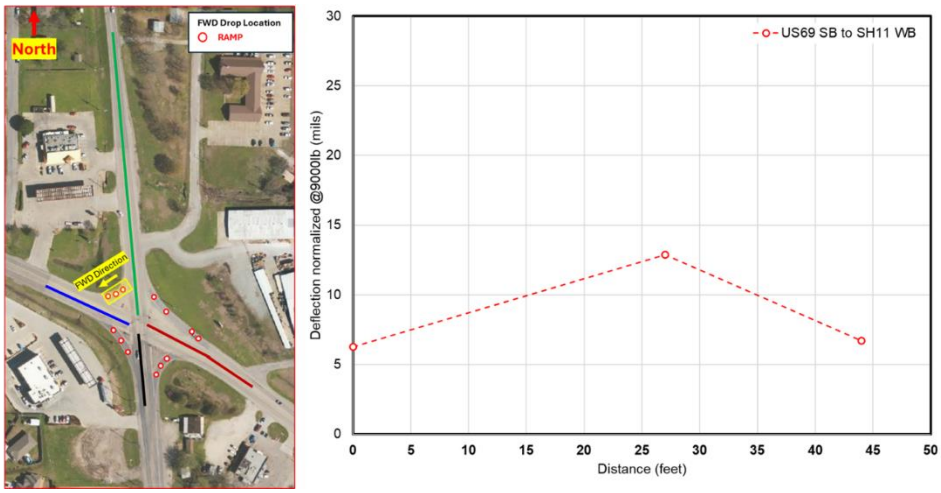

Figure A- 12 FWD Testing of Ramp from US69 SB to SH11 WB

From the FWD test observations, a distribution curve was plotted, as shown in Figure A-13, to analyze the statistical distribution of measured deflections. The results showed that the mean FWD deflection was approximately 11.59 mils, and the data trend followed a right-tailed normal distribution. The calculated standard deviation was 5.29 mils. The FWD test also aimed to select deflection data for use in the proposed new deflection-based design method. Based on the data trend, the third quartile deflection (15.21 mils) was chosen for further analysis, as it is a conservative measure and fits for our design purposes.

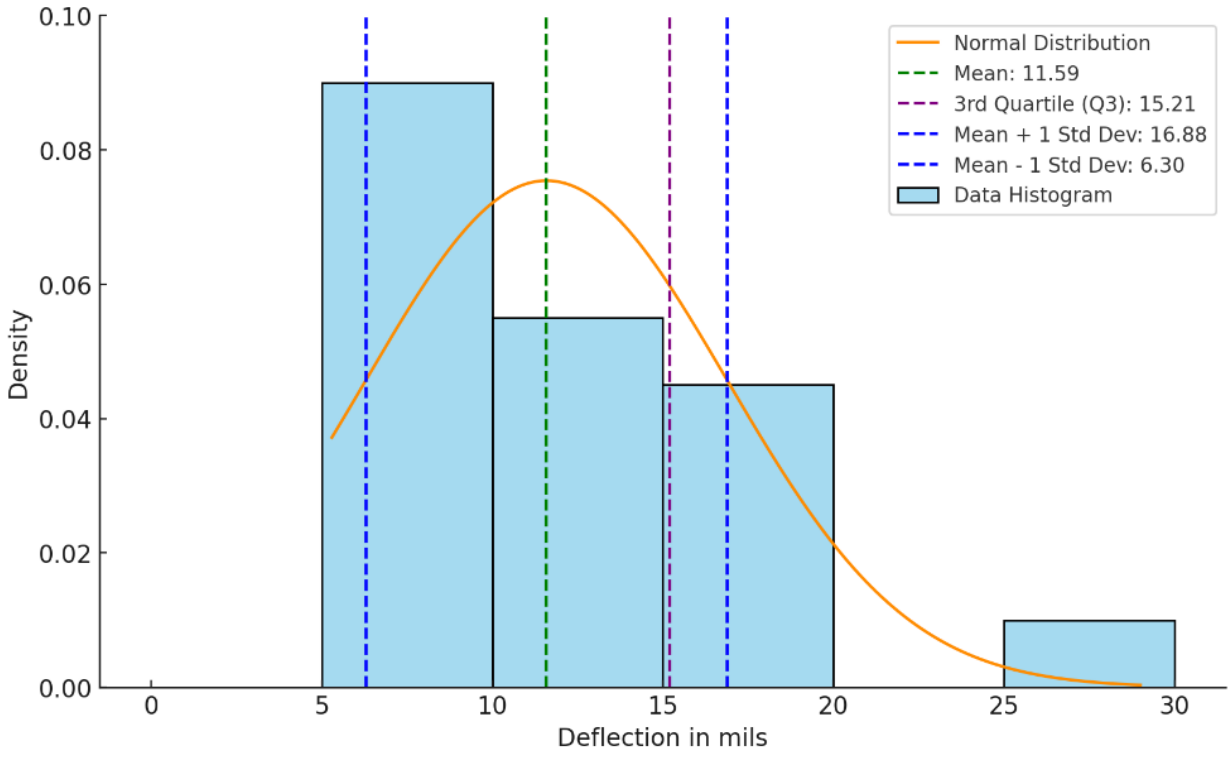

Figure A- 13 Histogram along with distribution curve of the FWD Testing results

DCP Testing

As mentioned earlier, DCP testing was conducted at six locations. Table A-2 shows the deflection measured in each location and their respective subgrade modulus. As seen the highest deflection was observed in SH11 EB in mainlane and ramp from US69 WB to US69 SB. This high deflection was attributed to lower subgrade modulus.

Table A- 2 Location where DCP Test was performed

Location	**Direction**	**Deflections (mils)**	**Subgrade Modulus (ksi)**
Ramp	From SH11 EB to SH160 SB	8.49	25.6
	From US69 WB to US69 SB	8.71	38.2
		15.17	7.4
		29.00	9.6
SH11 EB	Eastbound	19.07	12.4
		26.63	4.7

The coring operation was conducted to measure the HMA thickness and assess the condition of the base and subbase layers. Figure A-14 provides details on the base layer and HMA thickness, as measured by GPR and coring. Notably, SH 11 (eastbound and westbound), US 69 (eastbound and westbound), and all ramps showed no subbase beneath the HMA layer. In contrast, both US 69 and SH 160 (northbound and southbound) had concrete beneath the HMA. This finding aligns with observed high deflections at locations without a subbase beneath the HMA layer.

The subgrade was identified as black, soft, wet clay. While GPR was initially used to measure the existing HMA thickness, its results were compared with coring data from eight locations. Interestingly, the HMA thickness measured by coring was generally less than that indicated by GPR, raising questions about GPR's accuracy for measuring exact HMA thickness. To improve reliability, additional coring is recommended for comparison with GPR results. Moving forward, relying on coring is advisable, as it likely provides a more accurate representation of the subbase condition beneath the HMA layer with higher confidence.

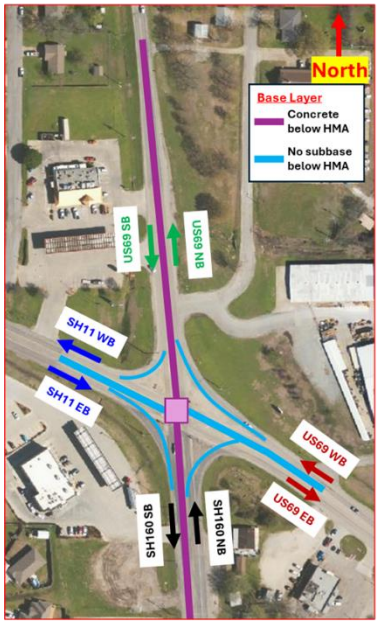

Highway	Direction	HMA Thickness	
		Using GPR (in inches)	Using Coring machine (in inches)
SH11	West Bound	12	9.25
	Turn Lane	10.25	
	East Bound	10.5	
US69	West Bound	9.5	8.25
	Turn Lane	10.25	
	East Bound	10.6	
	South Bound	11.5	9.25
	Turn Lane	10	
	North Bound	11.5	
SH160	South Bound	11.5	8.5
	Turn Lane	10	
	North Bound	10	
Ramp	From SH11 EB to SH160 SB	9	11
	From SH160 NB to US69 EB	10.5	8.75
	From US69 WB to US69 NB	11	9.25
	From US69 SB to SH11 WB	12.5	8.75

Figure A- 14 Base Layer condition and HMA thickness measured using GPR and

With the information collected on deflection and subgrade modulus, a graph was plotted to examine their relationship. As expected, Figure A-15 shows that deflection measured has a direct relationship with subgrade modulus. As deflection increases the subgrade modulus tends to decrease and vice versa.

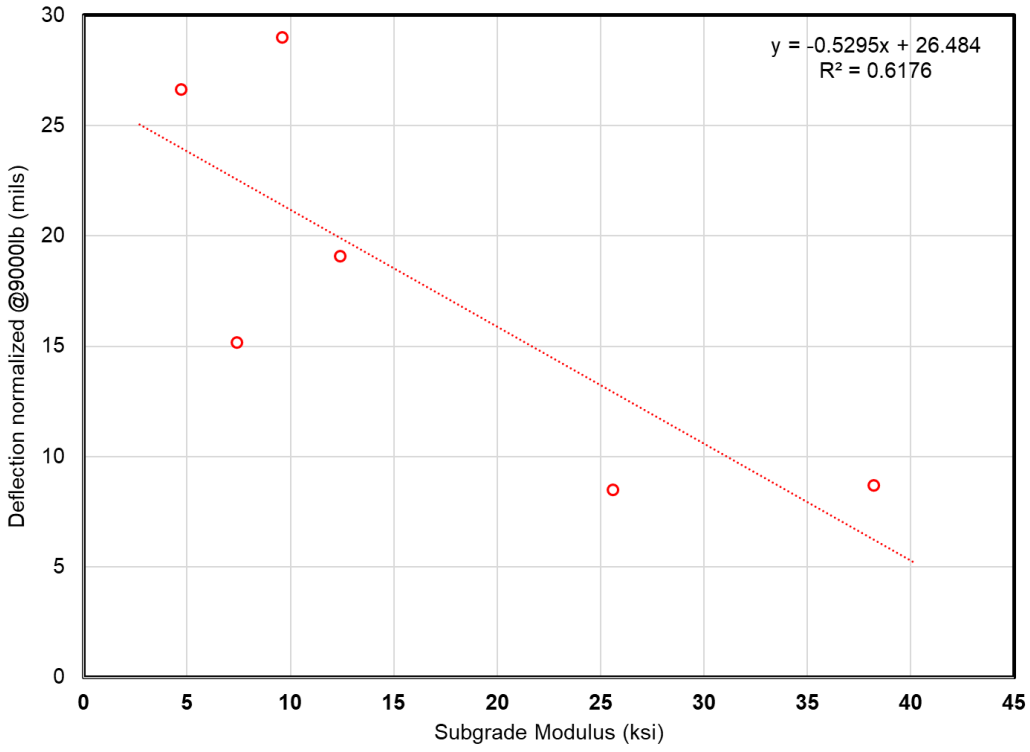

Figure A- 15 Relationship between Deflection and Subgrade Modulus

Summary

In summary, the two primary input factors required for this analysis are the future traffic ESALs value and the base deflection. Based on our investigation, we have chosen to use a base deflection of 11.59 ~ 12 mils, a mean value. Consequently, any deflection value exceeding 11.59 mils warrants further investigation, as performed here through DCP testing. Additionally, it is essential to recognize that the thickness and type of base layer can significantly influence deflection. Therefore, the engineer in charge should assess high deflection areas, potentially implementing retrofitting for localized sections to enhance reliability in the base deflection used for design.

As previously noted, the design traffic values are as follows:

- 10-year design period: 5 million ESALs → 7-inch overlay
- 20-year design period: 11 million ESALs → Use 8-inch overlay
- 30-year design period: 25 million ESALs → Use 10-inch overlay

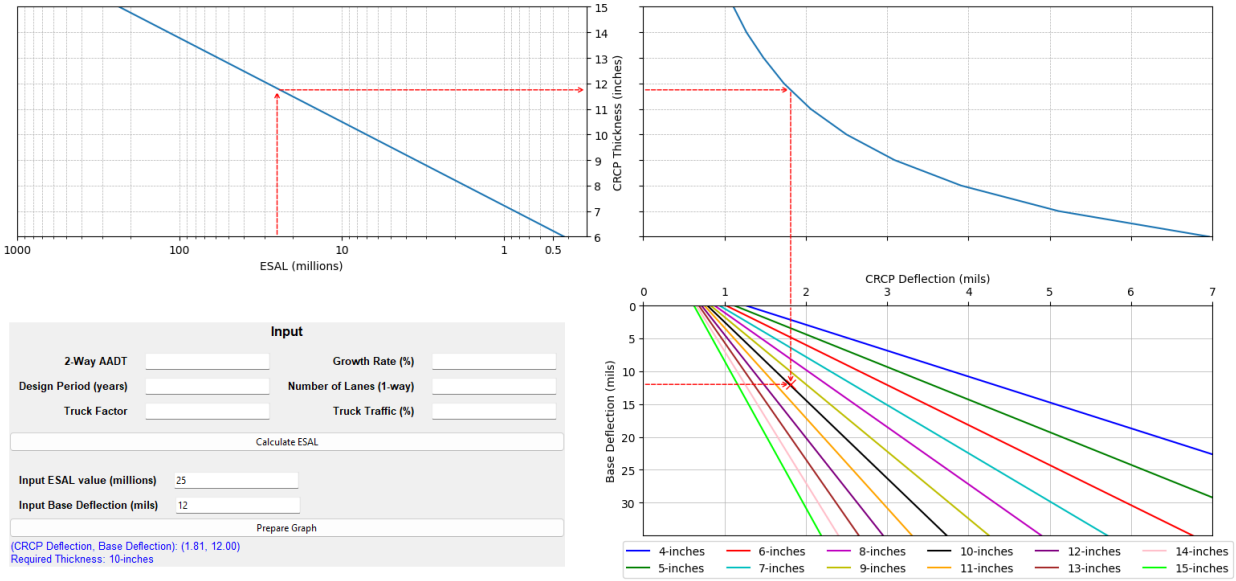

Figure A- 16 Deflection based Design Method Nomograph